

**AN INVESTIGATION INTO THE EFFECT OF MYRISTOYLATION ON
THE INTERACTIONS BETWEEN HIV-1 NEF AND CELLULAR
PROTEINS**

VICTORIA J BOULTON

A thesis submitted for the degree of Doctor of Philosophy

Department of Veterinary Pathology
Faculty of Veterinary Medicine
University of Glasgow
May 1998

© Victoria J Boulton

ProQuest Number: 13818617

All rights reserved

INFORMATION TO ALL USERS

The quality of this reproduction is dependent upon the quality of the copy submitted.

In the unlikely event that the author did not send a complete manuscript and there are missing pages, these will be noted. Also, if material had to be removed, a note will indicate the deletion.



ProQuest 13818617

Published by ProQuest LLC (2018). Copyright of the Dissertation is held by the Author.

All rights reserved.

This work is protected against unauthorized copying under Title 17, United States Code
Microform Edition © ProQuest LLC.

ProQuest LLC.
789 East Eisenhower Parkway
P.O. Box 1346
Ann Arbor, MI 48106 – 1346

GLASGOW UNIVERSITY
LIBRARY

11178 (copy 1)

GLASGOW
UNIVERSITY
LIBRARY

DECLARATION

The studies described in this thesis were carried out in the Department of Veterinary Pathology at the University of Glasgow Veterinary School between October 1994 and March 1998. The author was responsible for all the results except where it is stated otherwise. No part of this thesis has been presented to any university

Victoria J Boulton

May 1998

CONTENTS:

	Page number
Abbreviations	13
Symbols for amino acids	15
Acknowledgements	16
Summary	17
CHAPTER 1 INTRODUCTION	
1.1 HIV and the <i>Retroviridae</i>	21
1.1.1 Introduction	21
1.1.2 Prototype genes, <i>gag</i> , <i>pol</i> and <i>env</i>	23
1.1.3 HIV virus structure	26
1.1.4 Auxiliary genes	27
1.1.5 Viral cell tropism	31
1.1.6 Therapeutics	33
1.2 Nef	35
1.2.1 Introduction	35
1.2.2 Gene structure	35
1.2.2.1 Physical features	35
1.2.2.2 Significance of <i>nef in vivo</i>	38
1.2.3 The protein product of the <i>nef</i> gene	40
1.2.3.1 Characteristics	40
1.2.3.2 Myristoylation of Nef	41
1.2.3.3 Nef subcellular localization	44
1.2.4 Nef mediated virion infectivity	45
1.2.5 Nef disruption of cell signalling pathways	48
1.2.5.1 Nef phenotype	48
1.2.5.2 Nef putative interaction partners	49
1.2.6 Nef mediated CD4 down-modulation	51
1.2.7 The role of Nef in HIV immune evasion	54
1.2.8 Miscellaneous	55
1.3 Nef and the Src tyrosine kinases	56

1.3.1	Introduction to the Src tyrosine kinases	56
1.3.2	Evidence for Nef interactions with Src tyrosine kinases	59
1.4	Aims of the thesis	62

CHAPTER 2 MATERIALS AND METHODS

2.0	General chemicals and enzymes	67
-----	-------------------------------	----

MOLECULAR BIOLOGY TECHNIQUES

2.1	Molecular biology techniques - Materials	67
2.1.1.	Chemical and enzymes	67
2.1.2.	Radiochemicals	67
2.1.3.	Bacterial strain	67
2.1.4.	Cloning vectors	67
2.1.5.	Stock solutions	69
2.1.6.	Media and antibiotics	70
2.2	Molecular biology techniques– Experimental methods	70
2.2.1	Agarose gel electrophoresis	70
2.2.2	Polymerase chain reaction (PCR)	71
2.2.3	Restriction enzyme digests	71
2.2.4	DNA purification from agarose gels	71
2.2.5	Ligation of DNA molecules	72
2.2.6	Plasmid transformation using competent <i>DH5α</i> <i>E.coli</i>	72
2.2.7	Small scale alkali purification of <i>E.coli</i> plasmid DNA	72
2.2.8	Large scale purification of plasmid DNA from <i>E.coli</i>	72
2.2.9	Sequencing of DNA	74
2.2.9.1	Manual	74
2.2.9.2	Sequencing gel	75
2.2.9.3	LI-COR automated	75

YEAST PROTOCOLS

2.3	Yeast protocols– Materials	77
-----	----------------------------	----

2.3.1	Chemicals and enzymes	77
2.3.2	Radiochemicals	77
2.3.3	Yeast strain	77
2.3.4	Yeast interaction trap plasmids	78
2.3.5	Yeast media and supplements	79
2.3.5.1	Complete minimal (CM) dropout powder	79
2.3.5.2	Carbon sources	80
2.3.5.3	Dropout plates and media	81
2.3.5.4	X-Gal plates	81
2.3.5.5	10xBU salts	81
2.3.5.6	Nomenclature of media plus supplements	81
2.3.6	Storage and freezing of yeast	82
2.4	Yeast protocols- Experimental methods	82
2.4.1	Transformation of yeast by the high efficiency lithium acetate method	83
2.4.2	Testing baits for transcription activation	84
2.4.2.1	Constructing the transcriptional activation selection strain	85
2.4.2.2	Transcriptional activation assay	85
2.4.3	Repression assay	86
2.4.4	Selecting interactors from library transformants	87
2.4.4.1	Transformation of the library plasmid and determination of colony forming units (CFU)	87
2.4.4.2	Isolating interactors on Leu-plates	88
2.4.4.3	β -Galactosidase filter assay	88
2.4.5	Verifying the specificity of the interactions	89
2.4.5.1	RFLP analysis of PCR products	90
2.4.5.2	Primers for RFLP PCR	90
2.4.6	Yeast plasmid miniprep	91
2.4.7	Yeast cell lysis using glass beads	91
2.4.8	Labelling of Yeast with ^3H Myristic Acid	92

BACULOVIRUS PROTOCOLS

2.5	Baculovirus protocols – Materials	94
2.5.1	Chemicals and enzymes	94
2.5.2	Radiochemicals	94
2.5.3	Insect cell line	95
2.5.4	Baculovirus strain	95
2.5.5	Expression plasmids	95
2.5.6	Stock solutions	96
2.5.7	Preparation of culture medium	96
2.5.8	Growth and maintenance of insect cell cultures	96
2.5.9	Counting the Sf9 cells	97
2.5.10	Freezing, storage and recovery of Sf9 cells in liquid nitrogen	97
2.5.11	Preparation of glutathione-agarose (GA) -beads	98
2.6	Baculovirus protocols – Experimental methods	98
2.6.1	Transfection of <i>Spodoptera frugiperda</i> (Sf9) insect cells to generate recombination baculoviruses	98
2.6.1.1.	Preparation of viral DNA	99
2.6.1.2.	Transfection of Sf9 insect cells	99
2.6.1.3.	Plaque assay to harvest the recombinant virus	100
2.6.2	Verifying expression of the protein of interest by the recombinant baculovirus	101
2.6.3	Large scale production of viral stocks	101
2.6.4	Plaque assay for virus titre	102
2.6.5	Production of Sf9 cell lysates	102
2.6.5.1	Single baculovirus infections	103
2.6.5.2	Coinfections	103
2.6.6.	Purification of affinity reagents	103
2.6.6.1	Large scale virus infections GST-fusion protein purification	103
2.6.6.2	Lysis of infected cells and purification of GST fusion proteins	103
2.6.7	<i>In vitro</i> binding assay	104
2.6.7.1	Binding purified protein to GA-beads	105
2.6.7.2	Binding assay	105

2.6.8	<i>In vivo</i> binding assays	105
2.6.9	Metabolic labelling	106

PROTEIN BIOCHEMISTRY

2.7	Protein biochemistry– Materials	107
2.7.1	Chemicals and enzymes	107
2.7.2	Radiochemicals	107
2.7.3	Stock solutions	108
2.8	Protein biochemistry - Experimental methods	108
2.8.1.	SDS-PAGE gel analysis	108
2.8.2.	Coomassie staining	109
2.8.3.	Radioactive gels	109
2.8.4.	Western blot	110
2.8.4.1	Transfer to PVDF membrane	110
2.8.4.2	Western blot	110
2.8.4.3	Reprobing the membrane	110
2.8.5	Immunoprecipitation	112
2.8.6	Bradford assay	112
2.8.7	<i>In vitro</i> transcription-translation	112
2.8.8	Autophosphorylation assay	113
2.8.9	Protein kinase assays	113
2.8.10	HIV-1 protease experiments	114

CHAPTER 3 Use of the yeast interaction trap to investigate novel cellular interactions with HIV-1 Nef

3.0	General introduction	117
3.1	Results	120
3.2	Modification of the bait plasmid to accept proteins as N-terminal fusions	125
3.3	Verification of expression and myristoylation of Nef in pVEG	125
3.4	Activation and repression assays	128

3.5	Screening a Jurkat T-cell library with pVEG Nef for novel protein-protein interactions	132
3.6	Further investigation of groups A1, B1 and C1 – sequence data and specificity tests	139
3.6.1	Analysis of the sequence and specificity results obtained for groups C1 and B1	142
3.6.2	Re-analysis of group A2	146
3.6.3	Analysis of the specificity results obtained for Group A1	149
3.7	Further analysis of the Nef-A1 (p9) interaction	152

CHAPTER 4 Investigation of a putative Nef interaction with Lck

4.1	Introduction	156
4.2	Background	159
4.3	Summary of work presented hereafter	160
4.4	Construction of the recombinant baculoviruses	160
4.5	Confirming the authenticity of the proteins	161
4.5.1	Expression and kinase activity	164
4.5.2	Confirming the authentic acylation of Lck	164
4.6	<i>In vitro</i> binding assays	167
4.6.1	Overview of preliminary studies	167
4.6.2	Follow up <i>in vitro</i> binding studies	169
4.6.3	Identifying the cause of the differences between protein stocks	172
4.6.4	How were the protein conformations altering between stocks	175
4.7	Construction of constitutively active and inactive Lck mutants to assess conformational binding criteria	177
4.8	Confirmation of the expression and kinase activities of the mutant Lck recombinant baculoviruses; Lck G2A/K273R/Y505F (LckGKY) and Lck G2A/Y505F (LckGY)	179
4.9	<i>In vivo</i> binding studies	183
4.9.1	<i>In vivo</i> binding studies for LckGY and LckGKY	183
4.9.2	A comparative study of Lck mutant binding abilities to N-G	186

4.10	Identification of region in Nef important in mediating its <i>in vivo</i> binding to LckGKY	189
4.10.1	Investigation of Lck binding to different Nef alleles	189
4.10.2	Screening of a panel of Nef deletion mutants for interactions with LckGKY	191

CHAPTER 5 Analysis of Hck interactions with NEF

5.1	Introduction	197
5.2	Summary of results presented hereunder	198
5.3	Construction of the SH3, SH2 and SH3-SH2 domain fusions to the activation domain of pJG4-5 for expression and interaction analysis in the YTHS	199
5.4	Analysis of YTHS interaction between the Src homology regions and myristoylated Nef	202
5.5	Construction of recombinant baculoviruses	210
5.6	Verifying the authenticity of the recombinant baculovirus expressed mHck, Src and Fyn	210
5.6.1	Determining full length expression and kinase activity	210
5.6.2	Determination of authentic acylation of the proteins	213
5.7	<i>In vitro</i> binding assays	216
5.8	<i>In vivo</i> binding assays	219
5.9	Analysis of the contribution of the N-terminus of Nef to Hck binding	222
5.10	Analysis of the contribution of the N-Terminus of Hck to Nef binding	224
5.11	Screen of a panel of Nef mutants and isolates	228
5.11.1	Results from the Nef mutant screen	228
5.11.2	Results from the Nef isolate screen	232
5.12	Effect of Nef on Hck enzymatic activity	235

CHAPTER 6- Discussion

6.1	Screening for novel Nef interactors	239
6.2	Conformational requirements for the Lck interaction with Nef	245
6.3	Interactions of Nef with Hck	255
6.4	Final discussion	263

LIST OF FIGURES:

3.1	Summary of approach taken to modify the bait plasmid to accept proteins as N-terminal fusions	123
3.2	Results of the [³ H] myristic acid labelling of yeast	127
3.3	Activation assay for pVEG-Nef, pVEG-G2A and pEG-Nef	130
3.4	Results of the repression assay for pVEG-Nef, pVEG-G2A and pVEG-Nef	131
3.5	Classification of potential Nef interactors after the library screen	134
3.6	Results from the rescreening of the library interactors	138
3.7	Western blot analysis of interactor expression	141
3.8	Computational analysis of sequence data for groups C1 and B1	143
3.9	Results of the specificity tests	145
3.10	Computational analysis of sequence data for groups A2 and A1 (clone39)	147
3.11	Results of the specificity screen for group A1, clone 39	151
3.12	Quantitative analysis of amount of GST-39 bound to GA-beads	153
4.1	Analysis of expression and phosphorylation of recombinant baculoviruses expressing wtLck and AcLck	163
4.2	Establishing the authentic acylation of wtLck	166
4.3	Results from the preliminary studies	168
4.4	<i>In vitro</i> binding assay results of the crosswise comparison of reagents	171
4.5	Effect of serum on Lck binding to N-G	174
4.6	Autophosphorylation assays to compare wtLck, AcLck and oAcLck	176
4.7	Analysis of the expression and kinase activities of LckGKY and LckGY relative to AcLck, LckG2A and Lck273A	181

4.8	Results of <i>in vivo</i> binding assays for LckGY and LckGKY	185
4.9	Comparison of Lck wildtype and mutants ability to bind N-G	188
4.10	LckGKY <i>in vivo</i> binding assays for 5 different Nef alleles PCR2,3 and 4 HIV-1 clinical isolates, SIV J5 and Bru	190
4.11	<i>In vivo</i> binding assays for LckGKY plus the panel of Nef deletion mutants	194
5.1	Verification of SH3, SH2 and SH3-SH2 domain expression for Hck, Lck, Src and Fyn in yeast	201
5.2	Nef interactions with Hck and Src SH3 domains in the YTHS	207
5.3	Nef interactions with Hck and Src SH2 domains in the YTHS	208
5.4	Interactions between Nef and Src kinase SH3-SH2 domain fusions	209
5.5	Confirmation of kinase activity and expression of mHck, Src and Fyn	212
5.6	Confirmation of authentic acylation of mHck, Src and Fyn	215
5.7	<i>In vitro</i> binding experiments for mHck and Src	218
5.8	Results of the <i>in vivo</i> binding studies with Nef plus mHck and Src	221
5.9	Effect of HIV-1 protease cleavage on the N-G Hck complex	224
5.10	Results of <i>in vivo</i> binding studies for Δ 78hHck and G2AhHck	227
5.11	Results of mHck binding to the panel of Nef mutants	230
5.12	Comparison of mHck, G2A- and Δ 78- hHck binding to PAAP Nef	231
5.13	Screening Nef alleles for mHck binding	233
5.14	Comparison of the effect of wildtype and PAAP Nef on mHck activity	236

LIST OF DIAGRAMS:

1.1	Genomic organisation of HIV-1	25
1.2	A schematic representation of virion assembly	27
1.3	HIV-1 genome structure and mRNA expression	31
1.4	Summary of the <i>nef</i> gene structural features	38
1.5	Myristate bound to the N-terminal glycine residue	41
1.6	A schematic representation of the Nef polyproline type II helix	57
1.7	Schematic diagram of Lck	60
3.1	Construction of pVEG2	124

3.2	Map of pVEG2, including sequence around the polylinker	126
3.3	Orientation of samples for the rescreening of putative interactors	137
3.4	Orientation of plates for specificity screening of the interactors	140
4.1	A model for the activation of Src tyrosine kinases	182
5.1	Orientation of samples for the SH3, SH2 and SH3-SH2 interactor hunt with Nef as bait	203
5.2	Flow diagram of experimental procedure	223
5.3	Sequence alignment of BH10 Nef with the primary patient isolates (PCR2-5iso)	234
6.1	Homology of clone 39 to 3',5'-cyclic nucleotide phosphodiesterase	243

LIST OF TABLES

2.1	General use chemicals and enzymes, including abbreviations	65
2.2	Further general use chemicals and enzymes, including abbreviations	66
2.3	Chemicals and enzymes for yeast protocols including abbreviations	77
2.4	Table of amino acid quantities required for the complete minimal dropout powder	80
2.5	Nomenclature of media and dropout plates (in single letter and triple letter code)	82
2.6	Chemicals and enzymes for baculovirus protocols	94
2.7	Volumes used for different culture dishes/flasks	103
2.8	Chemicals and enzymes for protein protocols	107
2.9	Antibodies used in the studies, suppliers and amounts used	111
4.1	Summary of Nef mutants	193
5.1	Summary of PCR primers for the cloning of the SH3. SH2 and SH3-SH2 domains into pJG4-5	200

BIBLIOGRAPHY

268

ABBREVIATIONS

AIDS	Acquired immunodeficiency syndrome
AP-1	Activator protein
β -gal	β -galactosidase
CA	Capsid
CTL	Cytotoxic T Lymphocyte
DB domain	DNA binding domain
DNA	Deoxy-ribonucleic acid
EIF3	Eukaryotic initiation factor 3
ER	Endoplasmic reticulum
FCS	Foetal calf serum
GA-beads	Glutathione-agarose beads
G-protein	Guanine nucleotide binding protein
GPI	Glycosyl-phosphatidylinositol
GST	Glutathione S-Transferase
hCMV	Human Cytomegalovirus
HIV	Human immunodeficiency virus
IL2-R	IL2-Receptor
IN	Integrase
ITAMs	Immune-receptor-tyrosine-based activation motifs
kDa	KiloDaltons
Lck	Lymphoid cell kinase
LTR	Long terminal repeat
MA	Matrix protein
MAPK	Mitogen activated protein kinase
MHCI	Major histocompatibility complex
MIP	Macrophage inflammatory
NAK	Nef associated kinase
NaOV	Sodium orthovanodate
NC	Nucleocapsid
NCBI	National Center for Biotechnology Information
Nef	Negative factor

NES	Nuclear export sequence
NMR	Nuclear magnetic resonance
ORF	Open reading frame
PAGE	Polyacrylamide gel electrophoresis
PAK	p21 activated kinase
PBMC	Peripheral blood mononuclear cell
PCR	Polymerase chain reaction
PIC	Preintegration complex
PKC	Protein kinase C
PR	Protease
RACKS	Receptors for activated C-kinase
RANTES	Regulated upon activation, normal T expressed and secreted
Rev	Regulator of late gene expression
RFLP	Restriction fragment length polymorphism
RNA	Ribonucleic acid
rpm	Revolutions per minute
RRE	Rev-response element
RT	Reverse transcriptase
SDF-1	Stromal-cell derived
SH2	Src homology 2
SH3	Src homology 3
SIV	Simian immunodeficiency virus
TA domain	Transcriptional activation domain
TAR	Trans-activating response
Tat	<i>Trans</i> -activator protein
TCR	T-cell receptor
TNF	Tumour necrosis factor
U	Unit
UAS	Upstream activating sequence
Vif	Viral infectivity factor
Vpr	Viral protein R
Vpu	Viral protein U
Vpx	Viral protein X
YTHS	Yeast two-hybrid system

SYMBOLS FOR AMINO ACIDS

A	Ala	Alanine
C	Cys	Cysteine
D	Asp	Aspartic acid
E	Glu	Glutamic acid
F	Phe	Phenylalanine
G	Gly	Glycine
H	His	Histidine
I	Ile	Isoleucine
K	Lys	Lysine
L	Leu	Leucine
M	Met	Methionine
N	Asn	Asparagine
P	Pro	Proline
Q	Gln	Glutamine
R	Arg	Arginine
S	Ser	Serine
T	Thr	Threonine
V	Val	Valine
W	Trp	Tryptophan
Y	Tyr	Tyrosine

ACKNOWLEDGEMENTS:

Thanks are due to a number of people, but first and foremost to my supervisor Dr. Mark Harris for all his encouragement and support throughout the duration of my studies. Prof. Jim Neil for keeping an eye on me in Mark's absence, not to mention the lunchtime tennis matches. Tom McP. for generally looking after both me and my laboratory requirements. All in the north office; in particular Nighean for all her recent help and for our sanity Sunday afternoon excursions; ex-members Lizzie and Karen C and of course Andy the honorary member. All downstairs at molecular oncology and gene therapy. Also Graham, Sanya, Duncan, Nick, Flods and cuz P. for maintaining my humour, and Craig for maintaining his distance and allowing me to finish my studies! In particular I'd like to thank Ma, Pa and Grandpa without whose assistance and paternal support I could never have contemplated this.

SUMMARY:

The *nef* gene is conserved across the primate lentiviruses. It is an auxiliary gene and encodes a myristoylated 27-34kDa protein expressed early in the viral replicative cycle. Data from *in vivo* macaque studies and analysis of long term non-progressor cohorts has implicated *nef* as a critical factor in the progression from latent HIV infection to full blown AIDS. However the exact mechanism of action of Nef remains controversial. These studies were undertaken to investigate Nef interactions with cellular proteins. The yeast-two-hybrid-system (YTHS) was modified to express Nef as an N-terminal fusion protein, allowing interactions to be evaluated for the authentically myristoylated Nef species. Screening of a Jurkat T-cell library identified a novel Nef interaction with an uncharacterised polypeptide (clone 39). Specificity screens confirmed the authenticity of the interaction and the polypeptide was further demonstrated to bind HIV-1 p55Gag. The cDNA sequence had no homologies to known genes but 99% homology to a human expression sequence tagged (EST) cDNA and 76% homology to a mouse EST-cDNA sequence, however no protein homologies were found to either of these sequences. A fragment of the clone 39 peptide sequence was found to have significant homology to cAMP phosphodiesterase; thus raising the interesting possibility that Nef may be capable of binding native phosphodiesterases causing the deregulation of cAMP levels typically associated with HIV infection. As cAMP is a key secondary messenger influencing a number of cellular signal transduction pathways a Nef interaction with phosphodiesterase might also explain the pleiotropic functions ascribed to Nef.

A highly conserved (PXX)₃P proline motif in Nef had been previously been demonstrated to confer Nef binding to isolated Src homology 3 domains (SH3) of members of the Src tyrosine kinase family *in vitro*. The latter half of the studies described herein were therefore designed to determine whether Nef-SH3 complex formation was maintained *in vivo* in the context of the full length native proteins. Firstly Nef interactions with the T-lymphocyte specific kinase Lck were assessed. Nef was found to associate with Lck in a conformation-dependent manner. Nef binding was conferred by the open active conformation of Lck, indicative of the interaction occurring concomitantly with cell membrane receptor aggregation,

possibly during viral entry. The Nef interaction with Lck was found to be mediated at least in part by the conserved (PXX)₃P motif in Nef in conjunction with an N-terminal region in Nef. Secondly, Nef interactions with primarily Hck but also Src and Fyn were investigated. For this purpose both the YTHS and baculovirus expression systems were utilised. Interactions with native Nef and the isolated Src homology domains SH3, SH2 and SH3-SH2 were evaluated in the YTHS, the results of which demonstrated a conserved SH3 domain-mediated interaction with Nef for Hck and Src. No interaction was detected for Fyn. This result was corroborated by *in vitro* binding assays with the baculovirus expressed full length native proteins. The interactions between Nef and Hck was found to be conserved *in vivo*, however complex formation was independent of the Nef (PXX)₃P motif. Indeed deletion of a number of regions in Nef did not perturb the interaction, although unexpectedly the Bru laboratory isolate of Nef had severely impaired Hck binding ability. This suggested Hck binding was Nef isolate dependent and that subtle changes in amino acid sequence in targeted areas outside the (PXX)₃P motif were sufficient to inhibit the association. Results from peptide substrate assays to assess the effect of Nef on Hck kinase activity revealed that the (PXX)₃P motif was however critical for the Nef induced enhancement of Hck enzymatic activity.

CHAPTER 1

CHAPTER 1 - INTRODUCTION

	Page Number
1.1 HIV and the <i>Retroviridae</i>	21
1.2 Nef	35
1.3 Nef and the Src tyrosine kinases	56
1.4 Aims of the thesis	62

CHAPTER 1 - Introduction:

The *nef* gene is unique to the primate lentiviruses. It has been unequivocally linked with the destructive pathogenesis of HIV *in vivo* and as such, represents a challenge to basic research. Historically the function of Nef has provided much controversy and to date its precise role in viral infection is still unknown. In these studies the aim was to define the interactions between Nef and cellular proteins. The remit for the initial work was to identify novel cellular partners for Nef using the yeast-two-hybrid system. Further studies, using the baculovirus expression system and protein binding assays, were undertaken to analyse factors important in mediating the interaction of Nef with the family of Src tyrosine kinases. Principally the interactions of Nef with the T-lymphocyte specific p56Lck and the macrophage/monocyte specific Hck proteins were investigated.

In this chapter the basic features of the Retrovirus family are outlined. The significance of characteristics unique to the primate lentiviruses and current therapeutic strategies will be discussed. Following this, a review of the literature of Nef covering potential functions, cellular interactions and *in vivo* implications. A brief introduction to the Src kinases will be provided and then the aims of the project will be presented in detail.

1.1. HIV and the *Retroviridae*:

1.1.1. Introduction:

The human immunodeficiency virus type 1 (HIV-1) is a complex retrovirus. Together with HIV-2 and SIV (simian immunodeficiency virus) (Desrosiers et al., 1989), it is a member of the primate lentivirus subclass of retroviruses. HIV has been identified as the causative agent of AIDS (acquired immunodeficiency syndrome) in humans. Progression of the disease is characterised by a period of latency (average of 8 years) followed by the onset of AIDS. Disease correlates include selective CD4 T-lymphocyte depletion, wasting syndromes, neoplasms and a susceptibility to opportunistic infections. In contrast, SIV can exist apathogenically in some primate species, although in unnatural hosts such as

macaques (e.g. Rhesus) a similar debilitating and fatal disease profile occurs. Thus, macaques have provided an invaluable animal model for the study of disease pathogenesis, therapeutics and vaccine strategies (Desrosiers et al., 1989; Lewis and Johnson, 1995).

It was originally believed that the period of latency between infection with HIV and progression to AIDS was due to viral latency *per se*. However, it has emerged during *in vivo* studies of the kinetics of HIV infection, that the observed steady CD4 lymphocyte count during latency is not due to a lack of replication of the virus. It is conversely due to, the rapid turnover of the CD4 lymphocyte population (average 2 days) in response to high levels of virion production (Perelson et al., 1996; Ho et al., 1995). This observation has had enormous therapeutic implications (see section 1.1.6), since it follows that 98.5% of the circulating plasma viraemia is from newly infected cells. Hence, current dogma is that a shift from latency to AIDS is caused by the exhaustion of the regenerative capacity of the hosts immune system.

Retroviruses have both RNA and DNA components to their life-cycle (Varmus, 1988). There are 2 (+) sense RNA molecules per virion, each encoding all of the viral genes and regulatory apparatus. The defining feature of retroviruses is their ability to reverse transcribe their RNA genome to DNA, using the virally encoded reverse transcriptase (RT) (Goff, 1990). This reverse transcription event generates duplicated 3' and 5' ends, termed LTRs (long terminal repeats). The double stranded (-/+) DNA viral copy (or provirus) is then randomly integrated into the host chromosomal DNA. Once integrated the 5' LTR is specifically recognised by host cell transcription factors and acts as a promoter. The 3' LTR provides the polyadenylation signal for the mRNA transcripts. Most members of the retrovirus family are dependent on available transcription factors for their replication. Therefore, retroviruses establish chronic infections and as a consequence more commonly transform a cell, than destroy it e.g. oncoviruses. This cellular transformation occurs either, i) as a direct result of random integration leading to the disruption of cellular gene regulation or, ii) due to recombination of the

retrovirus with the cellular DNA, resulting in the incorporation of an oncogene (*v-*onc**) into the retroviral genome. Although viral oncogenes are cellular homologues they usually contain point mutations or fusions to *gag* sequences, which results in their transforming ability. Alternatively, retroviruses can exist benignly within the host chromosomal DNA. Many vertebrate species harbour endogenous proviral sequences in their genome, resulting from the historical integration of retroviruses into germ line cells. The biological significance of these endogenous retroviruses, in shaping genome plasticity and potentially conferring disease protection, is reviewed in (Lower et al., 1996).

Lentiviruses differ from other members of the retrovirus family because in addition to the prototypical *gag*, *pol* and *env* genes, they have a number of auxiliary genes. The existence of transcriptional regulatory genes among these, allows self regulation of viral replication. A further defining feature of the lentiviral infection conferred by the auxiliary gene products is an ability to infect quiescent cells (Goldfarb, 1995), see section 1.1.4. Normally retroviruses are reliant on the breakdown of the nuclear envelope during mitosis to successfully integrate into the host genome. This ability to infect quiescent cells and upregulate viral replication is consistent with the productive infection seen during lentiviral, and in particular HIV infection.

1.1.2. Prototype genes, *gag*, *pol* and *env*:

The genomic size for HIV is about 9.8Kb, with 3 major open reading frames (ORF) encoding the conserved retroviral *gag*, *pol* and *env* genes. Expression from the proviral LTR promoter results in the transcription of multiply spliced and full length viral mRNAs (Kieny, 1990). The primary transcript for HIV is a full length mRNA which is translated into the Gag and Pol polyprotein precursors. The full length Gag-Pol polyprotein precursor is only produced at a ratio of approximately 1:20 of the p55Gag precursor. Gag-Pol translation requires a (-1) frame-shift event to read through the Gag stop codon. The Gag-Pol polyprotein is subsequently proteolytically cleaved to form the Gag, matrix (MA)-p17, capsid (CA)-p24 and nucleocapsid (NC)-p7 and p6, proteins which comprise the internal structural

proteins of the virus, see section 1.1.3. Pol is cleaved to form the viral protease (PR)-p10, reverse transcriptase (RT)-p66/55 and integrase (IN)-p32 enzymes. The specific proteolytic cleavage of these proteins is performed by PR, which is activated during viral budding. The frame-shift mechanism allows the high levels of expression necessary for Gag structural proteins, in comparison to the relatively low levels for the Pol encoded enzymes. This read through ability represents a common translational control level among retroviruses e.g. the murine and feline leukaemia viruses, control their *gag* stop codon read through event by utilising RNA secondary structures.

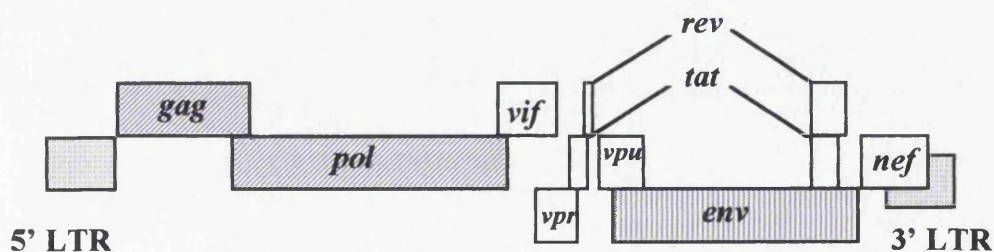
The Gag MA protein is myristoylated and targets the p55 Gag precursor to the cell surface membrane (Gottlinger et al., 1989; Spearman et al., 1994). A stretch of basic amino acids in the N-terminal 31 amino acids have been demonstrated to facilitate membrane targeting (Zhou et al., 1994). In the virion MA functions as an integral structural protein (see section 1.1.3.), but on virus entry a small percentage is tyrosine phosphorylated resulting in its association with the preintegration complex (PIC). In this context the MA helps target the PIC to the host nucleus (Bukrinskaya et al., 1996; Vonschwedler et al., 1994; Gallay et al., 1995a; Camaur et al., 1997). Multiple functions have also been proposed for the CA protein, inferred due to phenotypic changes within the viral particles caused by specific CA mutations (Dorfman et al., 1994; Zhang et al., 1996; Reicin et al., 1996). The N-terminal CA region confers important structural constraints on the viral core necessary for virion infectivity, while more C-terminal amino acid sequences are involved in virion assembly. MA, CA, NC and p6 are all necessary for virion infectivity (Lee and Linial, 1995; Furuta et al., 1997; Zhang and Barklis, 1997; Huang et al., 1995).

The HIV RT, encoded by *pol*, possesses both RNA dependent DNA polymerase and RNaseH activities. The molecule comprises a p66/51 heterodimer. The p51 species arises as a result of limited proteolysis of the C-terminus of p66. Crystallography studies (Jones et al., 1993; Stammers et al., 1994), in combination with sequence analysis and *in vitro* mutagenesis experiments, have implicated the

15KDa C-terminal region of p66 as the location of the RNaseH activity. The HIV RT lacks 3' to 5' exonuclease proof reading activity and as a result is highly error prone during DNA synthesis (Bebenek et al., 1989; Preston et al., 1988). This high ratio of mutagenesis provides a heterogeneous viral genome, which is thought to facilitate the virus in its evasion of the immune system. The viral IN also encoded by *pol*, acts to cleave and ligate the proviral into the host genome during integration.

The third major gene product is Env, which forms the viral envelope. The *env* transcript is singly spliced and is translated to form an apoprotein of 88KDa. This is subsequently glycosylated in the endoplasmic reticulum (ER) to form the gp160 precursor glycoprotein. The gp160 precursor is cleaved in the Golgi apparatus by cellular proteases, to form gp120, the envelope (surface) glycoprotein and gp41, the transmembrane envelope glycoprotein. These remain associated in an oligomeric complex that is transported to the cell surface for incorporation into the virion. During HIV virion entry into a target cell, the gp120 surface glycoprotein binds the CD4 cell surface receptor, which serves as the primary receptor for the virus. Selective binding of gp120 to secondary chemokine receptors drives the cellular tropism of the virus, for a review of the current literature see section 1.1.5. gp41 serves as a transmembrane anchor to which gp120 glycoprotein is noncovalently attached (Wyatt et al., 1997), see diagram 1.1 below for a schematic representation of the HIV-1 genome.

Diagram 1.1. Genomic organisation of HIV-1, structural genes and the 5' and 3' LTRs are shaded, the auxilliary genes are represented by open boxes:



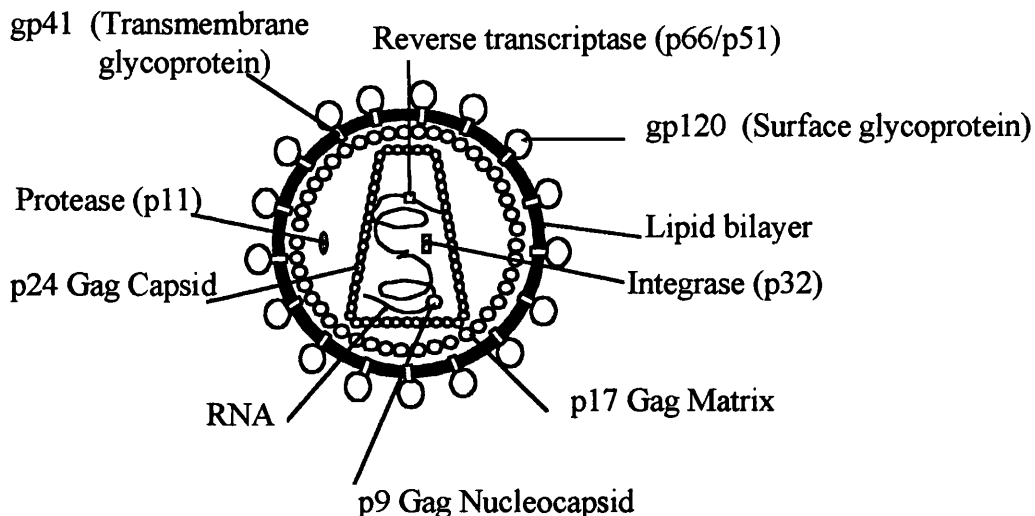
1.1.3. HIV virus structure:

HIV virion production occurs at the plasma membrane, via a self assembly process. The p55Gag and p160Gag-Pol precursors generate virus particles in association with gp120, gp41 and two copies of the viral (+) RNA genome. Particles bud from the membrane, incorporating host molecules incidentally (Cantin et al., 1997). Immature budding particles appear spherical by electron microscopy. Morphological changes occur within the particle, concurrent with budding, due to the cleavage of the p55Gag precursor by PR (Nakai and Goto, 1996). The viral particles are non-infectious prior to this maturation process. The mature virions are icosahedral in shape and approximately 110-122nm in diameter (Hockley et al., 1994; Nermut et al., 1994), see diagram 1.2 below. They are composed of an inner core surrounded by an outer lipid bilayer (envelope) formed from the cell membrane, in which characteristic spikes of envelope protein (70-80 in total), are anchored (Nakai and Goto, 1996). Each spike contains trimers (Weissenhorn *et al* 1997) of envelope glycoproteins. The MA Gag protein is a myristoylated protein and as such interacts with the hydrophobic phospholipids of the viral envelope. Mutations that block this modification completely inhibit viral assembly (Spearman et al., 1994; Morikawa et al., 1996). The MA protein of Gag is necessary for the incorporation of both gp120 and gp41 into the virion and a direct interaction between MA and HIV viral envelope, but not the viral envelope domains of other retroviruses, has recently been demonstrated (Lee et al., 1997).

The inner cone shaped, core of the virion is formed by an outer shell of Gag CA protein enclosing the dimeric RNA genome, in close association with the Gag NC protein and the viral enzymes RT, PR and IN. The NC proteins are very small, and rich in proline and basic amino acids, this in combination with two zinc finger domains gives them a high affinity for nucleic acid (Berthoux et al., 1997). The high concentration of NC in the inner core drives non-specific NC binding to the single stranded RNA genomes providing protection from nuclease attack. Further studies on NC have implicated a role for the zinc finger motifs in the specific recognition of the viral RNA genome in the cellular cytoplasm during encapsidation (Zhang and Barklis, 1997; Berkowitz and Goff, 1994; Berkowitz et al., 1995) and an

involvement of the basic amino acids in activating DNA strand transfers during reverse transcription to form the LTRs (Berthoux et al., 1997) reviewed (Darlix et al., 1995). Other auxiliary proteins also incorporated into the virion include - Nef, Vpr and Vpx although their exact location has not yet been determined.

Diagram 1.2. A schematic representation of virion assembly:



1.1.4. Auxiliary genes:

The auxiliary genes can be divided into early and late expressers. The early mRNA transcripts include the multiply spliced *tat* (*trans*-activator protein), *rev* (regulator of late gene expression) and *nef* (negative factor) transcripts. Late mRNA transcripts include for HIV-1, *vif* (viral infectivity factor), *vpr* (viral protein R), and *vpu* (viral protein U), see diagram 1.3. In HIV-2 and SIV the *vpu* gene is exchanged for *vpx* (viral protein X), with some exceptions involving variations of the inclusion of *vpr*, *vpu* and *vpx*. Tat and Rev have been implicated in the control of proviral expression and are both encoded by two separate exons flanking the *env* gene. Neither is incorporated into the virion, although both are essential for virion production. Tat is necessary for the elongation of the viral mRNA transcripts. A direct interaction of Tat with a distinct RNA *trans*-activating response region, termed TAR, located 40bp downstream from the transcription initiation site, has been widely demonstrated (Gait and Karn, 1993). However, recent studies have

suggested that Tat association with TAR is not directly responsible for the observed increase in RNA processivity. It has been shown using western blotting and cell-free transcription reactions (Keen et al., 1997), that the TAR element plays a role in recruiting RNA polymerase and cellular cofactors, but once transcription has been initiated, removal of TAR does not affect the Tat mediated elevated RNA synthesis. The function of Tat as a transactivator is not limited to viral transcription but also includes activation of cellular genes including, tumour necrosis factor (TNF), interleukin 6 (IL-6), CD4, IL-2, IL-2R α , IL-10, transforming growth factor- β 1 (TGF- β 1) and CD95 ligand. Since Tat is known to be released extracellularly and is successfully translocated to the nuclei of uninfected T-cells, it has been postulated that Tat facilitates the rapid loss of CD4 T-lymphocytes during progression to AIDS. A potential mechanism for this is via the sensitisation of uninfected cells to CD95 mediated apoptosis.

The second proviral regulatory protein Rev, also recognises a specific RNA element, the Rev-response element (RRE) (Gait and Karn, 1993), see diagram 1.3 below. Rev provides a mechanism whereby large unspliced viral, but not cellular mRNA, can be selectively translocated across the nuclear membrane to the cytoplasm (Dundr et al., 1996; Fischer et al., 1994; Fischer et al., 1995; Fritz and Green, 1996). In the absence of Rev the RRE which is located within the *env* gene mediates retention of transcripts in the nucleus. This results in transcript splicing and the production of the early mRNA transcripts including Rev. As Rev concentrations increase, hence RNA synthesis shifts to the production of viral late transcripts necessary for virion assembly. Investigation of the mechanism of Rev mediated nuclear export of RNA has led to the discovery of a nuclear export pathway, potentially conserved across all eukaryotic cells. It has emerged that the carboxyl terminus of Rev, the effector domain, acts as a nuclear export sequence (NES). This specifically targets the protein and the associated mRNA, to a putative exporting nuclear pore. It has been proposed that the NES-containing protein moves through the pore by sequential interactions with nucleoporins (Fritz et al., 1995). One hypothesis for the movement of the molecule through the pore, based on relative affinities of the NES for various nucleoporins, is that affinity for the

NES increases through the pore, being strongest on the cytoplasmic side (Fritz and Green, 1996).

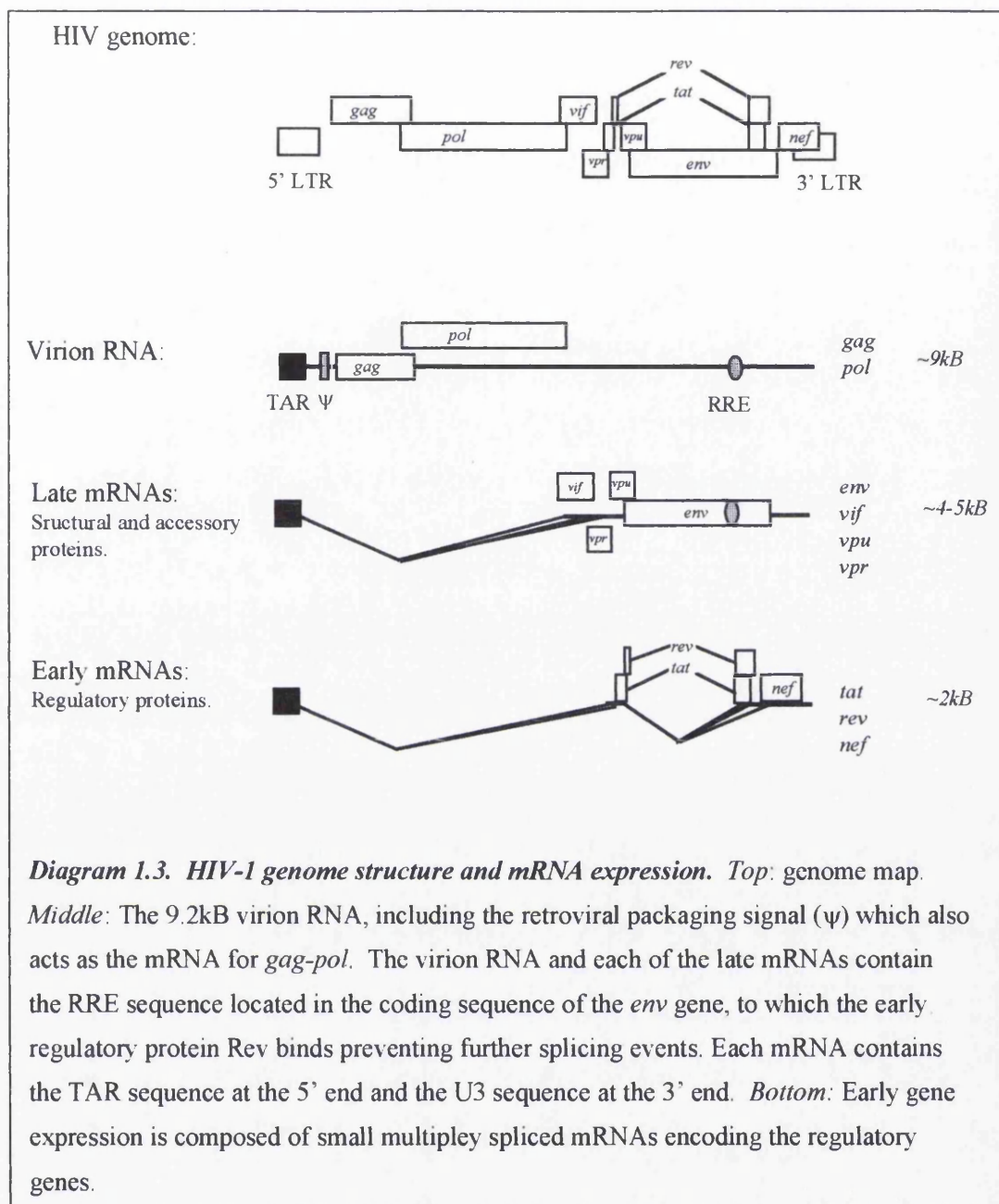
The third early transcript is *nef*, the characteristics of which will be discussed in depth in the following section, 1.2. This leaves the late transcripts, *vif*, *vpr*, *vpu* and *vpx* the expression of which is variable across different HIV-1, HIV-2 and SIV strains, but all are encoded by single exons. The strain specific and hence, to a large degree, species specific expression of *vpr*, *vpx* and *vpu*, argues a role for viral cell tropisms or virus-host interactions. Vif (Camaur and Trono, 1996), Vpr (Mahalingam et al., 1995) and Vpx (Wu et al., 1996) are all present in the virion. Similar to the Nef research effort, there has been much controversy surrounding the absolute requirement by the virus for these genes (Gibbs et al., 1995). However *in vivo*, where efficient viral replication, ability to infect quiescent cells and a diversity in cellular tropism are important in establishing persistent viraemia, it is likely that these auxiliary genes play a crucial role, in their respective hosts.

Vif is a highly basic, predominantly cytoplasmic, 23KDa protein. The primary function for Vif is believed to be during early viral infection, where it associates with the cellular cytoskeleton potentially aiding in the transport of the preintegration complex to the nucleus (Karczewski and Strebel, 1996). Other proposed functions for Vif include maintaining the stability of the viral nucleoprotein complex prior to integration of the provirus and aiding in viral assembly. In the absence of Vif a 1000 fold reduction in infectivity has been reported in some cell types.

Vpr is a 15KDa protein and also plays a role in targeting the preintegration complex to the nucleus although, like Vif it does not contain a conventional NLS motif. It is clear Vpr accumulates in the nucleus, but exactly how it mediates the translocation of the preintegration complex across the nuclear membrane is unknown. Competitive inhibition of the importin-dependent nuclear import pathway does not prevent Vpr nuclear entry, therefore the mechanism is independent from this classic NLS entry route (Stevenson, 1996; Silver, 1991). Expression of Vpr has also been shown to have a cytostatic affect, due to cell cycle arrest in the G₂ phase (Re et al.,

1995; Emerman, 1996). The observation that cells produce elevated levels of virus during G₂, suggests a role for Vpr in maximising virus production, before cells are destroyed by the hosts immune system - the half life of an infected T-cell being approximately 2 days (Perelson et al., 1996; Ho et al., 1995). Vpr and Vpx are both specifically packaged into the virion through association with the p55Gag precursor. They remain associated with p6 portion of Gag on viral entry in the preintegration complex. Vpx has regions of sequence homology with Vpr, hence it has been suggested they may be evolutionary duplicates of one another.

Vpu is a small 10KDa, hydrophobic protein. It associates with internal membranes of infected cells via a hydrophobic helix that serves as a membrane anchor. Proposed functions include the release of gp160 from complexes of CD4/gp160 that are retained in the ER. Vpu interacts with the cytoplasmic tail of CD4 causing its degradation (Willey et al., 1992; Lenburg and Landau, 1993; Chen et al., 1993; Willey et al., 1994; Buonocore et al., 1994) and the release of gp160 (Raja et al., 1994; Kimura et al., 1994; Fujita et al., 1997). A second recently proposed function for Vpu is an ability to form ion channels across the cellular membrane. The resultant increase in membrane permeability has been implicated in facilitating viral budding. One continuous theme emerging through the study of the auxiliary proteins is their pleiotropic nature. The apparent level of functional redundancy between proteins may reflect the different virus-host interactions required for infection across different cell types.



1.1.5. Viral cell tropism:

Early studies on CD4, the primary receptor for HIV, demonstrated that CD4 alone was not sufficient to confer susceptibility upon cells (Ashorn et al., 1990). It was shown that murine cells expressing human CD4 were capable of binding the HIV viral particles but the virus did not internalise, additional human factors were required for this process (Ashorn et al., 1990; Dragic et al., 1992; Dragic and Alizon, 1993). Determinants of HIV-1 cell tropism were mapped to a short region in the V3 loop of Env outside of the CD4 binding domain. Taken together this

implicated the existence of a further cellular receptors necessary for HIV cell tropism. Subsequently, the inability of murine NIH3T3-hCD4 cells to support HIV infection was exploited by the laboratory of Dr. E. Berger (Feng et al., 1996; Ashorn et al., 1993; Alkhatib et al., 1996). In these studies they transiently transfected NIH3T3-hCD4 cells expressing T7 RNA polymerase and cDNA library plasmid pools. The cells were then monitored for their ability to fuse with NIH3T3 cells, which expressed vaccinia encoded Env and contained the *E.coli lacZ* gene linked to the T7 promoter. *In situ* staining with X-Gal identified cell fusion events. This method allowed the identification of a gene which conferred susceptibility to HIV infection upon the CD4-hybrid cells (Feng et al., 1996). This gene encoded a chemokine receptor, a member of a family G-protein coupled receptors with 7 transmembrane spanning domains. They respond to chemokines which recruit leukocytes and lymphocytes to areas of inflammation. As predicted, the repertoire of HIV co-receptors has expanded as different cell types and HIV strains have been investigated (Bron et al., 1997; Sol et al., 1997; Alkhatib et al., 1997; Luo and Garcia, 1996) reviewed in (Unutmaz and Littman, 1997; Wilkinson, 1996; Broder and Collman, 1997; Berger, 1997). However, the two main receptor groups which correspond well to the main viral cell tropisms described, are the β -chemokine receptor, CC-chemokine receptor 5 (CCR5) (Deng et al., 1996; Alkhatib et al., 1996) and the α -chemokine receptor CXC-chemokine receptor 4 (CXCR4) (Feng et al., 1996). The names reflect their respective chemokine ligands, with the arrangement of the cysteines in a conserved motif either CXC or CC defining the subfamily groupings.

CCR5 is expressed primarily in peripheral blood mononuclear cells (PBMCs) and macrophages and has been identified as fundamental to the transmission of the virus (Deng et al., 1996; Alkhatib et al., 1996; Bieniasz et al., 1997). This correlates with tissue macrophages and dendritic cells being among those cell types exposed to the virus, and is consistent with the predominance of HIV macrophage-tropic strains (M-tropic strains) early in infection (Clark, 1996). Conversely, CXCR4 is expressed primarily in PBMCs and on some macrophages, but mainly in T-cells and immortalised cell lines. Hence it is primarily the co-receptor for T-lymphocyte

tropic (T-tropic strains) or dual tropic HIV strains (Feng et al., 1996; Bleul et al., 1997). The transition from predominating M-tropic to T-tropic HIV strains is concurrent with progression to AIDS and CXCR4 receptor usage. Previous studies had shown that exposure to HIV did not in every case lead to seroconversion. This lack of transmission has since been attributed to homozygous deletions in the CCR5 receptor, rendering it non-susceptible to HIV M-tropic infection (Dean et al., 1996). Similar resistance has been observed *in vitro* in the presence of the chemokine ligands for CCR5, such as RANTES (regulated-upon-activation, normal T expressed and secreted) and the macrophage inflammatory proteins (MIP) - α and - β , which are postulated to confer resistance via competitive inhibition of the receptor. Stromal-cell-derived factor (SDF-1), a chemokine ligand for CXCR4 behaves in the same way for T-tropic HIV strains (Bleul et al., 1996; Oberlin et al., 1996). Despite the undisputed requirement for chemokine receptors in HIV entry, relatively little is known as to their role in virus-cell fusion. One hypothesis is that binding of Env to CD4 and a chemokine receptor induces a conformational change in Env, exposing the N-terminal fusogenic region of gp41 in the process (Chang et al., 1997; Hill et al., 1997; Weissenhorn et al., 1996; Chen et al., 1995) promoting subsequent viral entry. Evidence for this mechanism is based on analogies to the influenza virus entry (Chen et al., 1995), in conjunction with the demonstration of a direct interaction between Env, CD4 and various chemokine receptors (Lee et al., 1997; Bieniasz et al., 1997; Hill et al., 1997).

1.1.6. Therapeutics:

The elucidation of the chemokine receptor family as a vital component in HIV infection has had important repercussions for the design of therapeutic agents. To date, the treatment of HIV has been limited to extending the lifespan of the patient, a complete cure has never been achieved. This destructive pathogenesis has been attributed to the plasticity of the viral genome caused by the highly error prone RT enzyme, which allows drug resistance strains to emerge rapidly. This has necessitated the administration of combination therapies which have been demonstrated to be more effective at suppressing HIV replication over longer periods of time (Larder, 1995). In addition, the nucleoside and non-nucleoside RT

inhibitors and the PR inhibitors currently available can have severe side effects on healthy bystander cells, resulting in complications such as, renal and hepatic dysfunctions. The discovery of the HIV co-receptors has provided a novel mechanism to selectively target HIV infected cells. Preliminary *in vitro* studies by two groups, (Mebatsion et al., 1997; Schnell et al., 1997), used engineered HIV cellular receptors expressed on the surface of modified viral vectors, as novel therapeutic agents. In the studies, both groups replaced the G-envelope protein of rhabdoviruses, either Rabies or Vesicular Stomatitis virus, with both CD4 and CXCR4 receptors. In order for these modified viral vectors infect cells in the absence of their G-envelope protein, both HIV gp120 and gp41 had to be present on the target cells, hence the selective targeting of only HIV infected cells. Mebatsion et al used replication incompetent viral vectors and were able to demonstrate a substantial reduction in HIV levels *in vitro*. In contrast, the viral vector designed by Schnell et al was capable of self-propagation and reduced HIV levels by 1000 fold. The latter vector was reported to remain viable for up to 30 days and was effective against further bursts of HIV infection that had initially escaped detection. Although these modified viral vectors clearly represent a unique mechanism by which to destroy HIV infected cells there are safety issues surrounding their use that will need to be resolved. An attractive alternative (Nolan, 1997) is that the co-receptors be incorporated into liposomes containing therapeutic agents able to chemically destroy HIV infected cells on fusion. The strategy of targeting HIV gp120 and gp41 proteins has the advantage over current therapies in that it has the potential to neutralise cell free virus. This is highly significant in the light of the rapid turnover of plasma virions identified by Ho et al and Perelson et al. In their work they emphasise the need to target HIV replication as opposed to stimulating the patients immune system. They cite the onset of AIDS as an indicator of the finite regenerative capacity of the immune system and suggest that viral levels increase as a direct result of the depletion of the host T4 lymphocyte population.

1.2. Nef:

1.2.1. Introduction:

The *nef* gene encodes one of the six HIV auxiliary proteins and is unique to the primate lentiviruses. The initial identification of antibodies to the Nef protein in the serum of HIV exposed individuals implied a functional role for Nef *in vivo* (Allan et al., 1985). However, early *in vitro* studies concluded that the *nef* gene was dispensable for viral replication and that its protein product imposed a negative regulatory effect on the rate of transcription from the viral LTR, hence the acronym *nef* (Yu and Felsted, 1992; Terwilliger et al., 1986; Ahmad and Venkatesan, 1988; Luciw et al., 1987). Subsequent research has attempted to clarify the viral requirement for Nef. *In vivo* data from macaque simian AIDS models established the existence of strong selective pressures for the conservation of *nef*, with engineered point mutations in the nucleotide sequence of *nef* rapidly reverting to wild type (Kestler et al., 1991; Sawai et al., 1996; Whatmore et al., 1995). The model also clearly illustrated, contrary to the described *in vitro* negative replicative effects of Nef, that *nef* incorporation into the viral genome was necessary for high viral loads and progression to simian AIDS. Despite the establishment of a crucial role for Nef in viral pathogenesis its mechanism of action still remains unclear, with no consensus on protein function yet agreed. Several studies have identified pleiotropic functions for the Nef protein, the most consistent of which include its ability to downmodulate CD4 expression from the cell surface, enhance viral infectivity and disrupt cell signalling pathways (reviewed (Harris, 1996; Trono, 1995)). However, the significance of these and other more infrequently reported multiple Nef phenotypes is still to be discovered. In this section, the current literature on Nef molecular biology, biochemistry and cellular interactions will be reviewed, with emphasis given to implications for the role of Nef in viral pathogenesis.

1.2.2. Gene structure of *nef*:

1.2.2.1. Physical features:

Alleles of *nef* are heterogeneous in length with the HIV-1 ORF being approximately 618bp (206 amino acids), extending to 750bp (250 amino acids) and 795bp (265

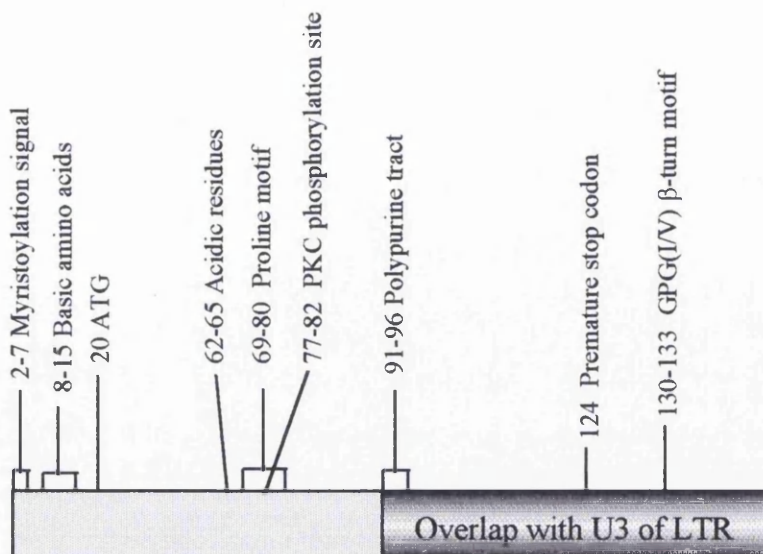
amino acids) for HIV-2 and SIV respectively (Allan et al., 1985; Harris et al., 1992; Shugars et al., 1993; Rud et al., 1994). The *nef* sequence is highly polymorphic between strains and even within isolates obtained from the same individual, sequence variation has been frequently reported. HIV-1 *nef* is located at the 3' end of the viral genome with ~56% of its C-terminal ORF overlapping the U3 region of the 3' LTR. U3 LTR sequences within the *nef* ORF include the polypurine tract and putative binding sites for the transcription factors chicken ovalbumin upstream promoter transcription factor (COUP-TF) (codons 125-140), activator protein (AP-1) (codons 133-135 and 138-139), nuclear factor 1 of activated T-cells (NFAT-1) (codons 151-163 and 176-180), upstream stimulatory factor (USF) (codons 190-195) and T-cell factor 1 alpha (TCF- α) (codons 202-206) (Shugars et al., 1993). The Nef protein is encoded by a number of variably spliced *nef*-specific mRNA transcripts, the significance of which is unknown since the *nef* ORF is totally contained on the 3' exon, one proposal is that these may constitute transitory species that occur during processing. These *nef*-specific transcripts form approximately 80% of all early transcribed mRNA, the remaining 20% comprising *tat* and *rev* specific transcripts, therefore inferring a substantial role for *nef* during early events in viral infection (Robert-Guroff et al., 1990).

Sequencing studies have been performed on several primary and laboratory *nef* isolates in order to ascertain conserved nucleotides potentially important for *nef* function (Shugars et al., 1993; Harris et al., 1992), a brief synopsis of which is given hereunder (summarised in diagram 1.4). Features identified at the N-terminus of *nef* have included (codon numbering as used Shugars *et al* 1993); an invariant N-terminal myristoylation signal (codons 2-7); a stretch of highly heterogenic nucleotides encoding predominantly hydrophobic and basic amino acids (codons 8-15); and a conserved ATG codon at position 20 which acts as an internal translation initiation site in HIV strains. To date, no second ATG has been found in the SIV strains analysed. Several studies have concurred that the highest degree of sequence homology between *nef* isolates is in the central region of the ORF. This region contains a putative recognition site for protein kinase C (PKC) phosphorylation RPMTYK (codons 77-82), located just upstream of a short run of acidic residues

(codons 62-65). Also, spanning the whole of the conserved region is a proline repeat motif (PXX)₃P (codons 69-80), which was thought to be significant because similar motifs form the recognition sites for SH3 domain containing proteins (Yu et al., 1994; Pawson, 1995), see sections 1.3, 4.1 and 5.1. Located immediately downstream from this amino acid motif is the polypurine tract (codons 91-96), containing 16 purine rich nucleotides, essential during viral replication for priming second strand synthesis during reverse transcription.

Towards the C-terminus of the *nef* ORF the only consistently conserved nucleotides identified, encoded a GPG(I/V) amino acid motif (codons 130-133) potentially important for structural constraints as the motif is indicative of a β -turn (Chou and Fasman, 1978; Shugars et al., 1993). In general, regions of least conserved sequence homology were located at the N- and C-termini of the ORF, with the exception of the myristoylation signal and a number of invariant codons. This was a surprising find since the 5 potential binding sites for cellular transcription factors together with an inverted repeat, necessary for cleavage and integration of the proviral DNA, were located at the C-terminus suggesting the existence of possible subtle sequence constraints at the RNA level in this region. The remaining feature potentially relevant to protein function was a clustering of premature stop codons in both laboratory and primary *nef* isolates, at codon 124. Functional motifs identified during these early characterisation studies of the *nef* gene have been consistently observed in most *nef* alleles since isolated (Huang et al., 1995; Huang et al., 1995; Du et al., 1995; Premkumar et al., 1996; Rousseau et al., 1997; Saksena et al., 1997; Dwyer et al., 1997).

Diagram 1.4. Summary of the *nef* gene structural features:



1.2.2.2. Significance of *nef* in vivo:

The importance of *nef* to viral replication *in vivo* was highlighted during macaque studies by Kestler *et al* 1991 and has subsequently been validated by a number of follow up macaque (Sawai *et al.*, 1996; Whatmore *et al.*, 1995) and SCID-hu mice (Aldrovandi and Zack, 1996) studies. Kestler *et al* initially demonstrated the rapid reversion of a stop codon (first detected at 2 weeks post-infection) at codon 93 in SIV_{mac239} *nef* to a coding codon, resulting in disease progression comparable to that caused by wildtype SIV_{mac239}. Significantly a 182bp deletion contained solely within the *nef* ORF led to a 100 fold reduction in viral burden in the rhesus macaques, with no disease symptoms. In further studies, these animals were found to be protected from subsequent challenge with wildtype SIV_{mac239} (Daniel *et al.*, 1992). The protection achieved using the deleted *nef* (Δnef) isolate provided the impetus for the use of attenuated HIV strains as potential vaccines (Gallimore *et al.*, 1995; Ruprecht *et al.*, 1996; StahlHennig *et al.*, 1996; Beer *et al.*, 1997). However, work by Baba *et al* 1995 using a Δnef , Δvpr SIV strain in neonatal macaques, suggested that the protection was saturable with higher viral doses still leading to disease. Despite this, a key role for *nef* in viral pathogenesis has been corroborated with the investigation of potentially functionally relevant point mutations (Sawai *et al.*, 1996) and short deletions (Whatmore *et al.*, 1995) in the *nef* ORF resulting in reversions

to the wild type *nef* sequence, thus confirming the replicative advantage to the virus of an intact *nef* gene.

Data obtained from human patients has also substantiated the requirement for *nef in vivo*. During the monitoring of the development of AIDS in human patients a small percentage (~5%) of HIV infected individuals, referred to as long term non-progressors, that had not developed AIDS were identified. These individuals were typically characterised as lacking clinical symptoms, immunologically normal with stable CD4 T-lymphocyte counts and had been infected for over 10 years. As a result of the outcome of the Δnef SIV studies the viral genomes of several distinct long term non-progressor cohorts were analysed for defects in their *nef* genes. Pertinently, sequence data from the Sydney Bloodbank cohort comprising 7 unrelated individuals infected from transfusions with the same contaminated blood, demonstrated a number of deletions in *nef* (Deacon et al., 1995). When the evolution of the mutations were mapped it emerged that the only deletions common to all the *nef* alleles were in their U3 overlap regions removing 46 codons, including a putative splice acceptor site located in this region of *nef* (splice acceptor 12) (Deacon et al., 1995). Other mutations potentially contributing to the attenuated viral phenotype included further variable deletions in the sequence unique to *nef*, plus duplication and rearrangement events in the untranslated U3 region. Subsequent work by Premkumar *et al* 1996 suggested that such gross mutations were not always required to abrogate *nef* function. The long term non-progressor in their study was found to harbour a point mutation at codon 138, the mutation of which had been previously linked to avirulent HIV and SIV strains (Dewhurst et al., 1992; Huang et al., 1995). Studies of viral infectivity in the human T-cell line, H9, demonstrated that a cysteine mutation at codon 138 disrupted viral infectivity. From this and results obtained in other long term non-progressor cohorts (Saksena et al., 1997; Rousseau et al., 1997) it has been proposed that subtle sequence variations in the *nef* gene can have important structural and hence functional implications. However, with notable exceptions in the long term progressor cohorts (Huang et al., 1995) it is likely the patient immunological subtype may also emphasize subtle mutant *nef* phenotypes.

1.2.3. The protein product of the *nef* gene:

1.2.3.1. Characteristics:

The size of the Nef protein, either 27kDa or 34kDa for HIV and SIV respectively, corresponds to the differences in size of their ORFs. Both are predominantly expressed as N-terminally myristoylated proteins, see below, although the existence of a minor species of HIV-1 Nef has also been reported (Nebreda et al., 1992; Kaminchik et al., 1994). This is produced due to the internal initiation of translation from a methionine at codon 20. Recently the presence of Nef as a virion protein was established and subsequently several studies demonstrated a further species of Nef which is present in the virion and is generated by specific cleavage by the viral PR, concomitant with viral packaging (Pandori et al., 1996; Welker et al., 1996; Bukovsky et al., 1997; Miller et al., 1997). The putative recognition site for this cleavage is between residues Trp57 and Leu58, yielding polypeptide products of 9kDa and 18kDa (Freund et al., 1994b). Incubation of Nef with PR *in vitro* has suggested that these cleavage products are stable and do not expose further protease recognition sites. However to date, only a 18-20kDa processed species of Nef has been detected in the virion, comprising approximately 50-95% (Pandori et al., 1996; Welker et al., 1996) of the total Nef protein. The whereabouts of the smaller N-terminal membrane targeted fragment of Nef is still to be ascertained.

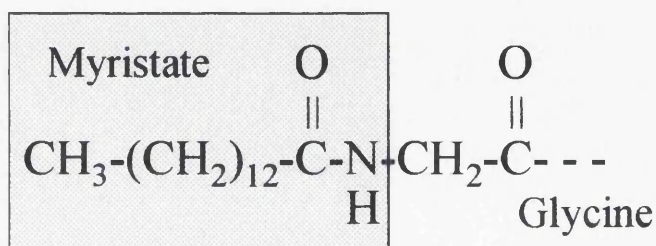
Biochemical analysis to determine whether Nef was capable of oligomerization was performed by Hodge et al 1995, who reported that the dimerization and to a lesser extent tetramerization of an HIV-2 allele of Nef occurred both *in vitro* and *in vivo*. They demonstrated the formation of oligomers was dependent on conserved leucine residues in a predicted α -helical region (residues 109-126) of Nef, in combination with putative intermolecular disulphide bond formation. Hodge *et al* also showed that the frequency of oligomerization *in vitro* was concomitant with increasing Nef concentrations, although in *in vivo* infected H9 T-cells, monomers, dimers and tetramers of Nef were all detectable. Interestingly, when the phosphorylation status of Nef was analysed it was found the only phosphorylated species of Nef was in the homodimers. This was not attributable to poor antibody epitope recognition during

the course of immunoprecipitation of the oligomers since it was reproducible with a variety of antibodies.

1.2.3.2. Myristoylation of Nef

As previously stated Nef is a myristoylated protein (Allan et al., 1985). Myristoylation is a cotranslational event driven by the presence of a specific myristoylation peptide signal at the N-terminus of a polypeptide (reviewed (Johnson et al., 1994; Bhatnagar and Gordon, 1998)). Proteins containing the motif are modified by the irreversible addition of a 14 carbon saturated fatty acid residue via amide bond formation with an N-terminal glycine residue, see diagram 1.5 below. The reaction is catalysed by the enzyme N-myristoyl transferase present only in the cytoplasm of eukaryotic cells. To date, structural studies on Nef have not taken into account the addition of this highly hydrophobic fatty acid residue at the N-terminus of Nef, the conformation of which is likely to influence the whole structure of the protein. Nuclear magnetic resonance (NMR) structural studies of Nef revealed that the N-terminal 39 residues of Nef together with an internal fragment between residues 159-173 were highly disordered (Freund et al., 1994a; Hadida et al., 1992). Similarly, in crystallography studies with Nef complexed to an R96I SH3 mutant of Fyn (Lee et al., 1996), an N-terminal truncation of 54 amino acids of Nef was required to obtain crystal diffraction of sufficient resolution for analysis (2.5Å). Pertinently, both studies used nonmyristoylated Nef for their initial analysis, it has hence been suggested (Harris, 1996) that structural order in these regions may be mediated by myristoylation.

Diagram 1.5. Myristate bound to the N-terminal glycine residue:



By analogies to other myristoylated proteins, it is possible that Nef may have a dynamic conformation, whereby the myristic acid residue is either sequestered into a hydrophobic pocket in the protein, or anchored into membrane phospholipid bilayers. In support of the former conformation, structural studies have identified a distinct accessible hydrophobic pocket on the surface of Nef, with crystallography analysis revealing 2 anti-parallel α -helices formed by residues 81-93 and 104-117 (Lee et al., 1996; Arold et al., 1997). Lining each helix are highly conserved hydrophobic residues which align to create the solvent accessible crevice. Structural studies have also located the N-terminus of Nef on the outside of the protein structure making it accessible to interactions with both its own surface and membrane structures. Similar hydrophobic pockets have been described for other myristoylated proteins e.g. Recoverin, a Ca^{2+} binding protein in photoreceptor cells, whose conformation alters by a Ca^{2+} -switch mechanism. Crystallography studies of recoverin identified a concave hydrophobic pocket consistent with a putative intramolecular interaction with its myristoyl group in the absence of Ca^{2+} (Flaherty et al., 1993; Ames et al., 1996; Ames et al., 1997). Also the resolution of cyclic AMP dependent kinase, crystallised with an intact myristoyl group, clearly demonstrated the ability of proteins to sequester their fatty acid attachment into a hydrophobic niche (Zheng et al., 1993). Available structural data for other myristoylated proteins with similar labile conformations including the Src non-receptor tyrosine kinase family, MARCKS the myristoylated alanine rich C kinase substrate and ARFS the myristoylated regulatory GTP binding proteins involved in vesicular transport, demonstrates the conservation of distinct surface hydrophobic pockets among these unrelated myristoylated proteins (more structural detail can be found at website <http://www.sdsc.edu/kinases/pk.home.html>).

The dynamic nature of the Nef structure is underscored by the abundant evidence for the latter, myristoyl membrane anchor conformation of Nef, in conjunction with a variety of emerging mechanisms for myristoylation acting as a key switch between different protein isoforms (reviewed (McLaughlin and Aderem, 1995)). Initial evidence for Nef membrane association came from cellular fractionation studies which revealed a Nef interaction with the membrane fraction that was abolished in

myristoylation defective Nef mutants (Kaminchik et al., 1994). Later it was demonstrated that myristoylation was also required for Nef virion association (Bukovsky et al., 1997). In viral genomes encoding a myristoylation defective Nef there was a profound reduction in the amount of Nef incorporated into the virion, resulting in a substantial attenuation of virion infectivity. Also, a direct interaction of Nef with CD4 was only demonstrable in the context of a myristoylated Nef in the presence of a membrane (Harris and Neil, 1994). Although these examples clearly corroborate a dependence on myristoylation for the membrane association of Nef the concept of it acting as a membrane anchor *per se* has been difficult to demonstrate. It is known that the addition of a myristic acid residue alone provides insufficient membrane affinity to hold a protein in position and that the membrane interactions of local amino acid sequences is crucial (Peitzsch and McLaughlin, 1993). Peptide study data has shown that the Nef N-terminal 26 amino acids facilitate the insertion of the myristic acid residue into the lipid bilayer, as the addition of a myristic acid residue to a peptide derived from internal Nef sequences did not disrupt liposome bilayers (Curtain et al., 1994; Curtain et al., 1997). Interestingly, a tyryptophan residue at position 5 was shown to be implemental in perturbing the phospholipid bilayer and when the peptide was added to a variety of cell cultures it was found to be cytotoxic to the cells (Curtain et al., 1997).

Work with other myristoylated proteins has identified a number of factors that are responsible for reversible membrane interactions including; specific protein-protein interactions with transmembrane proteins, e.g. p56Lck plus CD4 and CD8 (Veillette et al., 1988; Shaw et al., 1990); additional hydrophobic interactions provided by the palmitoylation of a nearby cysteine residue e.g. Src kinases, Guanine nucleotide binding protein (G-protein)-linked receptors and the α -subunits of heterotrimeric G-proteins; and electrostatic interactions between a cluster of basic amino acid residues within the protein and acidic phospholipids in the membrane bilayer e.g. MARCKS (Aderem, 1992; McLaughlin and Aderem, 1995). The latter, allows reversible membrane association by a process termed the "myristoyl-electrostatic-switch". This process is regulated by the phosphorylation of residues proximal to the stretch of basic residues within the protein.

Phosphorylation results in the repulsion of the protein from the phospholipids of the membrane and destabilization of the electrostatic interactions. Due to a concentration of basic residues between residues 7-22 of Nef with proximal Ser and Thr residues the possibility that Nef membrane association was regulated in this manner was examined. Previous work had shown Nef was phosphorylated *in vitro* by PKC and that phosphorylation levels were enhanced in recombinant vaccinia virus infected BHK21 cells on phorbol ester stimulation (Guy et al., 1987), this was corroborated by studies in our laboratory (Coates and Harris, 1995) and others (Bodeus et al., 1995; Luo et al., 1997). The extension of these studies to human Hela and Jurkat cells (Coates et al., 1997) revealed Nef phosphorylation of Ser residues and to a lesser extent Thr residues was inhibited by PKC specific inhibitors, but not inhibitors of mitogen activated protein kinase (MAPK) or cyclic AMP dependent kinase. Unexpectedly, after fractionation analysis phosphorylated Nef was found to be equally distributed between membrane and cytosolic pools. This implied Nef phosphorylation was either occurring at variable sites in the protein dependent on its subcellular localization or that other protein-protein interactions are responsible for its dynamic membrane association, since Nef is not palmitoylated.

1.2.3.3. Nef subcellular localization:

The intracellular distribution of Nef has been examined in numerous studies (Franchini et al., 1986; Yu and Felsted, 1992; Niederman et al., 1993; Kaminchik et al., 1994; Baur et al., 1994; Coates et al., 1997). The consensus from fractionation studies is that native Nef associates with primarily the membrane and cytosolic fractions of cells (Franchini et al., 1986; Yu and Felsted, 1992; Niederman et al., 1993; Kaminchik et al., 1994; Coates et al., 1997). There have been some reports of Nef interactions with the detergent insoluble cytoskeletal fractions, although this appears to vary among Nef isolates with some researchers seeing no association (Niederman et al., 1993; Kaminchik et al., 1994) (Harris personal communication). Where cytoskeletal association has been reported it was shown to be dependent on the (PXX)₃P repeat motif in Nef. In all cases myristoylation negative mutants of Nef were found exclusively in the cytosolic fractions. One isolated report using

immunofluorescence microscopy has also documented an abundance of the nonmyristoylated species of Nef present in the nucleus (Yu and Felsted, 1992), although others have not found this (Greenway et al., 1995). Limited evidence for extracellular Nef, has been provided by its ability to be secreted from stress induced yeast (Macreadie et al., 1995) and a study by Fujii *et al* 1993 which suggested Nef may be anchored extra-cellularly to the plasma membrane although there has been no confirmation of these initial studies. In general, due to the vast number of cell types and different Nef isolates used in Nef research it is accepted that while the occasional different cell type or Nef isolate may deviate, native Nef is predominantly distributed dynamically between the membrane and cytosol.

1.2.4. Nef mediated virion infectivity:

The Nef effect on viral infectivity has been dogged by uncertainty and conflicting results. Early studies on Nef utilised CD4 T-cell lines of malignant phenotypes or activated PBMC cultures, since the initial characterisation of HIV had shown propagation of the virus was dependent upon T-cell activation. It was in this background that Nef was originally demonstrated to have a negative affect on viral replication (Terwilliger et al., 1986; Luciw et al., 1987). Work with LTR reporter constructs concurred with Nef induced negative regulation on the rate of transcription (Ahmad and Venkatesan, 1988; Yu and Felsted, 1992). Evidence from subsequent reports controversially proposed no Nef effect (Hammes et al., 1989) or even a slight enhancement of viral replication by Nef (Kim et al., 1989; de Ronde et al., 1992). Further conflicting evidence came from the *in vivo* macaque data (see section 1.2.1.2), where the presence of *nef* was shown to increase viral load in the animals, hence inferring a positive role for Nef in viral replication. This contradictory data was rationalised by two studies (Miller et al., 1994; Spina et al., 1994) in which the *in vitro* tissue culture setting was adapted to more closely mimic that of an *in vivo* environment. By using quiescent CD4 lymphocyte and primary macrophage populations infected with different amounts of viral inoculum and activated at different times post-infection, Miller *et al* 1994 and Spina *et al* 1994 were able to show a positive viral replication effect for *nef*. In contrast, in the background of a continuous cell culture both groups reported no *nef* enhancement

of viral infectivity. Significantly, the *nef* mediated enhancement of infectivity was most prominent at low multiplicities of infection. This prompted speculation that *nef* inclusion was critical during early stages of infection, when maximal viral burst from infected quiescent cells is necessary for the virus to achieve a persistent infection. It was also proposed that in activated cells, cellular factors may mask the *nef* function possibly due to a redundancy in function between Nef and host proteins in this setting.

As well as the primary cell culture assay for the analysis of HIV replication kinetics, a single cycle assay in CEM cells was also developed (Chowers et al., 1994). The establishment of these reliable *in vitro* systems, facilitated the evaluation of the relative contributions of amino acid motifs in *nef* to the overall replication kinetics of the virus. Mutations that abolished myristoylation were shown to completely abrogate Nef induced enhancement of viral replication (Chowers et al., 1994; Goldsmith et al., 1995; Pandori et al., 1996). This suggested that myristoylation must either confer the protein conformation or subcellular location necessary for the Nef disruption of cell signalling cascades and the subsequent increase in virion production. Data concurring with the importance of the subcellular location of Nef was obtained by Baur *et al* 1994 in experiments using a CD8-Nef chimera, where Nef was substituted for the CD8 cytoplasmic sequences. Their results indicated that membrane associated CD8-Nef activated Jurkat T-cells. In contrast, cytoplasmic CD8-Nef appeared to inhibit the production of T-cell signalling markers. Further functionally critical amino acids identified in Nef for viral infectivity have included, a run of acidic residues (60-71) adjacent to the viral PR cleavage site (Iafrate et al., 1997) and the highly conserved (PXX)₃P repeat motif (residues 69-80) (Goldsmith et al., 1995; Saksela et al., 1995). As a consequence of the latter, Src homology 3 (SH3) domain containing proteins have been extensively investigated as potential interaction partners for Nef, due to their recognition of proline II helix motifs and their involvement in cellular activation pathways, discussed in more detail in section 1.3.

A number of studies have been undertaken to identify the mechanics of Nef stimulation of HIV replication. From these it is clear that Nef exerts its positive influence after viral entry into the target cell. It was demonstrated (Miller et al., 1995; Aiken and Trono, 1995) that a Δ Nef viral genome could be complemented *in trans* in the viral producer cells, but not in the target cells. This was explained by the observation of Nef inclusion in the virion. Furthermore, work by Miller *et al* 1997 has shown that by enhancing viral PR cleavage of Nef in the virion, an intact C-terminal core domain alone is insufficient to mediate the Nef phenotype. The mutations in Nef used to demonstrate this were all upstream of the PR cleavage site and hence were contained in the N-terminal fragment of Nef. It is therefore possible that either full length Nef is required for virion infectivity or that the N-terminal fragment plays a crucial role and the mutations in this region disrupted its function. A co-operative role for Nef with either the HIV envelope glycoproteins or cell surface CD4 during viral entry seems unlikely, as HIV-1 virions pseudotyped with the amphotropic murine leukaemia virus envelope glycoproteins show no disruption in their Nef mediated phenotype (Aiken and Trono, 1995). Nef enhancement of infectivity prior to viral genome integration was inferred by data from transfection studies where no differences in virion production was seen between wild type and Δ Nef genomes (Chowers et al., 1994). In addition, quantitative PCR analysis demonstrated that despite no detectable changes in both the viral RT activity and initial RNA levels in the presence of Nef, the rate of DNA synthesis was substantially increased (Aiken and Trono, 1995; Schwartz et al., 1995b). It has hence been suggested that Nef may act to stabilise the local environment of the preintegration complex, or even recruit cellular factors necessary for successful reverse transcription of the genome, such as cations or nucleotides. However, in view of the fact that no transcriptionally related cellular interaction partners have been described for Nef, the involvement of indirect interactions that could potentially stimulate their production seems more probable.

1.2.5. Nef disruption of cell signalling pathways:

1.2.5.1. Nef phenotype:

Accumulating evidence has suggested that Nef may also perturb cell signal transduction pathways, potentially contributing to the depletion of CD4⁺ lymphocytes and enhanced virion productivity during HIV infection. However, the reported alterations in intracellular signalling mediated by Nef, have not provided a clear indication of exactly how, when and where Nef affects these pathways. From *in vivo* Nef transgenic mice models (Skowronski et al., 1993b) it was evident that Nef expression, under the transcriptional control of a promoter derived from the δ subunit of the CD3-T-cell receptor (TCR) complex, selectively inhibited the production of thymic and peripheral T-cells. The CD4⁺ T-cell subset was identified as the most severely affected, although peripheral CD8⁺ T-cells in young animals were initially suppressed, but recovered as the animals matured. The intracellular mechanism for this observation was unknown but interestingly it was revealed that, despite decreased amounts of thymocytes, the activation status of these cells was elevated after specific stimulation with CD3 antibodies. Conversely, stimulation with phorbol ester and calcium ionophore, hence effectively bypassing the CD3-TCR complex, resulted in unaltered levels of cellular activation. Therefore, Nef was specifically enhancing CD3-TCR complex signalling without the subsequent T-cell differentiation and proliferation.

In vitro studies have analysed the levels of T-cell activation markers in T-cell lines after CD3-TCR stimulation and identified both decreased IL-2 and IL-2 receptor production and down-regulation of NF- κ B and AP1 transcription factors (Luria et al., 1991; Bandres and Ratner, 1994; Greenway et al., 1994; Greenway et al., 1995; Collette et al., 1996a; Collette et al., 1996b); thus implying that, contrary to the *in vivo* results, TCR distal events are inhibited by Nef expression in an *in vitro* setting. Consistent with this, a Nef block of early CD3-TCR complex proximal signalling was also evident as determined by the early activation antigen, CD69 (Iafraite et al., 1997). Early signalling events were unaffected by PMA or calcium ionophore stimulation. These two agents stimulate cells downstream from the CD3-TCR complex via protein kinase C activation or calcium dependent responses

respectively, it has therefore been postulated that the *in vitro* block to CD3-TCR signalling must occur either upstream of these pathways or to a putative parallel pathway. Explanations for the discrepancies between *in vivo* and *in vitro* data have been speculative, but are primarily based on the combinatorial effects of Nef. It has been postulated that the additional influence of the Nef perturbation of CD4 signalling pathways in the *in vivo* model could have a profound effect on the overall cellular activation. In addition, it has been demonstrated (Baur et al., 1994) that Nef expression targeted to the plasma membrane via a CD8-Nef chimera resulted in T-cell activation, in contrast cytoplasmic Nef expression inhibited activation. This raises the possibility that the high levels of Nef expressed in the *in vitro* systems meant increased levels of cytoplasmic Nef, concurring with the dominant inhibition of signalling pathways seen in these systems.

1.2.5.2. Nef putative interaction partners:

In order to identify how Nef was perturbing intracellular signalling, Nef interaction partners were investigated. Early work on Nef characterised it as a GTPase with autophosphorylation abilities that was phosphorylated on an N-terminal Thr 15 residue by protein kinase C (Guy et al., 1987). The catalytic activities initially associated with Nef have been refuted as a consequence of incomplete purification (Backer et al., 1991), but its phosphorylation albeit on variable Ser and Thr residues has been confirmed by a number of studies (Coates and Harris, 1995; Bodeus et al., 1995; Coates et al., 1997; Luo et al., 1997). In T-lymphocytes membrane bound Nef was found to be stably associated with a protein complex containing a cellular serine kinase (reviewed (Cullen, 1996)). The Nef complex contained two putative substrates of the kinase (62kDa and 72kDa) in T-cells, although in COS-7 and NIH3T3 cells only the smaller protein was detectable (Sawai et al., 1994; Sawai et al., 1995). Nef itself was not phosphorylated by the kinase. Nef mutations abolishing kinase binding included the Gly2 necessary for myristoylation, a double Arg motif (residues 137 and 138) and the (PXX)₃P motif (Wiskerchen and ChengMayer, 1996). All of these mutations were also demonstrated to abrogate Nef augmentation of viral replication and the first two prevented Nef down-modulation

of CD4. This has made it difficult to reconcile phenotypes solely attributable to the kinase association.

Data has subsequently shown that the Nef associated serine kinase was related to the p21-activated kinase (PAK) family of signal transduction molecules, which themselves are putative activators of the mitogen activated protein kinase (MAPK) family (Luo and Garcia, 1996; Nunn and Marsh, 1996). Activation factors of PAKs are small Ras-like GTP-binding proteins, Rac1 and Cdc42 normally linked to cell-surface receptors and involved in actin polymerization and endocytosis. It was demonstrated that dominant-negative mutants of Rac1 and Cdc42 blocked the activation of the PAK isozyme by Nef (Lu et al., 1996). A competitive inhibition was unlikely, because constitutively active Rac1 and Cdc42 mutants enhanced the Nef associated serine kinase activity, prompting speculation that Nef association with and activation of the serine kinase was via Rac1 and Cdc42. *In vivo* macaque studies using an SIV_{mac239} virus containing the double Arg mutation showed rapid reversion to wildtype implying a functional requirement for these residues (Sawai et al., 1996), whereas point mutations in the (PXX)₃P motif did not revert to wildtype (Lang et al., 1997). It has hence been proposed that the association of the PAK-like serine kinase is dispensable *in vivo* and that pleiotropic functions conferred by the double Arg mutation are of greater significance. The lack of reversion of the (PXX)₃P motif also had implications for SH3 mediated interactions, discussed in section 1.3 and section 6.3. A role for the Nef PAK-like kinase association has also been questioned by Luo *et al* 1996 and 1997, who have suggested it is Nef isolate dependent and is not sufficient for the enhancement of infectivity.

Initial investigations of the Nef associated kinase activity revealed two further kinases that specifically associated with the N-terminus of Nef (Baur et al., 1997). These have been identified as the non-receptor kinase p56^{Lck} (Lck) (discussed in more detail in section 1.3) and a serine kinase, distinct from the PAK-like kinase. The latter phosphorylated Nef and Lck *in vitro*. Deletion of a putative amphopathic helix at the N-terminus of Nef_{SF2} (Δ 16-22) which abrogated binding of the kinases *in vitro*, was shown to reduce Nef mediated enhancement of infectivity in primary

cell culture assays. However, successful incorporation of the mutant Nef into the virion was not demonstrated, therefore the decrease in infectivity may be attributable to the absence of Nef in the virion. A possible candidate for the N-terminal serine kinase is the theta isoform of protein kinase C (θ PKC). Recently a direct interaction between Nef and θ PKC has been demonstrated, which occurred independently of the substrate binding site (Smith et al., 1996). No data was presented regarding the phosphorylation status of Nef in these experiments. Notably, Nef expression in Jurkat T-cells was shown to decrease levels of cytosolic θ PKC without the concomitant increase of θ PKC in the particulate fraction. It was speculated that this may be due to a Nef mediated disruption of θ PKC binding to endogenous anchoring proteins or receptors for activated C-kinases (RACKs) rendering the activated kinase susceptible to proteolytic degradation. A Nef block or reduction of θ PKC activity would be consistent with the inhibition of CD3-TCR signalling pathways previously reported *in vitro*. An alternative suggestion is that the binding of Nef to cellular kinases is relatively non-specific and occurs purely to recruit kinases to the virion (Swingler et al., 1997). It is known that phosphorylation of the Gag MA protein on both Ser and Tyr residues is necessary during viral infection for nuclear targeting of the PIC (Bukrinskaya et al., 1996; Gallay et al., 1995b), therefore one of the functions of Nef may be to ensure successful packaging of suitable kinases into the virus particles.

1.2.6. Nef mediated CD4 down-modulation:

To date, cell surface down-modulation of the primary receptor of HIV and SIV, CD4 has been the only consistently reproducible function of Nef reported. It has been demonstrated to be cell type and Nef isolate independent (Abraham et al., 1991; Anderson et al., 1993; Garcia et al., 1993; Mariani and Skowronski, 1993; Foster et al., 1994), but is dependent on Nef myristoylation (Greenway et al., 1994). In addition, murine and simian CD4 molecules on the cell surface of murine T-cells (Garcia et al., 1993; Rhee and Marsh, 1994a), as well as murine CD4 of T-cells from transgenic mice were shown to be down-modulated by HIV-1 Nef expression (Brady et al., 1993; Skowronski et al., 1993a). The cytoplasmic domain of CD4 (38 amino acids) is sufficient for its down-modulation (Garcia et al., 1993;

Anderson et al., 1994), with a dileucine motif analogous to the endocytosis and lysosomal targeting signals found in CD3 γ and δ chains, identified as a crucial determinant (Aiken et al., 1994; Bandres et al., 1995; Grzesiek et al., 1996). Residues in Nef important for CD4 down-modulation cluster around the N- and C-terminal predicted flexible loops (residues 36-56 and 174-179) (Iafrate et al., 1997; Hua et al., 1997). Further mutational analysis of Nef has demonstrated that the down-modulation of CD4 is also independent of Nef mediated infectivity (Goldsmith et al., 1995; Saksela et al., 1995; Iafrate et al., 1997).

The mechanism for Nef accelerated CD4 down-modulation has been the subject of intense investigation. CD4 is a transmembrane glycoprotein of 55kDa and is normally anchored in the plasma membrane by association of its cytoplasmic tail with Lck (Veillette et al., 1988; Campbell, S. et al., 1995). The external domain of CD4 binds the non-polymorphic region of major histocompatibility complex class II (MHC II) and is recruited to the CD3-TCR receptor complex during TCR-MHCII antigen recognition where it acts as an enhancer of TCR signalling. Normally binding of CD4 to MHCII triggers PKC activation which phosphorylates serine residues in the CD4 cytoplasmic tail causing Lck dissociation and activation. Without the Lck membrane anchor CD4 is endocytosed and either directed to the lysosomes for degradation or recycled back to the cell surface (Veillette et al., 1989; Sleckman et al., 1992; Pelchen-Matthews et al., 1993). It was rapidly established that Nef expression did not disrupt the synthesis of CD4 mRNA or its transit through the endoplasmic reticulum and Golgi to the cell surface. However, it was noted that surface CD4 expression was inversely related to Nef expression suggesting Nef was inducing CD4 endocytosis. Mutation of the serine residues in the cytoplasmic tail of CD4 crucial for normal PKC mediated down-modulation were found to have no effect on Nef induced down-modulation of cell surface CD4, thus implying it was occurring via a novel mechanism (Garcia and Miller, 1991). Pulse-chase experiments revealed the half life of CD4 in cells expressing Nef was 4 fold lower than control cells, suggesting that Nef was promoting the degradation of CD4 (Rhee and Marsh, 1994b; Aiken et al., 1994). The introduction of lysomotropic agents, ammonium chloride and chloroquine inhibited CD4

degradation, confirming Nef was redirecting CD4 to lysosomes. This finding was corroborated by a number of groups (Rhee and Marsh, 1994a; Sanfridson et al., 1994). In addition, immunoelectron and immunofluorescence microscopy studies demonstrated the accumulation of CD4 in vesicles throughout the endosomal and lysosomal cellular compartments (Schwartz et al., 1995a; Sanfridson et al., 1997).

A direct interaction between Nef and the CD4 cytoplasmic domain has been demonstrated *in vitro* (Greenway et al., 1995; Grzesiek et al., 1996) and in the baculovirus (Harris and Neil, 1994) and yeast-two-hybrid expression systems (Rossi et al., 1996). In addition, evidence from overlapping HIV-1, HIV-2 and SIV CD4 target sites inferred a genetic conservation of CD4 recognition (Foster et al., 1994; Hua and Cullen, 1997). However it has been proposed that the association is likely to be transient as a stable interaction has not been demonstrated in mammalian cells and the K_D of a CD4 cytoplasmic pseudopeptide complexed with Nef was $\sim 1\text{mM}$ (Grzesiek et al., 1996). Conceivably, association of these two molecules could allow Nef to confer an altered mechanism of CD4 endocytosis. Pertinently, an elevation of Nef phosphorylation associated with PMA/PHA cellular stimulation has been demonstrated to correlate with enhanced CD4 down-modulation, suggesting Nef may mimic CD4 endocytosis signals (Luo et al., 1997). Furthermore, a series of recent studies have suggested a role for Nef as an adapter molecule between CD4 and the endocytic machinery (Mangasarian et al., 1997; Greenberg et al., 1997; Foti et al., 1997). The expression of Nef as a chimera with the green fluorescent protein in CD4 positive Jurkat T-cells was shown to co-localize with that of clathrin and the β -subunit of the AP-2 adapter protein complex at the plasma membrane (Greenberg et al., 1997). Clathrin is the primary component of hetero-oligomeric complexes which along with AP-2, forms coated pits at membrane invaginations (reviewed (Schmid, 1997)). It is involved in coated vesicle formation during endocytosis and the selective packaging of cargo and as a consequence the normal endocytosis of CD4. The expression of Nef was demonstrated by electron microscopy to specifically promote CD4 association with clathrin coated pits, since control experiments showed the rate of internalization of the transferrin receptor was unaltered (Foti et al., 1997). Nef expression in CD4 positive cells also increased the

percentage of cell surface area occupied by clathrin-coated structures. These Nef effects were shown to be dependent on the dileucine motif in the CD4 cytoplasmic tail. Nef in the context of a CD4-Nef chimera was also demonstrated to promote clathrin coated pit formation, hence it was suggested that Nef itself was a catalyst for pit formation (Foti et al., 1997). This has implications for the Nef mediated endocytosis of other cellular responses, however awaits confirmation in the context of native Nef. While these results are suggestive of a direct interaction between Nef, CD4 and components of the endocytic machinery, to date none has been demonstrated and a role for Nef as a connector molecule remains interesting but speculative.

1.2.7. The role of Nef in HIV immune evasion:

Recently it has been demonstrated that Nef expression increased the endocytosis rate of MHC-I molecules from the cell surface in a range of HIV-1 infected cells (Schwartz et al., 1996). Perturbation of MHCI presentation is a common strategy of immune evasion employed by many viruses e.g. adenovirus, human and murine cytomegaloviruses, herpes simplex viruses and poxviruses, and allows virus infected cells to avoid detection and destruction by cytotoxic T-lymphocyte (CTL) (reviewed (Oldstone, 1997)). It had been previously shown during vaccination studies that high levels of Nef specific CTLs (Gallimore et al., 1995) correlated with a reduced viral load in macaques. However, evidence that Nef expression conferred CTL resistance concomitantly with reduced cell surface MHCI epitope density was shown in cell culture by Collins *et al* 1998. While Δ Nef viruses were susceptible to CTL destruction, further work is necessary to confirm MHC-I down-modulation is the mechanism of CTL evasion. Another putative mechanism of CTL escape was proposed by Xu *et al* 1997. In their study they demonstrated CTL protection correlated with Nef induced increased FasL receptor expression on the surface of infected cells. FasL plays a crucial role in the apoptosis of lymphocytes and its expression is normally restricted to activated lymphocytes. FasL intercellular recognition of its counter ligand Fas, also a cell surface receptor, triggers apoptosis in the latter target cells. Research has revealed that during the pathogenesis of HIV there is a progressive loss of uninfected, both CD4⁺ and CD8⁺ T-cells. The Nef

enhancement of FasL expression on infected lymphocytes provides a mechanism by which this could occur. Levels of FasL expression are intrinsically linked to T-cell activation therefore Nef interaction with signal transducers such as those previously described in section 1.2. or the Src tyrosine kinases (section 1.3) could be instrumental in mediating enhanced FasL expression.

1.2.8. Miscellaneous:

With research currently being directed towards Nef cellular interaction partners there have also been a number of isolated associations identified for Nef. Briefly these include putative interactions with; β -COP a non-clathrin vesicle protein having possible relevance to Nef mediated endocytosis (Benichou et al., 1994); HsN3 a proteasomal subunit involved in nonlysosomal breakdown of misfolded proteins in eukaryotic cells e.g. MHC-I viral peptides (Rossi et al., 1997); p53 the anti-oncogene involved in apoptotic signalling pathways (Greenway et al., 1995); and a novel acyl Co-A thioesterase, inferring a possible role in the alteration of cellular fatty acid regulation (Watanabe et al., 1997). Nef has also been reported to bind RNA in cell free systems, having possible implications for the observed elevated levels of proviral DNA synthesis in the presence of Nef (Schwartz et al., 1995b). Despite an array of interaction partners it is clear Nef is having cellular effects that may not be mutually exclusive. It is likely that the key to the pleiotropic functions of Nef lies in its modulation of cell signalling pathways, conceivably simultaneously resulting in the down-regulation of specific cell surface molecules and enhancement of virion infectivity. The following section presents evidence for a Nef interaction with members of the family of Src tyrosine kinases which are highly conserved signal transducers and represent a putative Nef target.

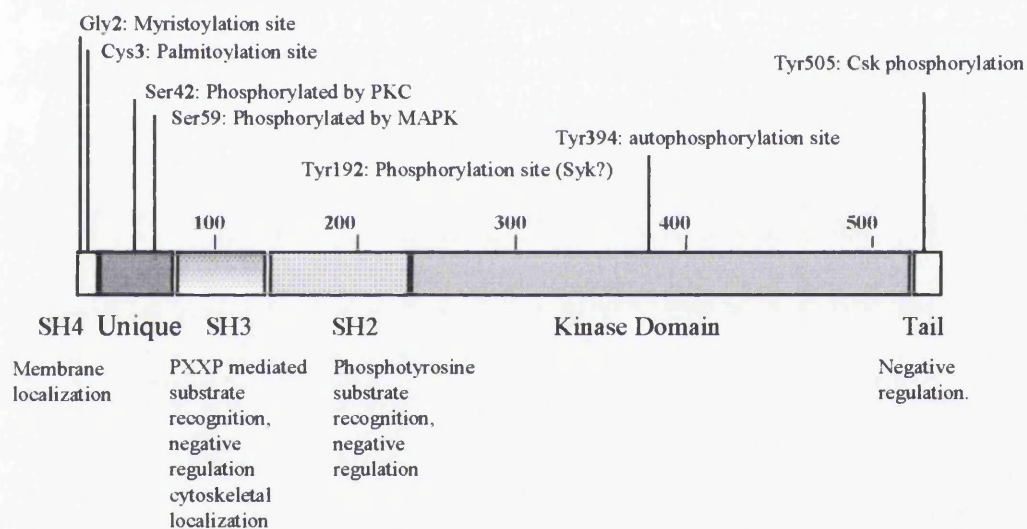
1.3. Nef and the Src tyrosine kinases:

1.3.1. Introduction to the Src tyrosine kinases:

The Src tyrosine kinases are a highly conserved family that regulate cellular responses to extracellular signals via their non-covalent association with transmembrane receptors (reviewed (Brown and Cooper, 1996; Mayer, 1997)). There have been 9 family members identified to date, including Src, Fyn, Yes, Fgr, Lyn, Hck, Lck, Blk and Yrk. At least one family member is expressed in all higher animal cell types examined, with the highest number identified in cells of haematopoietic origin. Family members are characterised by their unique mechanism for regulating their kinase activity and their distinctive domain structuring (see diagram 1.6.). Each comprises (from N- to C-terminus): i) A short amino-terminal sequence, containing a Gly2 residue necessary for myristoylation and membrane association. With the exception of Src and Blk all these proteins are reversibly palmitoylated on cysteine residues (normally positions 3 or 6). Palmitoylation has been directly implicated in the association of these proteins with glycosyl-phosphatidylinositol (GPI) linked proteins and plasma membrane microinvaginations called caveolae (see section 4.1) e.g. Lck, Fyn, Fyr, Lyn (Shenoyscaria et al., 1994; Stenberg et al., 1997), Hck (Robbins et al., 1995). ii) A unique domain, which is the only heterogeneous region between family members, varying in sequence and size (from 40 to 50 amino acids in Lyn, Hck, Lck and Blk extending to ~70 amino acids in Src, Yes, Fyn, Yrk and Fgr). The unique domain is responsible for mediating the differing protein interactions, subcellular localisations and kinase regulation of each member. iii) A Src homology 3 (SH3) domain (50-60 residues), which recognises left-handed poly-proline type II helices (see diagram 1.7.), similar domains are also found in cytoskeletal components (Yu et al., 1994; Alexandropoulos et al., 1995; Pawson, 1995). iv) A Src homology 2 (SH2) domain (~100 residues) which specifically binds phospho-tyrosine containing proteins (Songyang, 1993; Songyang and Cantley, 1995; Pawson, 1995). The SH3 and SH2 domains are non-catalytic modular domains common amongst cell signalling proteins and act as intermolecular adapters regulating enzyme-substrate recognition, enzyme activity and subcellular localization (Pawson, 1995). The specificity of the domains is conferred by localized amino acid sequence of their respective

recognition motifs (Songyang and Cantley, 1995). v) A catalytic tyrosine kinase domain (~250 residues), capable of *trans* and auto-phosphorylation, important for the transmission of external stimuli. vi) A short carboxy-terminal tail, consisting of a site for Csk tyrosine phosphorylation involved in the negative regulation of the catalytic domain. Intermolecular binding of the phosphorylated tail to the SH2 domain provides one mechanism of occluding the kinase active site from potential substrates (Amrein et al., 1993; Cooper and Howell, 1993).

Diagram 1.6. Schematic diagram of Lck to show sequence and post-translational features. Specific Lck posttranslational modifications are shown above the sequence along with the enzymes responsible. The characterisation of domains common to all Src family members is labelled below.



Currently, there have been three mechanisms of control proposed for the regulation of Src tyrosine kinase activity. The first and most established mechanism is provided by the reversible phosphorylation of the C-terminal tail (Cooper and Howell, 1993; Brown and Cooper, 1996). A paradigm for this is Lck, whereby negative regulation occurs due to Csk phosphorylation of the carboxy-Tyr505, as alluded to above. In this model the kinase is reactivated on dephosphorylation of Tyr505 by the transmembrane phosphatase CD45, hence disturbing the intramolecular association with the SH2 domain. However, mutagenesis and structural studies have revealed that dephosphorylation is not sufficient to fully activate the kinase and further

autophosphorylation of Tyr394 in the activation loop of the active site is necessary for high levels of kinase activity (Johnson et al., 1996; Yamaguchi and Hendrickson, 1996). The second model proposed as a result of recent crystallography studies (reviewed (Mayer, 1997)) (Brown and Cooper, 1996; Xu et al., 1997), shows the same intramolecular SH2 binding being activated not by CD45 but by a ligand to the SH3 domain: SH3 was shown to form intramolecular associations with a poly-proline type II helix formed by the linker region between the SH2 and kinase domain (Sicheri et al., 1997). Activation of the kinase has therefore been proposed to result from SH3 domain displacement, leading to an overall destabilization of the inactive structure and release of constraints on the kinase active site (Moarefi et al., 1997). This would allow autophosphorylation of the activation loop and subsequent upregulation of kinase activity. Interestingly, this study was performed using an N-terminally truncated Hck Δ 1-77, effectively removing myristoylation, palmitoylation and the unique targeting signals. The significance of this is discussed in chapter 5, since the ligand used in the study was Nef. There is also evidence from other members of the Src family of SH2 ligand mediated kinase activation e.g. Src and Fyn exhibit SH2 phospho-tyrosine dependent binding to pTyr residues in the PDGF and CSF1 growth factor receptors which has been reported to elevate the Src kinases catalytic activity (reviewed (Brown and Cooper, 1996)). In support of this activation mechanism, SH3 and SH2 domains have a higher affinity for their respective cellular ligands than their intramolecular binding motifs. This allows a specific ligand to compete for its domain and disrupt intramolecular associations. This model relies on the principle that neither the SH3 or SH2 domain intramolecular interaction alone is sufficient to maintain the inactive kinase conformation (reviewed (Mayer, 1997)).

The third putative control mechanism for Src kinase activity implicates structural changes that are independent of carboxy-terminal phosphorylation events (Nakashima et al., 1994; Pu et al., 1996). Pu *et al* 1996 demonstrated that low concentrations of mercuric ions (Hg^{2+}), which specifically bind sulfhydryl groups in proteins, caused a rapid elevation of Src kinase activity. Hg^{2+} can mimic cellular disulfide isomerase and cause the formation of a modified disulfide bond

(R-S-Hg-S-R) between 2 adjacent sulfhydryl groups (R-S). This activation was independent of C-terminal phosphorylation because cyanogen bromide cleavage of Src showed no reduction in phosphorylation of this residue, after Hg^{2+} treatment. These results were consistent with the observation of elevated Src tyrosine kinase activity in cells under oxidative stress. Oxidative stress can result from cellular exposure to agents such as oxidants (H_2O_2), ultraviolet radiation or heavy metal ions and leads to the production of oxygen radicals. These in turn promote disulfide bond formation among adjacent sulfhydryl groups catalysed by protein disulfide isomerase. Further data corroborating the importance of cysteine residues for Src kinase activity was obtained during mutagenesis studies of Lck by Veillette *et al* 1993. They demonstrated that mutation of either Cys 464 or 475 completely abolished all catalytic activity of Lck.

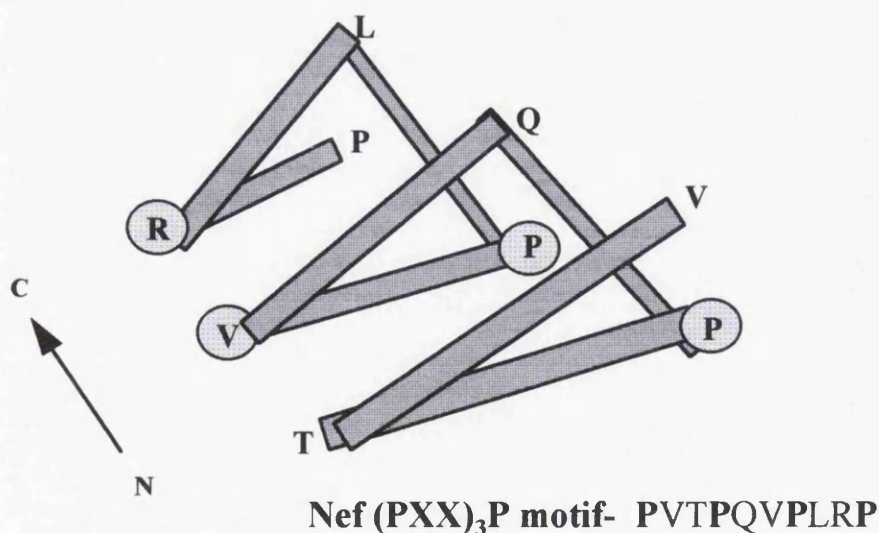
1.3.2. Evidence for Nef interactions with Src tyrosine kinases:

In order to gain an insight into the conflicting data obtained for the Nef mediated disruption of cell signalling cascades many groups investigated potential Nef interaction partners. The elucidation of the poly-proline type II helix as the consensus binding motif for SH3 domains, made Nef a suitable substrate/binding partner for SH3 containing proteins. Interactions with the family of cytoplasmic Src tyrosine kinases were examined since they are myristoylated, membrane associated proteins and importantly are intrinsically involved in the cellular activation pathways of haematopoietic cells.

Early work using filter binding assays (Saksela *et al.*, 1995), confirmed the $(\text{PXX})_3\text{P}$ motif mediated binding of Nef peptides to Hck and Lyn SH3 domains but not Lck and Fyn. However, when GST-Nef expressed in *E.coli* was bound to the SH3 domains it was found that only Hck SH3 retained its ability to bind Nef. Also in this assay, a second less conserved proline motif (residues 147-150) towards the C-terminus of Nef was necessary for binding in the context of full length nonmyristoylated Nef. Comparison of the growth kinetics of Nef⁺ viruses demonstrated that mutations in the conserved $(\text{PXX})_3\text{P}$ motif abolished Nef enhancement of virus replication. No affect on CD4 down-modulation was detected

(Saksela et al., 1995). Measurement of the affinities of these Nef-SH3 interactions revealed that full length Nef bound to Hck SH3 with a K_D of 250nM, the highest reported affinity for an SH3 interaction (Lee et al., 1995). However binding of a $(PXX)_3P$ peptide exhibited a reduced affinity ($K_D=91\mu M$) suggesting that other protein-protein interactions were important in stabilizing the association. Interestingly, in these latter studies using a soluble system, mutations in the C-terminal proline motif had no effect on Nef binding. Furthermore, a single R96I mutation in the Fyn SH3 domain was able to confer binding to the full length Nef with similar affinity to Hck SH3. It was concluded that residues in the "RT loop" of SH3 domains were crucial for specificity, and that the Nef association was dependent on hydrophobic interactions with the isoleucine residue in the RT loop. This high binding affinity of Nef as a ligand for Hck SH3 domains was exploited during a study on the mechanisms of activation of Src kinases (see sections 1.3.1. and 1.5.) (Moarefi et al., 1997). See diagram 1.7 below, for the orientation of Nef residues from the $(PXX)_3P$ motif in the PP-II helix.

Diagram 1.7. A schematic representation of the Nef polyproline type II helix, the circled residues form the SH3 binding surface, as detailed Arold et al 1997 the arrow indicates the direction from the amino to the carboxy terminus:



Hck is exclusively expressed in myeloid cells and although these cells have been implicated in maintaining a reservoir of HIV infection during disease pathogenesis

Hck is exclusively expressed in myeloid cells and although these cells have been implicated in maintaining a reservoir of HIV infection during disease pathogenesis Nef interactions with Hck did not explain the depletion of CD4⁺ lymphocytes. As Lck is expressed in T-cell lineages and moreover acts as a CD4 anchor it represented a putative Nef target in T-cells. Data from the Nef induced CD4 down-modulation studies revealed no consensus as to the effect of Nef on Lck. There were some reports that Lck dissociation from CD4 was accelerated in the presence of Nef (Anderson et al., 1994; Rhee and Marsh, 1994b) and indeed that its presence conferred enhanced Nef down-modulation of CD4 (Bandres et al., 1995). These results also raised the question as to the effect of the increased cytosolic levels of Lck, after Nef mediated CD4 down-modulation (Anderson et al., 1994). A number of groups have now demonstrated a direct interaction between Nef and Lck. The first of these (Greenway et al., 1995), used GST-Nef as an affinity reagent for *in vitro* binding studies with MT-2 cell and PBMC lysates. They determined that the interaction was dependent on the N-terminal region of Nef, since the use of GST-Nef25 (where the ORF started at the internal methionine, position 20) significantly reduced Lck binding. Furthermore, during normal cellular activation Lck is phosphorylated on serine residues within its unique domain, but in the presence of Nef this phosphorylation was inhibited. This inferred Nef was either blocking or inhibiting the Ser/Thr kinases PKC and MAPK. Preliminary data has suggested that Nef may be capable of direct interactions with both these kinases (Greenway et al., 1996; Smith et al., 1996). Subsequent studies using Nef peptides demonstrated a requirement for the (PXX)₃P motif in Nef for Lck SH3 and MAPK bindings. A Nef induced inhibition of both catalytic activities was also evident (Greenway et al., 1996). These results were corroborated by Collette *et al* 1996 who demonstrated a synergistic mode of action for Lck SH3 and SH2 domains in binding Nef and confirmed a Nef inhibition of Lck *trans* and auto- phosphorylation activities in CD4⁺ T-cells. Consistent with these reports, the N-terminus of Nef has recently been implicated in binding not only Lck, but also an unidentified serine kinase (Baur et al., 1997).

Final evidence in support of Nef interactions with members of the Src tyrosine kinase family comes from the investigation of a highly pathogenic strain of SIV, SIV_{pbj14}. This strain causes an acute illness in macaques and death within 10 days (Fultz et al., 1989). Unusually it is able to replicate in unstimulated PBMCs, apparently due to an inherent ability to activate the cells (Fultz, 1991). Genetic analysis revealed a double point mutation of RQ to YE (at positions 17 and 18) in the Nef ORF was sufficient to confer the phenotype to SIV_{mac239} (Du et al., 1995). This mutation resulted in the formation of a consensus sequence between residues 10-43 in SIV Nef for recognition by SH2 binding domains. Consistent with this Nef_{YE} was shown to bind Src in cotransfected COS cells, tyrosine phosphorylation of both Src and Nef_{YE} was also demonstrated. The wildtype SIV_{mac239} Nef bound Src and was tyrosine phosphorylated but to a lesser degree. It has been speculated that as Nef functions to enhance infectivity *in vivo*, the aggressive pathogenesis observed as a result of Nef_{YE} incorporation maybe due to an exaggeration of normal cell function.

1.4. Aims of the thesis:

The aims of these studies were two fold. Firstly, to identify novel Nef cellular interactions in order to aid in the characterisation of its pleiotropic phenotypes (chapter 3). Secondly, to further define the Nef interactions with members of the Src tyrosine kinase family (chapters 4 and 5).

To analyse novel cellular interactions the yeast-two-hybrid system was utilised which allowed library screening of protein-protein interactions. The system was modified to accept Nef as an N-terminal fusion, facilitating the screening of interactors in the context of a myristoylated Nef. Any potential Nef interaction partners isolated were sequenced and evaluated for the specificity of their interactions with Nef. The characterisation of Nef interactions with the Src tyrosine kinases fell into two categories. Initially Nef interactions with the T-cell specific Src kinase, Lck were examined using reagents available within the laboratory. The studies mainly addressed protein conformations necessary for the Nef-Lck

interaction, *in vitro* and *in vivo*. For this and subsequent studies using Hck, Src and Fyn the baculovirus expression system was used. This system had the advantage of allowing authentic posttranslational modifications of the proteins such as myristoylation, palmitoylation and phosphorylation potentially crucial to intermolecular interactions, whilst expressing the proteins to sufficiently high levels for alterations in protein-protein interactions to be detected. The latter was an important consideration because toxicity of both Nef and Src kinase proteins had been previously reported, therefore it might be anticipated that their coexpression would be unviable. Work with Hck was undertaken to confirm an interaction with Nef was possible in the context of the full length native proteins. Src and Fyn were included primarily as controls to verify the specificity of Nef interactions in this system. Determinants for Nef interactions with Hck were further evaluated, including the (PXX)₃P motif, in conjunction with assessments of the Nef affect on full length Hck activity. In addition the yeast-two-hybrid-system (YTHS) was employed to evaluate myristoylated Nef interactions with the isolated Src homology domains, SH3, SH2 and SH3-SH2 for each of Hck, Src and Fyn.

CHAPTER 2

CHAPTER 2 - MATERIALS AND METHODS.

	Page Number
2.0. General chemicals and enzymes	65
2.1. Molecular biology techniques- Materials	67
2.2. Molecular biology techniques- Experimental methods	70
2.3. Yeast protocols- Materials	77
2.4. Yeast protocols- Experimental methods	82
2.5. Baculovirus protocols- Materials	94
2.6. Baculovirus protocols- Experimental methods	98
2.7. Protein biochemistry- Materials	107
2.8. Protein biochemistry- Experimental methods	108

CHAPTER 2. Materials and methods:

2.0. General chemicals and enzymes:

Chemicals were obtained from the SIGMA chemical company, BDH chemicals, Boehringer Mannheim, Pharmacia or Life Technologies except where otherwise stated. All chemicals were of Analar quality. Enzymes, unless otherwise stated, were supplied by Life Technologies along with appropriate buffers. Chemicals common to each section are detailed below with their abbreviations while more specialised chemicals are detailed in their relevant section.

Table 2.1. General use chemicals and enzymes in alphabetical order, purchased from either BDH or SIGMA, including abbreviations (continued over page):

Purchased from:	
BDH, Poole, Dorset, UK	SIGMA, Poole, Dorset, UK.
2-mercaptoethanol	Ammonium hydroxide
Butanol	Ammonium persulphate (APS)
Caesium chloride (CsCl)	Ampicillin (Amp)
D (+) Glucose (Glu)	Aprotinin
Di-sodium-hydrogen-phosphate ($\text{Na}_2\text{HPO}_4 \cdot 7\text{H}_2\text{O}$)	Di-methyl-sulphoxide (DMSO)
Ethanol (EtOH)	Dithiothreitol (DTT)
Ethidium bromide (EtBr)	Ethylenediaminetetra acetic acid (EDTA)
Glacial acetic acid	Leupeptin
Glycerol	Lysozyme
N,N,N',N', Tetra-methyl-ethylene- diamine (TEMED)	
Polyethylene glycol MW4000 (PEG4000)	PepstatinA
Potassium acetate (KAc)	Magnesium chloride, $\text{MgCl}_2 \cdot 6\text{H}_2\text{O}$ (MgCl_2)

BDH, Poole, Dorset, UK.	SIGMA, Poole, Dorset, UK.
Potassium chloride (KCl)	Magnesium sulphate, $MgSO_4 \cdot 7H_2O$ ($MgSO_4$)
Sodium acetate (NaAc)	
Sodium azide	
Sodium azide	
Sodium chloride (NaCl)	
Sodium dodecyl sulphate (SDS)	
Sodium hydroxide pellets (NaOH)	TRIZMA® Base (Tris)
Sodium-dihydrogen-phosphate (NaH_2PO_4)	
Sucrose	
TritonX-100	

Table 2.2. Further general use chemicals and enzymes in alphabetical order, including companies purchased from and abbreviations:

Chemical/enzyme:	Company:
4- (2-aminoethyl) benzene-sulphonyl-fluoride -HCl (AEBSF)	Calbiochem-Novabiochem Corp.
Dimethyl formamide (DMF)	Rathburn Chemicals Ltd, Scotland
Electrophoresis grade agarose	Life Technologies Inc.
RNase A	Pharmacia
5-bromo-4-chloro-3-indolyl- β -galactosidase (X-Gal)	Melford Labs. Ltd, Ipswich, UK

MOLECULAR BIOLOGY TECHNIQUES:

2.1. Molecular biology techniques- Materials:

2.1.1. Chemicals and enzymes:

All detailed in general use chemicals, section 2.0.

2.1.2. Radiochemicals:

Redivue™ [$\alpha^{35}\text{S}$] dATP, specific activity, 1000Ci/mmol, used for manual sequencing, was purchased from Amersham Life Science, UK.

2.1.3. Bacterial strain:

E. coli DH5 α : F⁻, ϕ 80dlacZ Δ M15, *endA1*, *recA1*, *hsdR17*, (*r_K*⁻, *m_K*⁺), *supE44*, *thi-1*, *deoR*, *gyrA96*, *relA1*, (Δ *lacZYA-argF*), U169, λ ⁻. Purchased as competent cells from Life Technologies Inc.

2.1.4. Cloning vectors:

pCR™: *lacZ*⁺, *ampR*⁺, *kanR*⁺, plasmid designed for the specific cloning of PCR products, by making use of the non-template dependent addition of a single deoxyadenosine to the 3'-ends of duplex DNA molecules catalysed by *Taq* polymerase (Invitrogen).

PBluescript®II KS+/-: *lacZ*⁺, *ampR*⁺, T3 and T7 promoters flanking the polylinker, used for *in vitro* transcription-translation assays (Stratagene).

pGEX-4T-1: *ampR*⁺, pBR322-derived plasmid which carries part of the *Schistosoma mansoni* glutathione-S-transferase (GST) gene (Smith and Johnson, 1988) and a *tac* chemically inducible promoter for high levels of expression in *E. coli* (Pharmacia Biotech).

pAcCL29: *ampR*⁺, one of the original baculovirus vectors adapted by (Livingstone and Jones, 1989), contains a unique BamHI downstream from the polyhedrin promoter, plus an M13 intergenic region allowing single stranded DNA production

in bacteria in the presence of an M13 helper phage. Kindly provided by Dr Ian Jones, NERC Institute of Virology and Environmental Microbiology, Oxford, UK.

pAcES: *ampR*⁺, this was an inhouse modification of pAcCL29, a linker was incorporated into the BamHI site to generate the unique cloning sites EcoRI, SmaI and BamHI.

pAcGST: *ampR*⁺, this was an inhouse modification of pAcCL29 to include the coding sequence for Glutathione-S-transferase (GST) downstream of the unique BamHI site (Harris and Coates, 1993).

pEG202: A yeast-*E.coli* shuttle vector containing a yeast expression cassette that includes the promoter from the yeast ADH1 gene (pADH1), sequences encoding amino acids 1 to 202 of the bacterial repressor protein LexA (DNA binding and dimerization domains), a polylinker (containing unique restriction sites: *EcoRI*, *BamHI*, *SaII*, *NcoI*, *NotI* and *XhoI*) and the transcription terminator sequences from the yeast ADH1 gene (tADH1). It also contains an *E.coli* origin of replication (pBR ori), *ampR*⁺ gene, a yeast selectable marker gene (*his3*⁺) and a yeast origin of replication (2 μ ori). It confers upon a *his3*⁻ yeast strain the ability to grow in the absence of histidine and directs the constitutive expression of LexA fused to approx. 17 amino acids encoded by the polylinker, or a gene of interest inserted into the polylinker. Obtained as part of the yeast interaction trap system from Dr Roger Brent, Massachusetts General Hospital, Boston, USA.

pVEG': A modification of pEG202 including all the same elements except that the position of the polylinker was modified to allow fusion proteins to be expressed at the N-terminus of the LexA protein, see chapter 3 for a more detailed description.

pJG4-5: A yeast-*E.coli* shuttle vector that also contained a yeast expression cassette, including the inducible promoter from the yeast gene GAL1 (pGAL1) followed by 106 amino acids encoding an activation tag, a polylinker and the transcription terminator sequences from the yeast ADH1 gene (tADH). The

activation tag was made up of; the nuclear localisation signal from the SV40 virus large T-antigen (PPKKKRKVA), the bacterial B42 transcriptional activation domain and the haemagglutinin (HA-1) epitope tag (YPYDVPDYA). The plasmid also contained an *E.coli* origin of replication (pUC ori), amp^R gene, a yeast selectable marker gene (TRP1) and a yeast origin of replication (2 μ ori). Obtained as part of the yeast interaction trap system from Dr Roger Brent.

2.1.5. Stock solutions:

Ampicillin (1000x): 100mg/ml in ddH₂O. Filtered through a 0.22 μ m filter, aliquoted and stored at -20°C.

Agarose Gel loading buffer (10x): 50% glycerol, 0.5% bromophenol blue, 0.5% xylene cyanol, in 1x TBE. Stored at room temperature.

DNA size markers: Phi (ϕ) X174 RF DNA digested with *Hae*III. Lambda (λ) DNA digested with *Hind*III, both from Life Technologies Inc. Both used at 1 μ g/10 μ l.

Ethidium bromide: 10mg/ml stock in ddH₂O, working concentration 0.5 μ g/ml. Stored in the dark at room temperature.

Oligonucleotides: Oligonucleotides were synthesised on an Applied Biosystems 3818A Automated DNA Synthesiser (operated by Mr. T. McPherson, Veterinary Pathology, Glasgow University). DNA was eluted from the columns in 2ml of concentrated ammonium hydroxide and deprotected overnight by heating at 55°C. Deprotected oligonucleotides were lyophilised, resuspended in ddH₂O at 1 μ g/ μ l and stored at 4°C.

Polyacrylamide solution with urea (Easigel): Purchased from Scotlab, 6% polyacrylamide, 7M urea, 1x TBE, used for sequencing.

SOC: SOC was prepared by adding filter sterile 20mM glucose (from a 1M stock) and 10mM MgCl₂, 10mM MgSO₄ (from 1M stocks) to an autoclaved SOB

solution: 2% bacto-tryptone, 0.5% yeast extract, 10mM NaCl, 2.5mM KCl. This was then stored at 4°C.

TBE (10x): 0.9M Tris-HCl, 0.9M Boric acid, 25mM EDTA pH8.3. Stored at room temperature.

TE: 10mM Tris, 1mM EDTA, pH'd as required. Autoclaved and stored at room temperature.

X-Gal (5x): 40mg/ml in dimethyl formamide (DMF). Stored in aliquots protected from light at -20°C.

2.1.6. Media and antibiotics:

L-Broth: 1% (w/v) bacto-tryptone (DIFCO), 0.5% (w/v) yeast extract (DIFCO), 1% (w/v) NaCl in ddH₂O autoclaved and stored at room temperature. 1x ampicillin (100µg/ml) was added as required.

L-agar: as for L-broth, but also contained 1.5% (w/v) agar. 1x ampicillin (100µg/ml) or kanamycin (at 25µg/ml), were added just prior to pouring the plates (approx. 50°C).

2.2. Molecular biology techniques- experimental methods:

2.2.1. Agarose gel electrophoresis:

Gels containing 0.5-1.5% agarose (w/v) and 0.5µg/ml ethidium bromide in 1x TBE were used to separate and analyse DNA molecules. 50-100ml gels were poured in perspex tanks and wells were cast using appropriate combs. Gel loading buffer was added to samples at a final concentration of 1x, samples were then electrophoresed in 1xTBE at 5V/cm. Known concentrations of DNA size markers were run alongside the samples in order to gauge both product size and yield of DNA. Subsequent to electrophoresis, DNA fragments were visualised using a short wave UV transilluminator and photographed with a Polaroid camera.

2.2.2. Polymerase chain reaction (PCR):

The polymerase chain reaction allows the rapid amplification of selected regions of DNA from small amounts of starting template DNA (Saiki et al., 1985). All the necessary reagents were purchased from USB or Cambridge Bioscience and were used according to the manufacturers instructions. The *Thermus aquaticus* (*Taq*) DNA polymerase was used as the enzyme for the reactions since it leaves template independent deoxyadenosine overhangs at the 3' ends of duplex DNA which were easily cloned into pCR™ plasmids (Invitrogen). Amplification was initiated from primers targeted to specific regions of the template DNA by cyclical high temperature denaturation of template DNA, followed by annealing and polymerisation steps at lower temperatures. Standard reaction conditions were as follows: depending on the template 1-100ng of template DNA was added to a 50µl reaction mix containing, 5µl 10x reaction buffer (supplied with enzyme), 0.25mM of each nucleoside-tri-phosphate and 1µg of each primer. The reactions were carried out in 0.2ml thin walled micro-centrifuge tubes in a Perkin Elmer heated lid thermocycler. A typical cycling reaction was; denaturation at 94°C for 7 minutes and then 25 cycles of; denaturation at 94°C for 1 minute, annealing at 50°C for 1 minute, polymerisation at 72°C for 1 minute; with a 7 minute polymerisation at 72°C after the cycles. Samples were stored at 4°C overnight, but frozen at -20°C for longer storage.

2.2.3. Restriction enzyme digests:

These were carried out in the appropriate buffer supplied with the restriction enzyme (Life Technologies Inc.). Typically 1unit of enzyme per 1µg of DNA was sufficient, reactions were incubated at 37°C for 1.5hours.

2.2.4. DNA purification from agarose gels:

The GeneClean II® Kit from BIO 101, supplied by Stratech Scientific Ltd, was used to obtain highly purified DNA, as described in the manufacturers instructions. For ligation purposes it was assumed that 80% of the DNA was recovered by this procedure.

2.2.5. Ligation of DNA molecules:

Ligations were carried out according to the manufacturers protocols supplied with the T4 DNA ligase and 5x reaction buffer (Life Technologies Inc.). Generally, 50ng of plasmid DNA and a 3-4 fold molar excess of insert DNA were ligated in a volume of 20 μ l. Ligations were carried out overnight at 14°C.

2.2.6. Plasmid transformation using competent DH5 α *E.coli*.

For each transformation a 20 μ l aliquot of competent DH5 α *E.coli*, (stored at -70°C) was used; the number of aliquots required were thawed on ice. To each, 1 μ l of purified sample DNA/ligation mixture (approx. 20ng/ μ l) was added and mixed by pipetting. This was incubated on ice for 30 minutes. The mixture was then heat shocked at 42°C for 45 seconds, then returned to ice for a further 2 minutes. 80 μ l of SOC, was then added to each and the tubes were incubated for 1 hour at 37°C. Each transformation reaction was plated onto L-agar plates supplemented with the appropriate antibiotic. The plates were incubated overnight at 37°C to allow colony formation. This method was essentially adapted from the protocol originally described by (Hanahan, 1983).

2.2.7. Small scale alkali purification of *E.coli* plasmid DNA:

This method was originally described in (Maniatis et al., 1982). Colonies from the transformation plates were picked using a sterile toothpick and used to seed 2ml cultures of LB broth supplemented with ampicillin. These cultures were incubated overnight at 37°C with vigorous shaking, (180rpm). 1ml of culture for each was transferred to a micro-centrifuge tube and pelleted using a microfuge (13,000rpm/ 1 minute). The remainder of the culture was stored at 4°C. The medium was removed by aspiration and the pellet was then resuspended in 100 μ l glucose solution (50mM Tris pH 8.0, 50mM glucose, 10mM EDTA), by vortexing. To this 100 μ l of lysis buffer (0.2M NaOH, 1% w/v SDS), was added, the micro-centrifuge tubes were inverted several times to mix and left at room temperature for 5 minutes.

Next 100 μ l of 3M KAc pH5 (made in 20ml aliquots; 12ml 5M KAc, 2.3ml glacial acetic acid, 5.7ml water), was added and gently vortexed. The samples were then

centrifuged for 5 minutes in a microfuge (13,000rpm). The supernatant, approx. 300µl, was transferred to fresh micro-centrifuge tubes and to this 750µl of ethanol (EtOH) was added. The samples were incubated at -20°C for at least 15 minutes. Following this they were centrifuged for a further 5 minutes (12,000g) and the pellets washed in 70% EtOH. The pellets were dried under vacuum for 2 minutes, resuspended in 20µl TE containing 100µg/ml RNaseA and incubated at 37°C for 30 minutes.

2.2.8. Large scale purification of plasmid DNA from *E.coli*:

Bulk preparation of plasmid DNA was by the Triton lysis procedure outlined in (Maniatis et al., 1982) with final plasmid preparation by centrifugation on a CsCl/EtBr gradient.

For each plasmid to be purified an overnight 2ml culture of *E.coli* in LB broth supplemented with ampicillin was used to seed a 200ml culture. This was incubated overnight at 37°C shaking, (a 400ml culture was used if a low copy plasmid was to be purified). The bacteria were pelleted using either a Beckman JA14 (6 x 250ml) or JA10 (6 x 500ml) rotor at 8K for 5 minutes at 4°C. The medium was discarded and the pellet resuspended in 2.5ml 25% (w/v) sucrose, 50mM Tris-HCl pH 8.0 and transferred to 50ml Oakridge tubes (Beckman). To these 0.5ml of 20mg/ml lysozyme in 0.25M Tris pH 8.0 was added. The samples were incubated on ice for 5 minutes, then 0.5ml 0.5M EDTA was added and the samples were incubated on ice for a further 5 minutes. Next 4ml 2% (v/v) Triton X-100, 50mM Tris pH 8.0, 62.5 mM EDTA was added to each and incubated on ice for 15 minutes.

The samples were centrifuged for 30 minutes in a Beckman JA20 rotor at 20K, 4°C. The supernatant was transferred to a universal and 1g of CsCl per ml of supernatant added plus 100µl of 10mg/ml EtBr. This was divided between 2 heat sealing tubes (Beckman), VTi65, (approx. 5.5ml), the volume being made up to the top of the tubes using 1g/ml CsCl in TE buffer. The samples were centrifuged overnight for approx. 16 hours (Beckman, VTi65 rotor) at 55K, 20°C. To harvest the plasmid band the ultracentrifuge tubes were secured in a retort stand. The top of the tubes

were punctured using a syringe needle to prevent a vacuum forming when the plasmid band was drawn off. Then a syringe and needle was used to puncture the tube just below the lower closed circular plasmid band and the band was gently drawn off. When exceptionally pure DNA was required (for yeast transformations and baculovirus transfections) the plasmid DNA was transferred to Beckman TLV100 tubes (approx. 2ml) and centrifuged for 4 hours at 100K. The same method was used to harvest the plasmid band from these tubes. EtBr was removed from the samples by Butanol extraction.

Butanol extraction: In 15ml falcon tubes 5ml of saturated butanol was added to the samples, they were briefly vortexed and centrifuged to separate out the aqueous layer. The top layer was discarded and then 5ml of unsaturated butanol was added, the samples were briefly vortexed and centrifuged again and the top layer discarded. This process was repeated until all the EtBr had been removed, usually at least 3 times.

The sample volume was made up to 3ml with distilled water and 8ml of EtOH was added to precipitate the plasmid DNA. The samples were incubated at room temperature for 30 minutes, centrifuged at 3500rpm for 15 minutes, then the pellet was washed in 70% EtOH. The tubes were inverted on a paper towel to dry the pellets before they were resuspended in 450µl TE. This was transferred to microcentrifuge tubes and 50µl 3M NaAc plus 1ml of EtOH was added to each. The samples were allowed to precipitate for 20 minutes at room temperature and the DNA repelleted in a microcentrifuge, 13K, 5 minutes. Again the pellet was washed in 70% EtOH to remove any salt and then the pellet was dried under vacuum and resuspended in 200-500µl TE depending upon the amount of DNA (1-2µg/µl).

2.2.9. Sequencing of DNA:

2.2.9.1. Manual:

The T7Sequencing™ Kit from Pharmacia Biotech was used for manual sequencing with Redivue α[³⁵S] dATP. The kit utilised the original dideoxy base-specific termination of enzyme-catalysed primer extension reactions first described by Sanger et al (Sanger et al., 1977), except that T7 DNA polymerase was substituted

for the Klenow fragment of *E.coli* DNA polymeraseI due to its increased polymerization rate. The reactions were undertaken exactly as outlined in the manufacturers instructions using miniprep DNA as template.

2.2.9.2 Sequencing gel:

To run the samples a Biorad sequencing apparatus was used. The glass plates were cleaned with 70% EtOH and the back plate was siliconised with Repelcote (BDH) prior to assembly. A 20ml plug was poured, 20ml polyacrylamide mix (Scotlab), 90 μ l 25% (w/v) APS plus 40 μ l TEMED. Once set the sequencing gel was poured- 50ml polyacrylamide mix, 180 μ l APS, 40 μ l TEMED. Samples were heated to 95°C for 2 minutes and loaded immediately. The gel was run at approx. 2000volts, 60 watts.

2.2.9.3. LI-COR automated:

Automated DNA sequencing was carried out using a LI-COR model 4000 DNA sequencer. This had the advantage of being able to sequence 500-900bp DNA, however it was only used to confirm pCRTM sequences. This type of sequencing utilises infrared dye labelled primers which are incorporated into the DNA during the sequencing reactions. Sequencing reactions were performed as detailed in the Thermo Sequenase Fluorescent Labelled Primer Sequencing Kit supplied by Amersham Life Science. CsCl purified DNA was always used for automated sequencing. Mineral oil was layered over the reaction mix since the volume used was so small. After the thermocycling sequencing (denaturation 5 minutes at 95°C, 30 cycles of 95°C for 30 seconds, 55°C for 30 seconds, 70°C for 1 minute), 4 μ l of stop solution was added to each sample and the mineral oil removed as outlined in the manufacturers instructions. The samples were stored at -20 °C in the dark and remained stable for up to 2 weeks. Prior to loading on the sequencing gel the samples were denatured for 2 minutes at 95°C and put on ice. Gels were run according to LI-COR instructions.

The primers used to sequence the pCR™ plasmids were the universal primers modified to contain an infra red-label:

M13 (-29) forward primer: 5'- CAC GAC GTT GTA AAA CGA C -3'

Reverse primer: 5'- GGA TAA CAA TTT CAC ACA GG -3'

YEAST PROTOCOLS.

2.3. Yeast protocols- Materials:

2.3.1. Chemicals and enzymes:

Chemicals specific to this section are detailed in the table below, including abbreviations.

Table 2.3. Chemicals and enzymes for yeast protocols including abbreviations and companies purchased from.

Chemical/Enzyme:	Company:
Amino acids Di-methyl-sulphoxide (DMSO) Lithium acetate, C ₂ H ₃ O ₂ Li-2H ₂ O (LiAc) Zymolase	SIGMA, Poole, UK
Interaction Trap including host yeast strain, plasmids and Jurkat T-cell library.	R. Brent and R. Finley, Massachusetts General Hospital, USA
Salmon Sperm DNA	Life Technologies Inc.

2.3.2. Radiochemicals:

Metabolic label, ³H myristic acid, in EtOH, specific activity 40-60Ci/mmol, was obtained from Amersham Life Sciences, UK. Prior to use, aliquots were dried under vacuum and resuspended in DMSO 1mCi in 30µl DMSO per 5ml culture (0.2mCi/ml culture).

2.3.3. Yeast strain:

EGY48: LexAop-LEU2, *his3-*, *trp1-*, *ura3-*. This contained an integrated copy of the LEU2 gene in which the normal upstream regulatory sequences were replaced with 3 tandem LexA operators. The presence of both the LexA DNA binding domain (pEG202 or pVEG') plus the B42 bacterial activation domain (see pJG4-5)

were required for LEU2 expression which was necessary for the strain to grow in the absence of leucine. Auxotrophic selection markers were provided by the lack of *his3*, *trp1* and *ura3* genes allowing the cotransformation of the 3 plasmids used in the yeast-two-hybrid system. This yeast strain was supplied as part of the interaction trap kit kindly provided by Dr Roger Brent's laboratory (Massachusetts General Hospital, Boston, USA).

2.3.4. Yeast interaction trap plasmids:

All plasmids used for the interactor hunt were yeast-*E.coli* shuttle vectors and had an *ampR*⁺ gene and an auxotrophic selectable marker. Those that were used for cloning genes of interest are outlined in more detail in section 2.1. Plasmids were supplied as part of the interaction kit, except pVEG' which was a modification of pEG202, see chapter 3.

pEG202, pVEG' (*his3*⁺): Each encoded the bait protein either as C-terminal or N-terminal fusions, respectively, to the LexA DNA binding domain. The region of LexA expressed in the plasmid contained the bacterial DNA binding and dimerization domains which specifically recognised LexA operators cloned upstream of the reporter genes (*lacZ* in the pSH18 plasmid and the chromosomally integrated LexAop-LEU2 gene).

pRFHM-1, pSH17 (*his3*⁺): Control bait plasmids used for comparisons in the activation assay, pSH17-4 was inherently transactivating while pRFHM-1 behaved as a model bait protein in the assay.

pSH18-34 (*ura3*⁺): LacZ reporter plasmid used in addition to the LexAop-LEU2 reporter cloned into the genome. This plasmid contained the GAL1 TATA, transcription start and a small part of the GAL1 coding sequence fused to lacZ however the GAL1 upstream activating sequences (UAS's) had been replaced with

an XhoI site into which various numbers of LexA operators could be cloned, for these studies 4 were used, making the reporter highly sensitive.

pJK101 (*ura3+*): *LacZ* reporter plasmid used to measure repression by the LexA fusions indicating the ability of the fusions to enter the nucleus. It contained most of the GAL1 UAS's with a single LexA operator cloned between the UAS and the GAL1 TATA transcription start site. Therefore if a LexA DNA binding domain bound to the operator transcription of the *lacZ* gene was repressed.

pJG4-5 (*trp1+*): Encoded either individual, known, protein coding sequences (i.e. Src tyrosine kinases) or the Jurkat T-cell cDNA library fused to the C-terminus of the activation tag under the control of an inducible GAL1 promoter. The activation tag included a nuclear localisation signal, the bacterial B42 transcription activation domain and the haemagglutinin (HA-1) epitope tag which was useful for western blot analysis to confirm expression of the fusion proteins.

2.3.5. Yeast media and supplements:

Yeast was grown in a complete minimal media which contained a yeast nitrogen base, without amino acids (YNB) (purchased from DIFCO), a carbon source (galactose, raffinose [DIFCO] or D(+) Glucose [BDH]) and a mixture of nutrients (all amino acids were from SIGMA) the latter of which were varied depending on the auxotrophic selection required. See section 2.3.5.6. for the nomenclature of dropout medias and supplements.

2.3.5.1. Complete minimal (CM) dropout powder:

This contained a mixture of nutrients shown in Table 2.3.1 with one or a few omitted, hence- dropout powder. A dropout powder was made corresponding to each of the dropout medias required in the experiments i.e. for media lacking histidine (*his-*), the dropout powder used would contain all of the nutrients,

quantities of which are shown in Table 2.2.1, except for histidine. The dropout powders were made by grinding all the ingredients in a clean dry pestle and mortar until homogenous, this was then stored in the dark at room temperature.

Table 2.4. Table of amino acid quantities required for the complete minimal dropout powder:

Nutrient	Quantity (g).	Final conc. in media ($\mu\text{g/ml}$)
adenine	2.5	40
L-arginine (HCl)	1.2	20
L-aspartic acid	6.0	100
L-glutamic acid (monosodium)	6.0	100
L-histidine (his)	1.2	20
L-isoleucine	1.8	30
L-leucine (leu)	3.6	60
L-lysine	1.8	30
L-methionine	1.2	20
L-phenylalanine	3.0	50
L-serine	22.5	375
L-threonine	12.0	200
L-tryptophan (trp)	2.4	40
L-tyrosine	1.8	30
L-valine	9.0	150
uracil (ura)	1.2	20

2.3.5.2. Carbon Sources:

Stocks of the carbon sources were made separately and filter sterilised (20% (w/v) galactose, 20% (w/v) glucose, 20% (w/v) raffinose, all dissolved in ddH₂O). As

needed, galactose (Gal) and glucose (Glu) were each added to 2% final concentration, raffinose (Raf) was added to 1% final concentration.

2.3.5.3. Dropout plates and media:

For 1 litre of dropout medium 6.7g YNB without amino acids plus 2g dropout powder lacking the appropriate amino acid were added to 850ml of deionized water. This mix was autoclaved and the carbon source added prior to use from the filter sterile stocks. For the production of plates 20g/litre bacto-agar was added prior to autoclaving.

2.3.5.4. X-Gal plates:

For 1 litre the standard dropout media mix, was added to 800ml deionized water. This was autoclaved, the carbon sources were added and the mix allowed to cool to 65°C. Then 100ml of 10xBU salts (see below) and 4ml of 20mg/ml X-Gal dissolved in DMF (stored at -20°C), were added.

2.3.5.5. 10x BU SALTS:

For 1 litre, 70g $\text{Na}_2\text{HPO}_4 \cdot 7\text{H}_2\text{O}$, 30g NaH_2PO_4 adjusted pH to 7.0; autoclaved and stored at room temperature.

2.3.5.6. Nomenclature of media plus supplements:

The nomenclature for the dropout plates used in these studies is indicated in the table below:

Table 2.5. Nomenclature for media and dropout plates (in single letter and triple letter code):

Amino acid "dropped out":		Carbon Source added:	
Amino acid	Abbreviation	Carbon source	Abbreviation
histidine	H, His-	Glucose	Glu
leucine	L, Leu-	Galactose	G, Gal
tryptophan	T, Trp-	Raffinose	R, Raf
uracil	U, Ura-		

G/R UHT or Gal/Raf ura-his-trp- corresponds to plates supplemented with galactose and raffinose but lacking, in this example, the amino acids uracil, histidine and tryptophan; compared to Glu UHT or Glu ura-his-trp- which would be supplemented with glucose instead.

If the plates also contain X-gal an X will be added i.e. Glu UHT-X.

2.3.6. Storage and freezing of yeast:

Yeast were streaked onto the appropriate dropout plates and stored at 4°C for a maximum of 5 days. For longer term storage liquid cultures of an $OD_{600} = 1.0$ (approx. 3×10^7 cells/ml) were mixed with an equal volume of 65% (v/v) glycerol, 0.1M $MgSO_4$, 25mM Tris pH 7.5 and aliquoted into sterile microcentrifuge tubes and stored frozen at -70 °C.

2.4. Yeast protocols- Experimental methods:

2.4.1. Transformation of yeast by the high efficiency lithium acetate method:

This method was adapted from a method published by (Gietz et al., 1995). An overnight culture, of the appropriate dropout media, was grown at 30°C with

shaking (~150 rpm) and used to seed a 200ml culture. For high transformation efficiencies it was important to start the 200ml culture at $OD_{600} = 0.2$ or less and allow it to grow to $OD_{600} = 0.8$, so that the cells were in mid-log phase when harvested (an OD_{600} of 1.0 was taken to correspond to about 3×10^7 cells/ml). The culture was harvested by centrifuging at 500g for 5 minutes and the supernatant poured off. The cells were washed once in 10ml of sterile ddH₂O. These centrifuge steps and all the following manipulations were carried out at room temperature. The cells were resuspended in 5ml of filter sterilised LiAc/TE (10mM Tris HCl pH 7.5, 1mM EDTA, 100mM LiAc; made from a filter sterile stock of 1M LiAc, pH 7.5), pelleted again and the supernatant poured off.

Next the cells were resuspended in 1.0ml LiAc/TE, 50 μ l of this suspension provided enough competent cells to be transformed with 1 μ g of DNA. Generally for a single plasmid transformation 100ng was sufficient. The use of more than 1 μ g DNA per 50 μ l of cells resulted in the introduction of multiple plasmids in each yeast cell, this was used to advantage to allow multiple plasmids to be transformed simultaneously. However when transforming the library plasmid, where it was important not to introduce multiple plasmids in each yeast cell, a lower concentration of library plasmid DNA was used. This ensured that the selection assays were performed on only one library plasmid at a time.

After aliquoting the required amount of the yeast suspension the tubes were incubated at 30°C for 15 minutes, DMSO was added to a final concentration 10% (v/v), since it has been documented to improve efficiency by 3 to 5 fold. At this stage salmon sperm DNA was also added (5 μ l at 10 μ g/ μ l). 300 μ l of filter sterilised 40% PEG4000 in LiAc/TE (freshly made from stocks of 1M LiAc pH7.5, filter sterilised 50% PEG4000 in water, 1M Tris-HCl pH7.5 and 0.5M EDTA) was added. The tubes were gently vortexed to mix and subsequently incubated at 30°C for 30 minutes without agitation.

The transformations were then subjected to a heat shock at 42°C for 20 minutes after which they were immediately returned to room temperature. Before plating the cells were pelleted and the PEG solution removed. The cells were resuspended in sterile water and plated on the appropriate dropout plates.

For library transformations the following alterations to the protocol were included to increase efficiency: Aliquots of 150µl of competent yeast in sterile micro-centrifuge tubes were used. To each aliquot 2µg of library DNA was added and 200µg of carrier DNA (single stranded salmon sperm, in a total volume of 20µl). The volume of 40% PEG4000 in LiAc/TE was increased to 900µl. The number of aliquots used depended on the desired number of transformants and the expected transformation efficiency. In pilot transformations efficiencies of 10⁵ transformants per µg were achieved, therefore each aliquot was expected to yield 200,000 transformants, all of which was plated onto a single 24cm x 24cm plate. It was found the quality of the salmon sperm DNA, fresh solutions and the density of the cells when harvested were crucial in obtaining high transformation efficiencies.

2.4.2. Testing baits for transcription activation:

This assay was one of two assays which determined whether the proposed bait was suitable for use in the interactor study. The bait plasmid (either pEG202 or pVEG) encoded the protein of interest fused to LexA (a DNA binding domain that recognised the specific UASs). These LexA UASs were incorporated upstream of two reporter genes, an auxotrophic marker, Lexop-*leu2* encoded in the yeast genome, and *lacZ* encoded by the reporter plasmid (pSH18-34). For the bait to be suitable for use in an interactor hunt it had to successfully enter the nucleus and bind the LexA operators failing to transactivate either of the reporter genes, i.e. it should not possess any innate transactivation activity. This was determined by utilising the auxotrophic marker and comparing the growth of yeast cultures on

dropout plates +/- leucine. Typically both controls and baits grew at similar rates on plates containing leucine (Gal/Raf ura-his-), however if yeast growth was reproducibly diminished for a given bait, it indicated that its expression was toxic to yeast. Baits containing a non-activating LexA fusion did not grow after several days on plates lacking leucine (Gal/Raf ura-his-leu-). Any that activated transcription, i.e. grew equally on the Gal/Raf ura-his-leu- plates and Gal/Raf ura-his- plates, were discarded as unsuitable in this study.

2.4.2.1 Constructing the transcriptional activation selection strain:

To construct the selection strain, the host strain EGY48 was transformed using the LiAc method, with a URA3 lacZ reporter plasmid, (pSH18-34) and transformants selected on Glu ura⁻ plates. Plates were incubated at 30°C for 3-4 days. From these, three colonies were combined and grown in Glu ura⁻ liquid media and transformed with the HIS3 bait plasmid (pEG202 or pVEG-Nef) or control plasmids (pSH17-4 positive, pRFHM1 negative). Transformants were selected on Glu ura⁻his⁻ plates, incubated at 30°C, 3-4 days. Four individual colonies from each transformation were picked and each colony was used to inoculate 5ml Glu ura⁻his⁻ liquid cultures. The same four transformants were also streaked to another Glu ura⁻his⁻ plate for storage and later recovery. The plates were incubated at 30°C until colonies formed (about 3-4 days) and then stored at 4°C. If all four colonies behaved identically in the tests outlined below, any one was chosen to serve as the selection strain into which the library was introduced.

2.4.2.2. Transcriptional activation assay:

Liquid cultures were grown at 30°C with shaking to mid-log phase or $OD_{600} = 0.5$ (corresponding to about 1.5×10^7 cells/ml). Dilutions of 10^{-2} and 10^{-3} of each culture were made in sterile water. These were spotted in a volume of 10 μ l, together with the undiluted culture onto two plates either, Gal/Raf ura-his- or Gal/Raf ura-his-leu-. For side by side comparison both the bait plasmid being tested

and yeast containing the control plasmids were spotted onto the same plates. The plates were incubated at 30°C. (Note: galactose is used in the media because the actual selection will eventually be performed on galactose plates to induce expression of the activation tagged cDNA protein. Raffinose was added to aid yeast growth; it provides a better carbon source than galactose alone but does not block the ability to induce the GAL1 promoter). The growth of the cultures in the spots were monitored every 24hours for a period of several days. The yeast that did not grow on leucine minus plates were followed up with the repression assay, below.

2.4.3. Repression assay to show that the bait enters the yeast nucleus and binds the operators:

This was the second assay used to determine the suitability of a bait for an interactor hunt. It was performed to ensure baits that did not activate the auxotrophic LexAop-LEU2 reporter in the transactivation assay were able to enter the nucleus and bind the LexA operators.

In this instance the reporter plasmid was pJK101, which has a LexA operator positioned between the TATA transcription start site and UAS's. LacZ expression was induced by growth on galactose but was still detectable at lower levels in the presence of glucose because the negative regulatory elements in GAL1 that normally keep it repressed in glucose were not present in this plasmid. If LexA or a LexA fusion bound the LexA operator the *lacZ* gene activation was repressed indicating the bait could enter the nucleus. Yeast lacking LexA in the nucleus began to turn blue on the Gal/Raf plates after one day and appeared light blue on the glucose plates after two or more days, while yeast containing a bait that entered the nucleus and bound the operator turned blue more slowly, if at all.

The host strain, EGY48 was transformed with the plasmid pJK101 and selection for transformants was on Glu ura- plates. Three colonies were combined from these

plates and transformed with the HIS3 bait plasmid, pEG202 or pVEG (or HIS3 control plasmids, pSH17-4 positive, pRFHM-1 negative). These transformants were selected on Glu ura-his- plates. Four individual colonies from each transformation were picked and streaked in a patch onto Glu ura-his- and Gal/Raf ura-his- plates containing X-Gal. These were incubated at 30°C. The X-Gal plates were examined after 1, 2 and 3 days, those that remained white could be used for the interactor hunt, in this instance pVEG-Nef.

2.4.4. Selecting interactors from library transformants:

pVEG-Nef was used as a bait to screen a Jurkat T-cell cDNA library (cloned into pJG4-5). This was carried out in stages. Firstly it was confirmed using pJG4-5 alone that high efficiency transformation levels could be achieved with the pVEG-Nef, pSH18 selection strain. The library was then transformed without induction on Glu ura-his-trp- plates to prevent the loss of any potential interactors that might be toxic to the yeast. These colonies were harvested, stored and the colony forming units per ml (CFU/ml) determined. The colonies could then be screened for interactors using both the LEU2 and LacZ reporter constructs. Potential interactors were hence isolated for further investigation.

2.4.4.1. Transformation of the library plasmid and determination of colony forming units (CFU):

The Jurkat T-cell library, pJG4.5 (TRP1), was introduced into the selection strain, as outlined in the high efficiency lithium acetate method, under conditions designed to ensure that each individual transformed cell contained only one library plasmid. The transformants were plated onto Glu ura-his-trp- plates to maintain selection for the library plasmid (TRP1) and both the bait, pVEG (HIS3) and reporter, pSH18 (URA3) plasmids already contained within the selection strain. The plates were incubated at 30°C for 3 days or until the colonies were approximately 1 to 2mm in diameter. To harvest the colonies the agar plates were placed at 4°C for 2-4 hours

to harden the agar. The colonies were then washed off the plates by pipetting several times with 10ml of sterile TE (10mM Tris pH8, 1mM EDTA). The resulting cell suspension was transferred to a sterile 50ml Falcon tube and pelleted at 500g, 4°C, for 5 minutes. The cells were then washed a further 2 times with 2-3 volumes of sterile TE. The cells were finally resuspended in 1 pellet volume of glycerol solution (65% glycerol vol/vol, 0.1M MgSO₄, 25mM Tris pH 7.5) by gentle vortexing. Aliquots of 1ml were frozen at -70°C.

To determine the plating efficiency of the transformants an aliquot of the library transformation was thawed and serial dilutions were made in sterile water. 100µl of each dilution was plated onto 100mm Gal/Raf ura-his-trp- plates. The colonies that grew after 3 days at 30°C were counted and from this the plating efficiency in colony forming units (CFU) per volume of frozen cells was established.

2.4.4.2. Isolating interactors on leu- plates:

Library transformants which encoded a protein that interacted with the bait exhibited galactose-dependent growth on media lacking leucine and galactose dependent β -galactosidase activity. This was tested by thawing an appropriate number of aliquots to allow a final concentration of 10⁷ cells per 24x24cm plate. These cells were diluted 10-fold into Gal ura-his-trp- liquid media. To induce the GAL1 promoter and synthesis of the activation-tagged cDNA-encoded proteins they were incubated with shaking at 30°C for 4 hours. The cells were pelleted at 500g at room temperature for 5 minutes and resuspended in sterile water and plated onto Gal/Raf ura-his-trp-leu- plates. The selection plates were wrapped in para-film to prevent them from drying out and incubated at 30°C for 3-5 days.

2.4.4.3. β -Galactosidase filter assay:

To confirm that the colonies able to grow in the absence of leucine contained interacting proteins, the colonies were replica plated onto nitrocellulose filters in

order to assess expression of the *lacZ* marker by β -galactosidase assay. 24x24cm nitrocellulose filters were gently placed on the ura-his-trp-leu- dropout plates containing 1-2mm sized colonies. The orientation of the filters was marked for later reference and then the filters were immediately removed. The filters were immersed in liquid nitrogen for 1 minute to lyse the yeast. 3MM paper was cut to fit in the lid of a 24x24cm plate and 18ml per plate of buffer Z (60mM Na₂HPO₄, 40mM NaH₂PO₄, 10mM KCl, 1mM MgSO₂, 50mM β -mercaptoethanol, pH to 7.0, made fresh) containing 450 μ l per plate of X-Gal (40mg/ml in DMSO) was added. The nitrocellulose replica was placed colony side up on the 3MM paper being careful to avoid bubbles or wrinkles. This was then incubated at 30°C for between 30mins and 3 hours, until blue colonies were apparent.

2.4.5. Verifying the specificity of the interactions:

Once potential interactors had been identified the colonies were picked and streaked (on Glu UHT) plates to single colonies and glycerol stocks taken from one of the single colonies. The interaction was then double checked for each single colony by patching them onto Glu UHT-X, G/R UHT-X and Glu UHTL, G/R UHTL 100mm plates. This established which of the interactions were inducible, not due to mutations arising in the genomic DNA and confirmed the correct colonies had been picked. To confirm the library plasmids were interacting directly with the bait rather than non-specifically with LexA, the promoters, or some part of the transcription machinery, the library plasmids had to be rescued from the yeast.

Library plasmids were rescued from the yeast by performing a rapid yeast miniprep, see below. Since the library screen, after repatching to the dropout plates to confirm the interactions, yielded nearly 100 interactors it was decided before checking each individual cDNA for specificity it would be prudent to first check for duplicates. This was determined by PCR of the yeast miniprep DNA, followed by restriction fragment length polymorphism (RFLP) analysis of the PCR products. Once

duplicates had been identified the yeast miniprep DNA, containing all 3 plasmids used in the interactor hunt, was used to transform *E.coli*. Transformants were plated onto L-agar plates containing X-Gal and white colonies picked, thus excluding the *lacZ* reporter plasmid. Library plasmids were identified by restriction digests of miniprep plasmid DNA. Once isolated from *E.coli* the library plasmids were reintroduced to yeast containing LexA alone (pEG202) and unrelated baits (p55Gag and ORF94), to which they should not interact.

2.4.5.1. RFLP analysis of PCR products:

To identify duplicate interactors from the crude yeast miniprep DNA, PCR reactions (for a more detailed explanation of PCR see section 2.2) were set up as follows. In 0.5ml tubes, 13µl ddH₂O, 2µl 10x *Taq* polymerase buffer, 2µl dNTP mix (all 4 dNTPs at 2.5mM each), 1µl of each primer (0.1µg/µl), see below and 0.2µl *Taq* polymerase was added and to each 1µl of yeast miniprep DNA was added. The reactions were incubated in a thermocycler for 25 cycles of 92°C for 30 seconds, 65°C for 2 minutes and 75°C for 30 seconds. Next two tubes were set up for each PCR reaction containing 1µl of the appropriate restriction enzyme buffer and 1µl of either *AluI* or *HaeIII*, these restriction enzymes were chosen because they are frequent cutters and work well in the presence of the PCR reagents. To each tube 8µl of the PCR mix was added. The restriction digests were incubated at 37°C for 2 hours after which they were analysed on a 1.5% agarose gel (see section 2.2).

2.4.5.2. Primers for RFLP PCR:

5' primer derived from the library vector fusion moiety sequence:

BCO1 5'- CCA GCC TCT TGC TGA GTG GAG ATG -3'

3' primer derived from the ADH1 terminator sequence in the library vector:

BCO2 5'- GAC AAG CCG ACA ACC TTG ATT GGA G -3'

2.4.6. Yeast plasmid miniprep:

A 2ml overnight liquid culture of yeast was pelleted and the pellet resuspended in 1ml of TE (the OD_{600} of this suspension was between 2 and 5). The yeast were repelleted and resuspended in 0.5ml S buffer (10mM KPO_4 pH7.2, 10mM EDTA, 50mM 2-mercaptoethanol, 50mg/ml zymolase) and incubated at 65°C, 30 minutes. To this 166 μ l of 3M KAc was added and the samples were chilled on ice for 10 minutes. Subsequently they were centrifuged, 13K, 10 minutes and the supernatant poured into a fresh tube. The DNA was precipitated by the addition of 0.8ml of cold ethanol, incubated on ice for 10 minutes and centrifuged for a further 10 minutes. The ethanol was aspirated and the pellet washed with 70% ethanol. The pellet was dried under vacuum and resuspended in 40 μ l sterile ddH₂O. 1 μ l of this crude preparation was sufficient to transform *E.coli*.

2.4.7. Yeast cell lysis using glass beads:

This protocol was adapted from Current protocols, 1993, (Ausubel et al., 1993) for small scale preparations of yeast lysates. In general a 10ml culture of yeast in the exponential growth phase ($OD_{600} = 0.8$) was harvested, although this was scaled up according to requirements. The cells were pelleted by centrifugation at 500g for 5 minutes at 4°C. The pellet was washed with 10 volumes of ice cold dH₂O, repelleted and washed with glass bead disruption buffer (20mM Tris-HCl, pH 7.9, 10mM MgCl₂, 1mM EDTA, 5% glycerol, 1mM DTT, 1M KCl). The packed cell volume was estimated and the cells resuspended in 3 volumes of glass bead disruption buffer containing protease inhibitors (see section 2.5, under lysis buffers). The suspension was then transferred to a screw-capped micro-centrifuge tube. 4 volumes of chilled, acid-washed glass beads were added to the tube (glass beads were prepared by washing in 1M HCl for 1hour, followed by 3 washes with dH₂O after which they were autoclaved). From this stage onwards all buffers contained protease inhibitors.

The suspension containing glass beads was vortexed for 60 seconds and iced for 2 minutes. This process was repeated 5 times. The beads were allowed to settle and the supernatant decanted. To remove all the supernatant the bottom of the eppendorf was pierced with a needle and the tube placed in a second eppendorf. The two tubes were centrifuged at a low speed and the supernatant collected in the lower tube was pooled with the previously decanted supernatant. Next a further 2 volumes of the glass bead buffer was added to the beads and carefully mixed and collected as previously.

The pooled supernatants were adjusted to 1% Triton X-100 and 0.1% SDS, by adding a 1:10 vol. of 10% (v/v) Triton X-100, 1% (v/v) SDS, in glass bead buffer. These were incubated on ice for 30 minutes. The tubes were centrifuged at 13K for 10 minutes at 4°C and the lysate transferred to a fresh tube. If the lysates were to be immunoprecipitated (see protein protocols, 2.8) an aliquot was taken at this stage, lysates were otherwise stored at -20°C. Before immunoprecipitation the salt concentration was reduced to 0.5M KCl by adding an equal volume of glass bead buffer minus KCl, see section 2.8 for immunoprecipitation methods.

2.4.8. Labelling of Yeast with ³H Myristic Acid:

To confirm that proteins were being successfully myristoylated on their N-terminal glycine residue in yeast, ³H myristic acid was used to label yeast cultures during their exponential growth phase. Myristoyl proteins were then visualised by SDS PAGE and fluorography.

For labelling experiments, samples were grown in duplicate, one set were labelled with 100μCi per sample of ³H myristic acid while the second set were analysed by western blot (for method see protein protocols, 2.8). 3ml cultures were grown overnight and used to seed 5ml cultures at very low levels, when these cultures

reached $OD_{600} = 0.15$, the 3H myristic acid in DMSO was added (1mCi per sample was dried down under vacuum and resuspended in 30 μ l DMSO). 30 μ l of DMSO alone was also added to each of the yeast cultures to be analysed by Western blot. The cultures were then incubated at 30°C with shaking. The cultures were harvested when they reached an OD_{600} of 0.8. The washes and lysis of the yeast was essentially the same as outlined in the glass bead method detailed above except that the needle step was omitted and the final wash was doubled in volume. The lysates recovered were then immunoprecipitated overnight and analysed as outlined in section 2.8.

BACULOVIRUS PROTOCOLS:

2.5. Baculovirus protocols- Materials:

2.5.1. Chemicals and enzymes:

Chemicals and enzymes specific to this section are detailed below any others can be found in the general section at the start of this chapter.

Table 2.6. Chemicals and enzymes for baculovirus protocols including abbreviations and companies purchased from

Chemical/Enzyme	Company
Bsu-36I restriction enzyme	New England Biolabs
Lipofectin	Life Technologies
Low melting point (LMP) agarose	
Trypan blue stain	
Glutathione-agarose .	SIGMA, Poole, Dorset, UK
Neutral red viable stain	
Piperazine- N,N' -bis (2-ethanesulphonic acid) (PIPES)	
Reduced glutathione	

2.5.2. Radiochemicals:

^3H myristic acid and ^3H palmytic acid, in EtOH, specific activity, 40-60Ci/mmol , were purchased from Amersham Life Sciences Ltd, UK. Trans ^{35}S -Label™ (^{35}S *E.coli* hydrolysate labelling reagent containing 70% L-methionine, [^{35}S]), specific activity, 1177Ci/mmol (11.88mCi/ml) was obtained from ICN Pharmaceuticals Inc., USA.

2.5.3. Insect cell line:

Spodoptera frugiperda (Sf9) insect cell line, was a clonal derivative of the original Sf21 cell line which itself was derived from the ovarian tissue of the fall army worm.

Obtained from the American Type Culture Collection, accession number CRL-1711 (King and Possee, 1992).

2.5.4. Baculovirus strain:

AcMNPV.*lacZ* baculovirus (*Autographa californica*, multiple nuclear polyhedrosis virus) -(PAK6) (Kitts and Possee, 1993) which contains the *lacZ* gene under the control of the late polyhedrin promoter, allowing colour selection of recombinants. Kindly provided by Dr R.D.Possee, NERC Institute of Virology and Environmental Microbiology, Oxford, UK.

2.5.5. Expression plasmids:

pAcCL29, pAcES and pAcGST see 2.1.

2.5.6. Stock solutions:

Phosphate buffered saline (PBS): 100mM NaCl, Na₂HPO₄-7H₂O, 20mM NaH₂PO₄, adjusted to pH7.5. Autoclaved and stored at 4°C.

Neutral red viable stain: 0.1% (W/V) neutral red viable cell stain in PBS containing X-GAL at 0.4mg/ml final concentration (from a 40mg/ml X-GAL in DMF stock, stored at -20 °C). Filter sterilised and made fresh for each use.

Lysis buffers:

Protease inhibitors were added fresh prior to use, see below.

2x GLB lysis buffer (*Glasgow-lysis-buffer*): 2% (v/v) TritonX-100, 240mM KCl, 20mM PIPES/NaOH pH7.2, 60mM NaCl, 10mM MgCl₂, 20% (v/v) glycerol. Filter sterilised and stored at 4°C.

1x PBS lysis buffer: Autoclaved PBS with 1% (v/v) TritonX-100 added, stored at 4°C.

Protease inhibitors: for 1ml of buffer added, 1µl 10mM leupeptin (stored at -20°C), 5µl 1mM pepstatin A (stored at -20°C), 1µl aprotinin (stored at 4°C), 2µl 100mM

AEBSF (stored at 4°C), all supplied by SIGMA except AEBSF which was purchased from Calbiochem-Novabiochem Corp., USA.

Protein gel loading buffer (sample buffer): 62.5mM Tris-HCl pH6.8, 20% (v/v) glycerol, 2% (w/v) SDS, 5% (v/v) β -mercaptoethanol, 0.05% (w/v) bromophenol blue, in ddH₂O. Stored at room temperature.

2.5.7. Preparation of Culture Medium:

Bottles (500ml) of TC100 medium (Life Technologies Inc.) were stored at 4°C in the dark. Heat-inactivated foetal calf serum (PAA Labs.) and penicillin-streptomycin (P/S) (GIBCO), were aliquoted and stored at -20°C. Before use the bottles were wiped with 70% alcohol prior to placing in a Class II microbiological safety cabinet. Using aseptic techniques 50ml (10% v/v) of the foetal calf serum was added to 500ml TC100. Next 5ml of P/S (5000units/ml) was added. This supplemented medium was then referred to as complete TC100 medium and was stored at 4°C, in the dark.

2.5.8. Growth and maintenance of insect cell cultures:

All plastic flasks, petri dishes and pipettes were sterile wrapped and of cell culture quality. The insect cells were routinely grown at 28°C, with complete TC100 medium. For most purposes the cells were maintained as a monolayer although occasionally where larger volumes of cells were required spinner cultures were used (see L.A.King and R.D.Possee, 1992, for details of other culture methods). Cell culture work and virus infections were always carried out in separate Class II microbiological safety cabinets to remove the possibility of contaminating stock cells with virus.

For routine passage cell monolayers were seeded at a density of 6×10^6 cells in a volume of 40ml of complete TC100 medium per T162 flask and inspected under a microscope (x10 and x40 magnification) at intervals. The doubling time was approximately every 24hours. If the cells were round, healthy and confluent they were passaged, if the cells were over confluent and "sausage" shaped they were

discarded. Since healthy cells firmly adhered to the culture flasks it was possible to remove the medium containing any cell debris and replace it with 20ml of fresh medium. The cells were then dislodged by gentle scraping with a commercially available sterile cell scraper. An aliquot of this cell suspension was removed for counting and estimating the viability of the cells.

For the growth of cells in spinner cultures a Techne biological stirrer was used. To seed the flasks cells were added with complete TC100 medium to give a final volume of 50ml at 1×10^5 cells/ml. The cells were then placed at 28°C and stirred slowly at 30-40rpm. The cells were sampled daily for counting and harvested or passaged when the cell density reached $2-3 \times 10^6$ cells/ml.

2.5.9: Counting the Sf9 cells:

0.2ml of cells in suspension were counted using an improved Neubauer counting chamber after staining with an equal volume of trypan blue stain. Live cells were distinguished from dead cells by their ability to exclude the stain. The number of cells was determined by counting cells in the central large gridded area of the chamber ($1\text{mm}^2 \times 0.1\text{mm}$ depth, divided into 25 squares). Two areas of this size were counted and the number of cells averaged, then multiplied by the dilution factor (2 in this case). The count was then multiplied by 10^4 to obtain the number of cells/ml:

$$\text{i.e. } \frac{\text{count A} + \text{count B}}{2} \times 2 \times 10^4 = \text{number cells/ml}$$

Cell viability was generally about 80-90%.

2.5.10. Freezing, storage and recovery of Sf9 cells in liquid nitrogen:

On receipt of the Sf9 cells they were harvested at a low passage number from monolayer cultures into a small volume of fresh complete TC100 medium. This was achieved by pelleting the cells at a slow speed (500-800rpm) for 5 minutes and resuspending in fresh TC100 medium. Cells were only used for freezing if viability exceeded 90%. The cell concentration was adjusted to 5×10^6 cells/ml with complete

TC100, plus 10% DMSO. Cells were then aliquoted to suitable sterile cryogenic vials and placed at -70°C overnight. After 24 hours the cells were transferred to liquid nitrogen storage. In order to confirm successful freezing of the cells after 2 weeks one of the vials was removed from liquid nitrogen and thawed rapidly by hand. The tube was then swabbed with 70% alcohol and the cell suspension transferred to a T75 flask in a tissue culture hood and 15ml of complete TC100 medium added. The cells were incubated at 28°C for 24 hours and then the medium was replaced with fresh complete TC100. When the cells became confluent they were subcultured in the usual manner, see above.

2.5.11. Preparation of glutathione-agarose (GA) - beads:

GA-beads were prepared as follows; 85mg of GA-beads corresponding to 1ml packed volume, was weighed into a 15ml conical tube (Falcon) to which 15 ml of PBS was added. The tube was incubated on a rotator at 4°C for 30 minutes, after which the beads were pelleted (500g, 4°C , 3 minutes) and washed with ice-cold PBS. This wash was repeated for a second time and the beads were left with 4ml of PBS as a 20% (v/v) slurry. 0.1% (v/v) of sodium azide was added and the beads were stored at 4°C . Prior to use the beads were always washed in the buffer to be used for the subsequent experiment. A needle (gauge 19) and syringe was found to be the best method to remove any traces of wash buffer from the beads.

2.6. Baculovirus protocols- Experimental methods:

2.6.1. Transfection of *Spodoptera frugiperda* (Sf9) insect cells to generate recombinant baculoviruses:

The virus used for the transfection of *Spodoptera frugiperda*, Sf9, insect cells was termed PAK6. This baculovirus contained a *lacZ* gene under the control of the polyhedrin promoter, which allowed blue/white selection of recombinant viruses. The gene of interest was cloned into a transfer vector (pAcCL29, pAcES or pAcGST) which contained flanking viral sequences. Following cotransfection, homologous recombination occurred generating a virus containing the gene of interest under the control of the polyhedrin promoter. The polyhedrin promoter is a

late promoter which allowed the expression of recombinant proteins, such as the Src tyrosine kinases, which may have otherwise been toxic to the cells.

Prior to infection, to reduce the contamination of wildtype virus within the final recombinants, the baculoviral DNA was linearised at Bsu36I restriction sites within the *lacZ* gene and a downstream essential gene. This ensured that the only circularised, and hence infectious, virus genomes were those that had undergone recombination with the transfer vector, which replaced the essential gene coding sequence (Kitts and Possee, 1993). As detailed below lipofectin was then used to transfect these recombinant baculoviruses into Sf9 cells. Following this a plaque assay was performed on the supernatant obtained from the infected cells and single recombinants expressing the proteins of interest isolated. Protein expression was verified by using the plaques picked at this stage to infect Sf9 cells in a 24 well plate, these were subsequently harvested, lysed and protein expression determined by western blot analysis.

2.6.1.1. Preparation of viral DNA:

For each transfection of Sf9, insect cells, 200ng of wildtype baculoviral DNA (PAK6) was used. To linearise the DNA it was digested with an excess of Bsu36I (50U/ μ g DNA) and incubated at 37°C overnight. A small aliquot of the linearised DNA was run on a 0.8% (w/v) agarose gel (see molecular biology section 2.2) to confirm the digestion. Linearised DNA entered the gel whereas uncut DNA remained in the loading wells of the gel. Bsu-36I was inactivated by heating at 65°C for 10 minutes.

2.6.1.2. Transfection of Sf9 insect cells:

35mm culture dishes were seeded with 10^6 Sf9 cells in 2ml of complete TC100 medium. Sufficient dishes for the number of virus samples to be analysed and two for controls, mock and AcMNPV infected, were included. To give the cells time to adhere to the dishes they were incubated at 28°C overnight. The following day the cells were washed twice with 2ml of TC100 medium only, with no serum or antibiotics and left with 1ml of this unsupplemented medium.

The following step was carried out in a polystyrene container, either a bijou or a universal. For each transfection the linearised viral DNA (200ng) and plasmid DNA (1µg) were mixed in a total volume of 10µl, to this an equal volume of lipofectin (2:1,-lipofectin:H₂O) was added. The mixture was incubated at room temperature for 20 minutes. This was then added to the cells and incubated at 28°C for 4-5 hours after which 1ml of complete TC100 medium was added. The cells were incubated at 28°C overnight and the dishes placed in a sealed box to prevent them from drying out. The medium was changed to 2ml complete TC100 the following morning, the virus was harvested 2 days later.

2.6.1.3. Plaque assay to harvest the recombinant virus:

To harvest the virus the cells were resuspended by gentle pipetting and the suspension transferred to sterile micro-centrifuge tubes. These were then centrifuged at 6.5K in a microcentrifuge and the transfection supernatant containing the virus was removed and filtered through a 0.22µm filter (Costar, Spin-ex® columns). The supernatant containing the virus was then plaqued as follows to isolate the recombinant virus (*lacZ*-) from any *lacZ*+ virus still present: 35mm culture dishes were set up containing 10⁶ Sf9 cells in 2ml TC100 medium and allowed to adhere overnight. The following day the medium was removed and the virus was added to the cells either neat or at a dilution of 10⁻¹ (dilutions were made in TC100 medium), in a volume of 100µl and rocked at room temperature for 1 hour. The inoculum was removed and 2ml of a mixture (1:1 ratio) of 3% LMP (low melting point) agarose in H₂O (warmed to 45°C) and complete TC100 medium (room temperature) was added and allowed to set. Once set the agarose was overlaid with 2ml of complete TC100 medium. The plates were incubated at 28°C for 3-4 days.

To visualise the plaques in the Sf9 monolayer the plates were stained with 0.5ml per plate of neutral red viable cell stain, containing X-gal. The stain was added to each plate for 1 hour at 28°C. The supernatant was poured off and the plates inverted and left to stand in the dark, at room temperature, overnight. Any plaques formed

by recombinant viruses were white since they lacked the *lacZ* gene. Six white plaques per transfection were picked using fresh, sterile, plastic pastettes (Alpha Laboratories, Eastleigh, Hampshire, UK) and dispensed into separate bijoux containing 1ml of complete TC100 medium. The bijoux were vortexed to resuspend the virus and stored at 4°C.

2.6.2. Verifying expression of the protein of interest by the recombinant baculovirus:

A 24 well plate was seeded with 10^5 Sf9 cells per well. Once the cells had adhered to the plate 500µl of each resuspended virus (from the previous plaque picks) was added to the cells, the plate was sealed and incubated at 28°C. The cells were harvested 5-6 days later and transferred, by gentle pipetting, to screw-topped micro-centrifuge tubes. The cells were pelleted in a microcentrifuge, 6.5K, 5 minutes, the supernatant containing the virus was removed and stored at 4°C. The cell pellet was washed in PBS and repelleted as previously. The cells were resuspended in 100µl 1xGLB lysis buffer containing protease inhibitors and incubated on ice for 30 minutes. The cell debris was then pelleted in a microcentrifuge, 13K, 5 minutes and the lysates transferred to fresh tubes. 10µl of each lysate was analysed for protein expression by Western blot (see protein protocols, 2.8, for method). The lysates were stored at -20°C. Recombinant viruses expressing the proteins of interest were selected for expansion.

2.6.3. Large scale production of viral stocks:

Having obtained a purified recombinant baculovirus expressing the protein of interest it was necessary to build up a large working stock of the virus. (This method was scaled up when large amounts of virus was required for purification of GST-fusion proteins). 100µl of the stored supernatant from the second round 24-well assay was used to infect a T75 flask previously seeded with 5×10^6 Sf9 cells. After 7 days incubation at 28°C the medium was harvested, cell debris pelleted (500g for 5 minutes) and the supernatant filtered through a 0.22µm filter. This working virus stock generally contained between 10^7 and 10^8 plaque forming units (pfu) per ml (verified by plaque assay, see below) and was used to bulk up further

by infecting larger amounts of cells (e.g. 1.5×10^7 in a T162) at 0.1 pfu/cell. Again the virus was harvested after 7 days. At this stage some of the virus was aliquoted into 1ml amounts and stored in sterile eppendorfs at 4°C to form the working virus stock or frozen overnight at -70°C and then transferred to liquid nitrogen for longer term storage.

2.6.4. Plaque assay for virus titre:

Sufficient 35mm culture dishes were seeded with 10^6 Sf9 cells for the following titrations to be carried out in duplicate. Dilutions of the recombinant viruses were made (10^{-4} , 10^{-5} and 10^{-6}) in complete TC100 medium. The medium was removed from the Sf9 cells and 100µl of each dilution was added to the cells, as detailed previously in the plaque assay for harvesting the recombinant virus, 2.6.1.3. After 3-4 days the plaques were stained with neutral red viable cell stain and counted to determine the virus titres in pfu/ml (plaque forming units per ml). Virus titres were typically in the order of 10^7 pfu/ml. An example calculation is shown below:

e.g. If a 100µl seed at 10^{-5} dilution gave 20 plaques, 1ml would give 200 or 2×10^2 plaques at the same dilution. Therefore the undiluted virus titre is $10^5 \times (2 \times 10^2) = 2 \times 10^7$ pfu/ml.

2.6.5. Production of Sf9 cell lysates:

Typically monolayers of cells were used for virus infections. Flasks or dishes were seeded with the appropriate number of cells to yield subconfluent monolayers. These subconfluent cells were infected at a high multiplicity of infection (3-10 pfu/cell) for optimal protein expression. The medium was removed from the cells and the viral inoculum added and rocked for 1 hour at room temperature. For protein production the viral inoculum was not removed before the addition of complete TC100 medium. The cells were incubated at 28°C for 3-4 days. Cells were harvested to 15ml conical tubes by gentle pipetting, centrifuged (500g, 5 minutes, 4°C) and washed with 1ml of ice cold 1xPBS. The cells were transferred to screw-topped micro-centrifuge tubes and repelleted in a microcentrifuge (6.5K, 3 minutes) and finally resuspended in the appropriate amount of 1xGLB lysis buffer (see table). Cells were then incubated on ice for 30 minutes, cell debris was pelleted in a

microcentrifuge, 13K, 5 minutes and the lysate transferred to fresh screw-topped eppendorfs. Lysates were stored at -20°C.

2.6.5.1. Single baculovirus infections: The table below provides a guide to the equivalent volumes of virus: cells for the different scales of lysate production.

Table 2.7. Volumes used for different culture dishes/flasks:

Size of dish/flask	Number of cells o/n	Inoculum vol. min / max	Medium vol.	1xGLB vol.
35mm dish	1.0 x10 ⁶	0.1 / 0.5 ml	2ml	50-100µl
25cm ² flask	5.0 x10 ⁶	0.4 / 1.0 ml	5ml	150-500µl

2.6.5.2. Coinfections: Coinfections were essentially the same as single infections and were always carried out within the parameters of the table above. Care was taken to keep infection volumes equal within experiments, since different inoculum volumes were shown to affect efficiency of infection.

2.6.6. Purification of affinity reagents:

2.6.6.1. Large scale virus infections for GST-fusion protein purification:

In general subconfluent cells were infected at a high multiplicity of infection (3-10pfu/cell) for optimal protein expression. For each protein purified approximately 5xT162 flasks seeded with 2x10⁷ Sf9 cells in 30ml of medium were set up several hours prior to infection. The medium was removed and the viral inoculum added (3-10 pfu/cell, i.e. 6x10⁷ to 2x10⁸ pfu in total) in a final volume of 5ml. After the standard 1 hour rocking 30ml of complete TC100 medium was added to the flasks which were then incubated for 3 days at 28°C.

2.6.6.2. Lysis of infected cells and purification of GST fusion proteins:

The cells were harvested by agitating the flasks and gently pipetting several times, the cells were pelleted by centrifugation at 500g, 10 minutes, 4°C. The cell pellet was washed twice with 10-20ml of PBS by gently resuspending with a 10ml pipette

and then pelleted again (500g for 10 minutes, 4°C). Since the proteins used in this study were all cytoplasmic the cells were lysed in 1ml/flask of PBS containing 1% (v/v) TritonX-100 and protease inhibitors, for 30 minutes on ice. The cell debris was pelleted, 9K in sarstedt tubes (Sarstedt, Leicester), 4°C, 20 minutes and the supernatant transferred to a fresh 15ml polypropylene tube containing 1ml of preswollen GA-beads (see materials 2.5.11.). The lysate was incubated with the GA-beads at 4°C for 1 hour with constant mixing on a rotating wheel.

The beads were pelleted (500g for 3 minutes, 4 °C) and washed twice with >10 volumes of ice cold lysis buffer. The beads were then washed a further 4 times with ice cold 50mM Tris-HCl pH 8.0. During each wash the beads were resuspended by gentle inversion. After the last wash the beads were resuspended in 10 volumes of 50mM Tris-HCl pH 8.0 and poured into a 1ml disposable chromatography column (Biorad, polyprep). The column was allowed to pack but care was taken not to let it dry out. The fusion protein was eluted by adding 10x 250µl amounts of 50mM Tris-HCl pH8.0 containing 5mM reduced glutathione. Fractions were collected and each was assayed for protein content by Bradford assay (see 2.7 protein protocols). Fractions containing the protein were pooled and dialysed (visking tubing from BDH) overnight against two changes of 50mM Tris-HCl pH8.0. The integrity of the protein was verified by SDS-PAGE followed by Coomassie staining (see section 2.8). The protein was aliquoted and stored at -70°C in 100µg amounts.

2.6.7. *In vitro* binding assay:

Purified Nef-GST fusion proteins were used to investigate interactions with cellular proteins in a series of *in vitro* pulldown studies. The Nef-GST fusions were immobilised on GA-beads to act as affinity reagents in the experiments. Whole cell lysates containing the Src tyrosine kinases and other control proteins were precleared with GA-beads alone prior to the pulldowns with the affinity reagents. Once the pulldowns had been completed the results were analysed by western blot. The presence of both the proteins in the interaction was verified by stripping and reprobing the PVDF membrane, (see protein 2.8, protein protocols) with a second antibody.

2.6.7.1. Binding the purified protein to glutathione agarose (GA) beads:

To immobilise the purified GST fusion proteins on GA beads, 100µg of the protein was added to 50µl packed volume of GA-beads (final ratio of 2µg protein per 1µl packed beads). The total volume of the protein was made up to 100µl with 50mM Tris pH8.0, to ensure efficient mixing. The mixture was incubated on a rotating wheel (Blood mixer) at 4°C for 2 hours. Subsequently the beads were washed twice with 1ml 50mM Tris-HCl pH8.0. For immediate use the beads were resuspended (1:5, beads:buffer) in 1xGLB lysis buffer, however for storage at 4°C the beads were resuspended in 50mM Tris-HCl pH8. To confirm that the various proteins had bound equally to the GA beads, 5µl packed volume of beads were heated to 90°C in sample buffer and then analysed by SDS-PAGE and Coomassie staining (see 2.8, protein protocols).

2.6.7.2. Binding assay:

Unless otherwise stated for each binding assay 5µl of whole cell lysate was used. The lysates were precleared with GA-beads alone prior to the pulldowns. Generally 10µl of packed volume of GA-beads was used per pulldown and the volume made up to 100µl using 1xGLB containing protease inhibitors. If increased stringency was required the pulldowns were performed in the presence of 0.5M KCl, 5µl of lysate plus 1xGLB, 0.5M KCl. An aliquot of precleared lysate was taken and frozen at -20°C. The samples were precleared for 30 minutes, rotating, at 4°C. After preclearing the samples the beads were pelleted in a microcentrifuge at 6.5K for 30 seconds. 100µl of the supernatant was carefully transferred, using fine pipette tips to avoid carry over of beads, to 10µl packed volume of each of the affinity reagents. These were then incubated on a rotator at 4°C for 3 hours.

To remove any unbound protein the beads were washed several times in 1xGLB. If 0.5M KCl was used for higher stringency, the beads were washed 3 times in the increased salt wash and once in GLB alone (to remove the salt prior to electrophoresis), otherwise 4 washes in GLB alone was sufficient. The beads were then resuspended in sample buffer and analysed by Western blot.

2.6.8. *In vivo* binding assays:

Coinfections of the Src tyrosine kinases plus Nef-GST fusions were carried out as detailed above, 2.6.5.2. The *in vivo* pulldown assay was essentially the same as the *in vitro* pulldown assay, except a preclear step with GA-beads alone was not possible. As a result of this high stringency conditions were always used. Typically 40 μ l of the coinfection lysate was added together with 10 μ l of 1xGLB adjusted to 2.5M KCl and 50 μ l 1xGLB, 0.5M KCl to give a final salt concentration of 0.5M KCl. 10 μ l of packed volume of GA-beads alone was used as the affinity reagent in these pulldown assays. The samples were incubated for 3 hours, with rotating at 4°C and then washed 3 times with 1xGLB, 0.5M KCl, followed by one wash with 1xGLB to remove the salt. 15 μ l of 1x sample buffer was then added to the beads. The samples were then either frozen at -20°C or immediately analysed by western blot.

2.6.9. Metabolic labelling:

Radiolabelling was carried out in 35mm dishes, cells were infected as described, 2.6.5. After 24hours the medium was replaced with TC100 medium without methionine, containing 1% dialysed foetal calf serum (dialysed against PBS and stored at -20°C) and 50 μ Ci/ml ³⁵S or 100 μ Ci/ml ³H myristic or palmitic acid were added, cells were harvested as standard into 1xGLB and analysed by SDS-PAGE dried down and autoradiographed. In some cases samples were immunoprecipitated to enhance specific signals.

PROTEIN BIOCHEMISTRY:

2.7. Protein biochemistry- Materials:

2.7.1. Chemicals and enzymes:

Chemicals and reagents, including abbreviations, specific to this section can be found below. Any general chemicals will be found at the start of this chapter.

Table 2.8. Chemicals and enzymes for protein protocols including abbreviations and companies purchased from:

Chemical/Enzyme	Company
Secondary antibody conjugates Protein A agarose beads (Prot-A) Protein G agarose beads (Prot-G) Reduced glutathione	SIGMA, Poole, Dorset, UK
β -mercaptoethanol Coomassie Glycine Methanol Trichloroacetic acid (TCA) Tween 20 Anti-foam	BDH, Poole, Dorset, UK
Enhanced chemiluminescence detection reagents (ECL)	Amersham Life Science
Marvel (dried skimmed milk)	Local supermarket
Polyvinylidene difluoride (PVDF)	Millipore
Isopropyl-thio- β -D Galactopyranoside (IPTG)	Melford Labs. Ltd, Ipswich, UK

2.7.2. Radiochemicals:

[$\gamma^{32}\text{P}$] ATP, specific activity, 10Ci/mmol (10mCi/ml), for peptide substrate assays, supplied by Amersham Life Sciences.

2.7.3. Stock solutions:

Bradford's Reagent (5x): 10mg Coomassie, 5ml 95% (v/v) EtOH, 10ml 85% (v/v) orthophosphoric acid, made up to 100ml with ddH₂O. To avoid traces of phosphate detergents in glassware, this was made entirely in sterile 50ml polypropylene tubes. It was stored at room temperature in the dark. Before use filtered with a 0.22µM filter and diluted to 1x as required again avoiding all glassware.

Affinity reagents: Beads were stored in PBS containing 0.1% (w/v) sodium azide at a 1:5 ratio of beads:buffer. Prior to use the beads were aliquoted to give the required packed volume and washed with the buffer to be used in the subsequent experiment. A needle (gauge 19) and syringe was used to aspirate the buffer. Prot-G was used for rat and mouse antibodies, but Prot-A was used for rabbit antibodies.

SDS-PAGE loading buffer (sample buffer) (5x): 125mM Tris-HCl pH6.8, 40% (v/v) glycerol, 4% (w/v) SDS, 10% (v/v) β-mercaptoethanol, 0.05% (w/v) bromophenol blue, in ddH₂O. Stored at room temperature.

2.8. Protein biochemistry- Experimental methods:

2.8.1. SDS-PAGE (sodium dodecyl sulphate-poly-acrylamide gel electrophoresis) analysis:

The Biorad minigel system (Mini-Protean) was used for protein electrophoresis. Stock solutions were made of the following, which were diluted as required:

Ammonium persulphate: 10% (w/v) stock solution, stored at 4°C.

Resolving gel buffer (5x): 1.875M Tris, 0.5% (w/v) SDS, pH8.5 with conc.HCl stored at room temperature.

Stacking gel buffer (10x): 1.25M Tris, 1% (w/v) SDS, pH6.5 with conc. HCl, stored at room temperature.

Running buffer (5x): 0.25M Tris, 1.92M glycine, 0.5% (w/v) SDS, stored at room temperature.

In general 12.5% acrylamide gels gave sufficient resolution however when smaller polypeptides were being analysed a 17.5% gel was used. The acrylamide was bought as a 30% acrylamide, 0.8% bis-acrylamide, stock from Scotlab. The glass plates were cleaned thoroughly with 70% ethanol before the protein rigs were assembled. The resolving gel was then poured (12.5% acrylamide, 1x resolving gel buffer, plus per 10ml- 100µl APS, 10µl TEMED) and overlaid with water-saturated butanol, to ensure a flat interface. Once the gel had set the butanol was poured off and any traces removed with ddH₂O, the plates were dried with 3MM filter paper. The stacking gel (6% acrylamide, 1x stacking gel buffer, plus per 5ml- 50µl APS, 7.5µl TEMED) was then added and the comb carefully inserted. The comb was removed after polymerisation and the wells washed with 1x running buffer. Sample buffer was added to the protein and then the tubes were heated to 90°C for 2 minutes prior to loading. Seeblue pre-stained protein standards (Novex, USA) were run alongside the samples which as well as providing an indication of the size of the proteins also transferred to the PVDF membrane. ¹⁴C Rainbow markers from Amersham Life Sciences were run for radioactive samples.

2.8.2. Coomassie staining:

Gels were soaked in Coomassie stain (0.2% w/v Coomassie stain, 50% v/v methanol, 5% v/v glacial acetic acid) for 30 minutes and then destained in 50% (v/v) methanol, 5% (v/v) glacial acetic acid, until the bands became visible.

2.8.3. Radioactive gels:

Gels were soaked in destain, see Coomassie staining, for 5 minutes followed by 5 minutes soaking in "Enlightening", from Dupont, NEN, which amplifies the radioactive signal. The gels were subsequently dried under vacuum for 15 minutes at 80°C and autoradiographed.

2.8.4. Western blot analysis:

2.8.4.1. Transfer to PVDF membrane:

As PVDF membrane is hydrophobic it was first wetted in 100% methanol and then rinsed in ddH₂O, before equilibrating in transfer buffer (25mM Tris, 137mM Glycine, 20% v/v methanol). A Biorad Semi-Dry blotting apparatus was used to transfer the proteins from the SDS-PAGE gel to the PVDF as outlined in the instructions, for 30 minutes at 15volts. The membrane was then either immediately western blotted or sealed in a bag and stored at 4°C overnight.

2.8.4.2. Western blot:

The membrane was blocked for 30 minutes, room temperature, shaking, in 1x TBS-T (20mM Tris pH 7.6, 137mM NaCl, 0.1% v/v Tween) containing 10% (w/v) Marvel, followed by one rinse in TBS-T, and 5 minutes wash in TBS-T. The primary antibody was added at the appropriate dilution (see table 2.7.1) in TBS-T containing 5% Marvel, for 1 hour, with shaking (~40-60rpm). The antibody was removed and the membrane rinsed in TBS-T followed by one 5 minute wash and one 15 minute wash in TBS-T. The secondary antibody, horse radish peroxidase conjugated, was added at a dilution of 1 in 2000, except where otherwise stated, in TBS-T containing 5% Marvel. This was incubated for a further 30 minutes, shaking after which the membrane was washed thoroughly (4x 5minutes TBS-T) and the bound antibody visualised using the ECL detection system, as detailed in the manufacturers instructions.

2.8.4.3. Reprobing the membrane:

Antibodies were stripped from the blot by incubating the membrane in strip buffer (100mM 2-mercapto-ethanol, 2% w/v SDS, 62.5mM Tris pH6.8). This was carried out in a hybridization oven (Hybaid) with continuous rotation, at 60°C for 30 minutes. The membranes were then washed thoroughly in TBS-T (2x 30 minutes) before western blotting with an alternative antibody.

Table 2.9. Antibodies used in the studies, suppliers and amounts used:

Antibody (Ab)	Raised to	Supplier	Amount for i.p.	Dilution for western blot	Secondary Ab
Nef 1378 polyclonal	Bacterial expressed GST-Nef.	In house	n/a	1 in 20,000	α -sheep
Nef N-term Monoclonal	Bacterial expressed Nef.	In house	7 μ l	1 in 5,000	α -mouse
Nef 2/81c	Myristoylated Nef-6HIS.	Dr. J. McKeating, University of Reading, UK.	10 μ l	n/a	n/a
Lck 95	Peptide corresponding to residues 478-509 of murine Lck.	Dr. M. Marsh, University College London, UK	5 μ l	1 in 10,000	α -rabbit
Lck 97	Peptide within unique N-terminus	Dr. M. Marsh	5 μ l	n/a	α -rabbit
Hck (N-30) Polyclonal	Peptide corresponding to amino acids 8-37 of human Hck.	Santa-Cruz Biotechnology Inc., Wiltshire, UK. (cat. sc-72)	15 μ l	1 in 1,000	α -rabbit
Hck- MAb	33KDa protein fragment corresponding to amino acids 2-300 of human Hck.	Affiniti, Exeter, UK. (cat. H28520)	n/a	1 in 1,000	α -mouse
Fyn-MAb	Peptide corresponding to amino acids 85-206 of human Fyn.	Santa-Cruz Biotechnology Inc. (cat. sc-434)	n/a	1 in 1,000	α -mouse
Src	Peptide corresponding to amino acids 3-18	Santa-Cruz Biotechnology Inc. (c	n/a	1 in 1,000	α -mouse
pTyr-MAb (PY69)	Phosphotyrosine peptides	Santa-Cruz Biotechnology Inc. (cat. sc-21)	n/a	1 in 1,000	α -mouse
GST	Bacterial expressed GST	In house	n/a	1 in 500	α -mouse

2.8.5. Immunoprecipitation:

Lysates (in GLB) were adjusted to 0.5M KCl and incubated overnight at 4°C, on a rotator with the appropriate antibody. The following morning lysates were transferred to fresh tubes containing 10µl packed volume of either Prot-A or Prot-G beads, these were incubated for a further 4hours at 4°C. To reduce background a pre-clear step (30 minutes, rotating, 4°C), using the protein A or G beads, was utilized prior to incubating with the antibody. After precipitation the beads were washed 3 times using 1x GLB/0.5M KCl and 1x GLB (see section 2.5 lysis buffers) before resuspending in 15µl of sample buffer and analysis by SDS-PAGE.

2.8.6. Bradford Assay:

A standard curve using different amounts of BSA in duplicate (0-5µg) were pipetted into a 96 well plate in a volume of 10µl in 50mM Tris-HCl pH8.0. Samples to be analysed were also diluted into 10µl of 50mM Tris in duplicate. To each well 100µl of 1x Bradford reagent was added. Binding of Coomassie brilliant blue in the Bradford reagent to protein present in the samples causes a shift in the absorption maximum of the dye from 465 to 595nm (Bradford, 1976). The absorption of each of the wells at OD₅₉₅ can therefore be read and a standard curve plotted for the known concentrations of BSA. The standard curve was then used to work out the concentration of the sample proteins by using their absorption values to read off the amount of protein in mg/ml.

2.8.7. *In vitro* transcription-translation:

Coupled *in vitro* transcription-translations were carried out using Trans ³⁵S-Label™ and a TNT™ T7 Coupled Rabbit reticulocyte lysate kit supplied by Promega. Genes cloned into pSG5 plasmids under the T7 promoter (kindly donated by K.Coates) or pCR™ were (see 2.1) used as the template in this assay. Reactions were carried out in 50µl volume, 2.5µl Trans ³⁵S-Label™ and 1µg plasmid were added per sample. The reaction was incubated for 90 minutes at 30°C. Subsequently CaCl₂ was added to a 2.5mM final concentration, together with 0.1mg/ml RNaseA, the reactions were incubated for a further 15 minutes at 37°C.

2.8.8. Autophosphorylation Assay:

1 μ l of lysate was typically added to 20 μ l of kinase buffer (20mM PIPES pH7.2, 3.5mM MgCl₂, 3.5mM MnCl₂, 1mM NaOV) either plus or minus 10 μ M ATP. This was then incubated at 30°C for 30 minutes. The reaction was stopped by the addition of sample buffer to a 1x concentration. The samples were then analysed by Western blot using an anti-phosphotyrosine antibody.

2.8.9. Protein kinase assays:

Kinase activity assays were performed at 30°C in buffer containing 20mM Tris, pH7.5, 10mM MgCl₂, 800 μ M peptide substrate (RRLIEDAHYAARG), [γ ³²P] specific activity 10Ci/mmol (10mCi/ml) and 500 μ M ATP. This peptide has been reported to be an efficient substrate for Src family kinases, K_m=240 μ M for Src (Moarefi et al., 1997; Casnellie, 1991). Generally 3 μ l of lysate was added to an 80 μ l reaction volume. 10 μ l aliquots were removed from the reaction mix at time points required and the reactions terminated by the addition of an equal volume of cold 10% (w/v) TCA. These were briefly centrifuged and the supernatants spotted onto phosphocellulose paper, (Whatmann-P81), as described (Casnellie, 1991). The phosphocellulose pads were washed 5x 5 minutes in 400ml of 150mM phosphoric acid, rinsed in ethanol, dried and counted in a scintillation counter to measure the incorporation of ³²P into the peptide. Reactions were always carried out in duplicate. The activity of the kinase enzyme was measured in pmols of phosphate transferred to the peptide, which was calculated as follows:

The chemical concentration of the stock was calculated using the formula;

$$\text{Specific activity (mCi/mmol)} = \frac{\text{Radioactive concentration (mCi/ml)}}{\text{Chemical concentration (mmol/ml)}}$$

e.g.

Specific activity of the stock = 10Ci/mmol = 10,000mCi/mmol

and the radioactive concentration = 10mCi/ml

therefore, the chemical concentration = 10/10,000 = 1x10⁻³mmol/ml = 1 μ mol/ml

CHAPTER 3

CHAPTER 3

Use of the yeast interaction trap to investigate novel cellular interactions with HIV-1 Nef.

	Page number
3.0 General introduction	117
3.1 Results	120
3.2 Modification of bait plasmid to accept proteins as N-terminal fusions	121
3.3 Verification of expression and myristoylation of Nef from pVEG	125
3.4 Activation and repression assays to determine the suitability of pVEG-Nef as a bait in an interactor hunt	128
3.5 Screening a Jurkat T-cell library with pVEG-Nef for novel protein-protein interactions	132
3.6 Further investigation of groups A1, B1 and C1- sequence data and specificity tests	139
3.7 Further analysis of the Nef-A1 p9 interaction	152

CHAPTER 3: Use of the yeast interaction trap to investigate novel cellular interactions with HIV-1 Nef.

3.0. General introduction:

To date the function of Nef *in vivo* remains elusive although a variety of *in vitro* roles have been proposed. These include the downmodulation of expression of cell surface CD4, enhancement of HIV infection and disruption of cell signalling pathways. To understand how Nef can mediate these pleiotropic effects, attention has turned to the cellular proteins with which Nef interacts. A variety of interacting partners for Nef have been described, including CD4 (Harris and Neil, 1994; Rossi *et al*, 1996; Grzesiek *et al*, 1996b); the Src kinases- Lck (Collette *et al*, 1997; Collette *et al*, 1996b), Hck (Lee *et al*, 1995; Grzesiek *et al*, 1996a; Moarefi *et al*, 1997), Src (Lee *et al*, 1995) and Fyn (Arold *et al*, 1997); various serine kinases including, NAK (Nef associated kinase) (Sawai *et al*, 1994; Sawai *et al*, 1995; Baur *et al*, 1997) MAPK (Greenway *et al*, 1995; Greenway *et al*, 1996), θ PKC (Smith *et al*, 1996) and δ PKC (Saksela, 1997); β -COP (Benichou *et al*, 1994); HsN3 (Rossi *et al*, 1997); p53 (Greenway *et al*, 1995); and a novel acyl Co-A thioesterase (Watanabe *et al*, 1997; Liu *et al*, 1997). Despite the growing repertoire of Nef cellular interactors, there is still no consensus as to the functional significance for Nef *in vivo*.

The Nef interaction with β -COP was identified using the yeast-two-hybrid system (Benichou *et al*, 1994) and has gained recognition due to the Nef mediated increased endocytosis of both CD4 (Anderson *et al*, 1993; Rhee and Marsh, 1994; Schwartz *et al*, 1995) and MHC class 1 (Schwartz *et al*, 1996). β -COP is a ubiquitous protein found on non-clathrin coated vesicles and is involved in membrane trafficking of proteins. Exactly how a direct interaction with β -COP a non-clathrin endocytic component relates to the recent reports of Nef colocalization with clathrin and the AP-2 adaptor complex is unknown (Mangasarian *et al*, 1997; Greenberg *et al*, 1997; Foti *et al*, 1997). It is however interesting, that Nef mediated endocytosis is specific, leaving other cell surface receptors analysed so far unaffected. This suggests that the co-operation of Nef and the endocytic machinery

results in a targeted mechanism of downmodulation. Proposed mechanisms include, either a direct interaction involving β -COP, AP-2, clathrin or an as yet unidentified protein of the endocytosis machinery, with Nef acting as an adapter-molecule, or via an indirect action, such as perturbation of membrane anchoring caused by a Nef association with for example Lck.

Several studies have demonstrated Nef expression perturbs cell signalling pathways however these studies have been reliant on the monitoring of fluctuations in the expression of activation markers, such as IL-2, CD69, and NF κ B which can vary depending on the level of Nef expression and its subcellular location (Luria *et al*, 1991; Bandres and Ratner, 1994; Baur *et al*, 1994; Greenway *et al*, 1995; Collette *et al*, 1996a; Iafrate *et al*, 1997). The determination of Nef cellular interaction partners would therefore aid in the elucidation of its precise effect on cell signalling pathways. Putative binding partners identified to date include NAK, MAPK, θ PKC, δ PKC and the Src tyrosine kinases. The Nef interaction with NAK was first demonstrated by the coimmunoprecipitation of Nef with two serine phosphorylated proteins, of 62kDa and 72kDa respectively the identity of which remains unknown (Sawai *et al*, 1994; Sawai *et al*, 1995). Although recent studies have provided evidence that NAK is a member of the PAK family of serine kinases (Baur *et al*, 1997; Nunn and Marsh, 1995; Geleziunas *et al*, 1996), data from *in vivo* macaque studies (Lang *et al*, 1997) and from work with other Nef isolates (Luo and Garcia, 1996; Luo *et al*, 1997) has questioned the importance of this kinase association. Significantly, a number of other Nef interactions with serine kinases have now been identified (Greenway *et al*, 1996; Smith *et al*, 1996; Saksela, 1997), one proposal being that Nef retains a non-specific ability to recognise a variety of serine kinases (Swingler *et al*, 1997). If the latter hypothesis is accurate the elucidation of a wide range of Nef serine kinase interactions might be anticipated. Furthermore, the identity of the co-immuno-precipitates and whether these would remain the same for alternative serine kinases is unknown.

Currently, no direct interaction of Nef has been identified that exerts an effect on both CD4 downmodulation and infectivity, although these remain the most

conserved Nef phenotypes. Interactions of Nef with the Src tyrosine kinases represents an attractive explanation for the pleiotropic functions ascribed to Nef, due to their key role in signal transduction pathways and physical association with cell surface receptors. In addition high concentrations of the Src kinases have been identified in Triton insoluble complexes, indicative of associations with GPI-linked proteins, caveolae and the endocytic pathways (see section 4.1). However, the downstream affect of Nef interactions with the Src kinases *in vivo* is unknown. By elucidating cellular factors capable of binding Nef an insight into the repercussions of the Nef-Src kinase interaction may also be gained.

Evidence that Nef is capable of binding a number of cellular proteins potentially forming a complex has been provided by a number of studies (Harris and Coates, 1993; Cullen, 1996; Baur *et al*, 1997). By building a profile of these Nef cellular binding partners and the factors important for the interactions such as myristoylation or full length Nef expression a clearer picture of its role in viral pathogenesis will be obtained. To this end, we used the yeast-two-hybrid system to help elucidate novel protein interactions with Nef. The yeast-two-hybrid system (YTHS) was developed by Fields and Song (Fields and Song, 1989; Fields and Sternglanz, 1994). It was based on the observation that the yeast transcriptional activation protein, GAL4 was comprised of 2 domains that did not need to be covalently attached to cause transcription initiation. The first domain was the DNA binding domain (DB domain), which specifically recognised upstream activating sequences (UAS), the second a transcriptional activation domain, (TA domain). The crucial observation made by Fields and Song was that these 2 domains could be fused to independent protein sequences and still function as a transcriptional activator if their fusion partners brought them into the same spatial proximity. This functional domain separation has since been identified in other transcriptional activating proteins including the bacterial LexA protein and has led to the development of a variety of yeast-two-hybrid systems, see chapter 2 for details of the interaction trap system utilised for these studies.

The success of the yeast-two-hybrid as a research tool has already been highlighted in the HIV field, with the identification of the interaction between Cyclophilin A and HIV-1 Gag, latterly identified as necessary for the infectivity of the virion (Thali *et al*, 1994; Franke *et al*, 1994). With the aid of the yeast-two-hybrid system it was established that this Cyclophilin A association is dependent on the multimerization of p55 Gag. Further screening of randomly generated Gag deletions identified a minimal consensus region within the capsid (CA) domain necessary in conjunction with the multimerization signal in the nucleocapsid (NC) domain of Gag for binding to Cyclophilin A (Straus and Weiss, 1992; Colgan *et al*, 1996). The cyclophilins were originally identified as the cellular target for the immunosuppressive drug Cyclosporin A, therefore the identification of an interaction with Gag was also of therapeutic significance (Franke and Luban, 1996). The previous success of the yeast-two-hybrid system and its rapid *in vivo* screening of protein-protein interactions hence made it an ideal tool for investigating novel interactions of HIV-1 Nef.

3.1. Results:

As research continues it is becoming more likely that Nef exists in several distinct isoforms within the cell, which may contribute to its pleiotropic effects. It has been well documented that a 27kDa and 25kDa species of Nef exist, the smaller resulting from the initiation of translation from a downstream methionine. It has recently emerged that Nef is incorporated into the virion, where it is specifically cleaved by HIV protease to yield 2 fragments of ~9 and ~18kDa (Welker *et al*, 1996; Pandori *et al*, 1996; Bukovsky *et al*, 1997). The location of the small N-terminal fragment of Nef is yet to be determined. Protease cleavage only occurs in the virion, hence it is the full-length myristoylated Nef species that is present in abundance in infected cells. The only proteins identified to date that exclusively interact with this species of Nef are Lck, CD4 and NAK, the latter of which has been shown to be dispensable *in vivo*. Previous results within the laboratory had demonstrated that interactions of a number of Jurkat T-cell proteins were dependent on Nef myristoylation *in vitro* (Harris and Coates, 1993). To further identify these proteins

a Jurkat T-cell library, kindly provided by Dr R.Brent, was screened for interactions with myristoylated Nef using the yeast-two-hybrid system.

Initially the bait plasmid had to be modified to accept Nef as an N-terminal fusion protein, to allow myristoylation. The stability and myristoylation of Nef as an N-terminal fusion to the DB domain was then confirmed. Subsequently the suitability of Nef as a bait in the system had to be determined using the transcription activation and repression assays. Following this the screening of the Jurkat T-cell library was carried out. Potential cellular interactors with Nef were isolated, sequenced and investigated for the specificity of their interactions with Nef.

3.2. Modification of the bait plasmid to accept proteins as N-terminal fusions:

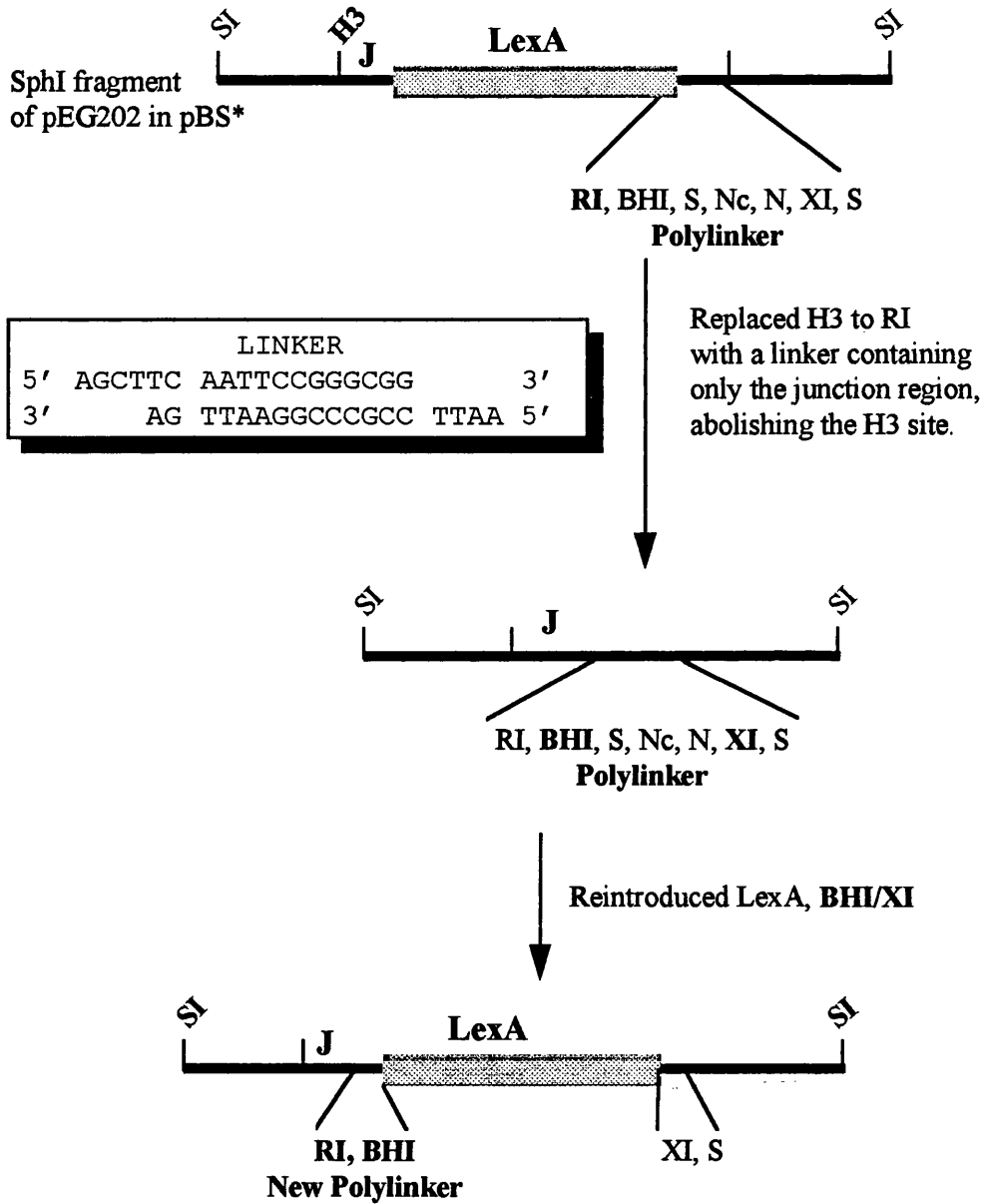
The original yeast interaction trap bait plasmid, pEG202 was constructed by E.Golemis in the lab. of Dr R.Brent, is described in detail in section 2.1. The only restriction site available upstream of the LexA DB domain, which could be used to make N-terminal fusions, was a HindIII site that was not unique. This necessitated the use of an intermediate cloning plasmid, into which a cassette containing the region of DNA for manipulation could be inserted (see figure 3.1 for this cloning process). For this purpose the region of DNA between the two SphI restriction sites (1.4Kb) in pEG202 was subcloned into a pBluescript® plasmid (Stratagene, see section 2.32.1) that had a modified polylinker containing an SphI site (see figure 3.1, step 1, for linker oligonucleotides used to modify pBluescript®). The LexA gene was then removed from the intermediate plasmid using the N-terminal HindIII site and a BamHI site in the polylinker (figure 3.1, step 3). Nef was amplified by PCR to incorporate a HindIII site and the required junction (~10bp) region between the ADH promoter and gene at its N-terminus, and an EcoRI site at its C-terminus. This was cloned into a separate pBluescript® plasmid (step 2). Adjoining Nef downstream in the pBluescript® plasmid was LexA which had been amplified to incorporate EcoRI and BamHI sites at its N- and C-termini respectively (step 2). The integrity of the resultant N-terminal Nef-LexA fusion was verified by *in vitro* transcription-translation from the T3 promoter in pBluescript® (figure 3.2). This

whole Nef-LexA cassette was then introduced into the intermediate plasmid using the HindIII and BamHI sites (step3). The SphI cassette was returned, containing the Nef-LexA cassette, to pEG202 and the resultant construct called pVEG-Nef (see figure 3.1 step 4). Nonmyristoylated Nef (G2ANef) was also cloned using this lengthy process, however a further modified pVEG was later constructed to allow a one step cloning process.

Figure 3.1. *Summary of approach taken to modify the bait plasmid to accept proteins as N-terminal fusions:*

pBluescript® was modified to introduce a unique SphI site with the linkers shown, this was then called pBluescript*. The SphI fragment from pEG202 containing the LexA gene and the polylinker was then subcloned into pBluescript* (step 1). Subsequently Nef was amplified by PCR to incorporate HindIII (H3) and EcoRI (RI) sites at its N- and C-termini respectively, this was cloned into a separate pBluescript® plasmid. LexA was amplified by PCR to contain RI and BamHI (BHI) and cloned adjacent to Nef (step 2). The Nef-LexA cassette was introduced into the pEG202 SphI fragment using the H3 and BHI sites therefore removing the original LexA gene (step 3). The SphI pEG202 fragment was then returned to pEG202 creating the pVEG-Nef plasmid (step 4). This process was repeated to create pVEG-G2A. The insert demonstrates the full length expression of Nef-LexA from the T3 promoter in the pBluescript® expression plasmid during *in vitro* transcription-translation assays, see section 2.8.7 for method. The products were immunoprecipitated with the Nef N-terminal monoclonal antibody and resolved by 12% SDS-PAGE. The gel was subsequently dried and autoradiographed. Lane 1, ¹⁴C rainbow markers, lane 2 Nef-LexA fusion (~55kDa), lane 3 pBluescript® only negative control, pBluescript®-Nef positive control (~27kDa).

Diagram 3.1. Construction of pVEG2:



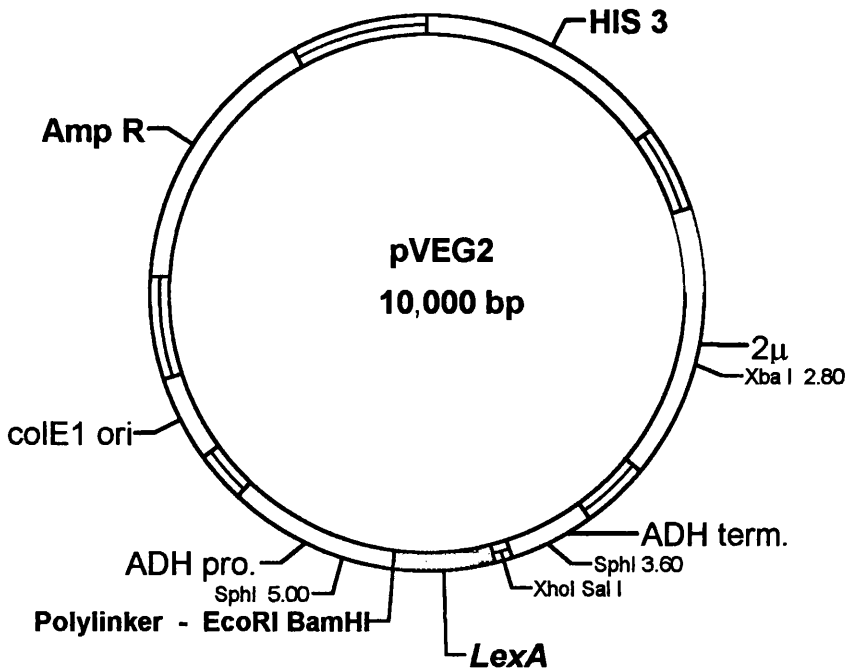
Key: RI-EcoRI, BHI-BamHI, H3-HindIII, Nc-NcoI, N-NotI, S-SalI, XI-XhoI, SI-SphI

In order to reconstruct pVEG to allow a single cloning step, it was necessary to include unique restriction sites between the junction region and the LexA gene. The following steps were carried out in the intermediate modified pBluescript® plasmid containing the 1.4Kb SphI fragment from pEG202. A linker was designed to span from the HindIII site, including the junction region to the EcoRI site at the 5' end of the polylinker. The EcoRI site was reconstituted while the HindIII site was abolished, see diagram 3.1. The linker region was sequenced and then the LexA gene was reintroduced into the original polylinker, after PCR amplification to incorporate BamHI and XhoI sites at its N- and C-termini. Thus maintaining unique EcoRI, SmaI and BamHI restriction sites N-terminal to the LexA gene. The modified SphI cassette was returned to pEG202. When cloning into these unique sites the gene of interest needed to contain an ATG and keep the ATG of the LexA gene in frame, see diagram 3.2. This plasmid was used to clone genes for the library specificity checks and will be referred to as pVEG2.

3.3. Verification of expression and myristoylation of Nef from pVEG:

Previous studies by Macreadie *et al* (Macreadie *et al*, 1993) have demonstrated the myristoylation of Nef in yeast and the ability of myristoylated Nef to enter the nucleus. Studies were performed to confirm that the DNA manipulations had not affected the expression capabilities of the pVEG plasmid and that Nef expressed as an N-terminal fusion to LexA was myristoylated. 5ml cultures of yeast expressing either myristoylated or nonmyristoylated Nef, or pEG202 were grown through the exponential phase in the presence of 0.5mCi ³H myristic acid per culture (~6 hours). Cultures were harvested in the late exponential phase, as outlined in section 2.4.8. The resultant lysates were immunoprecipitated with a Nef specific antibody (2/81c) (Harris and McKeating manuscript in preparation) and analysed by SDS-PAGE and fluorography. A band corresponding to the Nef-LexA fusion protein, was only detected in the lane containing the myristoylated Nef, see figure 3.2; thus confirming myristoylation of Nef expressed from the pVEG plasmid as an N-terminal LexA fusion. Cultures grown simultaneously and analysed by western blot confirmed equal levels of Nef expression (data not shown).

Diagram 3.2. Map of pVEG2, including sequence around the polylinker:



The sequence around the modified polylinker is shown below, the gene of interest requires an ATG and to fuse in frame with the ATG of the LexA gene.

GAATTCCCGGGGATCCATGAAA
 EcoRI BamHI Start of LexA

Figure 3.2. Results of the [³H] myristic acid labelling of yeast:

Yeast cultures (5ml) expressing either myristoylated Nef (pVEG-Nef), nonmyristoylated Nef (pVEG-G2A) or the bait LexA DB domain only (pVEG2) were grown to an OD₆₀₀≈1.0 in the presence of 0.5mCi [³H] myristic acid. The [³H] myristic acid was lyophilised prior to use and resuspended in 30μl DMSO per culture as detailed 2.4.8. The cultures were harvested as detailed section 2.4.7. and immunoprecipitated with the Nef antibody 2/81c. The immunoprecipitates were resolved by SDS-PAGE and analysed by fluorography (the example in this figure was exposed to film for 1 month). The pVEG2 negative control was loaded in lane 1, pVEG-G2A in lane 2 and pVEG-Nef in lane 3. A background band was visible in every sample, however a myristoylated Nef specific band was clearly detected in lane 3 at ~55kDa corresponding to the Nef-LexA fusion protein.

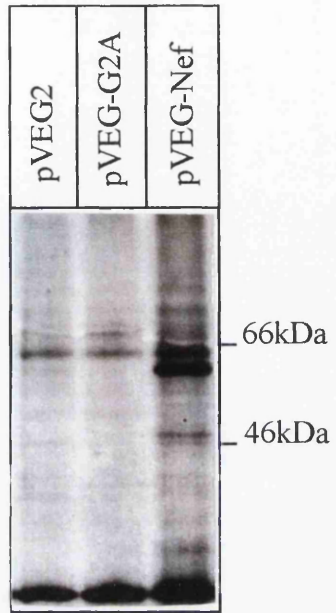


Figure 3.2.

3.4. Activation and repression assays to determine the suitability of pVEG-Nef as a bait in an interactor hunt:

To be a suitable bait for an interactor hunt the protein of interest, fused to the LexA DB domain, had to bind the UAS's within the nucleus without transactivating the reporter genes. Transcriptional activation activity was determined by monitoring the ability of the host yeast strains to grow on leucine. The LEU2 gene was a chromosomally integrated auxotrophic marker, utilised as a reporter gene in the interaction trap system. If the yeast became prototrophic for leucine it correlated with transactivation activity of the bait protein. Figure 3.3 shows a UH dropout plate compared to a UHL dropout plate. Yeast were spotted onto the plates at increasing dilutions, the UH plate which is permissive for all yeast examined confirmed equal culture densities. The UHL plate shows no growth for pVEG-Nef or pVEG-G2ANef indicating that Nef, as an N-terminal fusion to LexA, had no inherent transactivating capabilities. However pEG-Nef (Nef cloned into the original pEG202 plasmid as a C-terminal fusion), did appear to have a low level of transactivating ability. The differences in inherent transactivation, between N- and C- terminal Nef fusion proteins, was presumably due to the variable proximity of acidic stretches of amino acid sequences in Nef to the LexA DB domain. This meant that pEG-Nef would not make a suitable bait for an interactor hunt due to the high levels of false positives that would be obtained.

Since pVEG-Nef did not transactivate the reporter genes it was necessary to confirm it successfully entered the nucleus and bound the UAS. The repression assay, explained in more detail in section 2.42.4, was performed to determine the ability of the bait to reach the nucleus. A modified constitutively expressing LacZ reporter plasmid (pJK101) was cotransformed with the pVEG bait plasmid. This reporter plasmid contained a UAS between the ATG and TATA box, therefore if the bait bound the UAS transcription was blocked. To block the constitutive expression of LacZ a bait obviously had to enter the nucleus, this event could be determined by the formation of white colonies on plates containing X-Gal. Blue colonies would indicate the continued unhindered constitutive expression of the *lacZ* gene. Figure 3.4 shows the prospective baits spotted onto UH G/R plates

containing X-Gal. Both pVEG-Nef and pEG-Nef entered the nucleus and successfully blocked transcription of the *LacZ* gene as indicated by the growth of white colonies. A bait that was excluded from the nucleus was included as a control for blue colonies. The suitability of pVEG-Nef as a bait for the interactor hunt was therefore confirmed. These activation and repression assays were carried out every time a new bait was used for the interaction trap system, e.g. p55Gag and ORF94, see later.

Figure 3.3. Activation assay for pVEG-Nef, pVEG-G2A and pEG-Nef:

The activation assay was carried out as detailed 2.4.2. This example shows the pSH18-34 reporter plasmid plus pVEG-Nef, pVEG-G2A, pEG-Nef and the pSH17-4 control which possesses inherent transcriptional activation properties. Samples were spotted either undiluted (undil.) or at 1/100 or 1/1000 dilutions. The same samples were spotted onto the top (G/R UH) and bottom (G/R UHL) plates. All the samples grew on the G/R UH plate demonstrating similar culture densities for each sample. The lack of growth on the G/R UHL plate for pVEG-Nef and pVEG-G2A demonstrated they did not possess transcriptional activation properties. Colony growth was detected for pEG-Nef suggesting it would result in a large number of false positives if used as a bait in an interactor hunt. As expected the control transcriptionally activated the LexA-op-LEU2 gene.

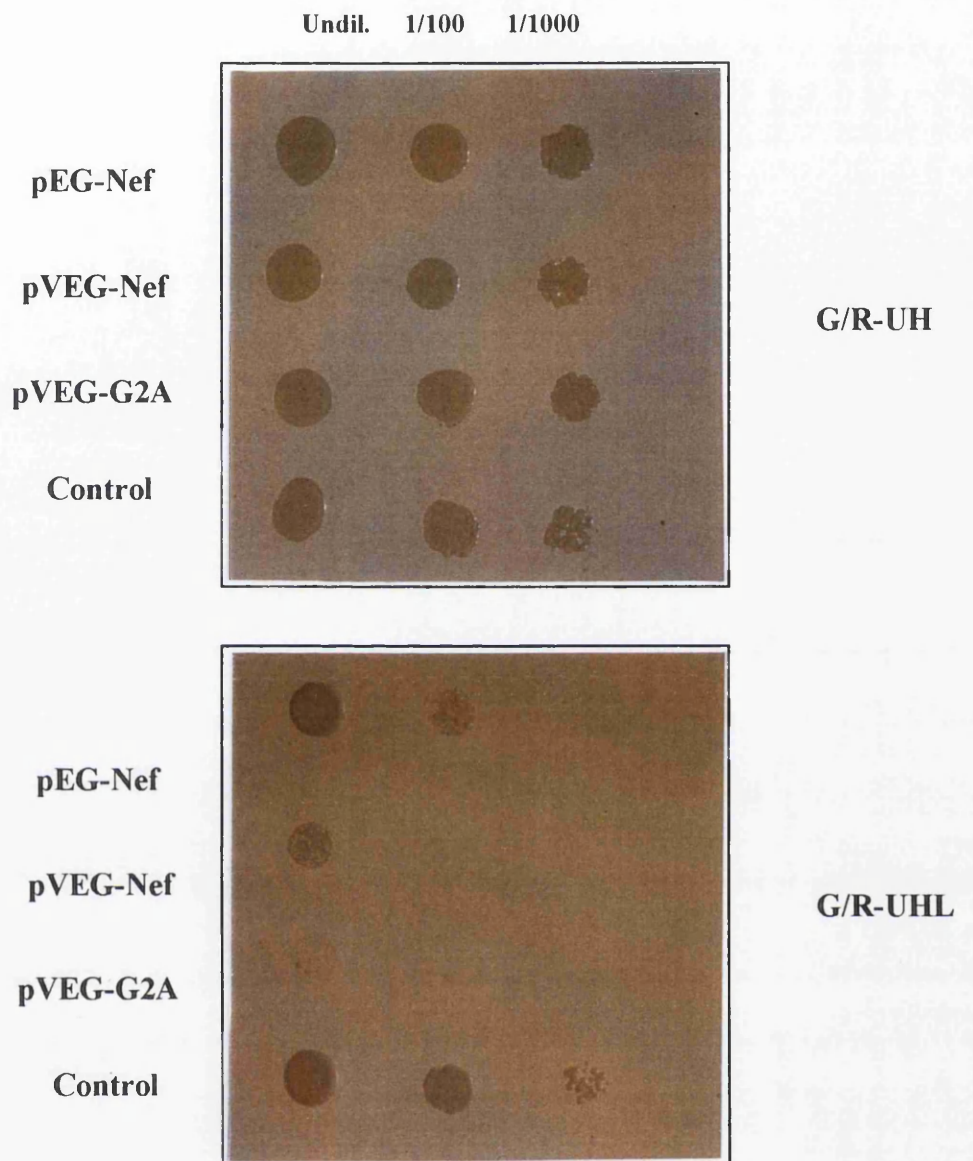


Figure 3.3.

Figure 3.4. Results of the repression assay for pVEG-Nef, pVEG-G2A and pEG-Nef:

This assay was performed to determine the baits ability to reach the nucleus the method is detailed 2.4.3. This example shows the pJK101 plasmid (detailed section 2.3.4.) transformed with either pVEG-Nef, pVEG-G2A and pEG-Nef or the pSH17 control (which was constitutively active). The growth of white colonies for pVEG-Nef and pVEG-G2A confirmed their ability to enter the nucleus and bind the LexA operator which was positioned such that it repressed transcription. A low level of transcriptional activation was detected for pEG-Nef consistent with its transcriptional activation capabilities.

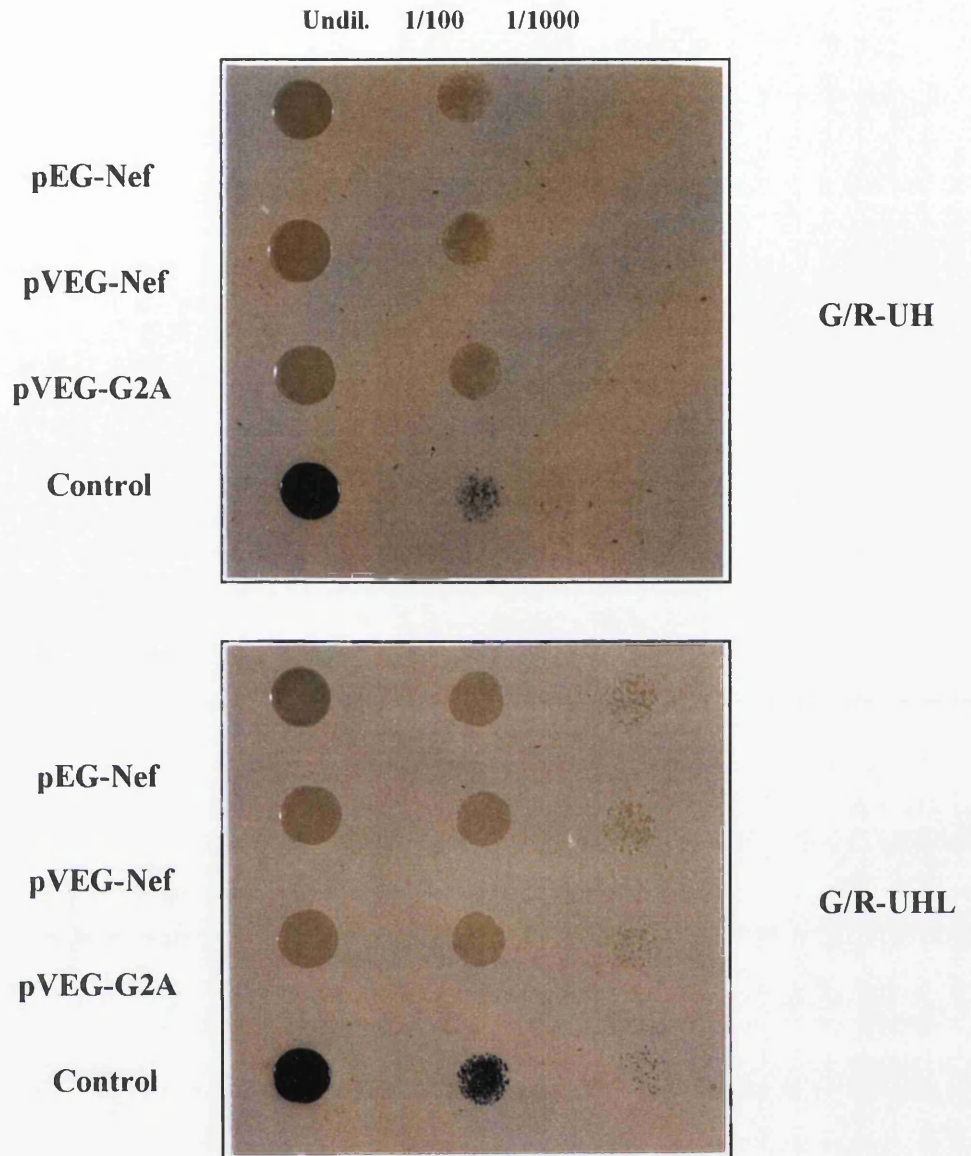


Figure 3.4.

3.5. Screening a Jurkat T-cell library with pVEG-Nef for novel protein-protein interactions:

The practicalities of obtaining high transformation efficiencies and physically screening a library are addressed in section 2.42.4. In the interactor hunt a final number of 92 potential Nef interacting colonies were obtained from the Jurkat T-cell cDNA library ($\sim 2 \times 10^6$ colonies were screened). Initially these potential interactors were divided into groups according to their RFLP (restriction fragment length polymorphisms) patterns, as determined by digestion with the frequent cutting restriction enzymes HaeIII and AluI. The graph in figure 3.5A shows the distribution of the colonies across the groups, with an example of the different RFLP patterns, figure 3.5B (the first 10 lanes are group A2 and the second 10 are group C1). The groups were sorted according to the strength of the interactions, as determined by the intensity of blue colouration when streaked on plates containing X-Gal (G/R UHT). Strong interactors were referred to as group A (either 1, 2 or 3 for different RFLP patterns), while group D was the weakest interactor group (compare 92 which was classified as group A and 91 which was classified as C in figure 3.5C). The graph distinctly shows, that there was 1 main interactor group, 3 smaller groups and 6 groups containing only 1 or 2 colonies. The initial categorisation of so many smaller groups arose due to ambiguities in RFLP patterns and ensured that all potential interactor groups were fully investigated, as will become clear. Library plasmids were isolated from the bait and reporter plasmids used in the system, then retransformed into *E.coli* for sequencing. Manual sequencing was carried out using BCO1 and BCO2 primers, designed within the library plasmid to sequence the 5' and 3' ends of the cDNA library inserts, see section 2.4. In parallel, each library plasmid was also retransformed back into yeast together with either pVEG-Nef or pEG202, plus the reporter plasmid (pSH18). This established the observed interactions were reproducible and did not result from a direct association with the LexA DB domain alone. For the larger groups A2, C1 and D2, 3-4 colonies from each were selected to be representative of the group. Where differences occurred during sequencing further members were examined.

After sequencing the distribution of the colonies across the groups altered. The majority of colonies sequenced from the weaker interaction groups had homology to colonies from larger groupings, with a few unsequenced due to practical difficulties. A summary of the reclassification of the interactors after sequencing is shown in the graph in figure 3.5D. The total number of different groups was reduced to 6.

Figure 3.5. *Classification of potential Nef interactors after the library screen:*

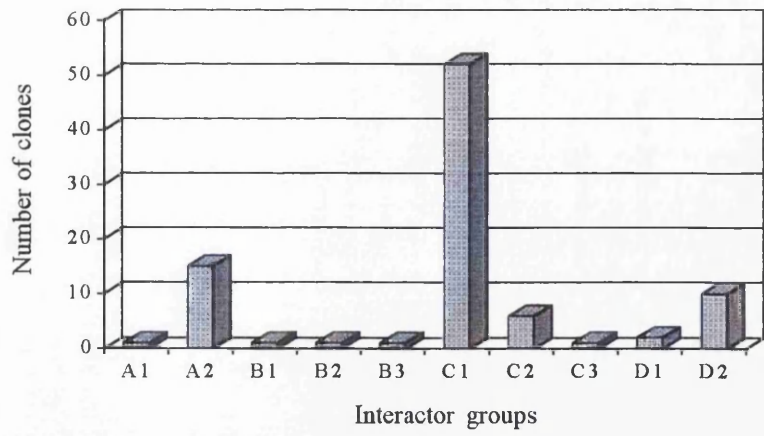
A. Distribution of potential interactors as classified by RFLP patterns (see B) and strength of β -galactosidase activity (see C). The strongest interactors were classified as A and the weakest D.

B. An example of the restriction enzyme digests used to classify the interactors. Lane 1 contains λ HindIII molecular weight markers, lane 2 contains ϕ X174 markers. Lanes 1-5 contain the same samples as 6-10 digested with *HaeIII* and *AluI* respectively, these were classified as A2 on the strength of their interaction. Lanes 11-20 contain 5 group C1 samples similarly digested.

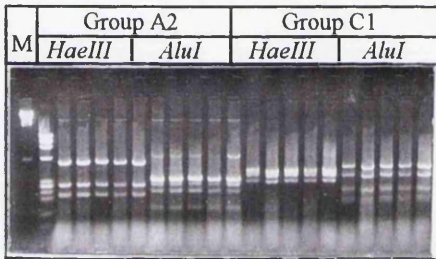
C. This is an example data set of the library screen. The samples are streaked on each plate anti-clockwise, starting left of top clone 83-clone 92. The top left plate is Glu UHT-X and demonstrates successful transformation of all plasmids. G/R UHT-X (top right) shows different strengths of the interactions (92 was group A2 and 91 group C1); Glu UHTL (bottom left) shows no growth and therefore no non-specific transactivation of the LexA-op-LEU2 reporter. G/R UHTL (bottom right) shows colony growth for each confirming the interaction.

D. Redistribution of the interactors after sequencing.

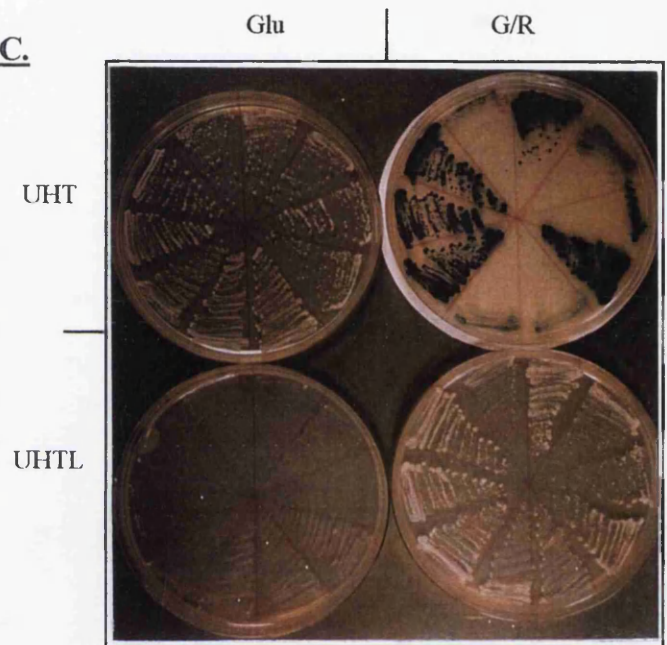
A.



B.



C.



D.

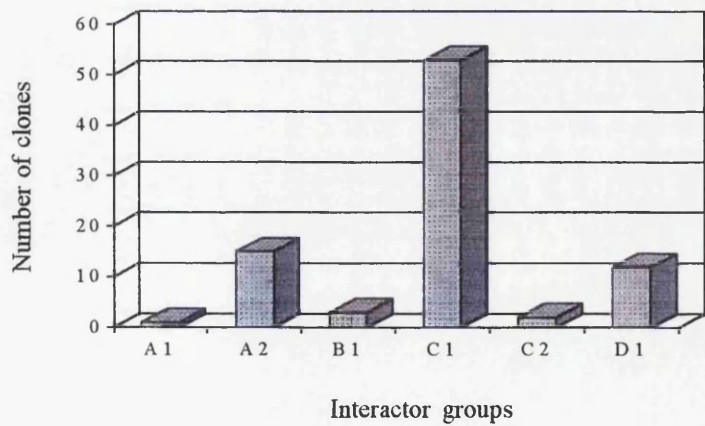


Figure 3.5

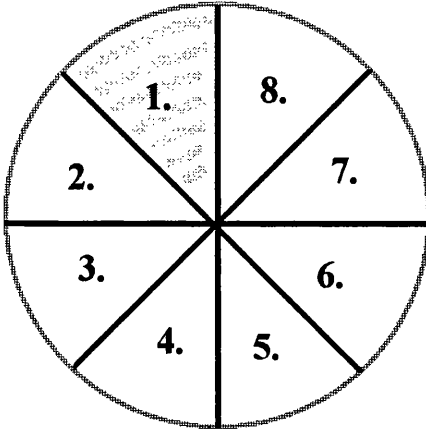
Interactors were selected for more detailed study on the basis of preliminary sequence data, in combination with the results obtained from the rescreening of the interactions. While groups A1 and A2 both maintained a strong interaction with Nef and did not activate the negative control, see figure 3.6 (see diagram 3.3 for plate orientation), at that time, the only significant nucleotide homology for both was with various uncharacterised cDNAs (as determined using FASTA and BLAST database searches of Genbank, CDS translations, PDB, Swissprot, Protein identification resource (PIR), EMBL, Expressed sequence tagged (EST) division, at the National Centre for Biotechnology Information (NCBI)). Amino acid homology with the A2 group was found mainly to zinc finger proteins, implicating it as a transcriptional activator. Since the *in vivo* presence of Nef in the nucleus is controversial and zinc finger proteins are common false positives found with the YTHS (Hengen, 1997), no further studies were performed for A2. However sequence available for clone 39, group A1, suggested some amino acid homology to a range of proteins involved in oxidative phosphorylation including, NADH dehydrogenase, ubiquinol-cytochrome-C reductase and cytochrome B. This clone was hence selected for further study. For groups B1 and B2 the interactions were shown to be reproducible although low transactivation levels of the LexA DB domain alone was seen for the LEU2 auxotrophic marker, see figure 3.6. However clone 40, group B1, had significant nucleotide homology to a 5Kb cDNA that contained a 3.5Kb ORF (open reading frame) previously proposed as a candidate gene, EHOC-1 (Epilepsy, HOIoprosencephaly Candidate-1) for progressive myoclonus epilepsy (Ac: U19252). EHOC-1 had been identified as encoding a putative transmembrane protein the function of which was unknown. Although the nucleotide homology for clone 40 was 3' to the ORF, the previous study had analysed cellular transcripts for the 5Kb cDNA using northern blotting. The existence of three 8, 7.5, and 5.3Kb mRNA species was determined, which were ubiquitously expressed across adult tissues. The prospect of altered splice patterns, resulting in the inclusion of the downstream sequences in these transcripts, made clone 40 a good candidate for further investigation. In contrast homology for group B2 was only found with uncharacterised cDNAs and the amino acid sequence had limited sequence homology to laminin, an adhesive glycoprotein found in the

extracellular matrix. Consequently group B2 was not investigated further during this study.

The largest interaction group, C1 had nucleotide sequence homology to several uncharacterised human cDNAs with amino acid homology to a *Saccharomyces cerevisiae* protein Pac10p (Ac: U29137). Pac10p was identified as one of a group of genes necessary in concert with the kinesin-related CIN-8p during mitosis in *S.cerevisiae*. The exact function of Pac10p is still to be elucidated therefore it provided few clues as to the identity of C1, except that it may play a role in mitosis. Several clones in C1 were rescreened for their specific interaction with Nef, all of which showed little or no activation of the LacZ reporter plasmid. However, despite a low level of transcriptional activation of LEU2 with the DB domain alone, levels of prototrophy for leucine in the presence of Nef were higher than in the absence of Nef. This inferred the interaction of C1 with Nef was specific, see figure 3.6. The number of clones isolated for C1 suggested an abundance of the transcript in the Jurkat T-cell library, it was therefore of interest to establish more conclusively the interaction of Nef with this group. No further work with group D1 was performed since rescreening the clones resulted in non-specific transcriptional activation of the reporter genes, see figure 3.6. Preliminary sequence data confirmed the cDNA had strong homology to a variety of zinc finger proteins.

Diagram 3.3. Orientation of samples for the rescreening of putative interactors:

A. Position of samples on each agar plate, on each plate 2 different putative interactors were analysed, 2 colonies were streaked for each:



1. pVEG-Nef+pJG4-5 library clone A
2. pVEG-Nef+ pJG4-5 library clone A
3. pEG202+pJG4-5 library clone A
4. pEG202+pJG4-5 library clone A;
5. pVEG-Nef+pJG4-5 library clone B
6. pVEG-Nef+pJG4-5 library clone B
7. pEG202+pJG4-5 library clone B
8. pEG202+pJG4-5 library clone B

B. Positioning of plates for each data set:

Glu UHT-X	G/R UHT-X
Glu UHTL	G/R UHTL

Figure 3.6. Results from the rescreening of the library interactors:

The library plasmids were isolated and retransformed with pVEG-Nef or pEG202 alone to confirm the authenticity of the interactions. In these examples the plates are orientated as shown in diagram 3.3.

A. Segments 1-4 are group A1 (clone39) and 5-8 are group B1 (clone 40). Only one colony picked for 39 retained a strong Nef interaction (segment 4 of each plate) as indicated by the growth of blue colonies on the G/R UHT-X plate and growth on G/R UHTL plate, the specificity was confirmed by the lack of colony growth on G/R UHTL or colour change on G/R UHT-X for 39 plus pEG202 (segments 1 and 2). Similar results were obtained for clone 40 of group B1, although a low background level of activation was occasionally detected on the Glu UHTL plates see segments 5 and 6 of bottom left plate in this example.

B. Segments 5-8 show a retransformed member of group A2 (clone 43). Segments 7 and 8 clearly show a retained strong interaction with Nef for both the β -galactosidase and LEU2 reporters. A slight activation of transcription was detected for the LEU2 reporter, segments 5 and 6 G/R UHTL (bottom right).

C. This data set shows two interactors from group C1 (clone 17 and clone 22). The reporter construct activation was similar for each, with low activation of both β -galactosidase and the LEU2 gene.

D. Results from the rescreen of D1 members demonstrated that all possessed inherent transactivating abilities in the absence of Nef, see segments 1 and 2.

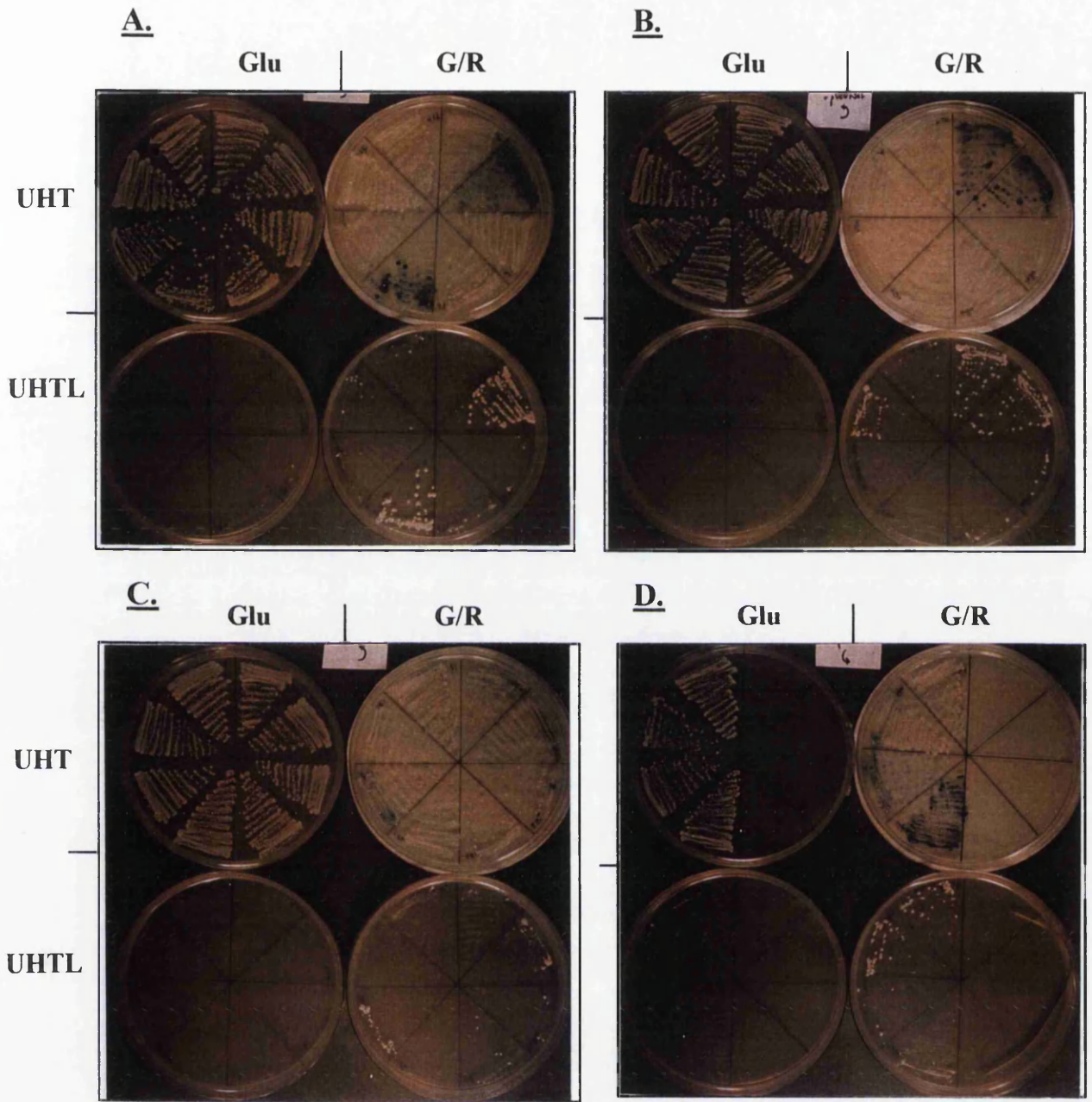


Figure 3.6.

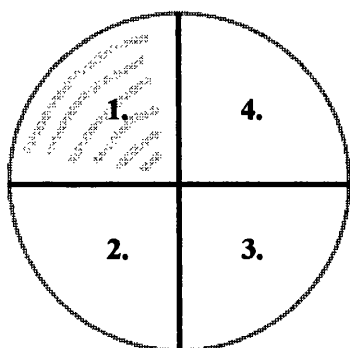
3.6. Further investigation of groups A1, B1 and C1- sequence data and specificity tests:

The individual clones comprising A1 (clone 39) and B1 (clone 40) together with a representative clone from C1 (clone 11) were subjected to further sequence analysis. To facilitate sequencing the cDNAs were subcloned into the pCR™ plasmid using PCR amplification with the BCO1 and BCO2 primers, see section 2.42.4. Automated sequencing was carried out with M13 forward and reverse primers, a typical sequence run provided 700bp of nucleotide sequence. A consensus nucleotide sequence for each cDNA was determined from several different pCR™ clones, allowing the prediction of the expected polypeptide length of the TA domain fusion. Figure 3.7 shows a western blot to confirm the actual size of the expressed fusion proteins. Western blot analysis was possible due to the incorporation of a haemagglutinin epitope tag in the TA domain. The blot revealed clone 39 was larger than its predicted size of 5kDa, running at ~24kDa including the activation tag corresponding to ~9kDa for clone 39. Clone 11 was significantly smaller than its predicted sequence resolving at only ~3kDa suggesting it was unstable, while clone 40 was ~4.5kDa in size consistent with the sequencing results. Interestingly when this blot was stripped and reprobed to determine the levels of Nef expression, elevated levels of Nef were seen in the clone 39 yeast cells, despite similar culture densities. This occurred consistently and suggested that expression of the clone 39 polypeptide reduced Nef toxicity to the yeast. This is in contrast to later studies with full length Lck (see section 5.4) where the co-expression of Nef resulted in complete toxicity to the yeast. The sequence data obtained for each clone was recently re-analysed by FASTA and BLAST programs to check for any homologies to newly submitted sequences. The results are shown in figures 3.8, 3.10 and 3.12 and will be discussed below in conjunction with the results of the specificity tests.

In order to establish whether the observed interactions with Nef were specific, it was necessary to cross pair them with further control LexA fusions. For this purpose two proteins, HIV-1 p55Gag and ORF94 containing myristoylation signals in their coding sequence were cloned into pVEG2. HIV-1 p55Gag is a

myristoylated protein precursor that is specifically cleaved by HIV-1 protease to form the integral structural proteins of the virion, as outlined in section 1.1. Its myristoylation in yeast has been previously determined. ORF94 is encoded by the human Cytomegalovirus (hCMV) and is produced during latent infection of granulocytes. ORF94 has a predicted myristoylation signal, although myristoylation of the protein has not been demonstrated. Prior to use as control baits in the interaction trap, pVEG2-p55Gag and ORF94 were screened in the activation and repression assays to confirm their suitability (data not shown). For the specificity tests all plasmids were freshly cotransformed with the library (potential Nef interactors) and reporter plasmids, plus one of the following, either: pVEG-Nef, pVEG2-Gag, pVEG2-ORF94 or pEG202. For easy comparison, each potential Nef interactor was streaked along with each of the baits on an individual plate, see figure 3.9, see diagram 3.4 below for orientation of the plates.

Diagram 3.4. Orientation of plates for specificity screening of the interactors:



1. pVEG-Nef+pJG4-5-library clone
2. pVEG2-Gag+pJG4-5-library clone
3. pVEG2-ORF94+pJG4-5-library clone
4. pEG202+pJG4-5-library clone

Figure 3.7. Western blot analysis of interactor expression:

Yeast cultures (3ml) were grown to an $OD_{600} \approx 1.0$ these were harvested and the pellet washed once in 1xPBS then resuspended in an equal volume of SDS-PAGE sample buffer. The samples were lysed by incubation for 5 minutes on dry ice followed by 5 minutes in a boiling water bath. The proteins were resolved by 17.5% SDS-PAGE, transferred to membrane and reacted with α -HA-1. Yeast cells alone used as the negative control (lane 1) demonstrated there was no yeast cross reactivity with the sera, a polypeptide of ~ 15 kDa was detected for the pJG4-5 plasmid alone consistent with TA domain expression (lane 2) a band of ~ 18 kDa was detected for clone 11, group C1 (lane 3) of which ~ 15 kDa comprised the TA domain and ~ 3 kDa the cDNA insert; a band of ~ 24 kDa was detected for clone 39, group A1 (lane 4) of which ~ 15 kDa was the TA domain and 9kDa the cDNA insert; clone 40, group B1 (lane 5) resolved at 19kDa corresponding to ~ 15 kDa TA domain and ~ 4 kDa cDNA insert.

3.6.1. Analysis of the sequence and specificity results obtained for groups C1 and B1:

Of all of the groups selected for further investigation, group C1 had the weakest observed interaction with Nef in the initial screens. The interaction was only detectable above background for the LEU2 auxotrophic marker. However, C1 contained the largest number of clones identified as potential Nef interactors, hence the decision to investigate the specificity of this Nef interaction further. During the specificity screen it was found that the interaction of C1 with Nef was capricious, see figure 3.9. The specific interaction with Nef could not be reconstituted despite earlier repeats, and it transactivated the reporter constructs in the presence of the DB domain (pEG202) alone (bottom right plate figure 3.9A, segment 4). No interaction above the transactivation level was seen with either the p55Gag control or ORF94 (segments 2 and 3). Preliminary sequence data had shown homology to *S.cerevisiae* Pac10p (section 3.5), but with recent re-analysis it transpired that C1 contained a fragment of the VHL (von Hippel Lindau) gene. VHL encodes a tumour suppressor protein implicated in the inhibition of transcriptional regulation. VHL protein is thought to interact with 2 subunits (B and C) of the elongin complex involved in transcriptional regulation; thus preventing their binding to and activation of the elongin A subunit. The activation of transcription by VHL in the yeast-two-hybrid system, is therefore contrary to its predicted inhibitory function, but is probably due to its affinity for the transcriptional apparatus in the context of its fusion to the TA domain. This suggests that early interactions seen for C1 with Nef, were in fact due to transcriptional activation and that for interactions within the yeast-two-hybrid system to be reproducible, both reporter genes must be transcribed, with minimal background activity.

Results obtained during the specificity screen for group B1, also concurred with those of group C1, see figure 3.9. In the original screens group B1 exhibited strong interactions with Nef. Some background levels of transcriptional activation of the LEU2 gene had been seen, but these were significantly lower than that seen in the presence of Nef. However, during the specificity screens the levels of transcriptional activation of the DB domain alone by group B1, obscured any potential Nef specific interaction (see figure 3.9B, bottom right plate segment 4). It was therefore unlikely that Nef was specifically interacting with group B1.

Figure 3.8. Computational analysis of sequence data for groups C1 and B1 (carried out at NCBI using BLAST and FASTA network services):

Group C1, clone 11:

This was found to have good homology to the tumour suppressor protein VHL. FASTA results are not shown as the amino acid homology obtained in BLAST searches was so high.

BLAST Results:

Sequences producing High-scoring Segment Pairs:	High Score	Smallest Sum P(N)	Sum N
U56833 VHL binding protein-1	271	8.6e-33	1
P48363 PA10_YEAST PAC10 PROTEIN.	62	2.6e-07	2
Z81587 T06G6.9 [Caenorhabditis ele.	65	4.9e-06	2
Q10143 YAS7_SCHPO HYPOTHETICAL 19.5 KD PROT.	78	3.1e-05	2

>gi|1465751 (U56833) VHL binding protein-1 [Homo sapiens]
Length = 166

Score = 271 (123.5 bits), Expect = 8.6e-33, P = 8.6e-33
Identities = 53/53 (100%), Positives = 53/53 (100%)

Query: 32 EDVDSFMKQPGNETADTVLKKLDEQYQKYKFMELNLAQKKRRLKGQIPEIKQT 84
EDVDSFMKQPGNETADTVLKKLDEQYQKYKFMELNLAQKKRRLKGQIPEIKQT
Sbjct: 1 EDVDSFMKQPGNETADTVLKKLDEQYQKYKFMELNLAQKKRRLKGQIPEIKQT 53

>sp|P48363|PA10_YEAST PAC10 PROTEIN>pir|S59741 PAC10 protein-yeast
(Saccharomyces cerevisiae) >gi|902026 (U29137) Pac10p
[Saccharomyces cerevisiae] >gnl|PID|e243428 (Z72863) ORF YGR078c
Length = 199

Score = 62 (28.3 bits), Expect = 2.6e-07, Sum P(2) = 2.6e-07
Identities = 12/33 (36%), Positives = 21/33 (63%)

Query: 52 KLDEQYQKYKFMELNLAQKKRRLKGQIPEIKQT 84
K E+ KYKFM+ + ++LK +IP+++ T
Sbjct: 40 KFQERLSKYKFMQESKLATIKQLKTRIPDLENT 72

Score = 55 (25.1 bits), Expect = 2.6e-07, Sum P(2) = 2.6e-07
Identities = 9/20 (45%), Positives = 15/20 (75%)

Query: 24 GIPEAVFVEDVDSFMKQPGN 43
GIP+A F+E+V+ +K P +
Sbjct: 14 GIPQAPFIENVNEIIKDPSD 33

Figure 3.9. Results of the specificity tests:

The orientation of the plates in this figure is illustrated in diagram 3.4.

A. Results for group C1, clone 11 show no detectable interaction with Nef (segment 1) and non-specific activation of the bait (segment 4, bottom plates).

B. Results for group B1, clone 40 as for group C1.

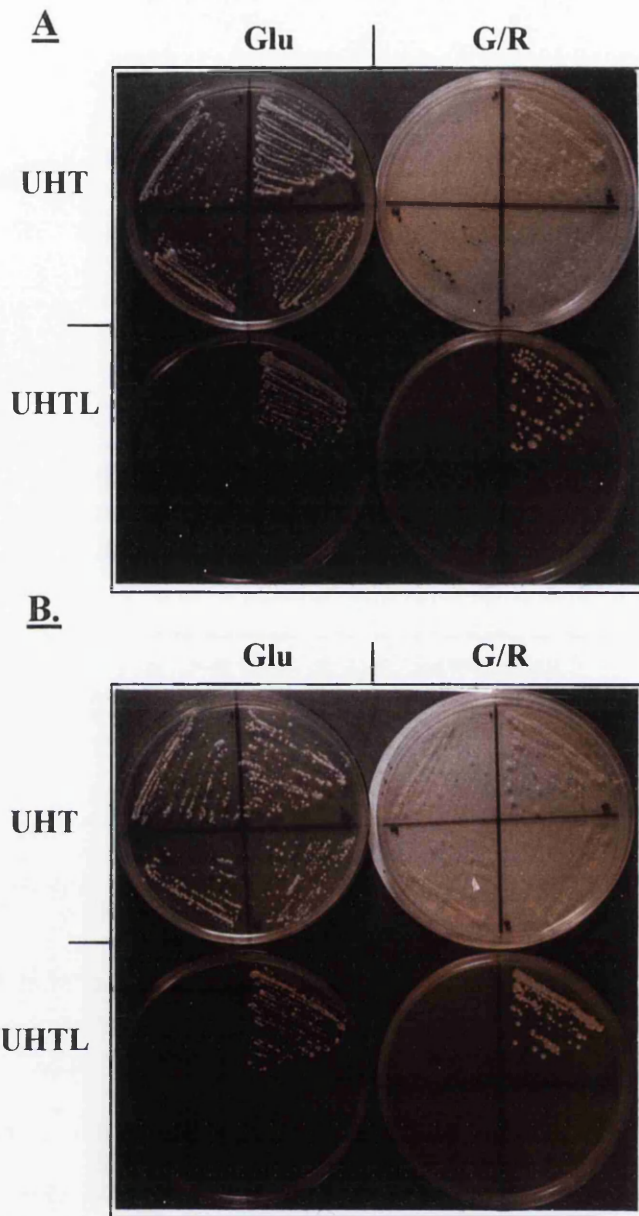


Figure 3.9.

3.6.2. Re-analysis of group A2:

Since the only reproducible interaction with Nef during the specificity screening was with the strongest interactor group A1, see below, it was decided to re-analyse the preliminary sequence data obtained for group A2. On re-analysis using FASTA and BLAST programs significant homology was found to the human eukaryotic initiation factor 3 (eIF3). The amino acid sequence was 96% homologous over the N-terminal 26 amino acids, after which there were several frameshifts, but there was a further 100% homology over 8 amino acids at residues 76-82 in eIF3 (see figure 3.10). The loss of homology at the amino acid level was due to frameshifts caused by discrepancies at the nucleotide level, these need resolving by further sequencing. The N-terminal region of eIF3, which was the location of the group A2 homology, has been recently implicated in RNA binding, explaining why previous database searches showed some homology to zinc finger proteins. It is now conceivable that a physiological interaction of Nef with eIF3 in the cellular cytoplasm may occur. However, further specificity studies may reveal, as for C1 and B1, that out of context this RNA binding domain is able to bind the LexA UAS's and activate the reporter constructs independently from Nef. Further investigation as to the specificity and reproducibility of this intriguing interaction is required. If genuine, the interaction of Nef with part of the translation initiation machinery suggests a role for Nef in recruiting the host translational apparatus. Therefore, selectively translating viral mRNA, providing a mechanism for the observed Nef enhancement of viral infection. Consistent with this, it has recently been demonstrated (Echarri *et al*, 1996; Echarri *et al*, 1997), that Nef has RNA binding capabilities.

Figure 3.10. Computational analysis of sequence data for groups A2 and A1 (clone 39):

Protein homologies identified for group A2:

The recent addition to the database of this translational elongation initiation factor provided a statistically significant match to clones from group A2.

FASTA Results:

```
Percent Similarity: 97.233   Percent Identity: 96.838
clone 11 x u54559.gb_pr2 eIF-p40 [Homo sapeins] ..

      1 gaattcggcaccgaggcggttgaaagatggcgtcccgcacgaaggaggtac 50
      | | | | | | | | | | | | | | | | | | | | | | | | | | | |
      1 .....GAAAGATGGCGTCCCGCAAGGAAGGTAC 28

      51 cggctctactgccacctctccagctccaccgcccggcncagcagggaag 100
      | | | | | | | | | | | | | | | | | | | | | | | | | | | |
      29 CGGCTCTACTGCCACCTCTCCAGCTCCACGCCGGCGCAGCAGGGAAAG 78

      101 g..aaagaaaggcggtcgggagattcagccgtgaagcaagtgcagata 148
      | | | | | | | | | | | | | | | | | | | | | | | | | | | |
      79 GCAAAGGCAAAGGCGGCTCGGGAGATTCAGCCGTGAAGCAAGTGCAGATA 128

      149 gatggccttgtggtattaaagataatcaaacattatcaagaagaaggaca 198
      | | | | | | | | | | | | | | | | | | | | | | | | | | | |
      129 GATGGCCTTGTGGTATTAAAGATAATCAAACATTATCAAGAAGAAGGACA 178

      199 aggaactgaagttgttcaaggagtgcttttgggtctggtttagaagatc 248
      | | | | | | | | | | | | | | | | | | | | | | | | | | | |
      179 AGGAACTGAAGTTGTTCAAGGAGTGCTTTTGGGTCTGGTTGTAGAAGATC 228

      249 .gcttgaaattaccaactgcttctttcc..... 275
      | | | | | | | | | | | | | | | | | | | | | | | | | | | |
      229 GGCTTGAAATTACCAACTGCTTTCCTTCCCTCAGCACACAGAGGATGAT 278
```

BLAST Results:

		Smallest	
		Sum	
Sequences producing High-scoring Segment Pairs:	High Score	Probability P(N)	N
U54559 eIF3-p40 [Homo sapiens]	120	2.6e-13	2

>gi|2351380 (U54559) eIF3-p40 [Homo sapiens]

Length = 352

Score = 120 (56.7 bits), Expect = 2.6e-13, Sum P(2) = 2.6e-13

Identities = 25/26 (96%), Positives = 25/26 (96%)

Query: 10 MASRKEGTGSTATSSSSTAGXAGK GK 35

MASRKEGTGSTATSSSSTAG AGK GK

Sbjct: 1 MASRKEGTGSTATSSSSTAGAAGK GK 26

Score = 45 (21.3 bits), Expect = 5.2, Sum P(2) = 0.99

Identities = 9/20 (45%), Positives = 15/20 (75%)

Query: 16 GTGSTATSSSSTAGXAGK GK 35

G+ +T++SS+ A GK GK

Sbjct: 9 GSTATSSSSTAGAAGK GK GK 28

3.6.3. Analysis of the specificity results obtained for group A1:

Group A1, clone 39 exhibited the strongest isolated interaction with Nef. During the specificity screening it became apparent that the Nef interaction with A1 was also the most reproducible. A1 consistently interacted with Nef and showed no transactivation capabilities with the DB domain (pEG202) alone. However, unexpectedly during the specificity screen, a strong interaction with p55Gag was also seen. No interaction was seen with ORF94. To verify whether the interactions of A1 were as a result of a direct interaction with the myristic acid molecule on these proteins, A1 was screened with nonmyristoylated Nef. The results of these specificity studies are compared in figure 3.11. From the results it was evident that the observed A1 interactions were not myristoylation dependent, because A1 consistently bound myristoylated p55Gag and both myristoylated and nonmyristoylated Nef. The interaction of a cellular protein with both HIV Nef and Gag is plausible since it is likely that they accumulate in similar cellular locations.

The cDNA contained in A1 was ~1000bp in size. When the fusion protein was analysed by western blotting it revealed the protein product to be only ~9kDa (p9), see figure 3.7. Sequencing results suggested A1 encoded a polypeptide of 43 amino acids, which was inconsistent with the expression of a polypeptide of ~9kDa inferring that either a posttranslational modification event had occurred or there were possible sequence discrepancies. BLAST searches produced no significant homologies to the complete A1 polypeptide sequence. However, a FASTA search revealed a 99% match over 195bp to the reverse complement of an EST tagged cDNA (Ac. N52259), which included non-coding sequences after the stop codon. The sequences differed by a single guanine nucleotide, causing a frameshift at amino acid 29 in clone 39 relative to the N52259 sequence. The N52259 sequence therefore encoded a polypeptide product of ~60 amino acids, more consistent with the 9kDa product detected in the western blot analysis. To further characterise A1 and to establish whether it was a fragment of a larger known protein, the UK Human Genome Mapping Project database facilities at Cambridge, were searched using the EST-BLAST program, for nucleotide sequence. This built up a profile of

the cDNA sequence surrounding A1, including any recently submitted sequences. Along with the previously identified N52259 human cDNA, a series of overlapping partial human cDNAs were retrieved. Several highly homologous mouse cDNAs were also identified, suggesting the existence of a mouse homologue e.g. 76% homology for mouse cDNA Ac: W90938. Two separate human and mouse consensus nucleotide sequences were generated for the cDNA in combination with the A1 query sequence. To avoid frameshifts resulting in spurious homologies, netBLAST and GAP-BLAST searches were performed at NCBI using the nucleotide sequence. These programs check for homologies in all possible reading frames. However, still no significant protein homologies were uncovered. The 60 amino acid N52259 peptide sequence also produced no statistically significant database matches. In addition, the nucleotide sequence was used to check for motifs (using Motifs, Profilescan at NCBI and Blocks at the Fred Hutchinson Cancer Research Centre (Henikoff and Henikoff, 1994)) although again nothing of significance was identified. The lack of homology found on screening the protein databases could be as a result of a series of frameshifts along the sequence, but in the absence of a longer polypeptide for analysis this could not be investigated further. However the existence of highly homologous cDNAs to A1, in both the human and mouse genomes implies the presence of A1 as an authentic transcript in the cell.

Figure 3.11. *Results of the specificity screen for group A1, clone 39:*

A. The colonies were streaked as shown in diagram 3.4. The interaction with Nef was maintained (segment 1), but it was also found to interact with p55Gag (segment 2), no interaction with ORF94 was seen (segment 3) and none with the negative control (pEG202) segment 4.

B. Segments 1 and 2 were pEG-Nef cotransformed with clone 39 for which no interaction was detected. PVEF-G2A and pJG4-5-39 were streaked in segment 2 and despite a poor level of colony growth on all plates (in this example) a specific interactions between the proteins was clearly evident. pVEG-Nef and pJG4-5-39 are shown in segment 4.

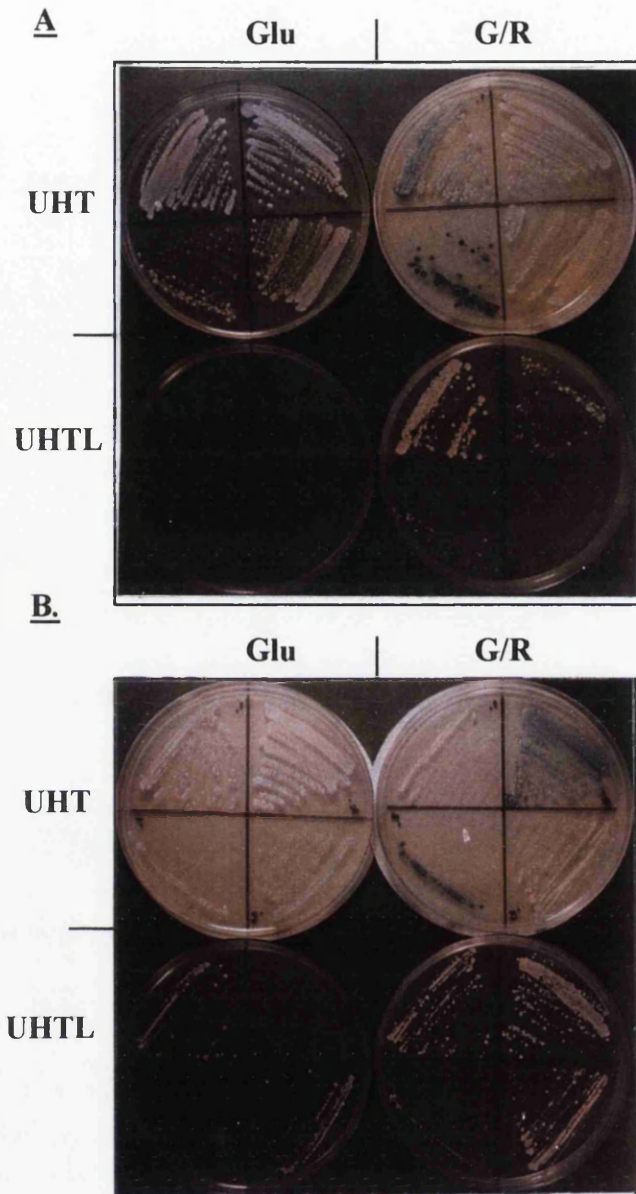


Figure 3.11.

3.7. Further analysis of the Nef -A1 (p9) interaction:

To further analyse Nef sequences important in the interaction with A1 (p9), *in vitro* coprecipitation assays were performed. p9 was cloned using the restriction sites EcoRI and XhoI into pGEX4T-1, a bacterial GST fusion expression plasmid; thus maintaining it as a C-terminal fusion protein, potentially important for its stability and interaction with Nef. The GST-p9 fusion was subsequently purified from bacteria and immobilized on glutathione agarose (GA)-beads, for use as an affinity reagent in *in vitro* binding assays. Problems were encountered with proteolysis, therefore for each sample ~3 times the standard amount of GST-p9 was bound to GA-beads as the affinity reagent, see figure 3.12. Protein binding assays were performed with ³⁵S-methionine labelled *in vitro* transcription and translation products, to determine protein specificity for GST-p9 *in vitro*. Proteins analysed included Nef, p55Gag, with CD4 and Lck as controls.

In vitro, no binding of GST-p9 to either Nef or p55Gag was seen. The lack of *in vitro* binding was unexpected considering the strength and specificity of the interaction of p9 with Nef and p55Gag *in vivo*. Observed binding differences between *in vitro* and *in vivo* usually implicates the involvement of cellular factors. However in this case, it seems more likely that practical considerations may have been affecting the binding potential. As previously observed, the purified GST-p9 was prone to proteolytic degradation. The lack of *in vitro* binding suggests that despite using increased amounts of GST-p9 as the affinity reagent there was still insufficient full length for Nef binding. It is also possible that the p9 protein was rendered inaccessible for Nef binding as a GST fusion. In the TA domain fusion, p9 was separated from the TA domain by the HA-1 epitope, such a linker region was absent in the GST fusion. It is conceivable that the linker region allowed the polypeptide to form secondary structures necessary for the interactions. Follow up studies will be required to circumvent these problems and further characterise the observed specific interaction of this short polypeptide with both Nef and p55Gag.

Figure 3.12. *Quantitative analysis of amount of GST-39 bound to GA-beads:*

E.coli expressed and purified GST-39 was bound to GA-beads along with GST alone as a control (150µg GST-39 was bound to 50µl packed volume of beads and 50µg GST was bound to the same volume of beads, as detailed 2.6.7.). 5µl of packed beads for each sample were analysed by 12% SDS-PAGE and Coomassie stained. The results shown in this figure demonstrate GST-39 was substantially proteolytically degraded, lane 1; GST alone is shown in lane 2.

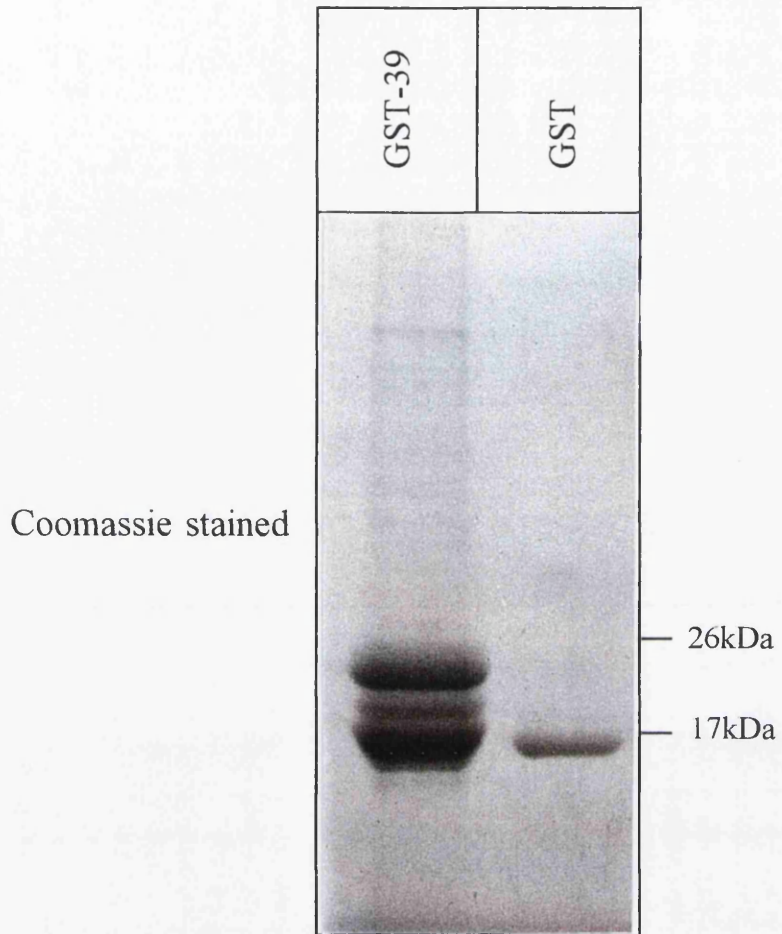


Figure 3.12

CHAPTER 4

CHAPTER 4 -
Investigation of a putative Nef interaction with Lck

	Page number
4.1 Introduction	156
4.2 Background	159
4.3 Summary of work presented hereunder	160
4.4 Construction of the recombinant baculoviruses	160
4.5 Confirming the authenticity of the proteins	161
4.6 <i>In vitro</i> binding assays	167
4.7 Construction of constitutively active and inactive Lck mutants to assess conformational binding criteria	177
4.8 Confirmation of the expression and kinase activities of the mutant Lck recombinant baculoviruses	179
4.9 <i>In vivo</i> binding studies	183
4.10 Identification of regions in Nef important in mediating its <i>in vivo</i> binding to LckGKY	189

Chapter 4: Investigation of a putative Nef interaction with Lck.

4.1 Introduction:

Similar to Src (reviewed (Brown and Cooper, 1996)), the *lck* gene (for lymphoid cell kinase) was first identified as a transforming agent. It was isolated during a study of a Moloney murine leukaemia virus-transformed lymphoblastoid cell line, where the integration site of the retroviral promoter caused a substantial elevation of tyrosine kinase activity in accordance with increased Lck expression (Marth *et al*, 1985; Voronova and Sefton, 1986). Its expression has since been predominantly detected in T-lineage cells (Marth *et al*, 1986; Abraham *et al*, 1991) and some B-cells (Perlmutter *et al*, 1988) and its dysfunction has been associated with lymphoid malignancies (Perlmutter *et al*, 1988; Adler *et al*, 1988; Marth *et al*, 1988). Lck expression is governed by 2 distinct promoters, the first of which is adjacent to the *lck* ORF and utilised in immature thymocytes, while the second is ~34kb 5' and active in mature thymocytes and peripheral T-cells (reviewed by (Anderson *et al*, 1994; Perlmutter *et al*, 1988)). The cellular requirement for 2 independent promoters is thought to be at the regulatory level as initiation from either produces the same transcript. The transcript encodes a 509 amino acid polypeptide that is cotranslationally myristoylated and subsequently palmitoylated. The polypeptide represents a typical Src non-receptor tyrosine kinase family member with the characteristic domain structure, outlined in section 1.3.1.

Lck, in conjunction with the variably spliced Src kinase, Fyn, has been implicated in amplifying cellular activation signals during antigenic stimulation of the TCR-CD3 receptor complex (Abraham *et al*, 1991; Glaichenhaus *et al*, 1991). The putative model for this outlined below, involves the "accessory" transmembrane receptors CD4 and CD8, to which Lck specifically associates via its unique N-terminal domain (Veillette *et al*, 1988; Shaw *et al*, 1989). Binding of Lck to the cytoplasmic tails of these receptors is mediated by common cysteine motifs potentially facilitating the co-ordination of a metal ion (Turner *et al*, 1990). During TCR-CD3 antigen recognition of either MHCI or MHCII the accessory receptors, CD8 or CD4 respectively are recruited to the TCR-CD3 complex. Cross-linking of CD4 has been demonstrated to cause the activation and dissociation of Lck which

subsequently phosphorylates the conserved tyrosine residues in the immune-receptor-tyrosine-based activation motifs (ITAMs) of CD3 (Straus and Weiss, 1992; Biffen *et al*, 1994). This phosphorylation event is thought to initiate the activation cascade by forming putative SH2 binding sites for molecules involved in signal amplification such as the Syk family of kinases (Latour *et al*, 1997). A critical role for Lck in TCR-CD3 signalling pathways has also been corroborated by *in vivo* mouse knockout studies. Consistent with its high levels of expression in immature lymphocytes, *lck* knockout mice exhibited pronounced thymic atrophy with severe depletion in their double-positive CD4+CD8+ thymocyte population (Molina *et al*, 1992). Intriguingly, in the Nef transgenic mice model a similar disruption of T-cell development was observed (Skowronski *et al*, 1993).

Lck has been reported to associate with a number of other cellular proteins (reviewed (Anderson *et al*, 1994)), for example the IL2-receptor (IL2-R), CD45 tyrosine phosphatase and glycosyl-phosphatidylinositol (GPI) anchored proteins e.g. the decay accelerating factor and CD59 (Shenoy-Scaria *et al*, 1993; Shenoy-Scaria *et al*, 1994; Parolini *et al*, 1996). Antibody cross-linking of the IL2-R results in Lck activation, however a crucial role for Lck in IL2-R signalling has been disputed as IL2-R positive cell types exist that do not express Lck (Anderson *et al*, 1994). One of the mechanisms proposed to activate the Lck kinase activity is dephosphorylation of its C-terminal Tyr505 residue by the transmembrane phosphatase CD45, see section 1.3.1. Significantly it was discovered in a study by (Gervais and Veillette, 1995) that the unique region of Lck was necessary for its activation by CD45 and membrane association *per se* was not sufficient. This inferred that specific protein-protein interactions are necessary for its activation, and that these interactions may be prevented by the binding of other molecules such as CD4 and CD8.

Antibody cross-linking experiments with GPI anchored proteins determined their ability to transduce intracellular signals via tyrosine kinase activation (Robinson, 1991). Subsequently it was demonstrated that both Lck and Fyn but not Src co-isolated with the GPI-anchored proteins, decay accelerating factor and CD59 in triton insoluble complexes (Shenoy-Scaria *et al*, 1993; Shenoy-Scaria *et al*, 1994;

Parolini *et al*, 1996). This association was dependent on authentic myristoylation and palmitoylation of the proteins, explaining the exclusion of Src from the complexes due to its lack of palmitoylation. It has been speculated that Lck and Fyn may mediate the intracellular signalling of GPI-anchored proteins. However, direct contact between the proteins is unlikely since they are each anchored into different leaflets of the lipid bilayer, Lck and Fyn are cytoplasmic whereas GPI-anchored proteins are extracellular. Current studies are hence addressing the possible involvement of a third transmembrane protein or possible inter-connecting lipids. GPI-anchored proteins have in the past been reported to associate with plasma membrane micro-invaginations termed caveolae, the primary constituent of which is caveolin (Parton, 1996). More recent studies using cationic colloidal silica particles have suggested these represent discrete areas on the cell surface with only a small percentage of GPI-anchored proteins associating with caveolae (Schnitzer *et al*, 1995; Hoessli and Robinson, 1998). Instead the GPI-anchored proteins have been detected in clusters in sphingolipid-cholesterol enriched rafts (Simons and Ikonen, 1997). The functional significance of this is unknown at present, but both structures have been implicated in initiating cellular activation cascades and both represent alternative endocytic pathways with which Lck may also be involved (Li *et al*, 1996; Deckert *et al*, 1996; Parton, 1996).

The studies described here were initiated in response to a number of observations that implicated Lck as a target for Nef *in vivo*. Nef mediated down-modulation of CD4 was one of the few consistently reproducible properties ascribed to Nef. In addition, evidence was accumulating to suggest that Nef possessed an inherent ability to disrupt cell signalling pathways. As previously outlined, in cells of lymphoid lineage Lck is putatively involved in a variety of cell surface signal transduction pathways, most notably in TCR-CD3 signal amplification. Lck is also known to function as a cell surface anchor preventing the interaction of CD4 with clathrin coated pits which constitutively endocytose associated macromolecules. Significantly it is the depletion of CD4⁺ T-lymphocytes that provides a marker for disease progression. T-cells have also been demonstrated to harbour a rapid, aggressive HIV-1 infection with associated high levels of virion production (Ho *et*

al, 1995; Perelson *et al*, 1996). It was therefore of interest to establish whether an interaction between Nef and Lck might play a role in the T-cell cytopathology of AIDS. As data had inferred a novel mechanism for Nef mediated CD4 down-modulation a direct interaction between Nef and Lck in the context of the full length native proteins was investigated. Criteria governing the binding was also investigated, to provide a clearer indication of exactly when the interaction occurs *in vivo*, allowing the possible consequences of the interaction to be evaluated.

4.2. Background:

Preliminary studies performed within the laboratory had indicated that a direct interaction between Nef-GST and a murine Lck was detectable *in vitro*. (Harris, 1995). Furthermore it was demonstrated that the interaction was dependent upon Nef myristoylation as it was not seen during binding studies using a nonmyristoylated Nef. The early results also suggested that an interaction between Nef and Lck was dependent on a specific Lck conformation, since the addition of the tyrosine phosphatase inhibitor sodium orthovanadate (NaOV) during cell lysis inhibited Lck binding to Nef. It was speculated that NaOV as a tyrosine phosphatase inhibitor may be acting on a baculovirus specific or insect cell phosphatase that was a functional homologue of the CD45 tyrosine phosphatase. This would prevent the dephosphorylation of Lck Tyr505, the C-terminal regulatory tyrosine residue, and maintain the kinase in its inactive configuration stabilized by the intramolecular association of the SH2 domain with phosphorylated Tyr505 (pTyr505). The corollary being that Nef interacted only with the kinase active conformation of Lck. These present studies were hence undertaken to further establish the Lck conformation required for Nef binding.

4.3. Summary of work presented hereafter:

Recombinant baculoviruses were constructed for each of the Lck proteins under investigation. Subsequently, the authenticity of the recombinant baculovirus expressed proteins were evaluated. Parameters examined included, expression of full length proteins, acylation (myristoylation and palmitoylation) and tyrosine kinase auto- and *trans* phosphorylation activities. Protein binding assays were performed to analyse the affinity of the recombinant Lck proteins for purified Nef during *in vitro* binding assays. These studies yielded unexpected results which resulted in a reappraisal of the experimental approach and the construction of additional Lck mutants. These mutants were used for further *in vitro* and *in vivo* binding studies to directly evaluate the importance of the active and inactive conformations of Lck in Nef interactions. In addition, a panel of Nef mutants were screened for their Lck binding ability to identify amino acids important in mediating the interaction, in particular the (PXX)₃P motif previously cited as an SH3 binding sequence.

4.4. Construction of the recombinant baculoviruses:

A murine Lck cDNA was subcloned from pSM.Lck (a gift from Dr. Mark Marsh, University College, London) into the baculovirus transfer vector pAcCL29. As no compatible sites were present both were blunt ended using Klenow and subsequently ligated. A recombinant baculovirus (AcLck) expressing Lck was generated by standard procedures as previously outlined (Harris, 1995). Subcloning maintained cDNA flanking sequences around the Lck ORF. In addition PCR amplification was necessary for the construction of mutant Lck clones required for the present studies, therefore a second wildtype recombinant baculovirus was generated using PCR primers (wtLck). This was cloned into the pAcES baculovirus transfer vector. The primers were designed to incorporate an EcoRI site for cloning and to reduce the amount of flanking non-coding cDNA sequence in the clone. A second 5' primer was also made to encode a nonmyristoylated Lck (LckG2A). In later studies a further 3' primer was made to mutate the C-terminal tyrosine 505 to a phenylalanine (LckY505F) to generate a constitutively active Lck. The K273A

Lck mutants were also amplified by PCR utilising the same primers for the respective mutants, however the template for PCR was pSM.LckK273A kindly donated by Dr. Mark Marsh. The primers used for PCR amplification are shown below:

Coding primers:

wtLck: 5'- NNNGAATTCAGGGATCATGGGCTGTGTCTGCAGC -3'

LckG2A: 5'- NNNGAATTCAGGGATCATGGCCTGTGTCTGCAGC -3'

Non-coding primers:

wtLck: 5'- NNNGAATTCAAGGCTGGGGCTGGTACTGG -3'

LckY505F: 5'- GAATTCAAGGCTGGGGCTGGAAGTGGCCCTC -3'

4.5. Confirming the authenticity of the proteins:

4.5.1. Expression and kinase activity:

Expression of the full length recombinant baculovirus Lck proteins was determined concomitantly with their autophosphorylation activity. *In vitro* autophosphorylation assays (+/- ATP) as detailed section 2.8.8, were performed on recombinant baculovirus infected Sf9 lysates. These were analysed for Lck expression and phosphotyrosine levels by western blotting. The anti-phosphotyrosine blot shown in the top gel of figure 4.1A compares the two independently derived wildtype Lck clones AcLck and wtLck to the LckG2A nonmyristoylated mutant and the kinase inactive mutant, LckK273A. Since the Lck proteins are significantly over expressed by comparison to any endogenous Sf9 cellular proteins the bands detected by the anti-phosphotyrosine antibody were solely attributable to Lck tyrosine phosphorylation. In all cases, with the exception of the Lck K273A kinase inactive mutant, in the presence of ATP the level of phosphotyrosine was elevated. The inhibition of tyrosine phosphorylation observed for the K273A mutant demonstrated by the lack of bands detected in the α -pTyr western blot, was consistent with the essential role for a lysine at this position in the phosphate transfer to Tyr394 during autophosphorylation. This inferred that the observed augmentation of tyrosine phosphorylation for the wildtype and nonmyristoylated Lck proteins was as a direct result of the autophosphorylation of Tyr394. If endogenous kinases were active on

Tyr394 we would have expected to see an increase in phosphotyrosine levels for K273A. Similar protein expression levels in the +/- ATP lanes were confirmed by stripping and reprobing the PVDF membrane (see section 2.8.4) with an anti-Lck antibody. Lck expression levels are shown in the bottom gel in figure 4.1A.

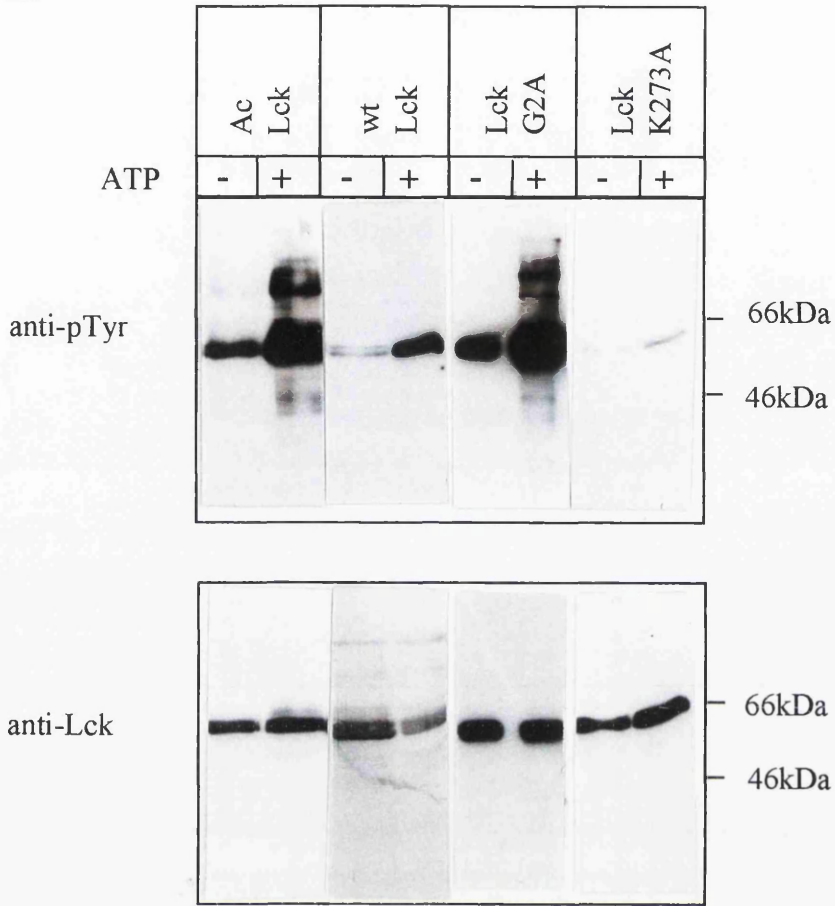
In order to establish the kinases were also active on an exogenous substrate, a peptide substrate assay was utilised, described in more detail in 2.8.9. In brief, the Lck kinase activity was measured by the number of phosphates transferred in 30 minutes to a peptide substrate documented to form an optimum substrate for Src tyrosine kinases (Casnellie, 1991; Moarefi *et al*, 1997). [$\gamma^{32}\text{P}$] was included in the reaction and the number of phosphates transferred calculated from scintillation counter readings. The results are presented in the bar graph in figure 4.1B. The number of pmols of phosphates transferred for wtLck was 6 fold higher than that observed for LckK273A, indicating that it maintained its kinase activity on an exogenous substrate. The Hck 30 minute reading was ~4 fold higher than that obtained for Lck. However, the amount of protein used for each assay was equilibrated by western blot analysis and therefore used protein specific antibodies. Hence, differing protein activities observed for Hck and Lck were most likely attributed to varying concentrations of each protein in the assay.

Figure 4.1. *Analysis of expression and phosphorylation of recombinant baculoviruses expressing wtLck and AcLck:*

A: Lysates from Sf9 recombinant baculovirus infected cells were made as detailed section 2.6.5 and autophosphorylation assays performed either $-/+$ ATP, as detailed section 2.8.8. The samples were resolved on a 12% SDS-PAGE gel and analysed by western blot. The top gel is an anti-phosphotyrosine (α -pTyr) blot and the bottom is an anti-Lck (α -Lck) blot. Lanes 1- 2 show AcLck $-/+$ ATP and lanes 3- 4 wtLck, both had elevated levels of tyrosine phosphorylation in the presence of ATP, corresponding to the ability to autophosphorylate Tyr394. Lanes 3- 4 contain LckG2A, which behaved similarly to the wildtype Lck clones. Lanes 4- 5 show the control kinase defective LckK273A mutant, for which no tyrosine phosphorylation was detectable.

B: The results from the peptide substrate assays (as detailed 2.8.9), summarised on a bar graph, clearly demonstrating that wtLck was active on an exogenous substrate, in contrast to LckK273 which was inactive. Hck was used as the positive control in these experiments and β -Gal was used as the negative control. The experiment was not quantitative.

A:



B:

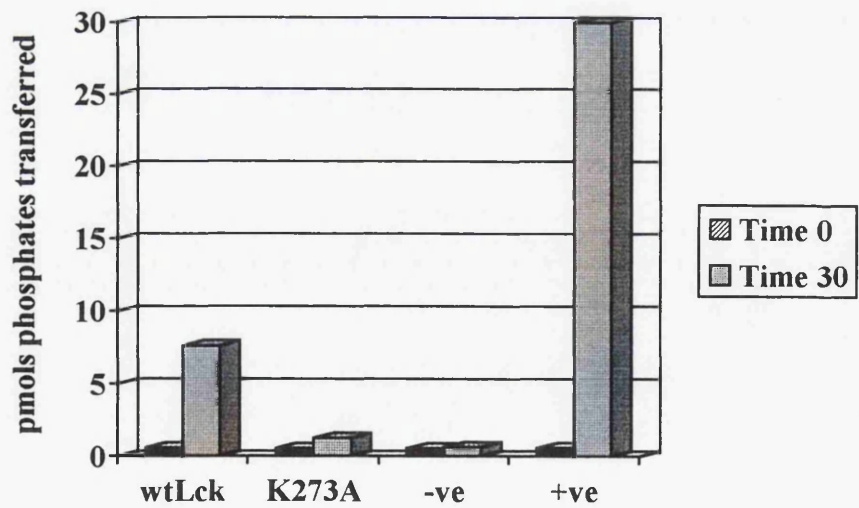


Figure 4.1.

4.5.2. Confirming the authentic acylation of Lck:

Acylation is a eukaryotic post-translational modification event which results in the addition of fatty acid side chains to specific protein motifs. Myristoylation occurs cotranslationally and results in the covalent attachment of a 14 carbon saturated fatty acid to an adjacent N-terminal glycine residue. The reaction is catalysed by the N-myristoyl transferase enzyme and is irreversible. In contrast, palmitoylation is a reversible event that occurs post-translationally at the cell membrane. Palmitoylation is typically dependent on myristoylation to target proteins to the membrane, where the addition of palmitate stabilizes the membrane association. Palmitoylation is catalysed by palmitoyl transferase which catalyses the addition of a 16 carbon saturated fatty acid to a cysteine residue via a thioester bond (reviewed (Mumby, 1997)). The baculovirus expression system was selected for use in these studies because it is eukaryotic and allows authentically acylated proteins to be expressed to high levels.

To ensure the proteins utilised in the interaction assays were authentically acylated, Sf9 cells were metabolically labelled with [³H] myristic and [³H] palmitic acid and subject to fluorography as detailed section, 2.6.9. In the experiments presented in this section the newly constructed wtLck was assessed for acylation, as previous work (Harris, 1995) had established authentic acylation of AcLck. The LckG2A and LckK273A recombinants were also analysed. The results can be seen in figure 4.2. Gel A shows cells labelled with [³H]] myristic acid. In lane 3 a band corresponding to wtLck at ~56kDa is clearly visible, confirming myristoylation of the protein. As expected the G2A Lck mutant (lane 4) which encodes an alanine at position 2 preventing myristate attachment, was not myristoylated. The kinase inactive mutant LckK273A was also authentically myristoylated as anticipated since the K273A point mutation was distal to the myristoylation signal (lane 5). Similar results were seen for labelling with [³H] palmitic acid, figure 4.2 gel B. However, the addition of palmitate by transesterification is a reversible process plus palmitate is upstream of myristate in the metabolic pathways. It was therefore possible that some of the palmitic acid label had been metabolised to myristate and the signal detected by fluorography in gel B was mainly due to myristoylation. To confirm that

the signal was caused by the incorporation of [^3H] palmitic acid the gels were treated with 1M hydroxylamine pH7.0. This treatment removes residues attached by thioester bonds, but has no effect on myristoylation. Figure 4.2 gels C and D show the results after 1M hydroxylamine treatment. Gel C containing the [^3H] myristic acid labelled proteins remained unchanged (compare to gel A), with the same bands detected in each lane. Conversely, gel D shows the loss of signal for wtLck and K273A confirming the label originally incorporated into these proteins was ^3H palmitic acid (compare to gel B); thus the authentic acylation of both wtLck and K273A Lck was confirmed.

Figure 4.2. Establishing the authentic acylation of wtLck:

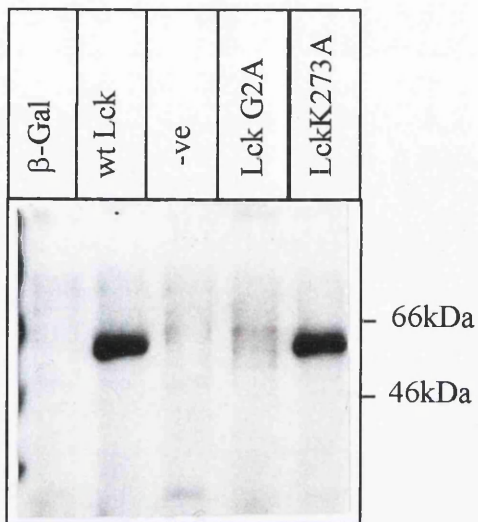
Sf9 cells were metabolically labelled with either [³H] myristic or [³H] palmitic acid and labelled proteins were detected by fluorography as described 2.8.1 and 2.6.9.

A: Results of fluorography of the [³H] myristic acid labelled samples. Lane 1; contained a β-Gal negative control; lane 2 shows the authentically myristoylated wtLck at ~56kD; lane 3 contained an Sf9 lysate negative control; lane 4 contained LckG2A a nonmyristoylated mutant of Lck; lane 5 contained LckK273A, the kinase defective mutant which was authentically myristoylated.

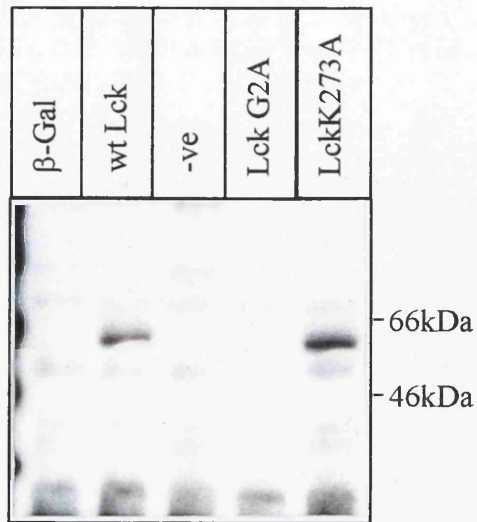
B: The same samples were labelled with [³H] palmitic acid. A signal corresponding to ~56kDa was detected for both wtLck (lane 2) and LckK273A (lane 5).

C and D: Determination of authentic palmitoylation. The same samples shown in A and B were reanalysed, but prior to fluorography the gels were fixed in destain for 10 minutes and subsequently incubated in 1M hydroxylamine pH7.0 for 30 minutes, to remove thioester bound palmitate. Gel C shows the [³H] myristic acid labelled samples were unaffected by the treatment whereas all detectable signal was lost in gel D for the [³H] palmitic acid labelled samples, indicating the label incorporated into the proteins in B was due to authentic palmitoylation.

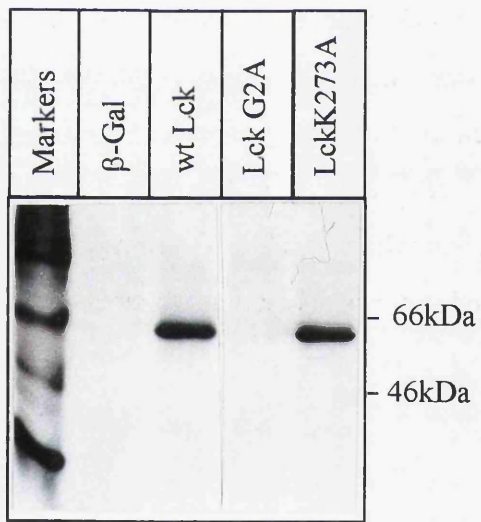
A.



B.



C.



D.

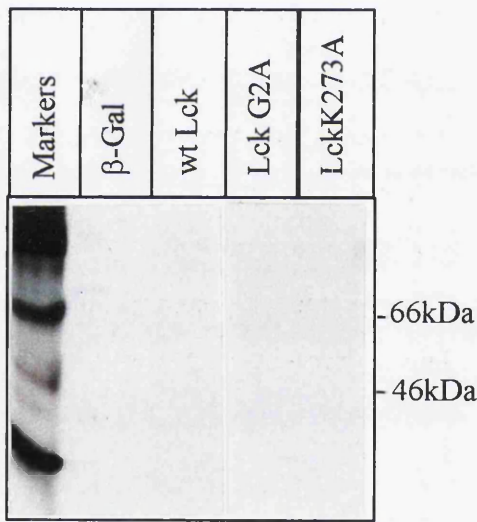


Figure 4.2.

4.6. *In vitro* binding assays:

For the *in vitro* assays throughout these studies, unless otherwise stated, the affinity reagents were baculovirus expressed affinity purified N-terminal GST fusions, bound to glutathione-agarose beads (GA-beads), as detailed in section 2.6. The Nef allele used for these studies, except where stated was BH10. The authenticity and functionality of the Nef isolates and mutants had been determined in previous studies with CD4, so will not be shown here (Harris and Neil, 1994; Cooke *et al*, 1997). The remit for these studies was to confirm the *in vitro* binding of Lck to Nef seen in preliminary experiments and to investigate an apparent loss of binding in the presence of NaOV, a tyrosine phosphatase inhibitor.

4.6.1. Overview of preliminary studies:

During preliminary studies within the laboratory *in vitro* binding assays were performed for AcLck with both Nef-GST (N-G) and nonmyristoylated Nef-GST (G2A-G) as affinity reagents. Data obtained from these studies, shown in figure 4.3A, demonstrated a direct interaction between full length acylated AcLck and Nef was dependent on Nef myristoylation *in vitro* (compare lanes 3 and 4 to lanes 5 and 6, gel A). Lck bound to the N-G affinity reagent was further analysed for autophosphorylation activity in the presence or absence of ATP (see section 2.8.8. for method). The anti-Lck western blot shown in figure 4.3A confirmed the N-G/Lck complex was aliquoted equally prior to the autophosphorylation assay with similar levels of Lck in both +/- ATP samples (lanes 3 and 4). As expected the levels of phosphotyrosine detected during the anti-phosphotyrosine western blot for the Lck lysate alone were elevated in the presence of ATP, consistent with autophosphorylation (compare lanes 1 and 2, C). In contrast, there was no detectable phosphotyrosine in Lck bound to Nef either minus or plus ATP, even at higher ECL exposure times (lanes 3 and 4, C). This preliminary data, since corroborated by our collaborators (Collette *et al*, 1996), suggested that Lck autophosphorylation activity was inhibited by Nef binding. In addition *in vitro* binding assays were performed on Lck lysates prepared in the presence of NaOV, a tyrosine phosphatase inhibitor. Under these conditions Lck binding was impaired (see figure 4.3B lanes 3 and 4). Taken together this data suggested that Nef bound the active conformation of Lck and in so doing rendered the kinase active site inaccessible to autophosphorylation.

Figure 4.3. Results from the preliminary studies:

In vitro binding assays were performed for AcLck plus either N-G or G2A-G. The complex immobilized on beads was aliquoted and subject to an autophosphorylation assay either +/-ATP. The results were analysed by western blot.

A: Depicts an anti-Lck blot of the binding assay. Lanes 1 and 2 are the AcLck lysate only control; lane 3 and 4 show a band corresponding to AcLck bound to the N-G affinity reagent. The absence of bands in lanes 5 and 6 demonstrate that AcLck was incapable of binding the G2A-G nonmyristoylated Nef affinity reagent.

B: A replica *in vitro* binding and autophosphorylation assay as shown in A and C except that the Lck lysates used as bait in these assays were prepared in the presence of NaOV. This anti-Lck blot shows that treatment of Lck with NaOV clearly impaired binding to N-G.

C: This shows the PVDF membrane in A stripped and reprobed with an anti-pTyr antibody. The AcLck lysate alone in lanes 1 and 2 provided a control for the autophosphorylation assay. The absence of detectable tyrosine phosphorylation in lanes 3 and 4 for AcLck bound to Nef suggested a Nef block to Lck autophosphorylation activity.

D: B stripped and reprobed with α -pTyr demonstrating no tyrosine phosphorylation was detectable after protein complex formation.

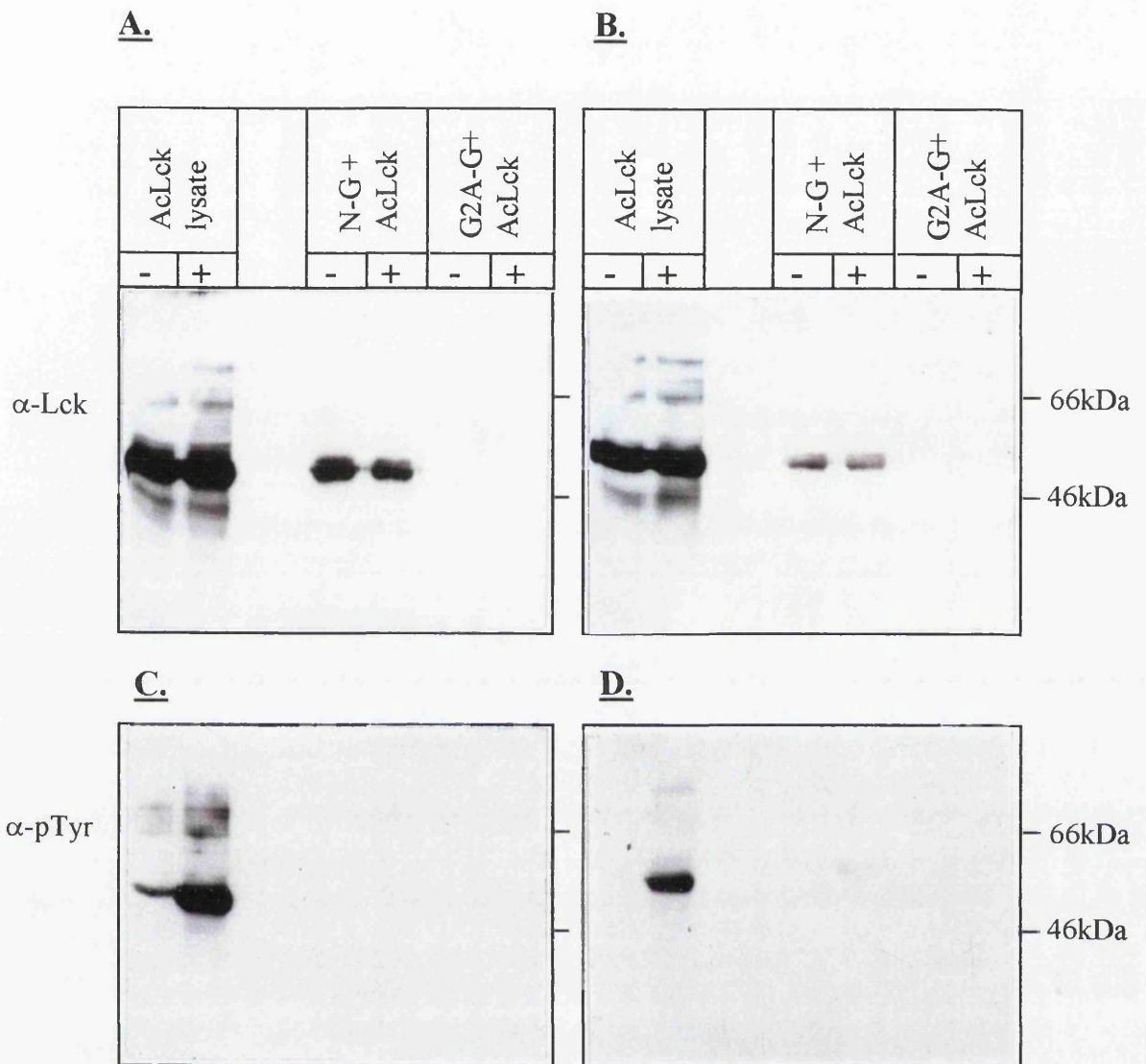


Figure 4.3

4.6.2. Follow up *in vitro* binding studies:

In the current studies standard binding assays were performed for the newly derived wtLck recombinant baculovirus using N-G, G2A-G and m-G as affinity reagents. Unexpectedly no interaction between Nef and wtLck was detectable (data not shown). The assay was repeated with freshly made lysates of the earlier constructed recombinant baculovirus AcLck substituted for wtLck and again the interaction could not be reconstituted. To reconcile the differences between the experiments and to ascertain whether the tissue culture media itself could be contributing by causing altered protein conformations, crosswise comparisons of all the reagents were carried out. This was facilitated by the availability of the original AcLck lysates (oAcLck) and GST affinity reagents (oN-G, oG2A-G and om-G) used in the preliminary studies.

The table in figure 4.4A summarises the 6 separate binding assays performed to identify compatible Nef-Lck binding partners (the numbers correspond to the sample sets shown in 4.4.B). Samples loaded onto the left-hand-side of each gel figure 4.4B (lanes 3,4 and 5) had the newly purified GST fusion proteins as their affinity reagents, while those on the right-hand-side had the original affinity reagents (lanes 7,8 and 9). The top gel in figure 4.4B shows the results for wtLck. If lane 3 is compared to lane 7 it is evident that as previously found there was no detectable binding of wtLck to N-G (lane 3). In contrast, oN-G bound low levels of wtLck (lane 7). In both assays no binding of wtLck to G2A-G or oG2A-G was seen (lanes 4 and 8). Almost identical results were obtained for AcLck, shown in the middle gel of figure 4.4B. However, when the original oAcLck lysate was analysed for binding to the affinity reagents (bottom gel), it was found low levels of oAcLck associated with the newly purified N-G (lane 3), at a level comparable to that seen for oN-G plus either wtLck or AcLck (lane 7, top and middle gels respectively). Significantly, when both sets of the original reagents were utilised (bottom gel, lane 7) the interaction was reconstituted. In lanes 2 and 6 of every gel each Lck lysate precleared with GA-beads was loaded, the amount corresponded to one fifth of the total input Lck lysate. Therefore oN-G bound ~10% of the total oAcLck. The preclear samples also illustrated that in every binding assay equivalent levels of Lck

protein were present. Similar to the preliminary *in vitro* binding studies Lck binding to Nef was found to be dependent on myristoylation (lane 8), although low levels of oAcLck binding to G2A-G was evident at higher exposures (lane 4). Figure 4.4C (second sheet) shows the loading of the affinity reagents on the GA-beads. This revealed the amount of the original reagents was ~2 fold greater than the newly purified stock which may have contributed to differences seen between the reagents.

These crosswise comparisons clearly indicated a fundamental difference between the original and newly produced stocks for both the affinity reagents and Lck lysates. In general, the original oN-G stocks had a higher overall affinity for all the Lck recombinant subclones (compare lane 7 of each gel to lane 3), which may or may not be attributable to varying concentrations since they were present in excess. Also, oAcLck bound Nef at significantly higher levels than the newly made AcLck lysate (compare middle and bottom gels). To identify factors governing the Lck and Nef association two questions were addressed. Firstly, what was the cause of the differences between stocks and secondly, how were the differences allowing the proteins to adopt more favourable binding conformations.

Figure 4.4. *In vitro* binding assay results of the crosswise comparison of reagents.

Table A: Summarises the reagents used in each assay (total of 6 individual assays).

B: Standard *in vitro* binding assays were performed to analyse discrepancies between different lysate and different affinity reagent stocks. A detailed account of the results are provided in the text. The top gel shows binding assays for wtLck, the middle for AcLck and the bottom for oAcLck. Lane 1 of each gel was loaded with the same Lck positive control to facilitate comparison of ECL exposures. Lanes 2 and 6 were loaded with precleared samples of each Lck lysate used for the respective assays. Lanes 3, 4 and 5 for each gel had the newly purified affinity reagents (N-G, G2A-G and m-G respectively) while lanes 7, 8 and 9 had the original affinity reagents (oN-G, oG2A-G and om-G).

C: Coomassie stained gel to quantitatively compare the amount of purified protein bound to GA-beads. Samples were resuspended in sample buffer and heated at 90°C for 2 minutes prior to loading, 5µl packed volume of GA-beads was loaded in each lane. Samples were loaded in the order, N-G, G2A-G, m-G, followed by oN-G, oG2A-G and om-G. The results show that there was an increased amount of protein bound to beads in the original samples.

A.

Binding assay No.	Lck Lysate			Affinity Reagent					
	wtLck	AcLck	oAcLck	N-G	G2A-G	m-G	oN-G	oG2A-G	om-G
1	✓			✓	✓	✓			
2	✓						✓	✓	✓
3		✓		✓	✓	✓			
4		✓					✓	✓	✓
5			✓	✓	✓	✓			
6			✓				✓	✓	✓

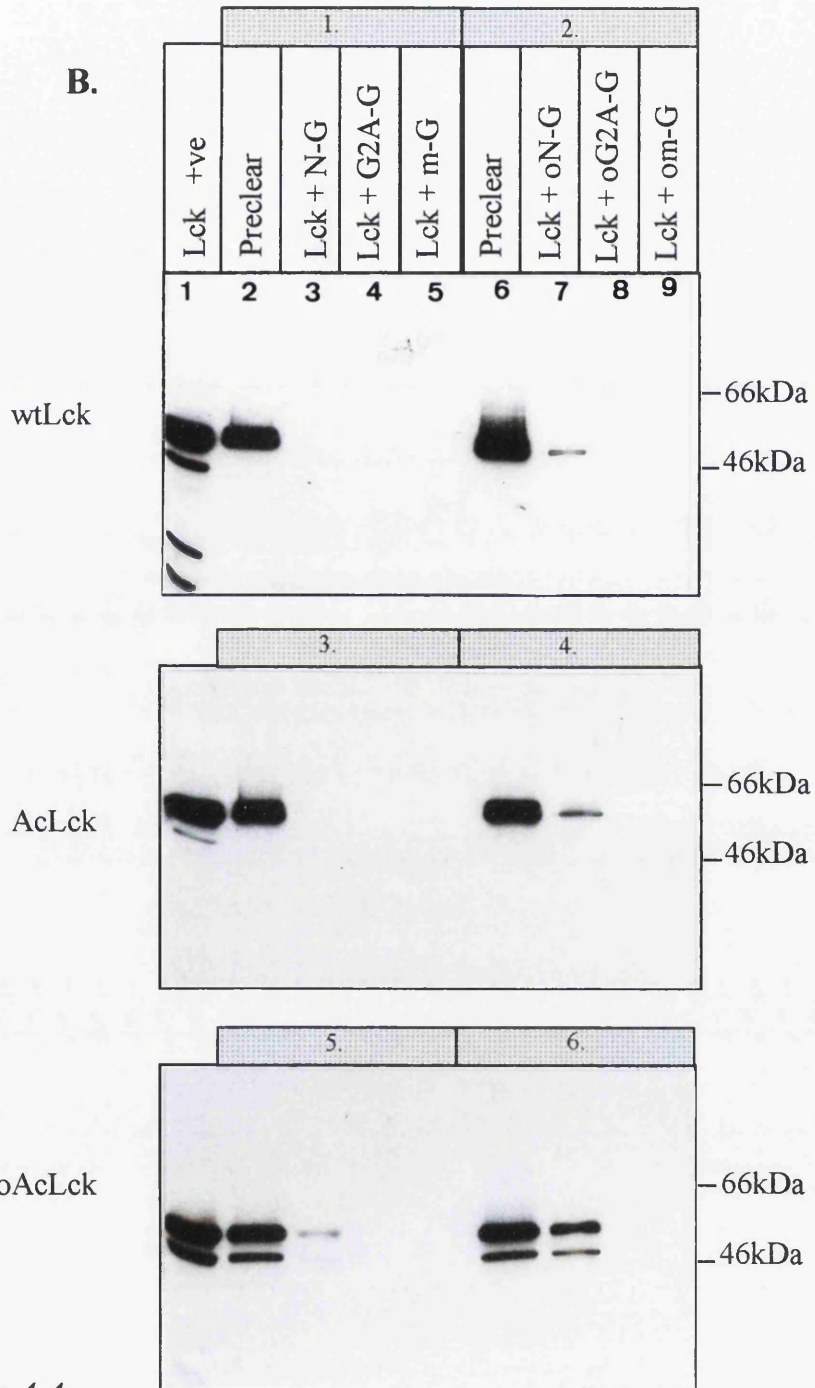


Figure 4.4.

C.

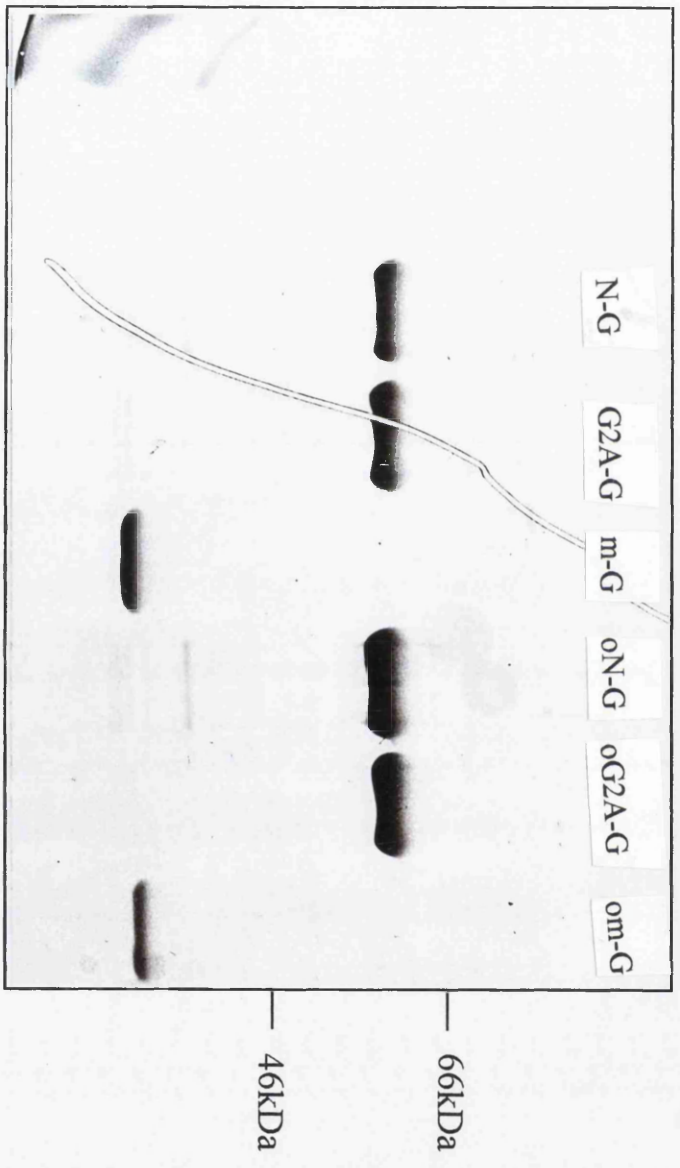


Figure 4.4 (cont.)

4.6.3. Identifying the cause of the differences between protein stocks:

As the results presented above demonstrated, variations in Lck-Nef binding occurred even when the same viral stocks were utilised, it was therefore concluded that either tissue culture or cell lysis conditions must be responsible. The most variable parameter among which was batch differences in the foetal calf serum used to supplement the TC100 medium. Serum comprises a complex mixture of biomolecules including, growth factors, cytokines, hormones, attachment and spreading factors, binding proteins, lipids, minerals and anti-proteases. It is hence difficult to control for differences between batches (Maurer, 1992). Slight alterations in, for example various inorganic minerals and trace elements such as Cu, Zn, Co, Mn and Se can abrogate cellular enzyme functions due to their critical role as enzyme cofactors. i.e. Selenite has been demonstrated to activate the enzyme glutathione peroxidase which is necessary for detoxifying otherwise cytotoxic oxygen radicals; therefore a selenite depletion in a batch of serum could potentially expose the cells to oxidative stress (Hewlett, 1991). Also concentration variations in other components such as growth factors (e.g. epidermal growth factor, fibroblast growth factor and platelet derived growth factor) and cytokines (e.g. IL-2, tumor necrosis factor (TNF), interferon γ , IL-12) normally involved in promoting cell proliferation and differentiation, could result in the alteration of an abundance of cell signal transduction cascades (Maurer, 1992).

To assess the impact of the serum on Lck association with Nef, Sf9 cells were grown for 1 passage in complete TC100 medium supplemented with 9 different serum batches. Once equilibrated the cells were infected with the AcLck recombinant baculovirus. *In vitro* binding assays were performed and the binding affinities of the Lck lysates (infected in different sera) for the same N-G affinity reagent ascertained. Figure 4.5A shows an anti-Lck western blot of the binding assays with N-G, while figure 4.5B shows an anti-Lck western blot of the precleared Lck lysates confirming levels of Lck were equal across the samples prior to immunoprecipitation. Lanes 1-7 were AcLck lysates produced from Sf9 cells grown in randomly selected commercially available serums, lane 8 was the same serum utilised for the preliminary studies (GIBCO) and lane 9 was the serum used

for the more recent experiments (PAA Laboratories). Overall the results of the binding studies (gel A) demonstrated that serum batches could significantly influence the ability of Lck to bind an invariant N-G affinity reagent (compare lanes 7 and 8). Due to the high exposure of the autoradiograph binding of AcLck to N-G in lane 9 was evident, however after 1 passage in the original sera there was a significant increase in the binding efficiency of AcLck to N-G in lane 8. Although the level of binding observed in lane 8 was not returned to that seen in previous experiments, (figure 4.3 and 4.4) this was probably attributable to the short amount of time the cells were passaged in the media for this experiment. These results therefore concurred with the prediction that the serum did have an effect on the ability of Lck to associate with Nef.

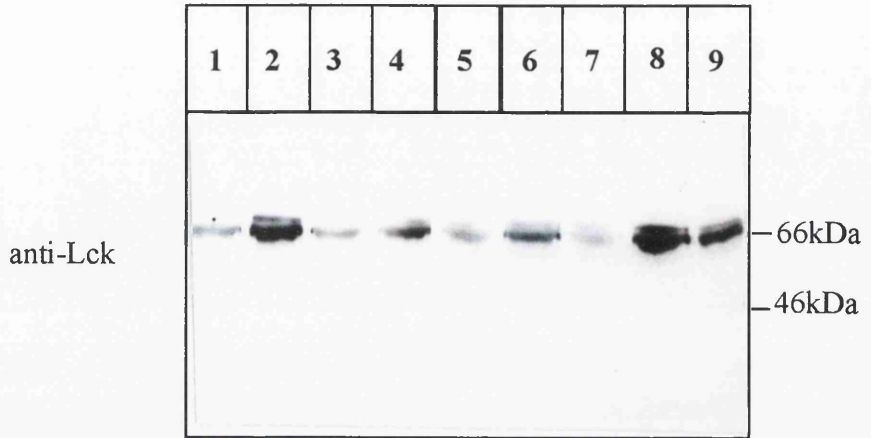
Figure 4.5. Affect of serum on Lck binding to N-G:

AcLck lysates were prepared from 9 individual batches of Sf9 cells each grown in different sera for 1 passage. The resultant AcLck proteins were analysed for their ability to bind N-G. Lanes 1-7 contain samples grown in random selected commercially available serum; lane 8 was the original serum; lane 9 was the current serum.

A: Results of *in vitro* binding assays; showing highly variable band intensity for AcLck demonstrating the different sera had a profound affect on the ability of Lck to bind Nef.

B: AcLck preclear samples, loaded the same as A confirming equivalent amount of AcLck was included in each assay.

A.



B.

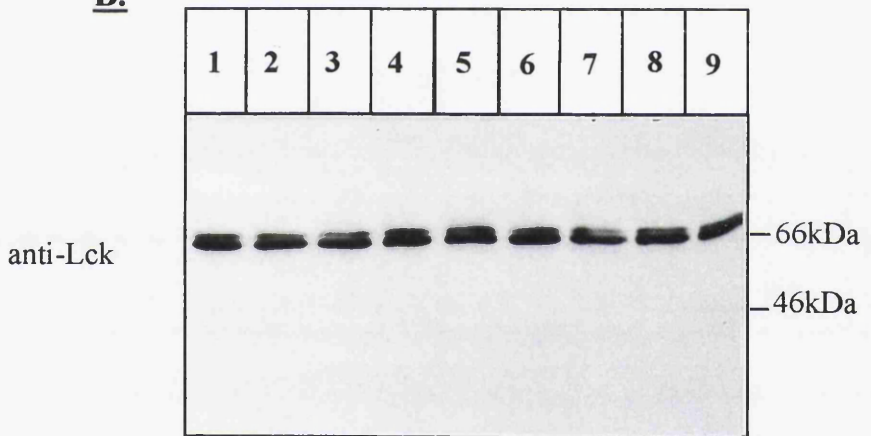


Figure 4.5.

4.6.4. How were the protein conformations altering between stocks:

It was conceivable that binding differences detected between Lck and Nef from different stocks may be as a result of the presence or absence of an intermediate factor. However, even if this was the case, the evidence from the NaOV experiments in the preliminary studies suggested it was Lck conformation dependent. The obvious affect of serum on the ability of Lck to associate with Nef and the intrinsic between serum factors and cell signal transduction pathways led us to compare the phosphotyrosine levels of oAcLck with those of AcLck and wtLck. Autophosphorylation assays were performed (as detailed 2.8.8) on the same Lck lysates utilised for the crosswise comparisons in section 4.6.2. Equivalent levels of Lck expression were confirmed by western blot analysis, figure 4.6B. The results of the autophosphorylation assay, see figure 4.6A indicated in accordance with earlier results (figure 4.1A) that both wtLck and AcLck had low background levels of phosphotyrosine (lanes 2 and 5) which elevated after incubation with ATP (lanes 3 and 6). In contrast, it was evident that by comparison oAcLck had elevated background levels of phosphotyrosine (lane 8) which did not substantially increase in the presence of ATP (lane 9).

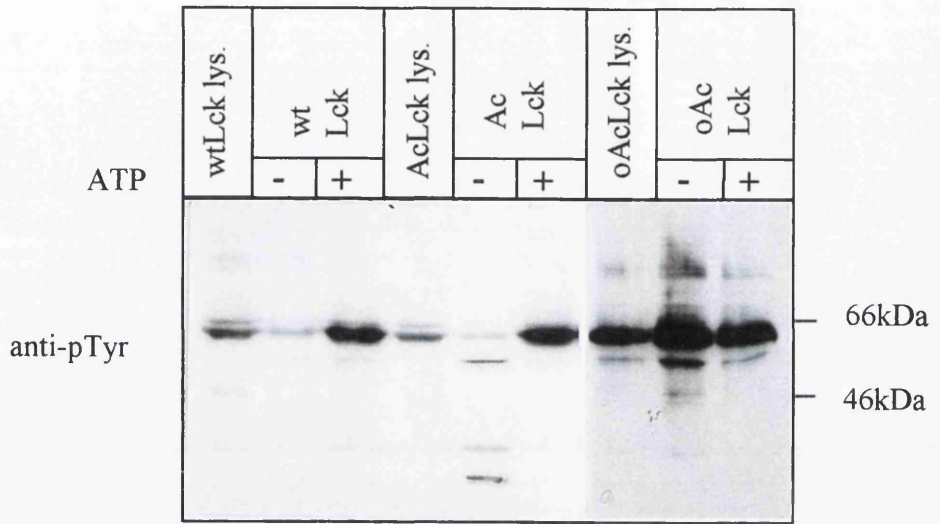
During the autophosphorylation assay presented in section 4.5.1. it was demonstrated the incubation of Lck with ATP correlated with an increase in tyrosine phosphorylation on Tyr394. The most plausible explanation for the high levels of pTyr in the oAcLck stock, irrespective of ATP, was that inferred phosphorylation of Tyr394 was saturated prior to the addition of ATP i.e. the oAcLck stocks were predominantly in the active kinase conformation. Conversely, the increase in phosphotyrosine levels on incubation with ATP for wtLck and AcLck suggested that these stocks were in the inactive conformation during the binding assays. However it was also possible that the elevated levels of phosphotyrosine were a result of saturated Tyr505 phosphorylation and that the kinase was predominantly inactive. The differential phosphorylation between stocks was were consistent with the original hypothesis and confirmed a distinct Lck conformation conferred its ability to bind Nef. To address this specific mutants were generated see below.

Figure 4.6. Autophosphorylation assays to compare wtLck, AcLck and oAcLck:

A: Depicts the results of the autophosphorylation assays analysed by western blot with an anti-pTyr antibody. Lanes 1-3 show wtLck, 4-6 AcLck and 7-9 oAcLck. The first lane for each is untreated lysate and the second two are the results of autophosphorylation assays either -/+ ATP. The autophosphorylation activities for wtLck and AcLck were similar, with low levels of tyrosine phosphorylation -ATP but high levels +ATP. In contrast, oAcLck (lanes 8 and 9) had equal phosphotyrosine levels either -/+ ATP, inferring it was constitutively active.

B: Gel A stripped and reprobed with anti-Lck to confirm equivalent levels of Lck in each lane.

A:



B:

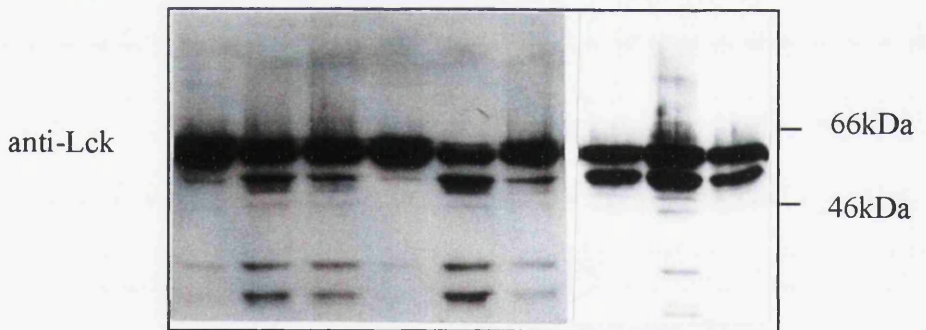


Figure 4.6.

It was clear from the crosswise comparison experiment that Lck conformation alone was not sufficient to reconstitute the Nef-Lck interaction, a distinction between the original and newly purified affinity reagents was also apparent. This could be as a result of the varying amounts of protein bound to the GA-beads, but as the affinity reagents were added in excess subtle differences would not normally be expected to greatly influence the amount of binding. The affect of the serum on Nef at this stage can therefore only be speculated. Nef phosphorylation on serine and threonine residues has been reported by our laboratory (Coates and Harris, 1995; Coates *et al*, 1997) and other groups (Guy *et al*, 1987; Bandres *et al*, 1994; Bodeus *et al*, 1995; Luo *et al*, 1997). In addition, our collaborators have identified tyrosine phosphorylation of Nef (Collette *et al*, 1996). However the significance of Nef phosphorylation is unknown, but may play a crucial role in enhancing Nef interactions with cellular proteins. Tyrosine phosphorylation of Nef could potentially transform it into an SH2 binding substrate, this in conjunction with the SH3 recognition motif, (PXX)₃P could provide the additional binding energy necessary for its interaction with Lck. As tyrosine phosphorylation is involved in the majority of cellular activation pathways, it is plausible that variations in sera may have induced variations in Nef tyrosine phosphorylation. Attempts to determine whether serum induced phosphorylation of Nef may influence its interaction with Lck were unsuccessful. This was due to insufficient sensitivity of the western blot analysis utilising anti-phospho serine/threonine and anti-phosphotyrosine antibodies.

4.7 Construction of constitutively active and inactive Lck mutants to assess conformational binding criteria:

To confirm whether Lck binding to Nef was dependent on Tyr394 phosphorylation *per se* or if the “open” active conformation was sufficient, two constitutively open Lck mutants were constructed. A single point mutation in the C-terminal regulatory tyrosine residue, Tyr505 of Lck has been demonstrated to confer cellular neoplastic transformation (Marth *et al*, 1988) analogous to that seen for p60^{c-Src} Tyr527 mutations (Courtneidge, 1985; Stover *et al*, 1994; Brown and Cooper, 1996). This Lck mediated neoplastic transformation occurs as a result of an inability of the

enzyme to regulate its kinase activity due to the disruption of the intra-molecular association of pTyr505 with the SH2 domain, hence maintaining Lck in the open conformation. As a consequence the Tyr505 mutation is accompanied by significant increases in Lck Tyr394 phosphorylation and enzyme activity. The first baculovirus transfer vector was hence modified to contain the Y505F Lck point mutation, as detailed in section 4.4. In addition, a second kinase inactive mutant K273A in combination with the Y505F mutant was constructed to provide an "open" inactive Lck conformation for comparison. A point mutation of lysine to arginine at position 273 in Lck has been reported to inhibit the transfer of a phosphate from ATP to Tyr394 (Carrera *et al*, 1993). As phosphorylation of Tyr394 is required for the kinase activity of the enzyme, the K273A mutation renders Lck inactive. However, when we attempted to introduce these two constructs into recombinant baculoviruses the expression of constitutively open conformations of Lck proved toxic to the Sf9 cells. As a result recombinant baculoviruses expressing Lck Y505F or Lck Y505F/K273A could not be generated. This suggested that the constitutively open myristoylated conformation of Lck was causing cytotoxic signal transduction via its SH3 and SH2 domains. To combat this nonmyristoylated derivatives of these mutants were constructed; thus removing Lck from cellular membranes where potential SH3, SH2 and kinase substrates are concentrated. This approach was prompted by a previous study by (Abraham and Veillette, 1990) in which expression of a nonmyristoylated Y505FLck mutant was reported to reduce the overall cellular tyrosine phosphorylation levels and oncogenic potential by comparison to a myristoylated Y505FLck mutant.

4.8 Confirmation of the expression and kinase activities of the mutant Lck recombinant baculoviruses; Lck G2A/K273A/Y505F (LckGKY) and Lck G2A/Y505F (LckGY):

Prior to evaluating the ability of the constitutively open Lck mutants to bind Nef it was necessary to confirm their authentic enzymatic modifications. The results of autophosphorylation assays for the newly constructed recombinant Lck baculoviruses compared to those obtained for the wildtype AcLck and controls (LckG2A and LckK273A) are shown in figure 4.7A. In this instance to compare levels of autophosphorylation between samples it is necessary to take into account their respective expression levels shown in figure 4.7B. Perhaps unsurprisingly it was found both of the open conformation Lck mutants were expressed at low levels relative to the Lck wildtype and controls. Intriguingly, the constitutively open active nonmyristoylated Lck mutant, LckGY shown in lanes 9 and 10 of figure 4.7 had no detectable background phosphotyrosine in the absence of ATP, even at higher exposures (gel A). LckGY was however capable of autophosphorylation in the presence of ATP, as evidenced by the increase of phosphotyrosine levels (lane 10). The triple mutant LckGKY as anticipated was not phosphorylated on tyrosine residues either minus or plus ATP concurrent with its open conformation and kinase defective mutations (lanes 7 and 8, gel A). This also confirmed the earlier hypothesis that phosphotyrosine reactivity was entirely due to Lck activity and not a cellular kinase.

By comparison to the open conformation mutants the kinase defective single mutant K273A was expressed to substantially higher levels (lanes 5 and 6, gel B). This was possibly as a result of Tyr505 phosphorylation occluding its SH3 and SH2 substrate binding sites together with an inability to phosphorylate Tyr394. The anti-phosphotyrosine blot for LckK273A revealed background levels of phosphotyrosine both minus or plus ATP, consistent with a low level of Tyr505 phosphorylation. The phosphotyrosine levels detected for LckG2A minus ATP (lane 3) were analogous to those detected in the original oAcLck sample. Significantly, the background levels were higher than those seen for K273A (lane 5), suggestive of substantial Tyr394 phosphorylation. The difference was not attributable to varying

protein concentrations as both G2A and K273A were expressed to equal levels (compare lanes 3 and 4 to lanes 5 and 6, gel B). The results for LckG2A incubated plus ATP showed a further increase in phosphorylation (lane 4), implying only a proportion of G2A was activated minus ATP. The AcLck wildtype autophosphorylation activity was similar to that seen in previous assays with elevated phosphotyrosine levels in the presence of ATP and negligible amounts minus ATP. AcLck was expressed at intermediate levels relative to the Lck mutants.

Figure 4.7: *Analysis of the expression and kinase activities of LckGKY and LckGY relative to AcLck, LckG2A and LckK273A:*

A: Autophosphorylation assay, analysed by western blot with an α -pTyr antibody. Elevated levels of tyrosine phosphorylation were detected for LckG2A -ATP (lane 2) suggestive of Tyr394 phosphorylation; lane 3 contains LckG2A +ATP. Lanes 5 and 6 contain the LckK273A kinase defective mutant which had negligible tyrosine phosphorylation. Lanes 7 and 8 were LckGKY, which had no detectable tyrosine phosphorylation due to the C-terminal Y505 mutation and a mutation in its kinase active site. Lanes 9 and 10 were LckGY which unexpectedly had no background tyrosine phosphorylation (despite mutations to constitutively activate it), however it was capable of autophosphorylation as evidenced by the increase in phosphotyrosine levels in the presence of ATP.

B: Gel A stripped and reprobbed with an α -Lck antibody to show the variable expression levels observed for each of the Lck samples.

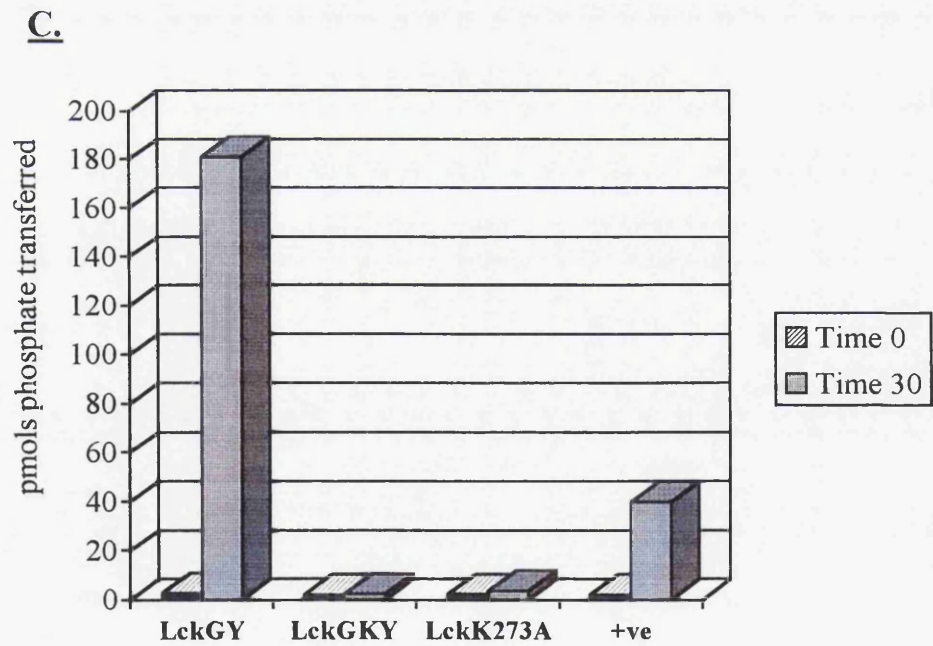
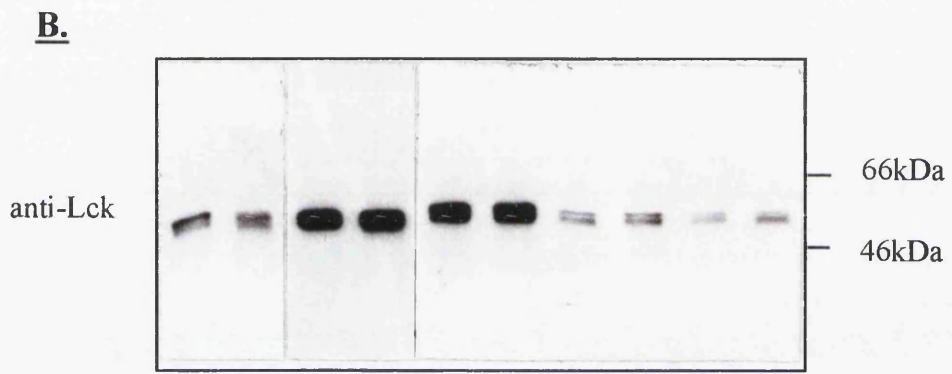
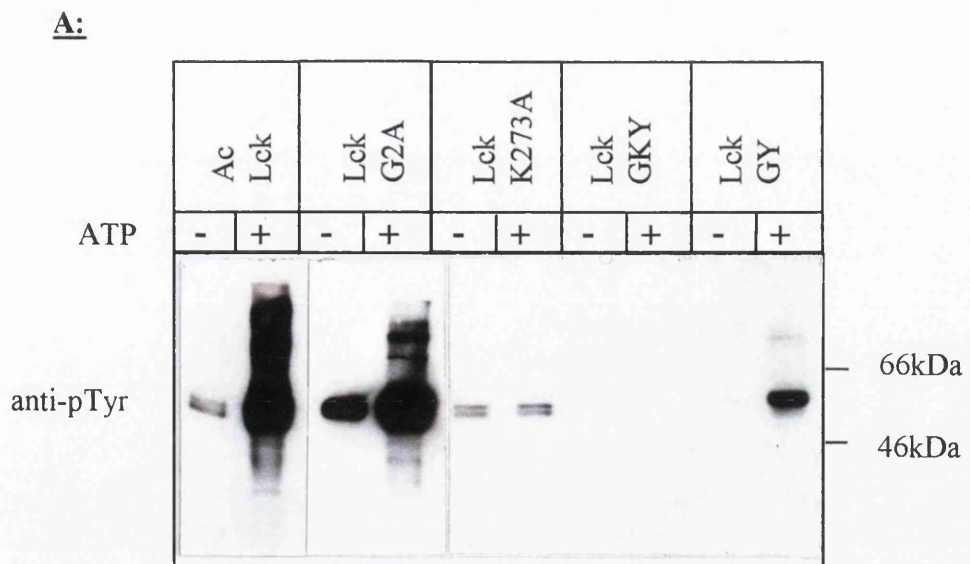
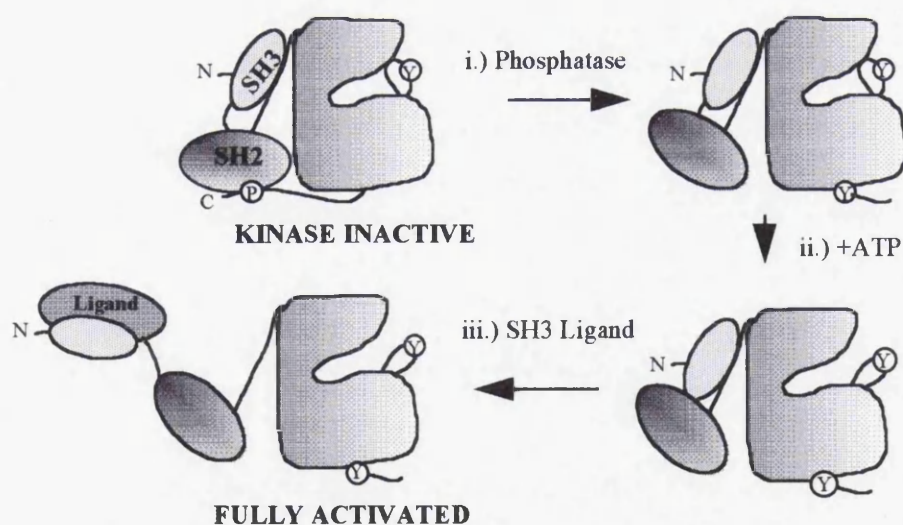


Figure 4.7.

One interpretation of this data, is that the removal of the nonmyristoylated Lck from cellular membranes allowed a level of kinase activity that could not be tolerated in the myristoylated wild type Lck. Whereas the inference from the results obtained for LckGY was that the Tyr505 residue or a conformation conferred by it was required for optimal autophosphorylation activity in the absence of high concentrations of ATP. It was speculated by Moarefi *et al* during their Hck activation studies (Moarefi *et al*, 1997) that variable partially active kinase conformations exist for Src kinases between the completely inactive and active conformations. In addition, external stimuli such as ATP have the potential to override any of these conformations converting an enzyme activity from a slow low background level, to a rapid high level of kinase activity. The results presented above concur with this hypothesis, with the autophosphorylation activities for LckG2A and LckGY being equivalent in the presence of ATP (if expression levels are taken into account), but variable at low ATP concentrations.

Diagram 4.1. A model for the activation of Src tyrosine kinases (adapted from Moarefi *et al* 1997):



To confirm the recombinant baculovirus Lck mutants maintained their enzymatic modifications on an exogenous substrate, peptide substrate assays were also performed (as detailed 2.8.9.). In the assay shown in figure 4.7C LckGKY and LckGY were compared to LckK273A with Hck as a positive control. As for the

wildtype Lck assays (section 4.5.1) an endpoint of 30 minutes was imposed and the total pmols of phosphates transferred over this period calculated. The Hck positive control used in this assay was not the same as presented in section 4.5.1., therefore the results are not directly comparable. However these results confirmed both the K273A, and K273A in combination with G2A and Y505F were kinase defective, while the double G2A, Y505F Lck mutant was highly active on an exogenous substrate.

4.9. *In vivo* binding studies:

If the previous *in vitro* binding results with the wildtype Lck proteins held true, one would predict that only the Lck species with elevated background levels of phosphotyrosine would bind Nef. In the panel of Lck mutants described above only the LckG2A mutant would therefore be expected to bind Nef, as the constitutively open active mutant LckGY had no detectable Tyr394 phosphorylation in the absence of ATP i.e. the conditions under which the binding assay is performed. For the assays outlined below the protein interactions were investigated *in vivo* after coinfection of Sf9 cells by the respective recombinant baculoviruses (see sections 2.6.5 and 2.6.8. for methods).

4.9.1. *In vivo* binding studies for LckGY and LckGKY:

Coinfections for LckGY and LckGKY with either N-G, G2A-G or m-G were assessed for protein interactions using the standard binding assay without the GA-bead pre-clear step (see section 2.6.8.). Unexpectedly it was discovered that the triple LckGKY mutant bound both N-G and G2A-G (lanes 6 and 7, figure 4.8A), but the active mutant LckGY did not associate with Nef (lanes 2 and 3). No association with the m-G negative controls were seen (lanes 4 and 8) confirming the specificity of the observed interactions. Higher exposures did reveal a faint band in lane 2 corresponding to LckGY binding to N-G, but this was not consistently reproducible. In fact, as apparent in the anti-GST western blot shown in figure 4.8B the co-expression of N-G or G2A-G with LckGY resulted in toxicity to the cells and invariably expression of one of the proteins was significantly reduced or lost all

together (lane 3, G2A-G expression was lost in this example). However, when co-expression was achieved as shown in lane 2, gel A there was only very minimal binding of LckGY to Nef. In contrast, co-expression of N-G with LckGKY appeared to increase LckGKY expression apparently reducing its cytotoxicity to the cells (data not shown). The lack of binding observed for LckGY corroborated the importance of elevated background phosphotyrosine levels for Nef association, but binding of LckGKY to Nef in the absence of LckGY binding represented an anomaly which will be addressed below.

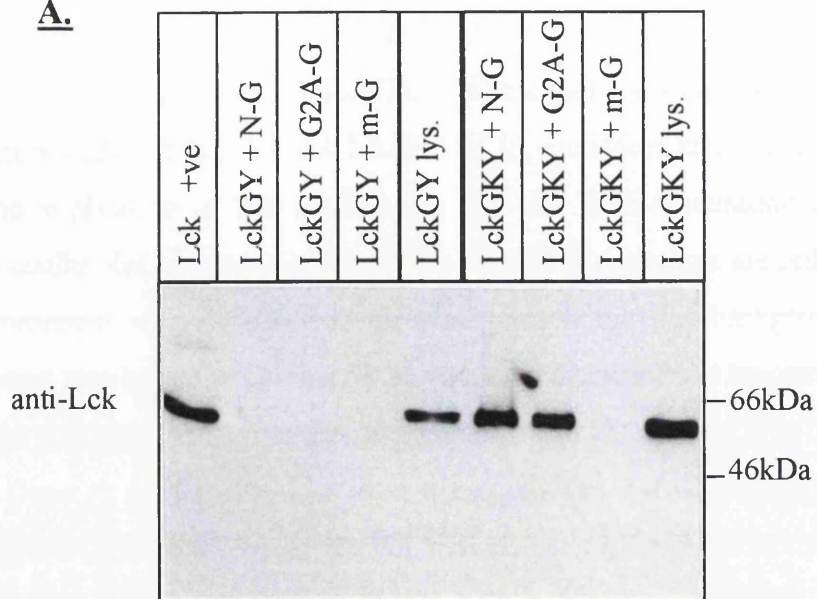
Figure 4.8. Results of *in vivo* binding assays for LckGY and LckGKY:

Coinfections of Sf9 cells were carried out for LckGY and LckGKY plus either N-G, G2A-G or m-G and *in vivo* binding assays performed as described sections 2.6.5. and 2.6.8.

A: *In vivo* binding assay, α -Lck western blot. Lane 1 is an AcLck positive control; lanes 5 and 9 contain LckGY and LckGKY lysates; lanes 2, 3 and 4 show there was no detectable binding of LckGY to either N-G, G2A-G or m-G respectively. Conversely the bands corresponding to Lck GKY in lanes 6 and 7 demonstrate its ability to bind both N-G and G2A-G. The lack of binding in lane 8 of LckGKY to m-G confirmed the specificity of the LckGKY interactions.

B: Gel A reprobed with an α -GST antibody.

A.



B.

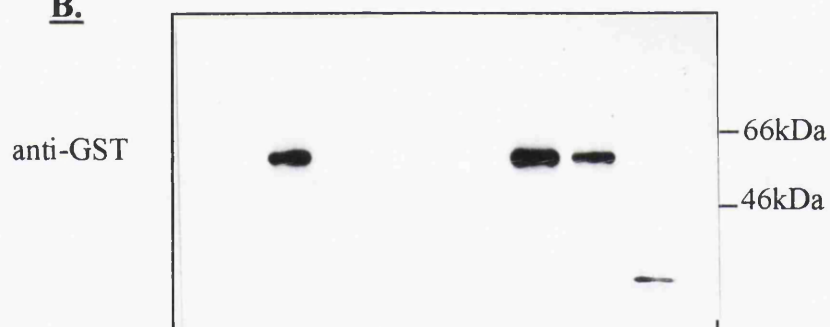


Figure 4.8.

* This also indicated that the coinfection of LckGKY with N-G in this example was not successful possibly due to a low multiplicity of infection ie. The amount of baculovirus per Sf9 cell, which for coinfections should be between 5-10 virions per cell.

4.9.2. A comparative study of Lck mutant binding abilities to N-G:

To directly compare the Nef affinity for the various Lck conformations, coinfections were set up simultaneously for each of LckGKY, LckGY, LckK273A, LckG2A, AcLck and β -Gal plus N-G. Western blot analysis of the results are shown in figure 4.9. Gel A shows an anti-Lck western blot of the various Lck mutants bound to Nef. As previously demonstrated the LckGKY mutant had a strong affinity for Nef (lane 2). Interestingly the Lck K273A bound Nef to equivalent levels as LckGKY (lane 4). The implication of this result being that the K273A mutation alone is sufficient to confer Nef binding, and the G2A and Y505F mutations are redundant. However, consistent with its observed elevated phosphotyrosine background the LckG2A mutant also bound N-G (lane 5), but with a reduced affinity by comparison to the K273A mutants. As in previous experiments no N-G binding was detected for LckGY (lane 3) with a very low level detectable for AcLck (lane 6). These results suggested that the G2A and K273A mutations may both contribute to the maintenance of an Lck conformation capable of Nef binding. The levels of N-G expression for each coinfection is shown in gel B. Reduced levels of N-G expression were shown for LckGKY, although this did not affect the amount of LckGKY bound suggesting the concentration of N-G in these assays is far in excess of the threshold level for binding*. The amount of Lck expression in each coinfection was quantitated by a separate western blot of the lysates prior to immunoprecipitation and found to be equivalent (see figure 4.9C).

These results therefore imply that both the LckG2A and LckK273A mutations cause the Lck protein to adopt similar conformations. As previously demonstrated the LckG2A mutant protein is predominantly in the "open" active conformation, so by analogy the K273A Lck mutant must be in the same configuration. The results from the autophosphorylation assays showing low levels of tyrosine phosphorylation for LckK273A consistent with a lack of Tyr505 phosphorylation support this hypothesis. Evidence for a possible open conformation of this mutant was provided in a recent study (Gonfloni *et al*, 1997). During an investigation of the role of the SH3-catalytic domain linker on the effect of enzymatic activity it was discovered mutations around the K273A site rendered the kinase constitutively

active. It is therefore possible that the K273A mutation causes the protein conformation to open but prevents kinase activity due to inhibition of the phosphate transfer reaction caused by the lack of the lysine residue at position 273.

Figure 4.9. *Comparison of Lck wildtype and mutants ability to bind N-G:*

Coinfections were performed as standard, each individual Lck recombinant baculovirus was coinfecting with the same amount of the N-G recombinant virus. Lysates were made and *in vivo* binding studies performed.

A: Results of the *in vivo* binding assay, western blot probed with α -Lck. Lane 1 was the β -Gal negative control which did not bind N-G. In lane 2 a band was detected at ~56kDa corresponding to LckGKY bound to N-G. Lane 3 shows LckGY did not bind N-G; but in lane 4 LckK273A bound to N-G at equivalent levels to that of LckGKY in lane 2. Lane 5 shows LckG2A had an intermediate binding level for N-G as evidenced by the reduced intensity of the band detected for LckG2A. A faint band in lane 6 was consistent with a very low level of binding of Lck to N-G.

B: Gel A stripped and reprobed with α -GST. Similar levels of expression for the affinity reagents were seen for β -Gal (lane 1), LckK273A (lane 4), LckG2A (lane 5) and AcLck (lane 6). Levels of N-G were reduced for LckGKY (lane 2) in this example, but did not impair the amount of LckGKY binding to N-G. No N-G expression was detected in the coinfection with LckGY (lane 3), consistent with cytotoxicity upon co-expression of the two proteins.

C: Quantitating the amount of Lck expression in the coinfection lysates. Each coinfection lysate was analysed by α -Lck western blot, prior to the binding assay to confirm equal Lck expression. The loading of the gel is the same as the above examples and the amount of Lck detected for each sample was equivalent.

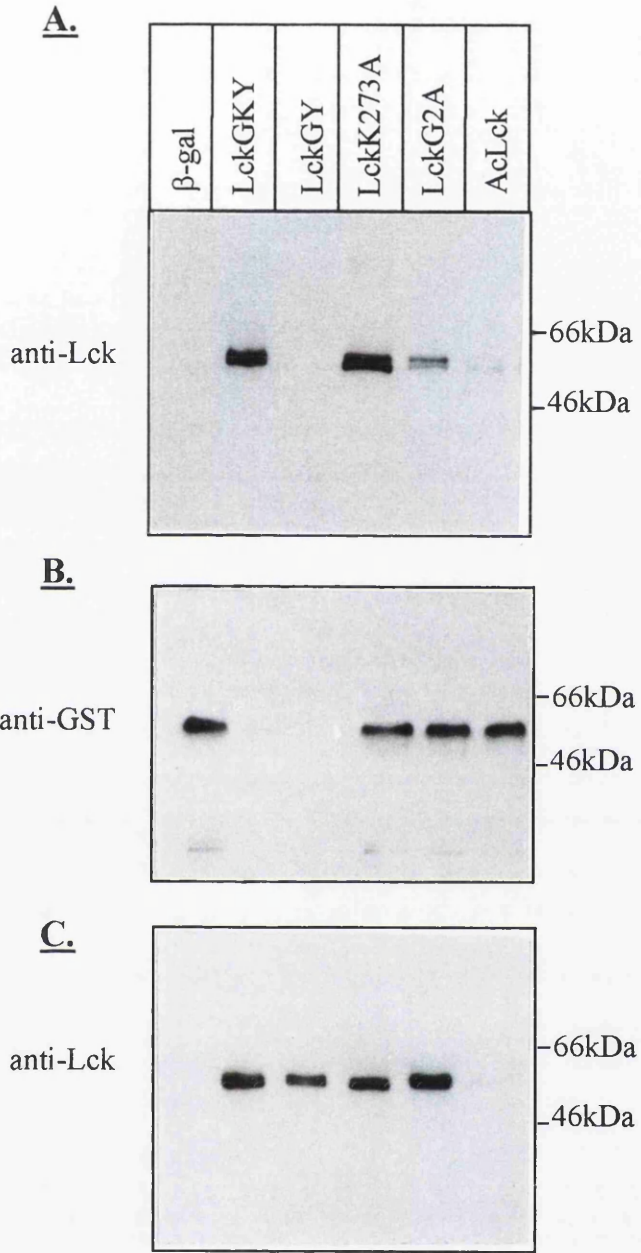


Figure 4.9.

4.10. Identification of region in Nef important in mediating its *in vivo* binding to LckGKY:

4.10.1. Investigation of LckGKY binding to different Nef alleles:

To assess whether the binding of LckGKY to BH10Nef was conserved between different Nef alleles a series of Nef alleles were assessed for their ability to bind LckGKY. These included; HIV-1 Bru Nef (from a laboratory adapted HIV strain similar to BH10); PCR2iso, PCR3iso and PCR4iso which are primary clinical Nef isolates (Harris *et al*, 1992) and a J5 SIV Nef allele (Rud *et al*, 1994), all of which were expressed from recombinant baculoviruses as GST fusions. The results of the *in vivo* binding studies are shown in figure 4.10A. The anti-Lck blot clearly demonstrates equal binding to N-G for each of the alleles from left to right, PCR4iso, PCR3iso, PCR2iso, followed by SIV J5 and Bru. Equivalent levels of expression for the N-G affinity reagent was determined by reprobing the PVDF membrane with an anti-GST antibody. It was noticeable at this stage that the level of N-G was slightly increased for the PCR4 primary isolate (figure 4.10B). However when the expression levels of LckGKY prior to the immunoprecipitation were analysed they were found to be the same (figure 4.10C). Taken together with the lack of variation seen in the binding study (gel A) this suggested that either subtle variations in the concentration of the affinity reagent had little effect on the amount of bound LckGKY, or that the PCR4iso isolate was not binding as efficiently as the other isolates. In an alignment of all the Nef alleles, PCR4iso differs in 24 amino acids from the BH10 consensus sequence, however as many as 30 amino acid changes were seen for PCR3iso (see diagram 5.3) . In addition the SIV Nef isolate is only 40% homologous in comparison to HIV-1 Nef. Further mutagenesis studies were carried out to analyse the specific amino acid requirements in Nef necessary for its interaction with LckGKY.

Figure 4.10. *LckGKY in vivo binding assays for 5 different Nef alleles; PCR2, 3 and 4 HIV-1 clinical isolates, SIV J5 and Bru:*

Coinfections and *in vivo* binding assays were carried out as standard. The results were analysed by α -Lck western blot. Levels of expression for the different Nef allele affinity reagents were determined by stripping and reprobing the PVDF membrane (As detailed 2.6.8 and 2.8.4). The coinfection lysates were also analysed for Lck expression prior to the *in vivo* binding assays, by α -Lck western blotting.

A: Results of the *in vivo* binding assay. The samples were loaded PCR2 (lane 3), PCR3 (lane 2), PCR4 (lane 1), SIV J5 (lane 4) and Bru (lane 5). Levels of LckGKY detected in each lane bound to each of the affinity reagents was similar.

B: Gel A stripped and reprobed with an α -GST antibody. Levels of Nef expression were equivalent for all except PCR4 (lane 3) which was slightly increased.

C: Quantitation of the levels of LckGKY prior to ~~Western~~ precipitation. The samples were loaded in the same sequence as the above examples and clearly show equivalent levels of LckGKY expression.

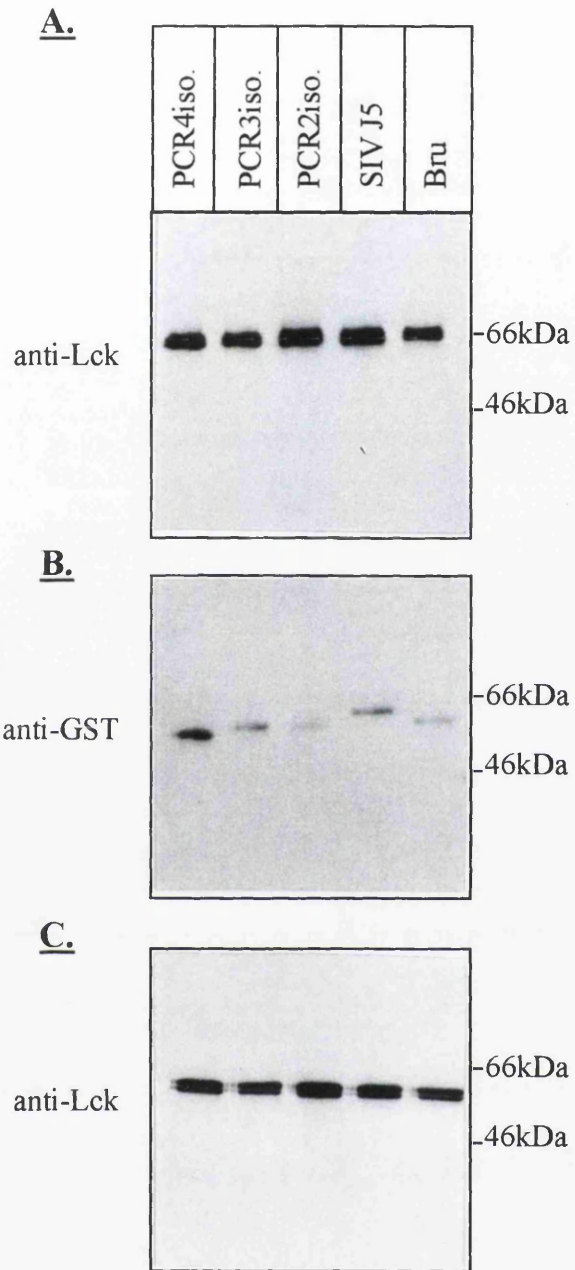


Figure 4.10.

4.10.2. Screening of a panel of Nef deletion mutants for interactions with LckGKY:

To determine the regions of Nef important for its association with LckGKY a panel of Nef mutants expressed as GST fusions (available within the laboratory) were screened for their ability to bind LckGKY during *in vivo* binding assays (see table 4.1 for a summary of the mutants). From these studies it was found deletions in multiple regions of Nef diminished its affinity for LckGKY (figure 4.11A). The two most severely impaired mutants were the PAAP mutant, containing two proline mutations in its (PXX)₃P motif (lane 3) and the Δ 36-65 mutation (lane 5). Binding for both the Δ 7-22 (lane 4) and Δ 74-98 (lane 6) mutants was also reduced by comparison to wildtype N-G (lane 1) and Δ 111-143 (lane 7) samples. Equal levels of LckGKY expression in the coinfecting lysates are shown in figure 4.11C. To confirm equivalent affinity reagent expression, the PVDF membrane shown in figure 4.11A was reprobbed with an anti-Nef polyclonal antibody. Elevated levels of Nef wildtype protein (lane 1) were probably attributable to increased antibody recognition since each of the deletion mutants had equivalent levels of expression and each had a reduced number of antibody epitope sites. The panel of Nef mutants was also screened for binding to LckGY, but as with the wildtype Nef no binding was detected.

These results were consistent with the predicted involvement of the (PXX)₃P motif of Nef mediating its interaction with the Lck SH3 domain. The secondary structure of the putative polyproline type II helix was essential to the interaction, as the mutation of the 2 central prolines in the PAAP mutant severely impaired Nef interaction with LckGKY. The intermediate binding seen for Δ 74-98 suggested that the first PXXP maintained affinity for the SH3 domain. The Δ 36-65 deletion removed a highly conserved short acidic region of Nef between 62-65, which notably has been demonstrated to be critical for Nef enhanced virion infectivity (Iafrate *et al*, 1997). In addition, amino acids 36-38 have been implicated in disrupting Nef mediated CD4 down-modulation (Iafrate *et al*, 1997). It would be tempting to speculate that an interaction in this region of Nef with Lck may provide

a mechanism through which it can simultaneously down-modulate CD4 and enhance virion infectivity.

The $\Delta 7-22$ mutation abrogates Nef interactions with cellular membranes possibly because it is enriched in hydrophobic and basic residues (Harris unpublished observations). The reduction in LckGKY binding with this mutant may result from the increased proximity of the Nef myristoyl group to the critical 36-65 amino acid region. Alternatively this region of Nef contains 2 consecutive serine residues at positions 8 and 9, which could potentially be phosphorylated in native Nef. Analysis of the purified N-G by mass spectrometry is currently in progress to determine the extent of Nef phosphorylation. Mass spectrometry of the deletion mutants will also determine the location of the phosphorylated residues. As the $\Delta 111-143$ Nef deletion which is enriched in tyrosine residues showed no reduced binding for Nef, we would predict that the tyrosine phosphorylation of Nef is not crucial for its interaction with Lck.

Table 4.1. Summary of Nef mutants:

Nef mutants- BH10 [except where stated]	Description of mutation	Refs.
$\Delta 7-22$	Concentration of hydrophobic and basic amino acids, potentially important for membrane interactions.	Harris unpublished observations
OM $\Delta 7-22$	As $\Delta 7-22$ except the Nef myristoylation signal was replaced by an optimum myristoylation signal.	
$\Delta 36-65$	A putative flexible linker region between the membrane anchoring region and the compactly folded core domain which starts at residue 66. Also contains the conserved acidic residues at position 62-65 linked to Nef mediated disruption of cell signalling pathways.	(Freund <i>et al</i> , 1994; Iafrate <i>et al</i> , 1997; Kawano <i>et al</i> , 1997)
$\Delta 74-98$	The proline motif PxxP (69-78) has been demonstrated to be important in mediating Nef interactions with Src family SH3 domains, this deletion removed the second half of the proline motif.	(Saksela <i>et al</i> , 1995; Lee <i>et al</i> , 1995; Lee <i>et al</i> , 1996; Arold <i>et al</i> , 1997)
PAAP	Point mutation of the two middle prolines to alanines from the PXXPXXPXXP motif (69-78). This mutation has been shown to abolish Hck SH3 domain binding to Nef.	(Saksela <i>et al</i> , 1995; Moarefi <i>et al</i> , 1997; Briggs <i>et al</i> , 1997)
$\Delta 111-143$	It has been suggested that the phosphorylation status of Nef may be important in mediating interactions. Since Src SH2 domains interact with phosphotyrosine residues this tyrosine rich region of Nef was deleted.	Collette <i>et al</i> Virology in press.

Figure 4.11. In vivo binding assays for LckGKY plus the panel of Nef deletion mutants:

The assays were performed as standard and analysed by α -Lck western blot. Nef expression levels were confirmed by stripping and reprobing the blots with α -Nef (1378 polyclonal). The level of Lck expression in the coinfection lysates was determined prior to the binding assays by a separate α -Lck western blot of the total lysate.

A: *In vivo* binding assays of the Nef point mutations and deletion mutants with LckGKY.

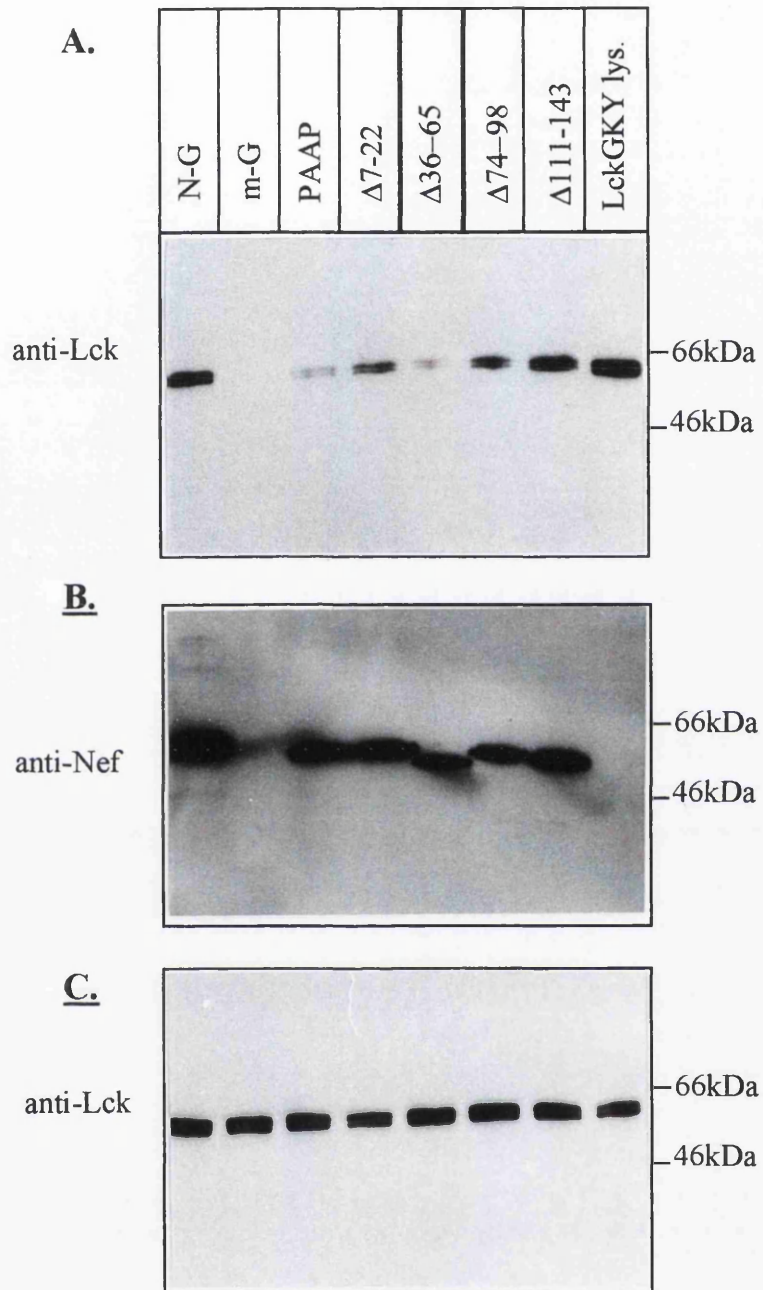


Figure 4.11.

CHAPTER 5

CHAPTER 5- Analysis of Hck interactions with Nef

	Page number
5.1 Introduction	197
5.1 Summary of results presented hereunder	198
5.3 Construction of the SH3, SH2 and SH3-SH2 domain fusions to the activation domain of pJG4-5 for expression and interaction analysis in the YTHS	199
5.4 Analysis of YTHS interaction between the Src homology regions and myristoylated Nef	202
5.5 Construction of recombinant baculoviruses	210
5.6 Verifying the authenticity of the recombinant baculovirus expressed mHck, Src and Fyn	210
5.7 <i>In vitro</i> binding assays	216
5.8 <i>In vivo</i> binding assays	219
5.9 Analysis of the contribution of the N-terminus of Nef to Hck binding	222
5.10 Analysis of the contribution of the N-terminus of Hck to Nef binding	224
5.11 Screen of a panel of Nef mutants to isolates to identify regions important for Hck binding and verifying the <i>in vivo</i> bind was not Nef isolate dependent	228
5.12 Effect of Nef on Hck enzymatic activity	235

Chapter 5: Analysis of Hck interactions with Nef.

5.1. Introduction:

The *hck* gene (for *haematopoietic cell kinase*) was isolated as a result of the cross-hybridization of its transcript with an *lck* cDNA probe (Quintrell *et al*, 1987). Its expression has been detected primarily in myeloid cells, particularly in monocytes and granulocytes and cells of B-lymphoid lineage (Quintrell *et al*, 1987; Zeigler *et al*, 1987; Perlmutter *et al*, 1988). The presence of high levels of Hck is reported to correlate with the differentiation of cells from precursors to mature leukocytes. Two Hck protein products have been identified in murine cells as a result of differential translational initiations from a single mRNA species, with a larger polypeptide generated from a CTG codon 63 bases 5' of the ATG (Lock *et al*, 1991). Subcellular fractionation of the isoforms revealed differing segregation patterns, the smaller p56Hck associated with membrane fractions while the larger p59Hck was present in both the cytosol and membrane fractions. This has subsequently also been observed for human Hck which encodes proteins of 59kD and 61kD. Further analysis has revealed that the differing subcellular locations are a result of the palmitoylation of the smaller Hck product (Robbins *et al*, 1995). In addition, palmitoylation has been demonstrated to direct Hck to Triton insoluble complexes, indicative of association with membrane sphingolipid cholesterol enriched rafts or caveolae. Evidence for Hck involvement in signal transduction pathways is limited, but by analogy to other Src family members an ability to transduce signals from transmembrane receptors seems highly likely. The recent crystallisation of Hck in its inactive form (Sicheri *et al*, 1997) published together with biochemical studies on its ligand mediated activation (Moarefi *et al*, 1997) provided an insight into the regulation of the Src family kinase activities, see section 1.3.1 and below.

Despite the fact that the function of Hck is one of the least well characterised of the Src tyrosine kinase family, its ability to bind Nef has been well documented. A strong interaction has been demonstrated between the SH3 domain of Hck and the (PXX)₃P motif of Nef. The affinity of this interaction was the highest ever reported for an SH3-PxxP interaction ($K_D=250\text{nM}$) (Saksela *et al*, 1995; Lee *et al*, 1995).

Data obtained during these studies suggested that the Hck SH3 interaction with Nef was not exclusively dependent on the conserved (PXX)₃P motif and other amino acid interactions were necessary to maintain the high affinity binding. The strength of the interaction implied that Nef would be capable of displacing endogenous Hck binding partners. This proved to be the case for Hck intramolecular interactions, where the SH3 domain stabilizes the inactive conformation by binding a left handed polyproline type II helix generated by the linker region between the SH2 and kinase domains (Sicheri *et al*, 1997). It was demonstrated that Nef was capable of preferentially binding the SH3 domain of inactive Hck causing its displacement and the subsequent activation of the enzyme (Moarefi *et al*, 1997). Pertinently, these studies utilised an N-terminally truncated Hck lacking the unique domain, and myristoylation/palmitoylation sites, encoding solely the sequences from the SH3 domain onwards. A nonmyristoylated Nef was used as a ligand during this and all of the afore-mentioned experiments. Studies of other Src family members have elucidated key roles for their unique N-terminal domains in mediating protein-protein interactions e.g. the unique region of p59Fyn is crucial for its association with cytoplasmic sequences present in the CD3 zeta (ζ), gamma (γ), epsilon (ϵ) and eta (η) a murine form of ζ , chains (Timson Gauen *et al*, 1992) which form part of the TCR complex; while the unique domain of Lck is necessary for its association with CD4 and CD8 (Shaw *et al*, 1989; Veillette *et al*, 1988), and activation by the tyrosine phosphatase CD45 (Gervais and Veillette, 1995). The studies outlined herein were hence undertaken to confirm whether the interaction of Nef with the Hck SH3 domain occurred in the context of the full-length native proteins. Mutagenesis studies were performed to evaluate the requirement for specific Nef motifs and the contribution of acylation plus the unique domain of Hck to the interaction was assessed. Finally, the effect of authentic acylation on the activation status of Hck in the presence of Nef as a putative SH3 ligand was also investigated.

5.2. Summary of results presented hereunder:

To evaluate the ability of myristoylated Nef to interact with the Hck SH3 domain, the yeast-two-hybrid system was utilised. Nef interactions with Hck SH2 and an SH3-SH2 domain fusion were also investigated. Src, Fyn and Lck were used as

controls for these experiments. Subsequently, the baculovirus expression system was employed to investigate the Hck-Nef interaction in the context of the full length native proteins. Recombinant baculoviruses were generated containing murine Hck plus chicken Src and human Fyn as specificity controls. Native protein expression was verified by western blot analysis, including phosphotyrosine detection to confirm autophosphorylation. Enzymatic activity on an exogenous substrate and authentic acylation of the proteins was also established. *In vitro* and *in vivo* binding assays were performed to assess the affect of Nef myristoylation on its interaction with native Hck. Following on from this, the ability of HIV protease to specifically cleave Nef between residues 57 and 58 was exploited to determine the role of the N-terminal region of Nef in the Hck interaction. Additional recombinant baculoviruses were generated to analyse the function of the Hck N-terminal acylation signals and unique region in the interaction. For these studies a human Hck clone was utilised to corroborate the observed murine Hck interactions. A panel of Nef mutants were screened for their ability to bind Hck, to analyse the contribution of specific residues to the overall efficiency of the interaction in the context of the native proteins. A Nef (PXX)₃P motif mutation was also included in the screen. Lastly, the affect of native Nef in comparison to the (PXX)₃P motif mutant of Nef on Hck kinase activity was investigated.

5.3. Construction of the SH3, SH2 and SH3-SH2 domain fusions to the activation domain of pJG4-5 for expression and interaction analysis in the yeast-two-hybrid expression system:

The Src homology domains, either SH3, SH2 or SH3-SH2, were amplified by PCR from cDNA clones of Hck, Src, Fyn and Lck. The primers for amplification are shown in the table below (table 5.1). Each was subcloned into the pCR™ plasmid before transfer into the activation plasmid of the yeast-two-hybrid-system (YTHS), pJG4-5. The restriction sites for cloning are indicated in the table, each non-coding primer also incorporated a stop codon. These constructs were transformed into yeast as detailed in section 2.4.1. and expression of the polypeptides was confirmed by western blotting. This was facilitated by the inclusion of an HA-1 epitope tag in

the activation domain fusion (see 2.1.4.). The results of the α -HA-1 western blots are shown in figure 5.1. The pJG4-5 plasmid has an inducible GAL1 promoter therefore extracts were made from both galactose induced and glucose repressed yeast cells. Due to the small size of the SH3 domains (~60 amino acids) they were resolved on 17.5% SDS-PAGE gels, however, the SH2 and SH2-SH3 domains were resolved on 12% SDS-PAGE. For each sample the same number of cells were lysed, however it was evident that the domains were expressed at variable levels. Polypeptides corresponding to the SH3 domains fused to the pJG4-5 activation domain (~160 amino acids in total) were detected at ~24kDa (gel A). For each no expression was detected without induction but by comparison to Fyn SH3 (lane 8), the expression levels for Lck SH3 (lane 2) and Src SH3 (lane 6) were significantly reduced. Hck SH3 expression was intermediate. Gel B confirms the expression of the SH2-activation domain fusions for each protein at ~30kDa, expression levels were more consistent for Lck (lane 2), Src (lane 6) and Fyn (lane 8) but slightly raised for Hck SH2 (lane 4). In gel C it is evident that both Src SH3-SH2 and Fyn SH3-SH2 fusions were expressed to elevated levels (~10 fold difference between expression levels for Lck and Fyn SH3-SH2).

Table 5.1. Summary of PCR primers for the cloning of the SH3, SH2 and SH3-SH2 domains into pJG4-5:

Prot.	SH3 PCR Primers	R.	SH2 PCR primers	R.
Hck, c:	5'-GAATTCTCTGAGGATACCATTGTG	RI/	5'-GAATTCTGGTTCTTCAAGGGGATC	RI/
nc:	5'-CTCGAGCTAAGAGTTAACACGAGCCAC	XI	5'-CTCGAGCTAACAGGGCACTGACAGCTT	XI
nc _{SH3/2} :	ATAGTTGCT		5'-GAATTCCTAACAGGGCACTGACAGCTT	RI
Src, c:	5'-GAATTCGGCGGCGTCACCACTTTC	RI/	5'-GAATTCTACTTTGGGAAGATCACT	RI/
nc:	5'-CTCGAGCTAGGAGTCTGAGGGCGCGAC	XI	5'-CTCGAGCTAGCAGACGTTGGTCAGGCCG	XI
Fyn, c:	5'-GAATTCACAGGAGTGACACTGTTT	RI/	5'-GAATTCGGTACTTTGGAAAAGT	RI/
nc:	5'-CTCGAGCTAGGAGTCAACTGGAGCCAC	XI	5'-CTCGAGGTAACAGGGAACTACTAGGCCG	XI
Lck, c:	5'-GAATTCCTGCAAGACAACCTGGTT	RI/	5'-GAATTCGGTTCTTCAAGAATCTG	RI/
nc:	5'-CTCGAGCTAGCTGTTTGTCTTCGCCAC	XI	5'-CTCGAGCTAGCAAGGACGGCTCAACTT	XI

c-coding primer; nc-noncoding primer; R.-restriction sites; RI-EcoRI; XI-XhoI.

Figure 5.1. Verification of SH3, SH2 and SH3-SH2 domain expression for Hck, Lck, Src and Fyn in yeast:

Yeast were grown at 30°C to an $OD_{600} \approx 0.5$, when they were pelleted and washed in PBS and subsequently grown for a further 4 hours either + galactose and raffinose or + glucose. Cells were harvested and lysed by incubation in an equal volume of protein sample buffer on dry ice for 5 minutes followed by 5 minutes in a boiling water bath (all materials and methods can be found in sections 2.3, 2.4 and 2.7). The samples were analysed by western blot (17.5% SDS-PAGE for SH3 and 12% for SH2 and SH3-SH2 fusions) with an α -HA-1 antibody. HA-1 was incorporated as an epitope tag in the B42 transcription activation domain of pJG4-5.

A: Western blot of the SH3 domains -/+ galactose induction for Lck (lanes 1 and 2), Hck (lanes 3 and 4), Src (lanes 5 and 6) and Fyn (lanes 7 and 8). For each no expression was detected minus galactose induction. All of the SH3 domains resolved at ~24kDa corresponding to ~60 amino acids plus the ~100 amino acids encoding the activation tag (see 2.1.4).

B: The SH2 domains were loaded in the same order as A. The SH2 polypeptides were only detected in the presence of induction, resolving at ~30kDa corresponding to the ~200 amino acids in total for each SH2 domain plus the activation tag.

C: As for A and B, the SH3-SH2 domains resolved at ~40kDa.

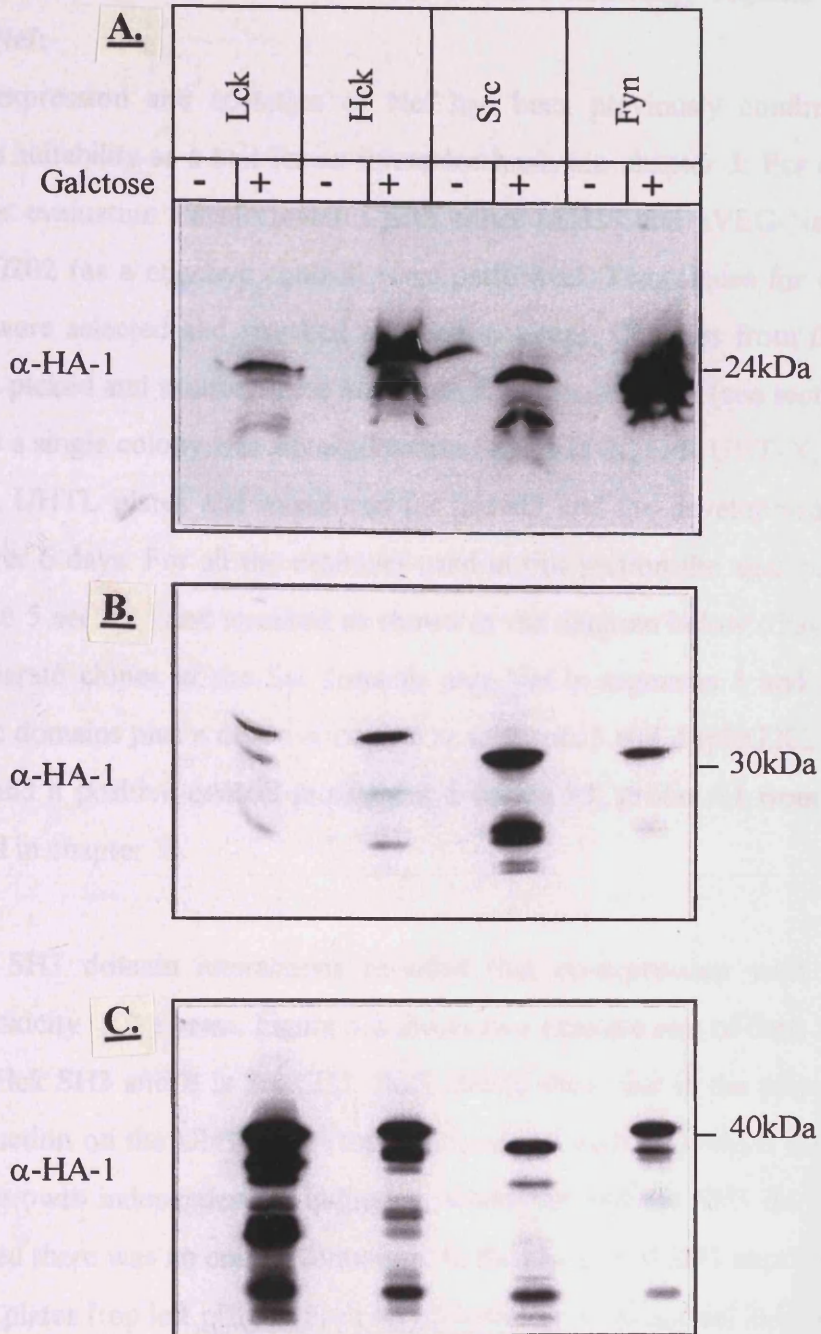


Figure 5.1.

5.4. Analysis of YTHS interactions between the Src homology regions and myristoylated Nef:

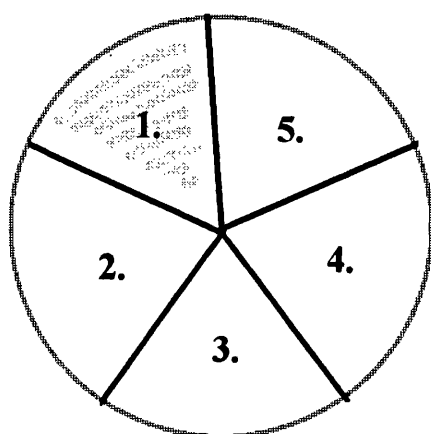
The authentic expression and acylation of Nef had been previously confirmed, together with its suitability as a bait for an interactor hunt, see chapter 3. For each interaction under evaluation transformations with either pSH18 and pVEG-Nef or pSH18 and pEG202 (as a negative control) were performed. Two clones for each transformation were selected and streaked to single colonies. Colonies from these plates were then picked and utilised in the interactor hunt. As standard (see sections 2.4.4. and 2.4.5) a single colony was streaked across Glu UHT-X, G/R UHT-X, Glu UHTL and G/R UHTL plates and monitored for growth and the development of blue colonies over 6 days. For all the examples used in this section the agar plates were divided into 5 sections and streaked as shown in the diagram below (diagram 5.1), with 2 separate clones of the Src domains plus Nef in segments 1 and 2, 2 clones of the Src domains plus a negative control in segments 3 and 4 (pEG202 bait plasmid alone) and a positive control in segment 5 (clone 39, group A1 from the studies presented in chapter 3).

Studies on the SH3 domain interactions revealed that co-expression with Nef resulted in cytotoxicity to the yeast. Figure 5.2 shows two example sets of data. A is the data set for Hck SH3 and B is Src SH3. Both clearly show that in the presence of galactose induction on the UHT plate (top right plate of each set) which should support colony growth independent of induction, when Nef and the SH3 domains were co-expressed there was no colony formation. In the absence of SH3 expression on the Glu UHT plates (top left plate of each set) colonies grew as normal indicating that all 3 plasmids required for the system to work had been successfully transformed. We were hence unable to assess the ability of myristoylated Nef to interact with the Hck SH3 domain in the YTHS. Cytotoxicity was also evident for the SH2 domains. However, there was sufficient colony formation to determine none of the SH2 domains interacted with Nef in this system, as evidenced by the presence of white colonies for all of the proteins under investigation (top right plate of each set). Examples of these studies are shown in figure 5.3; A is the Hck data set and B is Src SH2. Despite only a low level of blue colour development for the

positive control in these examples, from previous experience this was sufficient to detect any protein-protein interactions (compare to results shown in figure 5.4). In addition no colony growth was seen on the G/R UHTL plate (bottom right of each set), indicating there was no transcription of the second LexAop-LEU2 reporter construct.

Diagram 5.1. Orientation of samples for the SH3, SH2 and SH3-SH2 interactor hunt with Nef as bait:

A. Position of samples on each agar plate:



1. pVEG-Nef + pJG4-5 SH3/SH2
2. pVEG-Nef + pJG4-5 SH3/SH2
3. pEG202 + pJG4-5 SH3/SH2
4. pEG202 + pJG4-5 SH3-SH2
5. pVEG-Nef + pJG4-5 clone 39 (+ve)

B. Positioning of plates for each interactor data set:

Glu UHT-X	G/R UHT-X
Glu UHTL	G/R UHTL

In contrast, to the results obtained for the isolated SH3 and SH2 domains the Hck SH3-SH2 domain fusion showed a strong interaction with Nef (segments 1 and 2), particularly when measured by the β -Gal reporter construct, see figure 5.4A, compare Nef+Hck SH3-SH2 to the positive (segment 5) and negative+SH3-SH2, controls (segments 3 and 4) top right plate of the set. As in the previous studies

co-expression of Nef+Hck SH3-SH2 did result in some toxicity but even at a severely compromised level of colony growth the interaction between the 2 proteins was still visible, see figure 5.4B. This co-expression induced toxicity limited the effectiveness of the LEU2 auxotrophic marker as a reporter in these studies. In a typical experiment the growth obtained for two proteins (X and Y) under investigation on G/R UHTL (bottom right plate of each set in these examples) would be compared to that obtained for the negative control (pEG202 DNA binding domain only) and the pJG4-5 “protein Y” construct. If colony growth for the proteins X and Y together was substantially more than the negative control and Y the proteins can normally be determined interactors. However, in these present studies where the co-expression of proteins X and Y resulted in toxicity, comparison of colony growth was an unreliable marker for protein interactions. This is exemplified by the lack of colony growth for Nef+Hck SH3-SH2 on G/R UHTL plates and the presence of growth for the negative+Hck SH3-SH2. Growth on the negative+Hck SH3-SH2 segment might suggest that the Hck SH3-SH2 fusion was bypassing the Nef bait protein and binding directly to the DNA binding domain triggering transcription. However, as described above, a low level of colony formation can result from some negative controls especially since in these experiments the plates were incubated for 6 days. Consistent with this the colony growth seen for the negative control in these experiments was irregular and developed between 4-6 days of incubation (see figure 5.4 A and B, bottom right plates). In contrast, colony growth for the positive control developed within 2 days and showed a regular colony growth. This inferred that the colony growth seen for the negative control on the G/R UHTL plates did not result from the Hck SH3-SH2 domain binding directly to the LexA DNA binding domain. It was therefore concluded that the interaction observed for Hck SH2-SH3 and Nef in the presence of the β -Gal reporter reflected a genuine interaction between the two proteins.

A similarly strong interaction was also detected for Nef and the Src SH3-SH2 domain fusion, figure 5.4C top right plate. To our knowledge this is the only report of a wildtype Nef interaction with Src. A previous study demonstrated an increase in tyrosine phosphorylation of a modified SIV_{mac239} Nef allele when co-expressed with

Src (Du *et al.*, 1995). This allele had been mutated to determine the minimum sequence requirement necessary to confer the highly pathogenic phenotype associated with the pbj₁₄ Nef allele. Point mutations RQ to YE at positions 17 and 18 were sufficient to cause an acute SIV infection in macaques and the ability to transform *in vitro* cell lines similar to the pbj₁₄ phenotype. It was proposed that this was due to the observed increase in tyrosine phosphorylation of Nef and creation of an optimal SH2 consensus binding sequence in the N-terminus of Nef. It would be tempting to speculate from our results that wildtype Nef binds Src *in vivo*, but with a reduced affinity to the pbj₁₄ allele and as a consequence causes a chronic disease pathogenesis as opposed to the acute infection seen for SIV pbj₁₄. Notably the BH10 allele of Nef has no tyrosine residues within the designated SH2 consensus sequence. However, it has emerged recently that SH2 binding sequences exist that are not tyrosine phosphorylation dependent e.g. Raf1 serine/threonine kinase interaction with Fyn and Src SH2 domains was found to be dependent on serine phosphorylation of Raf1 (Cleghon and Morrison, 1994); similarly a cyclin-dependent kinase homologue, p130^{PITSLRE} was also found to bind SH2 domains via an N-terminal serine and glutamic acid rich sequence (Malek and Desiderio, 1994). Lastly, no interaction was detected between Nef and Fyn SH3-SH2 as determined by the formation of white colonies in the presence of X-Gal, see figure 5.4D. Co-expression of Nef and Lck SH3-SH2 once again was toxic to the yeast and no colonies grew, see figure 5.4E, right hand plate. Growth on the Glu UHT plate confirmed the presence of all 3 plasmids required for the system (left hand plate).

Although interactions between myristoylated Nef and the Hck SH3 domain could not be directly evaluated due to cytotoxicity, the lack of interaction between Nef and Hck SH2 suggested that the interaction observed for the SH3-SH2 domain was predominantly mediated by the SH3 domain. These results were consistent with those previously reported and inferred that the Nef interaction with the Hck SH3 domain could be maintained in the presence of Nef myristoylation. The data also implicated a similar mode of interaction between Nef and Src SH2-SH3. This is the first report to our knowledge of a Src interaction with a wildtype Nef allele. These results in combination with a recent report of a Nef-Fyn SH3 interaction (Arold *et*

al, 1997) as well as the previously documented interactions with Lck SH3 and SH2 (Hill *et al*, 1997), Hck SH3 (Saksela *et al*, 1995; Lee *et al*, 1995), Lyn SH3 (Saksela *et al*, 1995) and a Fyn SH3 R96I mutant (Lee *et al*, 1995; Lee *et al*, 1996) infer a conserved ability of Nef to interact with members of the Src tyrosine kinase family. It also suggests that as more members of the family are investigated further Nef-Src kinase interactions may be discovered. To investigate whether these interactions were conserved in the context of the full length native proteins the baculovirus expression system was utilised, the results of which are presented in the following sections.

Figure 5.2. *Nef* interactions with *Hck* and *Src* SH3 domains in the YTHS:

pVEG-Nef was used as a bait in these studies, pEG202 was the DNA binding domain negative control and the prospective interactors were expressed on G/R induction as activation domain fusions. The positive control was clone 39, group A1 from the library screen in chapter 3. The interactors were streaked across 4 agar plates, Glu UHT-X, G/R UHT-X, Glu UHTL and G/R UHTL (see diagram 5.1), a detailed description of the reporter constructs for this YTHS can be found in section 2.4.

A: Interaction between Hck SH3 and Nef. This shows co-expression of Nef and Hck SH3 (segments 1 and 2) on the induced G/R UHT-X (top right) and G/R UHTL (bottom right) plates was toxic to the yeast. Successful transformation of all 3 plasmids was confirmed by growth on the Glu UHT-X plate (top left).

B: Interaction between Src SH3 and Nef. As for A co-expression of the two proteins resulted in no colony formation.

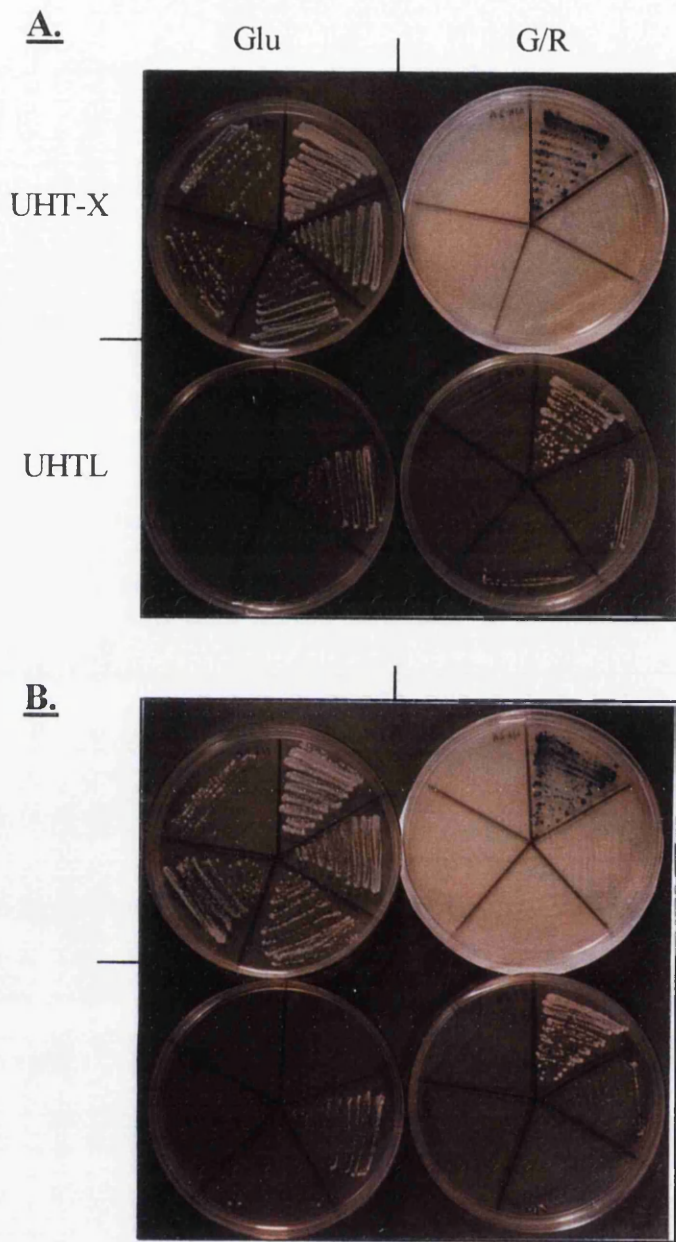


Figure 5.2.

Figure 5.3. *Nef interactions with Hck and Src SH2 domains in the YTHS:*

These studies were performed as standard see figure 5.2, for orientation of the plates see diagram 5.1.

A: Nef + Hck SH2 showed a similar yeast growth profile to Src SH2 + Nef. In this picture the G/R UHTL plate (bottom right) has been rotated anti-clockwise by one segment, so the colonies growing in segment 1 (see diagram 5.1) are in fact the positive control and those in segment 2 and 3 are Nef + HckSH2 etc.

B: No interaction was seen for Src SH2 and Nef (segments 1 and 2), as determined by the lack of colour change for yeast grown on the G/R UHT plates in the presence of X-Gal (top right plate).

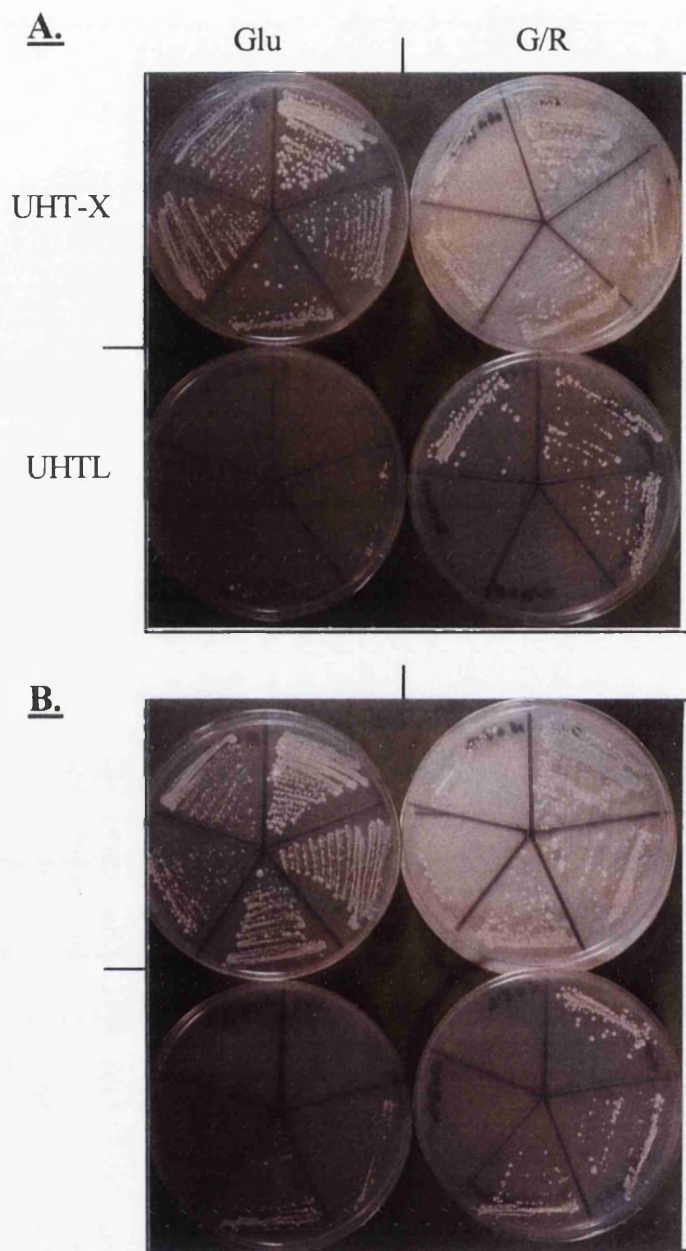


Figure 5.3.

Figure 5.4. Interactions between Nef and the Src kinase SH3-SH2 domain fusions:

A: Hck SH3-SH2 and Nef. The formation of small dark blue colonies on co-expression of Hck SH3-SH2 and Nef (segments 1 and 2) on the G/R UHT-X plate (top right) indicated a strong interaction between the proteins. See text for a full explanation.

B: Hck SH3-SH2 and Nef. Another example of the Hck SH3-SH2 interaction with Nef showing that even when very small colonies were obtained a colour change was still apparent on the G/R UHT-X plate.

C: Src SH3-SH2 and Nef. A strong interaction was visible as for Hck SH3-SH2 in A, on the G/R UHT-X plate (top right).

D: Lck SH3-SH2 and Nef. Only the Glu and G/R UHT-X plates are shown in this picture. Colony growth on the Glu UHT-X plate on the left-hand side confirmed all 3 plasmids had been transformed, however the lack of colony growth for Lck SH3-SH2 and Nef (segments 1 and 2) on the G/R UHT-X plate showed co-expression of the 2 proteins was toxic.

E: Fyn SH3-SH2 and Nef. The plates shown are as for D. Although only limited colony growth for Fyn SH3-SH2 and Nef was visible (segments 1 and 2), they were white colonies indicating there was no interaction between Fyn SH3-SH2 and Nef in this assay system.

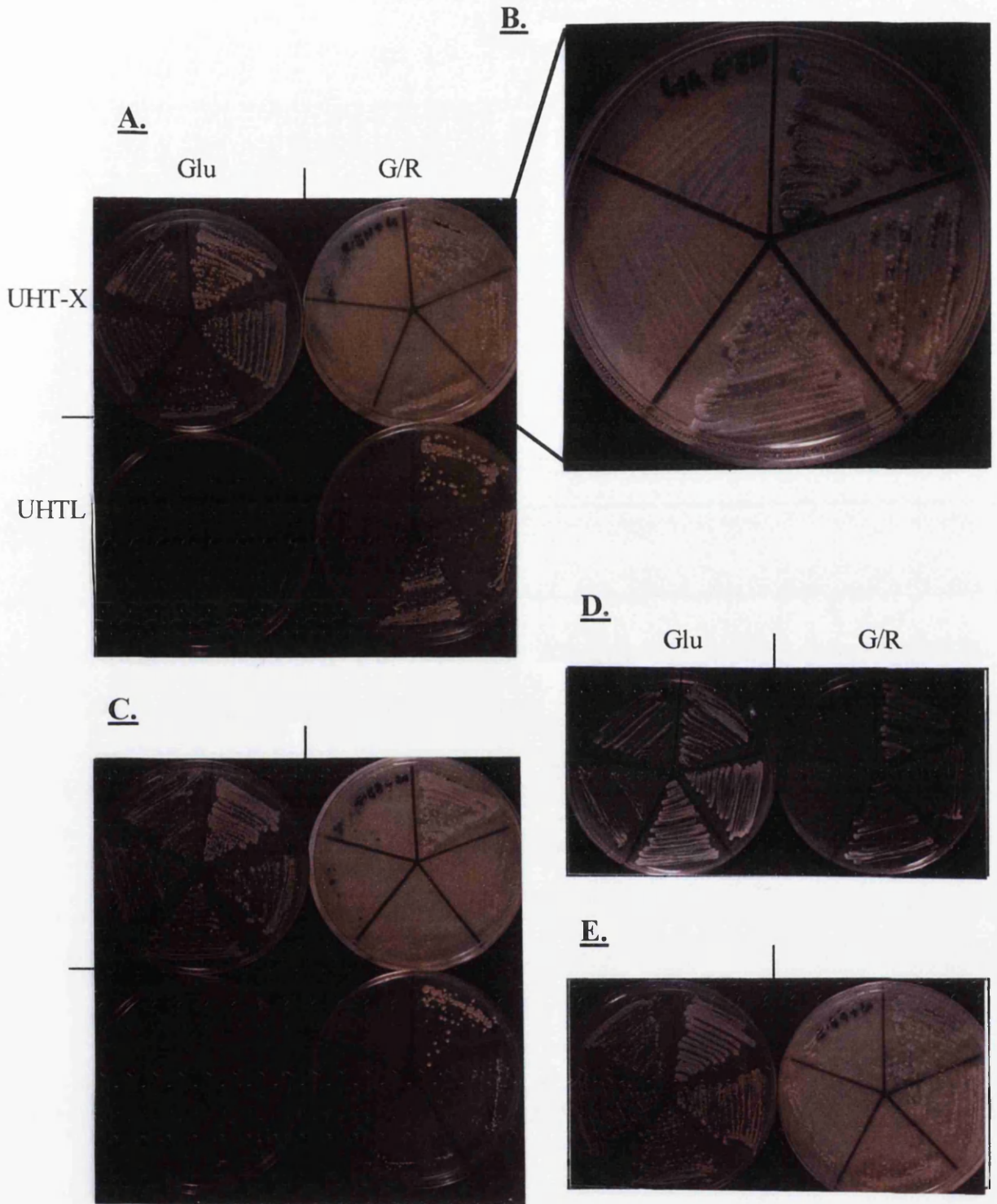


Figure 5.4.

5.5. Construction of recombinant baculoviruses:

The murine Hck (mHck), chicken Src and human Fyn cDNA clones were kindly provided by Dr. Mark Marsh (University College, London). Recombinant baculoviruses were generated from the pAcES transfer vector containing each cDNA subcloned as either EcoRI fragments (mHck and Fyn) or an EcoRI/XhoI fragment (Src). The human Hck (hHck) cDNA clone was donated by Prof. Kalle Saksela (University of Tampere, Finland). This was amplified by PCR to allow the production of a nonmyristoylated species of the protein (G2AhHck) and removal of the unique region (Δ 78hHck), EcoRI restriction sites were also incorporated (see below for primers). Unfortunately attempts to subclone the wildtype Hck cDNA to the pAcES transfer vector were unsuccessful.

Coding primer for G2AhHck:

5'-GAATTCAGATTGATGGCGTGCATGAAGTCC-3'

Coding primer for Δ 78hHck:

5'-GAATTCAGATTGATGGCAGGCTCTGAGGACATC-3'

Noncoding primer for hHck:

5'-GAATTCTCATGGCTGCTGTTGGTAGTC-3'

5.6. Verifying the authenticity of the recombinant baculovirus expressed mHck, Src and Fyn:

5.6.1. Determining full length expression and kinase activity:

Lysates of Sf9 cells were infected with recombinant baculoviruses containing either the mHck, Src or Fyn cDNAs, were prepared as detailed section 2.6.5. The lysates were subjected to autophosphorylation assays and protein expression was determined concomitantly with autophosphorylation activity. Western blot analysis with the standard anti-phosphotyrosine antibody (PY69 from Santa-Cruz see table 2.9) detected an increase in tyrosine phosphorylation for Src (lane 4) and Fyn (lane 6) in the presence of ATP, consistent with the Lck experiments in chapter 4. This confirmed both proteins had retained their abilities to autophosphorylate their active site tyrosine residues (Tyr416 and Tyr417 respectively). Notably, in the presence of

ATP a second faster migrating species of Fyn was detected suggesting either phosphorylation of the protein exposed it to proteolytic degradation or that the overall charge of the protein was altered affecting its electrophoretic mobility. Only background levels of phosphotyrosine were detected for both proteins in the absence of ATP suggesting the kinases were in the inactive conformation. Equivalent levels of protein +/- ATP were confirmed by reprobing the membranes with their respective protein specific antibodies, see figure 5.5.B, lanes 3 and 4 show an α -Src blot, while 5 and 6 show an α -Fyn blot.

In contrast, when the Santa Cruz α -pTyr antibody was used as a probe for tyrosine phosphorylation in mHck, no bands were detected. However, when the proteins were assessed for kinase activity on an exogenous substrate (see below) mHck was found to be highly active. As exogenous enzymatic activity requires phosphorylation of the active site residue Tyr411, this inferred mHck was capable of autophosphorylation. Western blot analysis was repeated with an alternative α -pTyr antibody, 4G10 (from Upstate Biotechnology Incorporation) which successfully detected mHck phosphotyrosine. The results are shown in figure 5.5A demonstrated that similar to Src and Fyn, background phosphotyrosine levels were low with a substantial increase in the presence of ATP as a result of autophosphorylation. The inability of the α -pTyr Santa-Cruz antibody to detect phosphorylation of the Hck active site Tyr411 residue suggested that pTyr411 was presented in a different conformation compared to the autophosphorylation sites of Lck, Src and Fyn. This variation in configuration of the active sites for these enzymes was probably a reflection of their differing substrate specificities.

To confirm the proteins were active on an exogenous substrate, peptide substrate assays were performed as detailed in section 2.8.9. The results shown in figure 5.5C confirmed all the proteins were enzymatically active. As the levels of protein expression had been determined by western blot equivalent amounts of protein for each of mHck, Src and Fyn could not be guaranteed, hence the apparent variations in activity.

Figure 5.5. Confirmation of kinase activity and expression of mHck, Src and Fyn:

Standard autophosphorylation and peptide substrate assays were performed to determine the kinase activity of the enzymes as sections 2.8.8. and 2.8.9.

A: Autophosphorylation assays analysed by α -pTyr western blotting; the standard α -pTyr antibody was used for Src (lanes 3 and 4) and Fyn (lanes 5 and 6) and 4G10 from Upstate Biotechnology Incorporation for mHck (lanes 1 and 2), see text. All samples were incubated $-/+$ ATP and all showed increased tyrosine phosphorylation levels in the presence of ATP, indicative of ATP induced autophosphorylation.

B: Confirmation of equivalent expression levels in the $-/$ ATP samples; the membranes shown in A were stripped and reprobbed with the protein specific antibodies i.e. α -mHck, α -Src and α -Fyn.

C: Bar graph representation of the results of the exogenous phosphotransferase activity of the enzymes. Activity of the enzymes is shown in pmols of phosphate transferred to the peptide substrate at either time 0 or after 30 minutes (time 30). The reduced activity seen for Src and Fyn probably corresponds to reduced levels of expression in the lysates used for this experiment by comparison to mHck. The negative control in this experiment was β -Gal.

5.6.2. Determination of authentic acylation of the proteins:

To confirm that the proteins for use in the binding studies were authentically acylated metabolic labelling experiments were performed with tritiated palmitic or myristic acid as outlined in section 2.6.9. The results of the fluorography detection are shown in figure 5.6. As expected mHck, Src and Fyn were myristoylated with bands corresponding to ~60kDa detected for each, lanes 1, 2 and 3 respectively in figure 5.6A. However, the results from [³H] palmitic acid metabolic labelling showed bands for Src and Fyn but not mHck. This was an apparent anomaly as both wildtype mHck and Fyn contain cysteine residues at position 3 (also in position 6 for Fyn), the putative location for palmitoylation, however wildtype Src does not contain a cysteine residue until residue 193 and is not normally palmitoylated. These results suggested that either Src contained a cryptic palmitoylation site recognised by the Sf9 cells or that a point mutation had been introduced into Src during cloning. As alternative palmitoylation sites generally occur proximal to transmembrane regions or other fatty acid residues such as prenylation (for a recent review see (Mumby, 1997)) palmitoylation of wildtype Src in Sf9 cells seemed unlikely. Unfortunately technical difficulties have made the latter proposal difficult to prove, but it represents the most likely cause for the detection of [³H] palmitic acid in Src. The possibility of the signal being a result of metabolism of palmitic acid to myristic acid was ruled out by treatment of the gel with hydroxylamine which removed all detectable fluorography signal consistent with the removal of palmitate (data not shown), see 4.5.2 for method.

The intensity of the bands detected for each of the proteins in the [³H] myristic acid labelling experiment suggested that mHck was expressed at reduced levels by comparison to Src and Fyn. To determine if mHck was palmitoylated but expressed at insufficient levels to be detected, a lysate of [³H] palmitic acid labelled cells infected with the recombinant baculovirus expressing mHck was immunoprecipitated with an mHck specific antibody. Metabolically labelled β -Gal was used as a negative control for the immunoprecipitation studies. The [³H] myristic acid labelled mHck served as a positive control. The results are shown in figure 5.6.6. The [³H] myristic acid samples were loaded on the left-handside of the

gel. Lane 1 contains β -Gal which confirmed the specificity of the α -mHck immunoprecipitation antibody and in lane 2 an ~ 60 kDa protein was specifically immunoprecipitated corresponding to myristoylated Hck. In lane 3 again no bands were detected for the β -Gal palmitic acid negative control, however an mHck specific band was detected in lane 4 confirming its authentic palmitoylation. Again hydroxylamine treatment removed any detectable signal confirming authentic acylation of mHck (data not shown).

Figure 5.6. Confirmation of authentic acylation of mHck, Src and Fyn:

Recombinant baculovirus infected Sf9 cells were metabolically labelled with either [³H] palmitic acid or [³H] myristic acid for 24 hours as detailed 2.6.9. Cells were harvested and then lysed in 1xGLB. Proteins were resolved by 12% SDS-PAGE and subsequently detected by fluorography. The examples shown in A and B were exposed to film overnight, C was exposed for 20 days.

A: Determination of myristoylation, the samples were loaded Hck, Src, Fyn, lanes 1, 2 and 3 respectively. Bands were detected in each lane at ~60kDa, confirming the proteins authentic myristoylation. The relative intensities of the bands also reflected their relative abilities to be palmitoylated (B).

B: Determination of palmitoylation. Bands corresponding to Src (lane 2) and Fyn (lane 3) were detected for palmitate metabolic labelling but none for Hck (lane 1).

C: Immunoprecipitation of metabolically labelled Hck samples; lane 1 contained a β -Gal negative control for myristoylation, lane 2 was a [³H] myristic acid labelled Hck sample included as a positive control; lane 3 contained a [³H] palmitic acid β -Gal negative control and lane 4 shows the authentically palmitoylated Hck protein detected after immunoprecipitation.

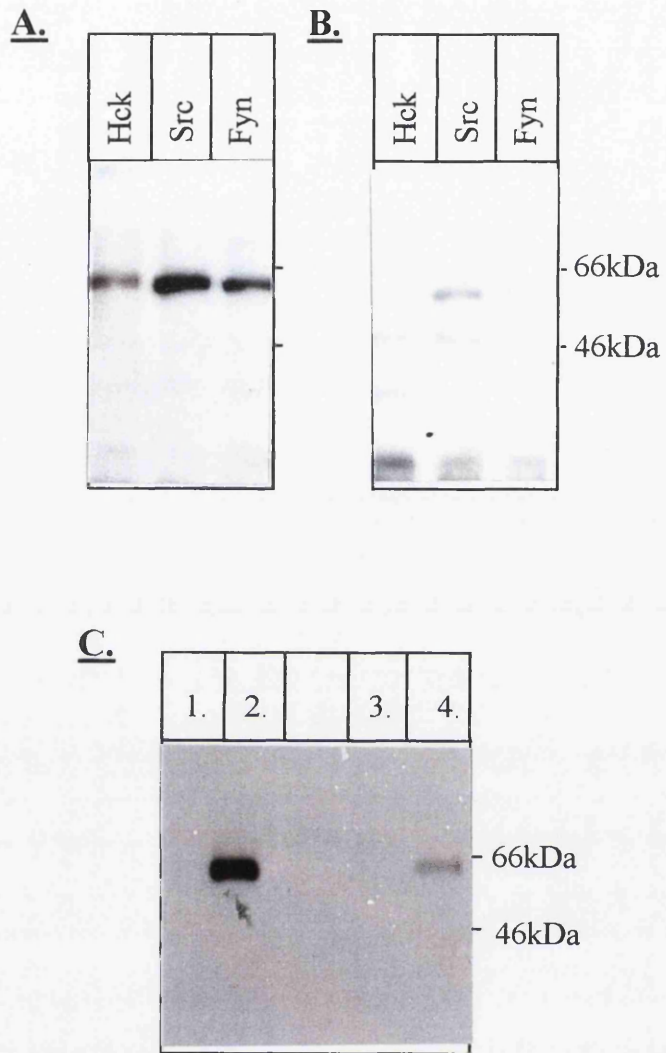


Figure 5.6.

5.7. *In vitro* binding assays:

In vitro binding assays were performed to evaluate whether the Hck SH3 mediated binding to Nef was conserved in the context of the native proteins. Binding of Nef to native Src and Fyn was also investigated in this assay. In addition the contribution of Nef myristoylation was assessed. The affinity reagents used for these *in vitro* binding studies were BH10 Nef (N-G), nonmyristoylated Nef (G2A-G) and myristoylated GST (m-G) which served as a specificity control for binding. Binding assays were performed as standard (detailed in sections 2.6.5; 2.6.6; 2.6.7) for each of Hck, Src and Fyn. In the example shown in figure 5.7 the binding assays were carried out in duplicate for each sample.

The results of the *in vitro* binding assays demonstrated specific binding of mHck to N-G, with binding to G2A-G detectable at reduced efficiency. Gel A lanes 1 and 2 show a band corresponding to the correct molecular weight ~56kDa for p56 mHck bound to the N-G affinity reagent. A similar fainter band was detected in lanes 3 and 4 consistent with G2A-G binding. The specificity of the interactions were confirmed by the lack of corresponding bands in the m-G lanes (5 and 6). These results demonstrated that Nef and Hck retained the ability to interact in the context of the full length acylated proteins. Furthermore, the intensity of the bands in lanes 1 and 2, compared to 3 and 4 suggested that myristoylation enhanced the interaction *in vitro*. The results from *in vitro* binding assays with Src are shown in figure 5.7B. It was found Src also bound N-G (lanes 1 and 2) more efficiently than G2A-G (lanes 3 and 4), albeit binding was at a reduced overall level compared to that seen for Hck. This corroborated our earlier results of a Nef-Src SH3-SH2 interaction identified in the YTHS and confirmed as with Hck that the interaction occurred in the context of the full length acylated proteins. In contrast, no association of Nef with Fyn was detectable in this assay (data not shown). Since these experiments an interaction has been reported between nonmyristoylated Nef and the SH3 domain of Fyn *in vitro*, indeed the complex crystallised (Arold *et al*, 1997). However our data suggests that this interaction was not sufficient to mediate binding between the native proteins. Notably, the results from the autophosphorylation assays suggested Fyn was in the inactive conformation. It would be interesting in future studies to determine whether

the Nef interaction with Fyn SH3 was sufficient to confer Nef binding to the 'open' active Fyn conformation analogous to the Nef-Lck binding demonstrated in chapter 4. As both Fyn and Lck are involved in TCR-CD3 signal transduction a Nef interaction with both proteins could have a drastic affect on T-cell receptor activation of cells. The amount of affinity reagent bound to the GA-beads used through-out all of these experiments was determined by SDS-PAGE and Coomassie blue staining and is shown in figure 5.7C.

Figure 5.7. *In vitro* binding experiments for mHck and Src:

GST fusion proteins were expressed and purified from Sf9 cells as described 2.6.6. and bound to GA-beads to generate the affinity reagent for the *in vitro* binding studies. Affinity reagents included N-G, G2A-G plus m-G which was included as a control for specificity. The method for the binding assays is outlined in detail in section 2.6.7, briefly mHck, Src and Fyn lysates were precleared with GA-beads and then incubated with the affinity reagents at 4°C for 3 hours with rotation. The complex bound to the GA-beads was subsequently resolved by 12% SDS-PAGE and bound proteins detected by western blot with either α -Hck, α -Src or α -Fyn antibodies. Only the results for the mHck and Src binding assays are shown in this figure, samples were loaded in duplicate.

A: Results of the *in vitro* mHck binding assay; lanes 1 and 2 show proteins associated with the N-G affinity complex, the ~56kDa α -Hck specific bands, confirmed mHck interaction with N-G. Lanes 3 and 4 show mHck did bind G2A-G but with reduced efficiency. The absence of bands in lanes 5 and 6 confirmed the specificity of the interactions.

B: Results of *in vitro* Src binding assays. The detection of Src specific bands in lane 1 and 2 plus 3 and 4 confirmed its ability to bind both N-G and G2A-G in the context of the full length acylated proteins. Lanes 5 and 6 contain the m-G negative control.

C. Coomassie stained gel of the affinity reagents (N-G, G2A-G and m-G) bound to 5 μ l (packed volume) GA-beads. Lane 1 contained N-G, lane 2 G2A-G and lane 3 m-G. These results show the amount of G2A-G bound to the beads was slightly less than N-G.

5.8. *In vivo* binding assays:

To establish whether the same specificity of Nef binding to the Src kinases was maintained *in vivo*, coinfections of recombinant baculoviruses expressing either N-G, G2A-G or m-G plus Hck, Src or Fyn were performed. Whole cell lysates expressing both proteins were analysed in *in vivo* binding assays as detailed 2.6.8. In these assays a preclear step with GA-beads was not possible therefore higher stringency washes (0.5M salt) were employed. Figure 5.8 shows the western blot results for each of the precipitations.

The results of the mHck binding assay are shown in figure 5.8A and demonstrated as for the *in vitro* assays that mHck maintained its ability to interact with N-G in the context of the native proteins *in vivo* (lane 2). However in these *in vivo* studies equivalent binding of mHck to G2A-G was also apparent (lane 3). Low levels of binding were seen for mHck and m-G (lane 4), but this was probably due to the removal of the preclear step. In contrast, for the *in vivo* Src studies a high background level of Src binding was detected using all 3 affinity reagents, inferring a non-specific interaction with the GA-beads (Gel B). It was therefore impossible under these assay conditions to investigate the Src-Nef protein interactions *in vivo*. Future experiments will need to address this problem. The same problem was also encountered with Fyn (data not shown). To confirm equivalent levels of GST fusion expression the blots were stripped and reprobed with α -GST, shown in C and D respectively. Levels of mHck expression prior to the precipitation were also shown to be equivalent for each affinity reagent in a separate western blot (data not shown).

To confirm that the Hck-Nef interaction was not an artifact of the GA-bead pulldown assay, lysates of coinfecting cells were immunoprecipitated with α -Hck and analysed by western blot with the α -Nef polyclonal 1378 antibody. The results of the α -Nef blot are shown in figure 5.8E and demonstrated that both myristoylated and nonmyristoylated Nef were specifically co-immunoprecipitated with the Hck specific immune complex (lanes 1 and 2 respectively). This polyclonal Nef antibody was raised to Nef-GST and is cross reactive with GST therefore the lack of GST

precipitation, as determined by the absence of bands in lane 3, provides good evidence for the specificity of the Hck-Nef interaction. A recent study (Briggs *et al*, 1997) has since corroborated these results and demonstrated the ability of Nef to form a stable complex with Hck in Rat-2 fibroblasts. In addition they confirmed the previous reported *in vitro* activation of Hck by Nef was maintained *in vivo* and ultimately resulted in the formation of transformed foci of cells.

Figure 5.8. Results of the *in vivo* binding studies with Nef plus mHck and Src:

Sf9 cells were coinfecting with N-G, G2A-G and m-G plus either mHck, Src or Fyn. The resultant lysates were immunoprecipitated with GA-beads (as detailed section 2.6.8) and the results analysed by western blot.

A. Results of the *in vivo* mHck binding to Nef (α -Hck western blot) demonstrated both N-G (lane 2) and G2A-G (lane 3) were capable of forming stable complexes with Hck. In each lane bands at ~56kDa were visible corresponding to mHck. The lack of mHck binding to m-G (lane 4) confirmed the specificity of the interactions. An mHck lysate alone was loaded in lane 1 as a control for the blot.

B. Results of the *in vivo* Src binding assay. Binding of Src to N-G, G2A and m-G was visible in lanes 2, 3, and 4 corresponding to non-specific binding of Src to the GA-beads. A Src lysate positive control was loaded in lane 1.

C and D. These are the same membranes shown in A and B stripped and reprobed with and α -GST antibody, therefore sample loading is the same as A and B. The results show that the affinity reagents were expressed to similar levels.

E. Results of the immunoprecipitation of Hck (with an α -Hck antibody) from coinfecting lysates demonstrates that the association of Nef and Hck is stable and independent of the immunoprecipitation reagent. The gel was probed with α -Nef (polyclonal 1378); lane 1 shows a band corresponding to Nef-GST at ~52kDa, lane 2 is G2A-G. No binding for m-G was detected in lane 3.

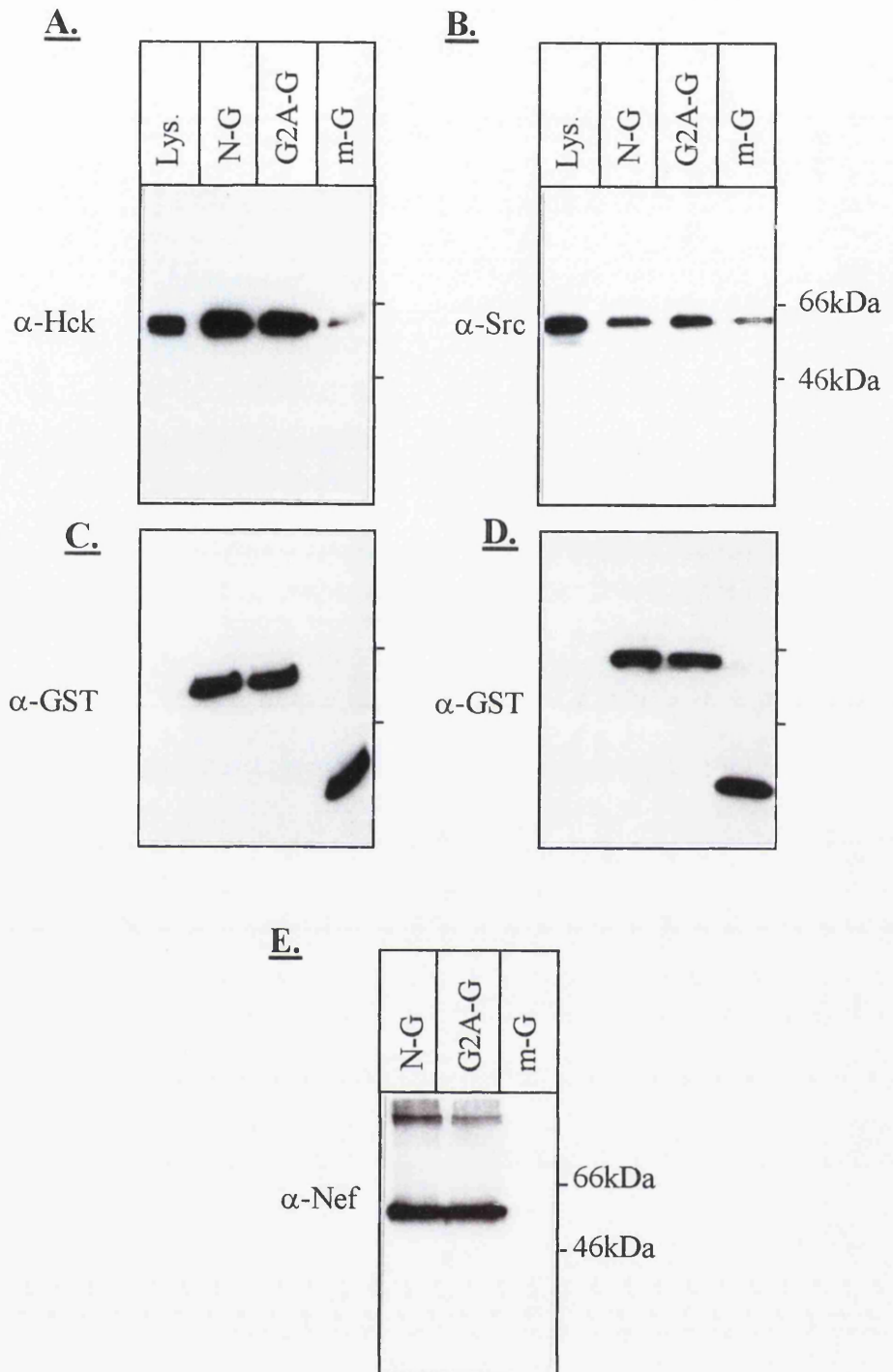


Figure 5.8.

5.9. Analysis of the contribution of the N-terminus of Nef to Hck binding.

As binding of Nef to mHck was unaffected by Nef myristoylation it was decided to investigate whether the N-terminal truncated species of Nef was sufficient to confer the *in vivo* interaction. This species of Nef is normally found associated with the virion and results from the specific cleavage of Nef by HIV protease (Pandori *et al*, 1996; Welker *et al*, 1996; Bukovsky *et al*, 1997; Miller *et al*, 1997). This was assessed by treating Nef immunoprecipitated complexes with HIV-1 protease and monitoring for the release of mHck. The results shown in figure 5.9 (a flow diagram of the method is shown below in diagram 5.2) demonstrate binding of mHck to both N-G and G2A-G was unaffected by the protease cleavage of Nef. The immunoprecipitate bound to beads after protease cleavage is shown in A. If lanes 1 and 2 (minus protease) are compared to lanes 5 and 6 (plus protease) it is clear similar levels of mHck remain bound to both N-G and G2A-G in the presence of protease. This was confirmed by analysing the protein released into the supernatant after protease cleavage. An α -Hck western blot of the supernatants is shown in B, the mHck lysate positive control in lane 9 is the same as gel A to facilitate quantitative comparison of the blots. The lack of Hck detectable in C after protease cleavage demonstrated that the Nef-Hck complex remained stably associated. Both of these blots were subsequently stripped and reprobed with α -GST to establish successful HIV protease cleavage of Nef.

N-G lysate alone was included as a control for protease cleavage and is shown either -/+ protease in lanes 4 and 8 respectively. Incubation with protease resulted in the production of 2 smaller Nef species. As the putative protease cleavage site was between residues 57 and 58 we would have expected a polypeptide of 57 amino acids to be released, corresponding to ~ 7.5 kb. This accounted for the N-G polypeptide detected at ~ 45 kDa (N-G was ~ 52 kDa), but not the smaller N-G species suggesting that an alternative protease cleavage site may also exist in this BH10 *nef* allele. Also, protease cleavage of the N-G lysate utilised in these studies did not result in 100% cleavage of Nef. Further studies of protease cleavage with purified N-G (data not shown) gave similar results suggesting it was a Nef conformational effect not an Sf9 lysate artifact. Notably the Nef cleavage pattern

was the same for both G2A-G (lane 6, gel B) and N-G (lane 5, gel B) complexed with mHck suggesting the same cleavage site(s) remained accessible during mHck binding. The α -GST blot of the proteins released into the supernatant (gel D) revealed similar background levels of GA-bead dissociation for all samples, suggesting this was a result of long incubation periods required for the experiment (~4hours). From these results it can be concluded that the affinity of mHck for the N-terminal truncated virion produced Nef is equal to its affinity for the full length native Nef. However, it should be noted that the lack of release of Hck could be due to the residual full length Nef remaining bound to the GA-beads.

Diagram 5.2. Flow-diagram of experimental procedure:

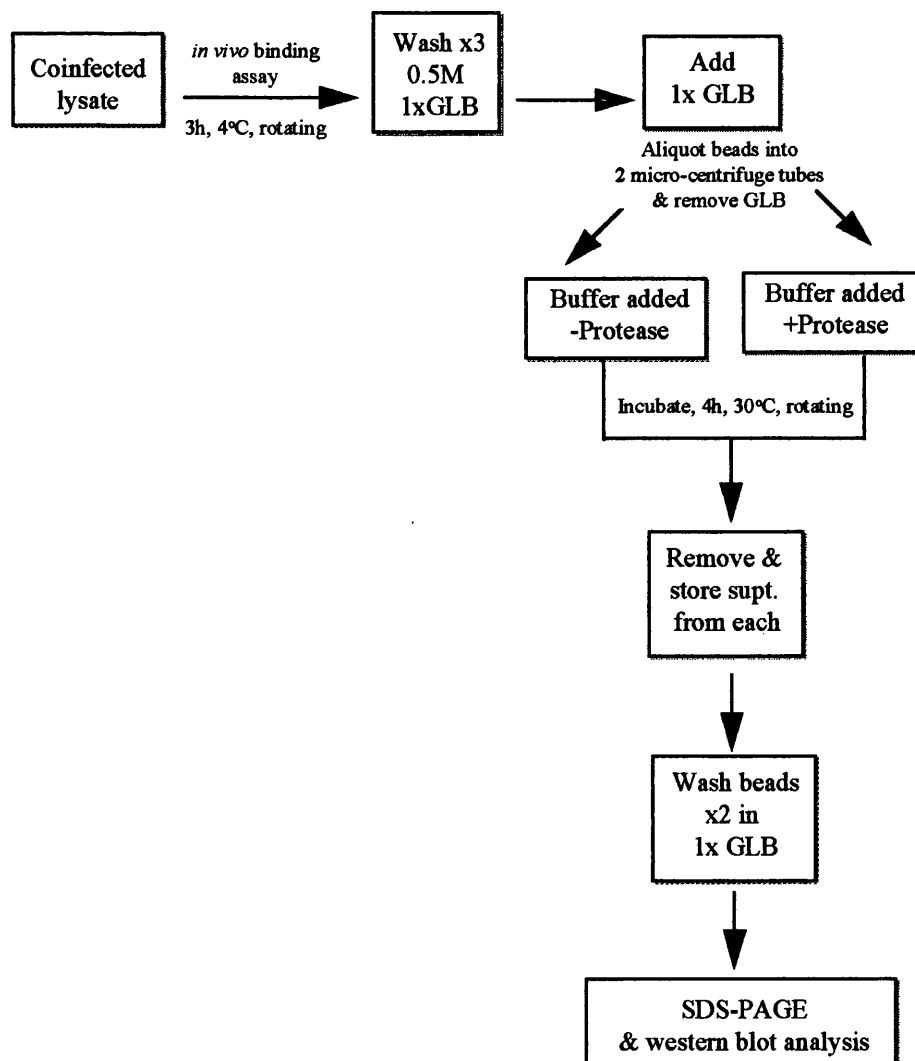


Figure 5.9. *Effect of HIV-1 protease cleavage on the N-G Hck complex:*

A summary of the protocol used for these experiments is shown in the flow-diagram in diagram 5.2. Standard *in vivo* binding assays were performed on coinfecting lysates. The complexes bound to GA-beads were subsequently divided in 2 and incubated either +/- protease at 30°C on a rotator for 4 hours. The supernatant was retained and analysed in parallel to the complex bound to beads by western blot.

A. Results of protease treatment of the Hck-Nef complex bound to beads. This shows an α -Hck western blot of immunoprecipitations with either N-G (lane 1), G2A-G (lane 2), m-G (lane 3) minus protease or plus protease lanes 5, 6 and 7 respectively. Lanes 4 and 8 contain an N-G lysate alone. The results show that Hck was detected in lanes 1, 2, 5 and 6 and that binding was independent of protease treatment. An Hck lysate positive control is in lane 9.

B. Protein released into the supernatant after protease treatment. This shows an α -Hck blot, loaded as for gel A. Lane 9 is loaded with the same Hck lysate as gel B, demonstrating that the exposure is comparable to gel B. Faint bands were detected for Hck both +/- protease.

C. Gel B stripped and reprobed with α -GST to confirm protease cleavage of N-G. N-G was cleaved from ~52kDa to 2 smaller species ~45kDa and ~43kD in lanes 5,6 and 8 consistent with incubation with HIV-1 protease. In the absence of protease 1,2 and 4 N-G remained full length at ~52kDa.

D. Gel C stripped and reprobed with α -GST. This confirmed that any Hck detected in the supernatant in gel C was as a result of affinity reagent dissociation from the GA-beads and not due to N-terminal Nef fragment release. Faint bands were detected consistently across both +/- protease treated sample sets.

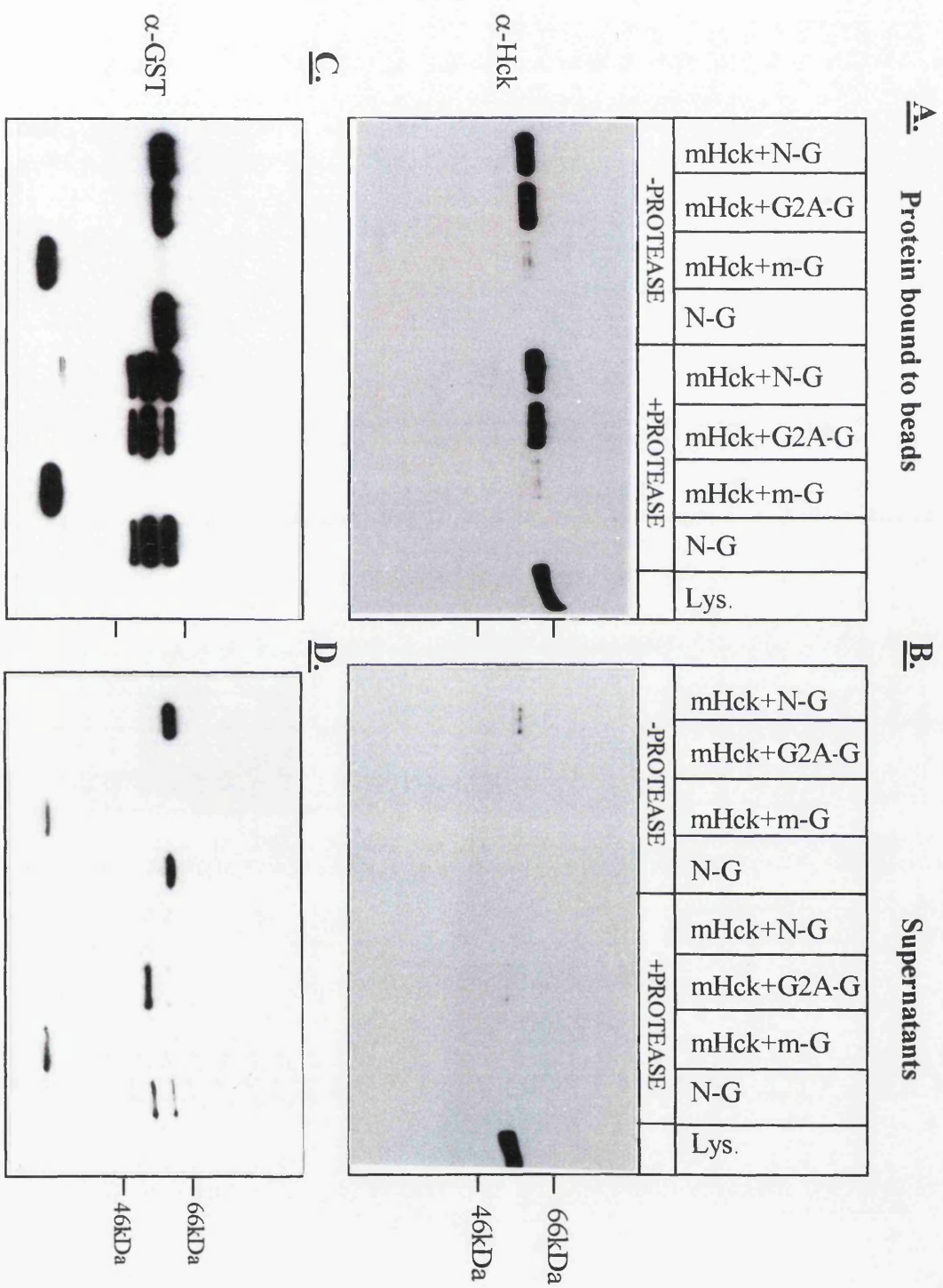


Figure 5.9.

5.10. Analysis of the contribution of the N-terminus of Hck to Nef binding:

To assess the impact of the unique N-terminal domain of Hck on Nef binding *in vivo* it was necessary to make an N-terminally truncated Hck. *In vitro* studies reported at the time by Moarefi *et al* 1997, had demonstrated that a bacterial expressed Nef was capable of activating an N-terminal truncated human Hck clone. In order to make a direct comparison to these studies a recombinant baculovirus was generated expressing a similarly truncated human Hck, $\Delta 78\text{hHck}$ see section 5.5. A nonmyristoylated G2AhHck mutant was also constructed, but unfortunately cloning difficulties were encountered for the wildtype hHck cDNA. The hHck clone was kindly donated by Prof. Kalle Saksela (University of Tampere, Finland) and was the same allele of Hck used in the experiments by Moarefi *et al*. These constructs not only allowed us to investigate the importance of the Hck unique region in Nef binding *in vivo* but also corroborate our previous results with the murine Hck. Authentic kinase activity of the enzymes is shown in figure 5.14.

In vivo binding assays performed for $\Delta 78\text{hHck}$ and G2AhHck demonstrated that they retained their ability to bind both native Nef and nonmyristoylated Nef *in vivo*. As the $\Delta 78\text{hHck}$ protein lacked its unique domain an alternative α -Hck antibody for western blot detection was utilised, purchased from Affiniti, Exeter, UK (see table 2.9), termed α - $\Delta 78\text{hHck}$ herein. The results of the assays are shown in figure 5.10. The level of binding detected for $\Delta 78\text{hHck}$ was not directly comparable to that for G2AhHck as the α - $\Delta 78\text{hHck}$ antibody gave high levels of background for G2AhHck. The standard α -Hck antibody (Santa Cruz, see table 2.9) was therefore used as a probe for G2AhHck. Figure 5.10A shows an α -Hck western blot of the results for the binding assay with G2AhHck. Lanes 1 and 2 show significant levels of binding of G2AhHck to both N-G and G2A-G with none detectable for m-G (lane 3) confirming the specificity of the interaction. The apparent increase in binding of G2AhHck to N-G in this example was explained when the membrane was stripped and reprobred with α -GST. The α -GST western blot analysis revealed levels of N-G were substantially elevated by comparison to G2A-G and m-G. In contrast, results from the $\Delta 78\text{hHck}$ *in vivo* binding assays suggested $\Delta 78\text{hHck}$ bound with a reduced affinity to nonmyristoylated Nef by comparison to N-G. Figure 5.10B

shows an α - $\Delta 78\text{hHck}$ western blot of the results. The amount of $\Delta 78\text{hHck}$ bound to N-G in lane 1 is ~ 7 fold more than that bound to the G2A-G affinity reagent (lane 2). This was a genuine manifestation of different binding efficiencies as equivalent levels of the affinity reagents were confirmed by stripping and reprobing the blot with an α -GST antibody shown in D. In addition, for each of the experiments equivalent levels of Hck in the coinfecting lysates prior to immunoprecipitation were confirmed on separate blots (data not shown).

From these results it can be concluded that nonmyristoylated hHck binds to both myristoylated and nonmyristoylated Nef with equal efficiency similar to the binding observed for the wildtype mHck isolate. However, the latter results for $\Delta 78\text{hHck}$ suggest that myristoylation does enhance the stability of the Nef-Hck complex because in the absence of Nef myristoylation binding of the $\Delta 78\text{hHck}$ was reduced. As differences between N-G and G2A-G Hck binding were only seen for $\Delta 78\text{hHck}$ the results implied both myristoylation and the unique domain of Hck serve to enhance the interaction and that the removal of each individually is not sufficient to perturb the interaction. This raises the possibility that the Hck-Nef complex is formed by an accumulative number of weak interactions acting in concert and modifications such as myristoylation maybe necessary to stabilize the interaction under physiological conditions. To determine regions in Nef essential for the interaction and to confirm the observed *in vivo* interaction was Nef isolate independent a panel of Nef mutants and isolates were screened for their ability to interact with Hck.

Figure 5.10. Results of *in vivo* binding studies for $\Delta 78hHck$ and G2AhHck:

In vivo binding assays were performed as detailed previously. $\Delta 78hHck$ binding to the affinity reagent was determined by α - $\Delta 78hHck$ (Affiniti) western blot, while G2AhHck was detected by the standard α -Hck (Santa Cruz). Subsequently both membranes were stripped and reprobed with α -GST antibody to determine levels of affinity reagent expression.

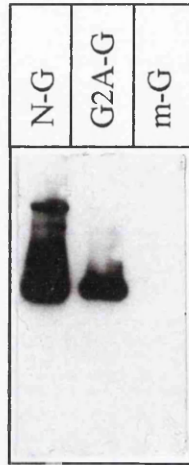
A. Results of *in vivo* binding assay for G2AhHck. These demonstrated that G2AhHck bound to N-G (lane 1) and G2A-G (lane 2) specifically with no binding to m-G (lane 3). N-G was expressed to higher levels see C consistent with increased G2AhHck binding in this example.

B. Results of *in vivo* binding assay for $\Delta 78hHck$, western blot (α - $\Delta 78hHck$). Lane 1 shows increased binding of $\Delta 78hHck$ to N-G by comparison to binding levels in lane 2. No binding to the m-G negative control in lane 3 was observed.

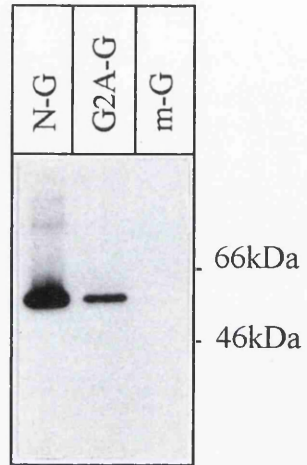
C. A, stripped and reprobed with α -GST showing increase levels of N-G in lane 1 by comparison to G2A-G (lane 2) and m-G (lane 3).

D. B, stripped and reprobed with α -GST confirming equivalent levels of expression of the affinity reagents.

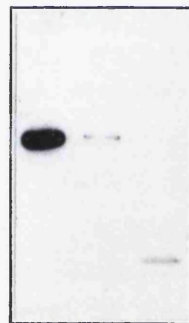
A.



B.



C.



D.

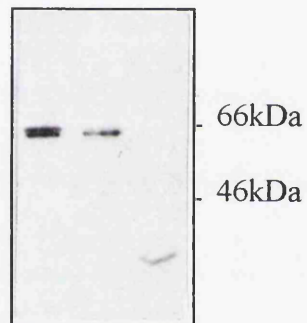


Figure 5.10.

5.11. Screen of a panel of Nef mutants and isolates to identify regions important for Hck binding and verify the *in vivo* binding was not Nef isolate dependent:

5.11.1. Results from the Nef mutant screen:

Nef mutants were screened for interactions with murine Hck *in vivo*. Results obtained for G2A- and $\Delta 78$ - hHck will also be presented. Coinfections and *in vivo* binding assays were performed as previously outlined and the relative binding affinities of Hck for the various Nef mutants and alleles determined. The Nef mutants screened, including a description of the salient points for each are shown, table 4.1.

The results of the coinfection binding assays for the murine Hck are shown in figure 5.11. A, shows the uniform binding of Hck to each of N-G, G2A-G, $\Delta 36-65$, $\Delta 74-98$, $\Delta 111-143$, PAAP, $\Delta 7-22$, $OM\Delta 7-22$ (lanes 1, 2, 4, 5, 6, 7, 9 and 10 respectively). The apparent reduction in Hck binding to the 3 deletion mutants (lanes 4-6) was explained by the reduced levels of expression observed for these mutants (see B). These results therefore implied that Hck bound to each of the Nef mutants with equal efficiency as the wildtype N-G. To ensure the results had not been affected by variable Hck levels a separate α -Hck western blot of the coinfecting lysates was performed. This confirmed equivalent levels of expression of Hck in each of the coinfecting lysates (see C). The binding of mHck to PAAP was unexpected as previous studies had demonstrated an intact (PXX)₃P motif in Nef was critical for the association (Saksela *et al*, 1995; Moarefi *et al*, 1997; Briggs *et al*, 1997). To establish binding to the PAAP Nef mutant observed in our current studies was not an anomaly of the mHck isolate the experiments were repeated for G2AhHck and $\Delta 78$ hHck. The results shown in figure 5.12 clearly demonstrated binding of G2A- and $\Delta 78$ - hHck to the BH10 PAAP-G mutant (lanes 1 and 4, A) consistent with the mHck results. To confirm these results were not an *in vivo* phenomenon the assay was repeated *in vitro* for mHck plus PAAP compared to N-G, G2A-G and m-G (see C and D) and again mHck bound PAAP with an equal efficiency as N-G and G2A-G. This suggested that either the conformation adopted

by the proteins expressed in Sf9 cells differed from the previous studies or that the loss of binding was Nef isolate dependent.

The screening of the remainder of the Nef mutants for G2A- and Δ 78- hHck binding gave similar results to those seen for mHck. The conserved Hck ability to bind to the panel of Nef mutants, suggested either; i) a critical motif had been maintained throughout the mutants; or ii) multiple Hck binding sites exist in Nef and the elimination of one is not sufficient to destabilize the Hck association.

Figure 5.11. Results of mHck binding to the panel of Nef mutants:

In vivo binding assays were performed as standard (see sections 2.6.5. and 2.6.8.) and the results analysed by western blot.

A. Results of the *in vivo* binding assay for mHck with the Nef mutants as the affinity reagents. This α -Hck western blot shows equal mHck binding in all lanes except lane 3 which was the m-G negative control. Samples were loaded N-G (lane 1), G2A-G (lane 2), Δ 36-65 (lane 4), Δ 74-98 (lane 5), Δ 111-143 (lane 6), PAAP (lane 7), mHck lysate positive control (lane 8), Δ 7-22 (lane 9), OM Δ 7-22 (lane 10).

B. The same blot as shown in A, stripped and reprobed with α -GST, demonstrating the affinity reagents were expressed to similar levels.

C. A separate α -Hck western blot of the coinfecting lysates prior to immunoprecipitation, confirming equivalent levels of mHck expression in all samples.

Figure 5.12. Comparison of mHck, G2A- and Δ 78- hHck binding to PAAP Nef:

In vivo binding assays were carried out for G2A- and Δ 78- hHck plus either PAAP Nef, N-G or m-G (see sections 2.6.5. and 2.6.8. for methods). In addition an *in vitro* binding assay was performed for mHck plus the same affinity reagents including G2A-G.

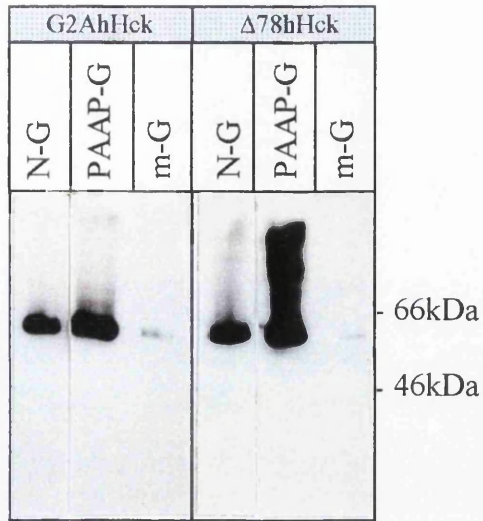
A. *In vivo* binding assays for G2A- Δ 78- hHck. Equal binding to the PAAP Nef mutant was apparent for both Hck derivatives (lanes 1 and 4) by comparison to the BH10 N-G wild type (lanes 3 and 6). Specificity was confirmed by lack of binding to m-G for each (lanes 2 and 5). The G2AhHck blot was probed with α -Hck and the Δ 78hHck with the α - Δ 78hHck antibody.

B. The same membranes as shown in A both stripped and reprobed with α -GST confirming equivalent levels of affinity reagents were present.

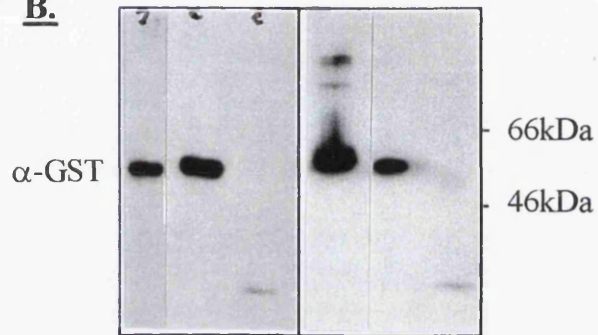
C. *In vitro* binding assay of mHck with PAAP-G (lane 1), N-G (lane 2), G2A-G (lane 3) and m-G (lane 4), the method is detailed 2.6.7. Equivalent binding of mHck to all except the m-G specificity was detected.

D. C reprobed with α -GST.

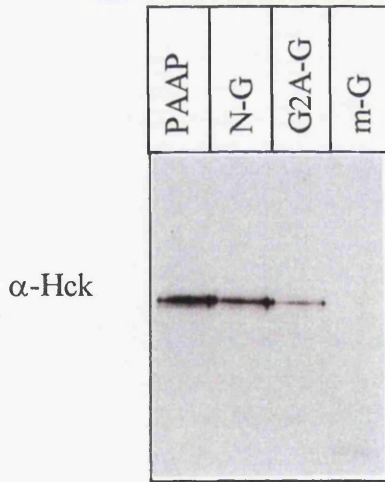
A.



B.



C.



D.

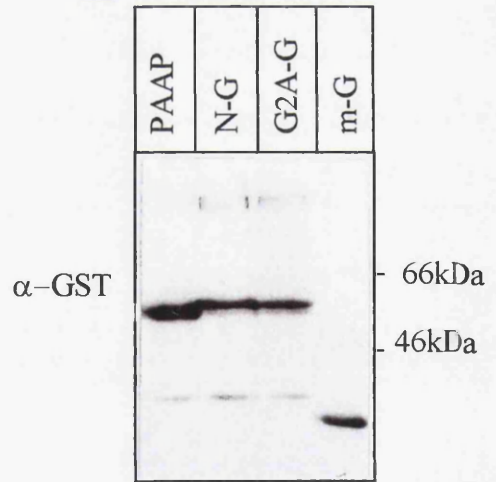


Figure 5.12.

5.11.2. Results from the Nef isolate screen:

To determine whether the Hck binding affinity for Nef isolates was inherently variable *in vivo* binding assays were performed for BH10, Bru (a laboratory HIV strain derived Nef similar to BH10); PCR2iso, PCR3iso, PCR4iso, PCR5iso (Harris *et al*, 1992)(all primary patient Nef isolates); and SIV J5 (Rud *et al*, 1992). It was found mHck was capable of consistently binding all of the PCR patient isolates at equivalent levels to BH10 Nef (A, lanes 1-4). Similar results were also obtained for the SIV J5 Nef isolate (lane 8) although this consistently expressed to lower levels mHck binding was proportional to expression levels. However unexpectedly the Bru Nef isolate was consistently impaired in mHck binding (lane 7). In the example shown in figure 5.13 mHck binding levels to Bru in A are equal to those observed for SIV J5, but if the levels of the affinity reagents are compared in B, Bru is expressed at ~14 fold higher levels than SIV J5. In addition, Bru-GST (lane 7) is expressed at equal levels relative to N-G (lane 6, B) but the amount of mHck associated with Bru in the binding assay was ~10 fold less than that detected for BH10 Nef. The Bru amino acid sequence only differs from BH10 by 7 amino acids (see diagram 5.3) and none of these changes are in the conserved Nef motifs. There are 2 point mutations to threonine residues, A16T and N52T, which could potentially result in the generation of serine/threonine kinase substrate sites, but the remaining changes are all highly conservative. Mass spectrometry studies are currently in progress to analyse whether the introduction of 2 additional threonine residues in Bru resulted in its phosphorylation in Sf9 cells.

Figure 5.13. Screening Nef alleles for mHck binding:

In vivo binding assays were performed for mHck with the laboratory Nef alleles BH10, Bru, the primary isolates PCR2iso, PCR3iso, PCR4iso, PCR5iso and SIV J5 (see section 2.6.5. and 2.6.8.) as affinity reagents. The complex bound to GA-beads was analysed by western blot, α -Hck was used as a probe for mHck binding, the membrane was subsequently stripped and reprobed with α -GST.

A. Binding of mHck to the different Nef alleles. This demonstrated that mHck bound the primary Nef isolates at equivalent levels PCR5iso (lane 1), PCR4iso (lane 2), PCR3iso (lane 3), PCR2iso (lane 4). The specificity of the interaction was confirmed by m-G in lane 5. Binding to BH10 (N-G) is shown in lane 6. In this blot it appeared levels of mHck binding to Bru and J5 were similar (lanes 7 and 8), however if the expression levels of the affinity taken into account (see B) it is evident Bru was a poor affinity reagent for mHck.

B. Expression levels of the affinity reagents, A reprobed with α -GST therefore loading is the same as in A. PCR2iso-PCR5iso were expressed at the same levels (lane 1-4), as were N-G (lane 6) and Bru (lane 7). SIV J5 was expressed at a substantially reduced level (lane 8) consistent with the reduction in mHck binding.

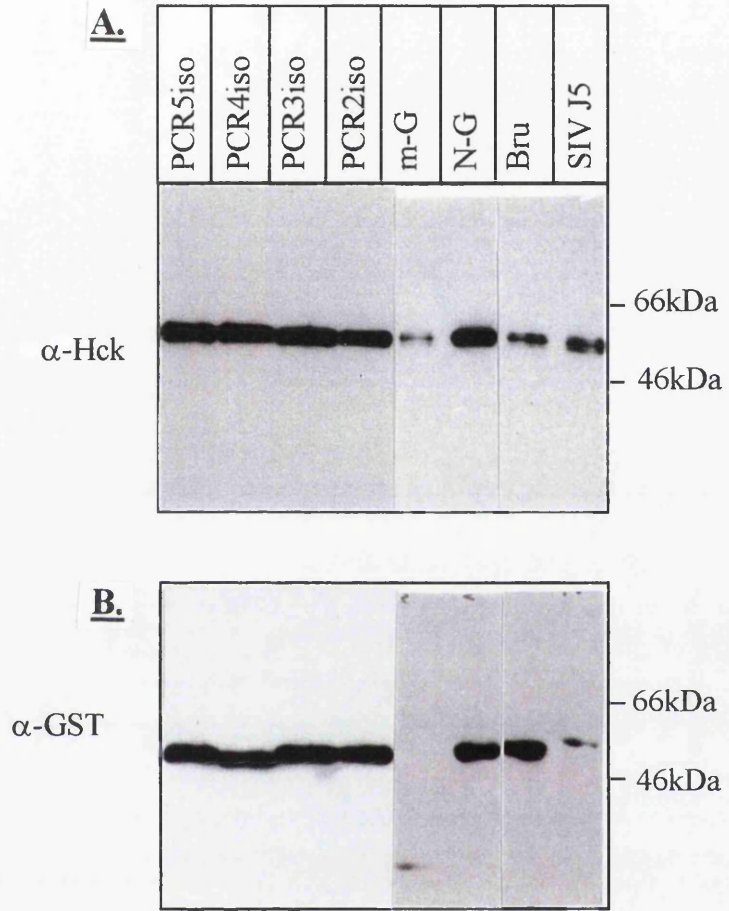


Figure 5.13.

5.12. Effect of Nef on Hck enzymatic activity:

To determine if the PAAP BH10 mutant bound Hck in the same manner as wild type Hck the effect on enzyme activity was investigated. The Nef (PXX)₃P mediated binding to Hck via its SH3 domain had been demonstrated to activate the kinase activity. We therefore hypothesised that as the PAAP BH10 mutant was clearly binding independently of the (PXX)₃P motif, the effect on Hck activity may also be perturbed. Peptide substrate assays were carried out as described section 2.8.9. In this experiment increasing concentrations of N-G, Nef-6His (described elsewhere (Harris and Coates, 1993)), PAAP-G or m-G were added to each Hck sample and the number of phosphates transferred to a peptide substrate in 30 minutes determined. The results are presented in the bar graph in figure 5.14. Increasing concentrations of Nef-6His resulted in enhanced Hck kinase activity. However, it was found increasing m-G levels did slightly enhance Hck enzyme activity. The recent reports of reducing conditions causing the formation of sulfhydryl bonds and subsequent enzyme activity (see section 1.3) are consistent with this m-G observed activation of mHck. However, a clear difference between N-G and PAAP-G was still evident. Increased concentrations of N-G resulted in the elevation of enzyme activity, while PAAP had no detectable effect on enzyme activity in this assay. This confirmed the hypothesis that binding of Nef to Hck involves an additional interaction, independent of the (PXX)₃P-SH3 domain binding. Furthermore it suggested that Nef is capable of binding Hck without the accompanying increase in enzyme activity. However significantly, native Nef retained its Hck activation ability corroborating the results of Moarefi *et al* 1997, who proposed that SH3 domain recruitment by the (PXX)₃P motif in Nef leads to enhanced enzyme activation.

Figure 5.14. Comparison of the effect of wildtype and PAAP Nef on mHck activity:

Peptide substrate assays were performed for equal amounts of mHck in the presence of varying concentrations of either N-G, PAAP-G, m-G, Nef-6His or BSA (0, 2 or 5 μ g). These were carried out in duplicate and the results averaged. The results of the number of phosphates transferred to a peptide substrate after 30 minutes are shown in the bar graph. It was clear increasing concentrations of Nef-6His resulted in elevated mHck enzymatic activity with a significant increase in the number of phosphates transferred detectable. BSA had no effect on kinase activity and although m-G did enhance enzyme activity slightly (see text) the levels of activity in the presence of N-G were almost doubled. Significantly increasing concentrations of PAAP did not effect mHck enzyme activity.

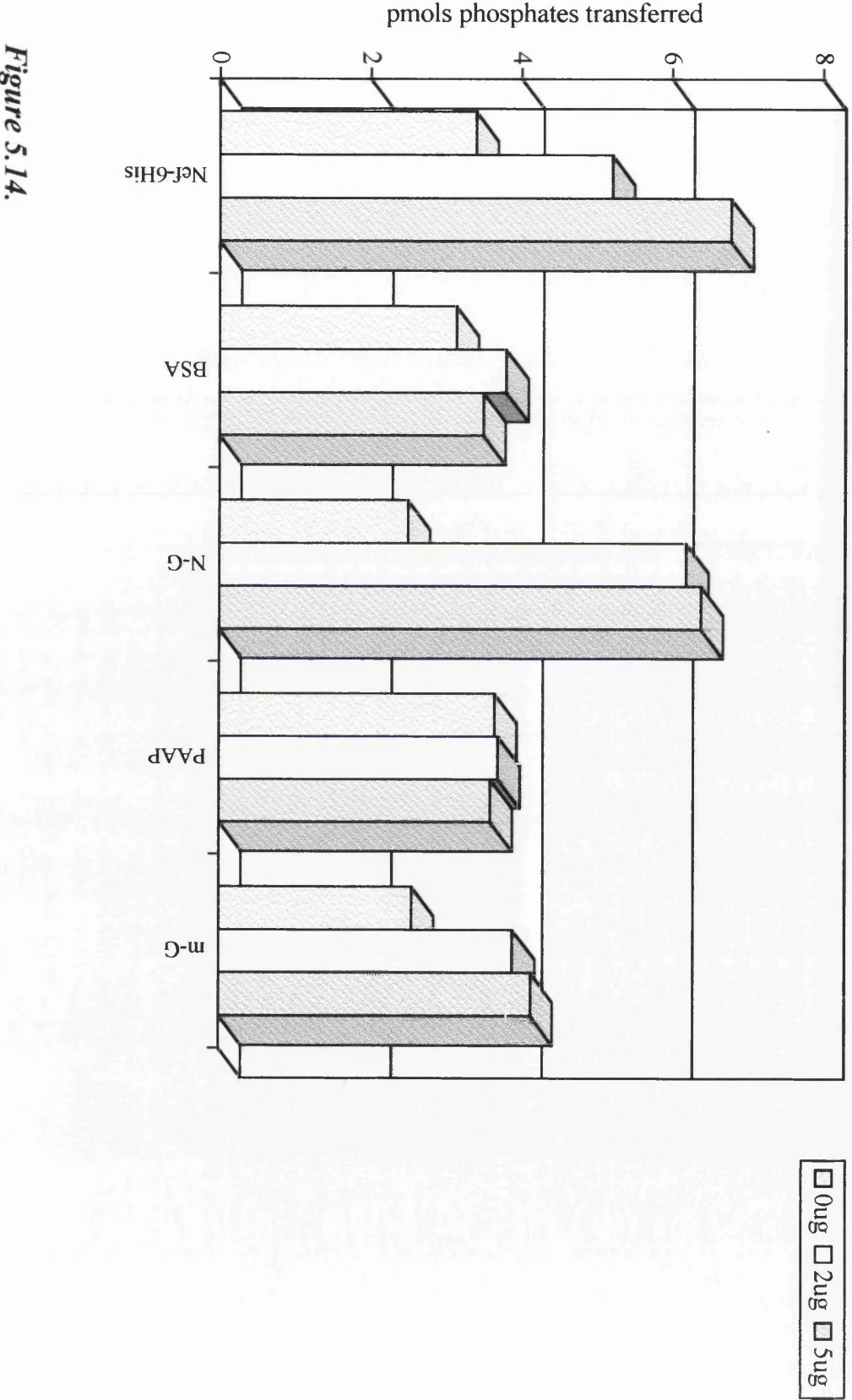


Figure 5.14.

CHAPTER 6

CHAPTER 6 - DISCUSSION

	Page number
6.1 Screening for novel Nef interactors	239
6.2 Conformational requirements for the Lck interaction with Nef	245
6.3 Interactions of Nef with Hck	255
6.4 Final discussion	263

CHAPTER 6- DISCUSSION:

6.1. Screening for novel Nef interactors:

Studies on Nef have revealed a wide variety of functions each with a corresponding hypothesis as to the implications for HIV pathogenesis. In an attempt to understand the pleiotropic nature of Nef an increasing number of groups have been investigating potential endogenous cellular binding partners for Nef. As the *nef* transcript comprises 70% of the early viral mRNA it might be predicted that any potential cellular interaction partner would be similarly abundantly expressed. Moreover, at this stage in the viral life-cycle Nef is expressed predominantly in its full length myristoylated form. The cotranslational addition of myristate to the N-terminus of Nef could have important consequences for both its subcellular location and by analogy to other myristoylated proteins its overall structural configuration; thus exerting a strong influence on its intracellular binding partners. To investigate Nef protein-protein interactions it was therefore necessary to utilise a system that would express Nef in its native conformation and simultaneously allow the rapid screening of protein-protein interactions. The YTHS represented an ideal tool for these purposes.

At this time available YTHS were not sufficiently developed to allow expression of the bait protein as an N-terminal fusion. The pEG202 bait plasmid supplied with the interaction trap system was therefore modified by a complex cloning procedure to accept bait-cDNA N-terminally to the DB domain (see section 3.2). This left the N-terminus of the bait protein under investigation accessible for posttranslational modifications, such as myristoylation required during these experiments. The generation of pVEG2 as an alternative bait plasmid will provide a valuable basic research tool for protein interactions dependent on free N-termini or an N-terminal modification. In addition, if the results obtained in the activation assay for the pVEG-Nef and pEG-Nef (the N- and C- terminal fusions respectively) constructs set a precedent, it is possible that by expressing some proteins as N-terminal fusions inherent transactivating properties will be circumvented, allowing the proteins to be

used as a bait in the system. This is in contrast to the drastic steps of deleting regions of acidic amino acid sequences normally recommended for transactivating baits. The experiments performed in these studies confirmed that the full length expression of myristoylated and nonmyristoylated Nef, p55Gag and ORF94 as DB domain fusions in pVEG and pVEG2 was stable and non-toxic to yeast. The suitability of the protein fusions as baits in the YTHS was assessed by the activation and repression assays. These showed that pVEG(2)-Nef, -p55Gag and -ORF94 were capable of entering the nucleus and binding the UAS but did not possess intrinsic transcriptional activation properties. The studies also confirmed the authentic myristoylation of Nef in this system. Previous work by Macreadie *et al* 1993 has demonstrated the ability of a myristoylated Nef to enter the nucleus (Macreadie *et al*, 1993).

The human haploid genome is 2.8×10^6 kb; given that we were screening a Jurkat T-cell cDNA library for Nef interaction partners and that mRNA populations reflect the relative abundance of protein expression in a cell to ensure a reasonably complete library screen it was necessary to screen 10^6 - 10^7 clones (Old and Primrose, 1989). In these studies $\sim 2 \times 10^6$ colonies were screened, consistent with our hypothesis that Nef interactors would exist among the enriched mRNA population. A total number of 92 potential interactors were identified which on RFLP and sequencing analysis partitioned into 6 groups. On the basis of; preliminary sequence data; strength of the detected interactions as determined by β -galactosidase activity; and the number of interactors within each group; groups A1, B1 and C1 were selected for further investigation. A representative from each group was isolated and retransformed back into yeast where they were reassessed for their ability to interact with the Nef-DB domain fusion, a negative control (pEG202 encoding the DB domain only) and the 2 specificity controls p55Gag and ORF94. From these results it was determined that only one clone was genuinely interacting specifically with Nef, clone 39, from group A1.

The largest group of false positives was in fact the largest group of identical clones isolated, group C1. C1 was found to have homology to the recently cloned VHL

(von Hippel Lindau) gene encoding a tumour suppressor protein involved in transcriptional regulation. Although false positives are a common problem with the YTHS (Hengen, 1997) the isolation of this protein probably also reflected the Jurkat T-cell line used as the cDNA source for these studies, as the expression of oncogenic proteins is likely to be enhanced in continuous cell lines. Other false positives isolated included 2 different groups of polypeptides with significant zinc finger protein homology. The isolation of zinc finger containing DNA binding proteins represents an ongoing problem with the YTHS and arises as a result of their expression in the context of an activation domain fusion. In addition Nef exhibited a spurious interaction with a polypeptide derived from cDNA encoding the EHOC-1 (Epilepsy, HOIoprosencephaly Candidatie-1) gene. A database of YTHS false positives is currently being compiled by E.A.Golemis from the laboratory of Dr.R.Brent. From the data made available to date it is evident that a number of proteins are consistently isolated during interactor hunts and due to either specificity problems or physiological reasons, are classified as false positives. As with EHOC-1 there is often no apparent reason why these proteins are isolated except perhaps their relatively high level of expression. Frequently isolated cDNAs include for example, heat shock proteins, ribosomal proteins, cytochrome oxidase, ferritin and proteasome subunits. Interestingly, the HsN3 proteasomal subunit has recently been reported by Rossi *et al* 1997 to specifically interact with Nef. These studies were predominantly performed in the YTHS and in view of the results compiled by E.A.Golemis it appears proteasome subunits may be inherently 'sticky' proteins in the YTHS. Future studies in alternative expression systems will therefore be required to confirm this Nef interaction.

The specificity of the clone 39 interaction in the YTHS with both Nef and p55Gag was intriguing, especially given the strength of the interaction as determined by β -galactosidase activity. The lack of interaction observed *in vitro* was therefore unexpected and as detailed in section 3.7 was probably a result of practical considerations. The cDNA insert in clone 39 was ~1000bp, however it was found to encode a polypeptide of only 43 amino acids as determined by sequencing, although western blot analysis suggested the transcript encoded a polypeptide of ~9kDa.

FASTA DNA analysis revealed statistically significant homology to a human cDNA (Ac: N55259) in that the Poisson P value was <0.01 (the Poisson P value is calculated by the FASTA program and is the probability of the match occurring by chance given the number of residues in the query sequence and the database). The homology of N55259 to clone 39 was found to extend through to the untranslated region, up to 195bp. The N55259 cDNA sequence included a frame shift caused by an additional guanine at codon 29 relative to clone 39 (clone 39 numbering). It therefore encoded a 60 amino acid polypeptide more consistent with the 9kDa product detected by western blot analysis. The N55259 cDNA sequence was hence utilised to screen the HGMP EST tagged cDNA databases in an attempt to identify further flanking DNA sequences with possible known protein homologies. These searches revealed the existence of a mouse homologue, but no flanking cDNA sequence data. Partial cDNA sequences identified during the database searches were used to compile consensus DNA sequences for both human and mouse cDNA sequences. BLAST searches of these consensus sequences revealed no statistically significant protein sequence similarities.

In view of the problems encountered during the sequencing clone 39 due to stretches of high concentrations of guanine and cytosine nucleotides it was also possible that the N52259 sequence contained inaccuracies. This was supported by the calculation of the number of amino acids theoretically required to form a 9kDa polypeptide which is nearer 80 amino acids. Recent reanalysis of the clone 39 peptide sequence alone in the absence of the N52259 frame shift revealed 75% homology over a 12 amino acid stretch to 3',5'-cyclic-nucleotide-phosphodiesterase. This homology reduces to only ~21% if taken over the whole peptide sequence and is lost completely if the N52259 frame shift is included. As 3',5'-cyclic-nucleotide phosphodiesterase is a specific regulator of 3',5'-cyclic-adenosine monophosphate (cyclic-AMP) a Nef interaction with this protein could be highly significant. Phosphodiesterases hydrolyse cAMP to AMP, this is an essential process as cAMP acts as a second messenger for many hormones, including epinephrine, glucagon, luteinizing hormone, melanocyte stimulating hormone and thyroid stimulating hormone. Significantly cAMP is involved in

physiological processes such as the degradation of storage fuels, acid secretion by the gastric mucosa and the dispersion of melanin pigment granules, each of which is severely affected during AIDS. Consistent with this elevations in cellular cAMP levels have been detected in HIV infected cells (Nokta and Pollard, 1991; Hofmann *et al*, 1993). In addition a number of lines of evidence make it a plausible Nef target. It has been proposed that elevated levels of cAMP cause an early block in T-cell signalling events (Tamir and Isakov, 1991; Tamir and Isakov, 1994; Tamir *et al*, 1996) resulting in transcription inhibition of IL-2, IL-2R and c-Jun expression. Furthermore, increased cAMP levels have been found to block the shift in electrophoretic mobility indicative of Ser59 phosphorylation which was also reported to be inhibited by Nef expression (Greenway *et al*, 1995a) see section 6.2. This cAMP block of Lck serine phosphorylation has been proposed to result from an inhibition of PKC and MAPK activities (Tamir *et al*, 1996) again consistent with reports of Nef effects (Greenway *et al*, 1996; Smith *et al*, 1996). Intriguingly it has recently been demonstrated that elevated levels of cAMP in myeloid cell lines results in the selective inhibition of CD4 endocytosis, suggesting in the presence of high concentrations of cAMP Nef expression may be required to target CD4 to clathrin coated pits (Foti *et al*, 1997). It would therefore be of interest to determine whether clone 39 represents a novel phosphodiesterase. Future studies will also be required to determine whether Nef is capable of binding other phosphodiesterase family members and to establish the effect of this interaction on cellular cAMP levels. In addition the interaction of p55Gag with clone 39 raises the possibility that phosphodiesterases may be recruited to the virion. Further work will also be required to address which Gag polypeptide mediates the interaction, it is even possible phosphodiesterase interactions may influence the micro-environment of the PIC.

Figure 6.1. Homology of clone 39 to 3', 5'-cyclic-nucleotide phosphodiesterase:

```

pir||A36317 3',5'-cyclic-nucleotide phosphodiesterase C
           cAMP-specific - human
           Length = 686
Score = 40 (19.8 bits), Expect = 0.18, Sum P(2) = 0.17
Identities = 7/12 (58%), Positives = 9/12 (75%)

Query:     20 CTAVPSKETCQE 31
           C A S+ETCQ+
Sbjct:    . 18 CKATLSEETCQQ 29

```

The results obtained during the specificity study for clone 39 demonstrated that its interaction with Nef was myristoylation independent. This was contrary to the prediction that myristoylation would influence protein-protein interactions, but does not preclude the existence of such myristoylation dependent interactions. The development of false positive databases, plus automated sequencing techniques will make future YTHS library screenings more efficient. This should also facilitate comparative library screenings where both myristoylated and nonmyristoylated Nef could be used as baits to screen the same library. Ideally library sources should be primary cell lineages to ensure the mRNA population is not qualitatively distorted. A comparative study of different cell lineages would also be beneficial to distinguish between Nef binding partners in T-cell lineages and those of myeloid origin. The β -galactosidase reporter construct would allow the relative affinities of the interactions in each cell type to be determined. In addition, multiple library screenings would identify ubiquitously expressed Nef cellular targets, potentially alluding to those that are of functional significance in all cell types maximising the potential targets for therapeutic drug design.

In summary of the data obtained during this study; the modification of the bait plasmid to accept cDNA inserts as N-terminal fusions to the DB domain was successful increasing the repertoire of proteins that can be used as baits in the system; myristoylation was not found to mediate the clone 39 interaction detected for Nef, but as only one putative interaction was identified it is likely that further screening would reveal further interactors; clone 39 showed a strong specific interaction for myristoylated and nonmyristoylated Nef and p55Gag in the YTHS but it was not reproducible *in vitro* under the conditions used in these experiments; clone 39 showed strong homology to both human and mouse cDNA EST tagged sequences, but only limited protein sequence homology to 3',5'-cyclic-nucleotide phosphodiesterase, further studies will be necessary to establish whether this limited homology reflects a Nef ability to interact with 3',5'-cyclic-nucleotide-phosphodiesterase.

6.2. Conformational requirements for the Lck interaction with Nef:

The results presented in these studies clearly demonstrated Lck conformational dependent Nef binding. Furthermore multiple regions in Nef were found to contribute to Lck binding including the highly conserved (PXX)₃P motif and a region between residues 36-65 previously implicated for Nef mediated virion infectivity. A summary of the results obtained followed by a discussion of the functional implications of an Lck conformational dependent interaction with Nef will be detailed below.

A detailed investigation of the Lck conformation compatible with Nef binding was prompted by two observations. Firstly, Lck binding to native Nef was severely impaired after a change in foetal calf serum (FCS) used to supplement the complete TC100 media for Sf9 cell culture, and secondly a similar loss of binding had been noted in previous experiments when the Lck lysates were prepared in the presence of NaOV. A further comparison of Nef binding affinities for Lck expressed in lysates from Sf9 cells grown in media supplemented with different FCS batches revealed a marked variability in the level of Lck bound to Nef for each sera. As FCS is comprised of variable concentrations of innumerable biomolecules all providing a subtle balance between cell proliferation, differentiation and apoptosis and all intrinsically linked with cell signal transduction pathways, it was hypothesised that Lck conformation was being altered by the varying sera. If this hypothesis was correct it followed that Lck enzymatic activity would also be effected. In accordance with this, α -pTyr (PY69, Santa Cruz) western blot analysis of the different Lck stocks demonstrated an increase in overall tyrosine phosphorylation in stocks compatible with Nef binding. To address whether this increase in tyrosine phosphorylation was due to a saturation of the active site Tyr394 phosphorylation indicative of the active “open” kinase conformation, or conversely the inactive Tyr505 phosphorylated Lck form, recombinant baculovirus Lck mutants were constructed.

A constitutively “open” active Lck was constructed by mutating the C-terminal Tyr505 to Phe. This mutant had a two fold effect, as well as constitutively activating Lck by disrupting the intramolecular association of pTyr505 with the SH3 domain, it also removed the alternative Tyr505 phosphorylation site. Detection of tyrosine phosphorylation for this mutant would therefore be solely attributable to Tyr394 phosphorylation. However it was found expression of the Y505F mutation both separately or in combination with a kinase inactivating K273A mutation in the phospho-transfer site of the active site of the enzyme, was toxic to Sf9 cells. This resulted in the inability to generate recombinant baculoviruses expressing the Y505F mutation in this background. A further G2A mutation was necessary to facilitate the production of recombinant baculoviruses expressing this Y505F mutant protein. The reduced toxicity of LckY505F in this context was probably due to the removal of the protein from cell membranes. It is well documented that Lck signalling at the cell membrane is necessary for T-cell activation and removal from the membrane impairs signalling (Abraham and Veillette, 1990). Consistent with this the oncogenic potential of a nonmyristoylated Y505F Lck mutant was much reduced compared to myristoylated LckY505F (Abraham and Veillette, 1990). This is a conserved family characteristic as myristoylation is also required for the transforming capacity of v-Src in fibroblasts (Cross *et al*, 1984; Kamps *et al*, 1985; Catling *et al*, 1993).

Kinase assays for LckGY demonstrated its *trans* and auto-phosphorylation activity, but unexpectedly despite its open conformation LckGY did not have an elevated background level of Tyr394 phosphorylation. The reasons for this are unclear but may be related to its cytotoxicity. That LckGY expression was barely tolerated by the cells was evident when it was co-expressed with Nef, resulting in a dramatic reduction in the levels of expression for each protein. This was consistent with its recruitment to the membrane by myristoylated Nef. The kinase assays for LckGKY revealed that it was kinase defective consistent with the K273A substitution in the active site, no phosphotyrosine was detected by western blot analysis either -/+ATP. This also confirmed that levels of phosphotyrosine detected in previous autophosphorylation assays were due to Lck autophosphorylation activity and not

endogenous cellular kinases phosphorylating Tyr394 in the active site. Autophosphorylation assays were also performed for LckG2A and LckK273A. The results from these revealed LckG2A was predominantly in the active conformation with elevated levels of Tyr394 phosphorylation in the absence of high concentrations of ATP. A low level of tyrosine phosphorylation was detected for LckK273A which confirmed that the increases in tyrosine phosphorylation detected for the previous Lck species occurred on Tyr394. Furthermore the low level of tyrosine phosphorylation detected for LckK273A implied that the PY69 Santa Cruz, antibody did not detect Tyr505 phosphorylation or that the K273A mutant was not tyrosine phosphorylated and was in the open conformation.

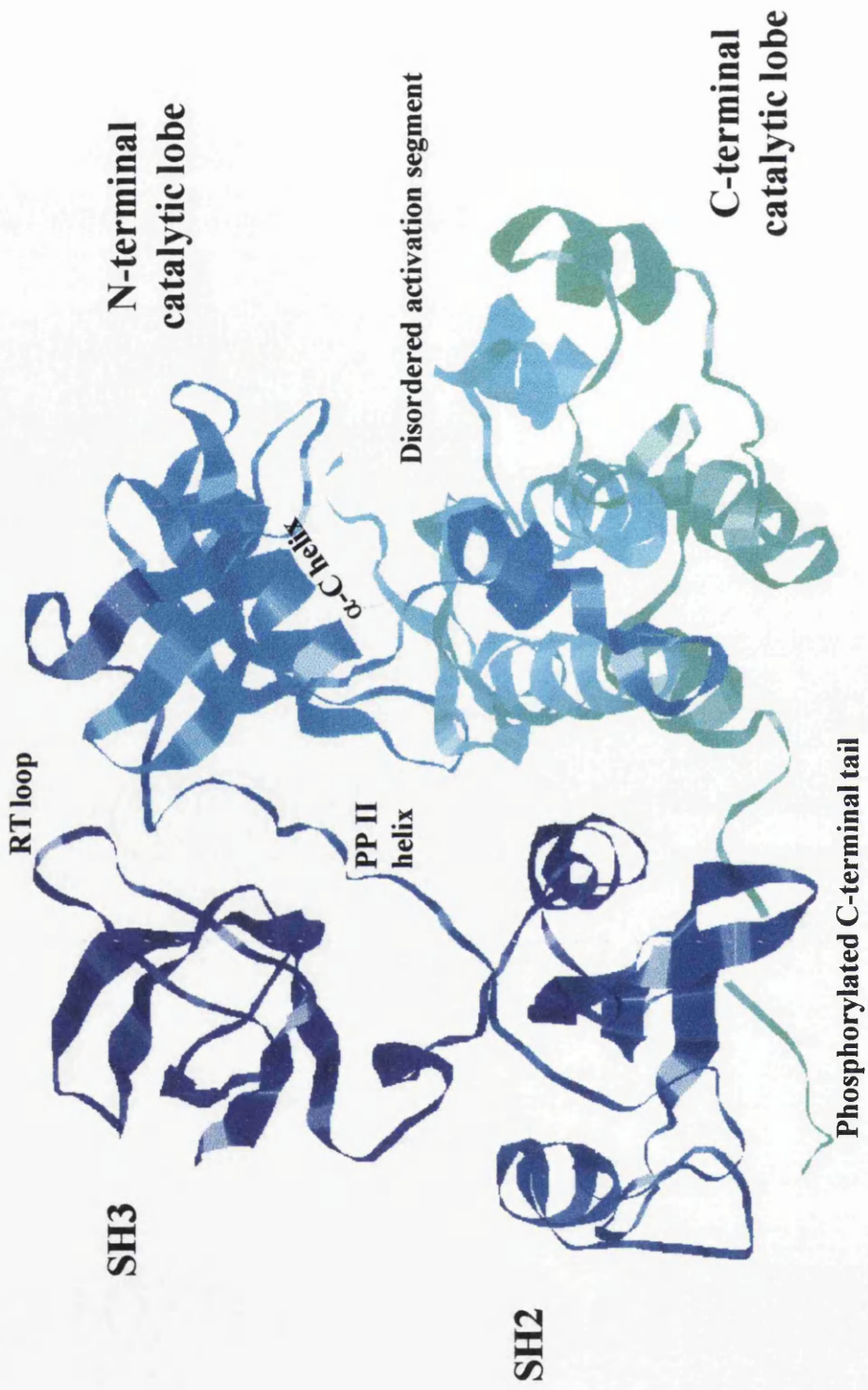
From the results obtained for Lck expressed in the presence of different sera it was predicted that Nef binding should correlate with elevated Lck tyrosine phosphorylation. However screening of these multiple Lck mutants also allowed us to assess whether Nef complexed with the “open” or “closed” conformation of Lck and whether Tyr394 or Tyr505 phosphorylation was required. A lack of Nef binding for LckGY observed in the *in vivo* binding assays inferred either Tyr394 phosphorylation was necessary for the Nef interaction with the open conformation or that it complexed with the closed conformation of Lck. However it is difficult to interpret the results of this experiment due to the cytotoxicity exhibited following co-expression of Nef and LckGY. Significantly, Nef binding was detected at high levels for LckGKY and LckK273A and to an intermediate level for LckG2A, of which only LckG2A maintained elevated phosphotyrosine levels and enzyme activity.

The efficiency of Nef binding to LckGKY suggested that the open Lck conformation was required for Nef binding and furthermore that Tyr394 phosphorylation was not necessary for the interaction. The requirement of an open conformation was further corroborated by LckG2A-Nef binding. The intermediate binding of LckG2A to Nef seen during the binding assays was consistent with only a percentage of the Lck expressed in the lysate complexing with Nef. Evidence for a variable LckG2A conformation in the lysates was provided by the results of the

autophosphorylation assays: These demonstrated that, despite elevated background levels of tyrosine phosphorylation for LckG2A, an increase in the presence of ATP was still observed. This confirmed that background Tyr394 phosphorylation levels were not saturated. It therefore followed that only a percentage of LckG2A present in the lysate was in the active conformation and compatible with Nef binding, consistent with the intermediate amount of LckG2A detected complexed to Nef in the *in vivo* binding assays. The LckK273A mutant was included as a control for the inactive conformation of Lck in these experiments, therefore its high affinity binding to Nef was unexpected. However data from a recent study (Gonfloni *et al*, 1997) demonstrated that mutations in this region of Lck render the kinase constitutively active inferring this mutant was in fact in the open conformation. In this study the role of the linker region between the SH2 and N-terminal lobe of the catalytic domain of the Src kinases in activating the enzyme was analysed. Mutations of P274E and Q269E introduced into the β 3 loop of Lck, proximal to the α -C helix were found to abrogate the kinase regulatory ability of the C-terminal tail, rendering the kinase constitutively active. These results argue that the conformation of the β 3/ α -C loop plays a dominant role in determining Lck kinase activity. If this observation is extended to the results obtained in our current study, a conformation for the K273A mutant Lck may be envisaged where the α -C helix is in the active orientation. This would cause the overall protein structure to open and occupy the active configuration, but remain kinase defective due to the absence of the crucial lysine 273 residue necessary for phosphate transfer. On the basis of these results we propose that that Nef selectively binds the open conformation of Lck and that complex formation can occur independently from both Tyr394 phosphorylation and Gly2 myristoylation.

The most complete crystallography studies performed to date, have resolved the structures of human Hck (Sicheri *et al*, 1997), human Src (Xu *et al*, 1997) and chicken Src (Williams *et al*, 1997) in their inactive C-terminally regulated conformations; all lacking their acylation signals and unique N-terminal domains. The structures revealed the catalytic domain comprises two lobes. The smaller N-terminal lobe is comprised of a 5 stranded anti-parallel β -sheet with a single helix

Diagram 6.2. Structure of human Src as resolved by Xu et al 1997,
taken from <http://www2.ebi.ac.uk/pdb/index.shtml>



(α -C). The α -C helix contains a highly conserved glutamate residue (Glu 310 in Src) the position of which is crucial for the activity of the enzyme and is indirectly involved in the positioning of the α and β phosphates of ATP. It is the position of this α -C helix that mutations in the β 3 loop are thought to affect (Gonfloni *et al*, 1997). The larger C-terminal lobe is predominantly α -helical and contains the active site tyrosine residue (Tyr 416 in Src) which localised to a disordered flexible loop in the crystal structure (activation segment), plus residues involved in substrate binding. The lobes are stabilized in the inactive conformation by associations with the SH3 and SH2 domains, which dock on the back of the catalytic domain and are thought to restrict the access of ATP to the active site, as illustrated below, diagram 6.1. The SH2 domain binds the C-terminal pTyr505 tail, while the SH3 domain forms a tripartite interaction between the SH3 ligand binding surface, a polyproline type II helix formed by the SH2-catalytic domain linker and the back of the small lobe of the catalytic domain. The inactive kinases exhibited a closed configuration of their N- and C- terminal lobes, with a solvent exposed positioning for the α -C helix. It has been proposed that phosphorylation of the active site Tyr416 would result in a widening of the cleft, reorientation of the α -C helix and activation of the enzyme (Xu *et al*, 1997). However the precise order of events is unknown at present. Evidence for a dramatic conformational change for the activation segment has been provided by the crystallisation of the Lck catalytic domain in its active configuration (Yamaguchi and Hendrickson, 1996). However it has also been demonstrated that Tyr394 phosphorylation and partial activation of Lck can occur in the presence of Tyr505 phosphorylation (D'Oro *et al*, 1996), a similar phenomena has been reported for Src (Boerner, 1996). These conformations are consistent with the proposal put forward by Moarefi *et al* 1997 that various degrees of activity exist for Src kinases. The results from our current study however suggest that the local configuration of the catalytic domain is not sufficient to confer Nef-Lck complex formation. Moreover the results indicated that a completely open Lck conformation was essential for Nef binding. This suggested that motifs occluded in the closed protein structure mediate the Nef interaction.

The concept of an open conformation of Lck conferring Lck-Nef binding ties in well with the recent reports of this association (Collette *et al*, 1996; Greenway *et al*, 1995b; Greenway *et al*, 1996; Baur *et al*, 1997). Studies on the CD45 phosphatase regulation of Lck have revealed that in cell lines lacking CD45 such as fibroblasts, Lck resides in its pTyr505 inactive state, conversely in CD45 positive cell lines such as PBMCs, Jurkat T-cells and MT-2 cells Lck is predominantly in its open conformation (Gervais and Veillette, 1995). Significantly the recent reports of Lck-Nef complex formation used these T-cell lines (Collette *et al*, 1996; Greenway *et al*, 1995b; Greenway *et al*, 1996; Baur *et al*, 1997). In addition similar *in vitro* co-precipitation assays were performed in two of the studies (Collette *et al*, 1996; Greenway *et al*, 1996) using the SH3 and SH2 isolated domains expressed as GST fusions as affinity reagents. The results from the studies concurred that the SH3 domain alone was able to precipitate Nef and that the efficiency of the interaction was greatly enhanced in the GST-SH3/SH2 domain fusions. *In vitro* peptide binding assays delineated the (PXX)₃P motif in Nef as critical for the SH3 domain interaction. The studies presented here corroborate and extend these earlier results and demonstrated that in the context of the native proteins the Nef (PXX)₃P motif remains critical for the interaction. The results demonstrated that the mutation of the 2 central prolines severely impaired Lck binding. However deletion of the second half of the motif (Δ 74-98 Nef) did not have such a drastic effect on complex formation suggesting two adjacent prolines are sufficient to maintain the PP-II helix structure. Significantly there are only two prolines in a PxxP motif in the SIV and HIV-2 Nef isolates (Rud *et al*, 1994; Lang *et al*, 1997)

A second region of Nef implicated in our current studies as important for Lck binding was the residues spanning positions 36-65. As the Lck SH2 domain has been identified to significantly enhance Lck-Nef interactions it would be tempting to speculate that amino acids 36-65 might be involved in this interaction. It had been previously proposed (Collette *et al*, 1996) that tyrosine phosphorylation of Nef may contribute to the SH2 domain association. However follow up studies in which all the tyrosine residues in Nef were systematically mutated revealed that Nef tyrosine phosphorylation was not required for the interaction (Collette *et al*, Virology in

press). In this context, a number of reports have detailed phosphotyrosine independent substrate binding to various SH2 domains including; a cyclin dependent kinase homologue p130^{PITSLRE} (Malek and Desiderio, 1994), Raf as a substrate for Fyn and Src SH2 domains (Cleghon and Morrison, 1994), Bcr binding to Abl SH2 domain (Pendergast *et al*, 1991; Muller *et al*, 1992), each of which is dependent on either serine or threonine phosphorylation instead. Notably Nef contains 2 adjacent serine residues at positions 45 and 46 which were deleted in the Δ 36-65 Nef mutant. These serines are also conserved in SIV-J5 where they are located at positions 51 and 52. Furthermore, serine phosphorylation of Nef has been demonstrated in a number of studies although the serine residues targeted have not been elucidated (Coates and Harris, 1995; Bodeus *et al*, 1995; Luo *et al*, 1997; Coates *et al*, 1997). For future studies it would therefore be interesting to determine whether mutation of these residues produced the same reduction in Lck binding as the Δ 36-65 Nef mutant and whether this correlates with a reduction in Nef serine phosphorylation. In addition data from Baur *et al* 1997 demonstrated that the N-terminal 22 amino acids of SF-2 Nef were sufficient to confer a low level of binding to Lck with any increase after 35 amino acids conferring the same level of binding as the N-terminal 94 amino acids. There are at least 2 serine residues in the N-terminal 22 amino acids of most Nef alleles making this another region worth investigating for SH2 binding in future studies. The requirement for this region of Nef would be consistent with the reduction in Lck binding observed for the Δ 7-22 Nef isolate in these current experiments. Further mutagenesis studies will be required to address the importance of these various N-terminal serine residues in conferring Lck SH2 binding.

Taken together the results presented here and from others (Collette *et al*, 1996; Greenway *et al*, 1995a; Greenway *et al*, 1996) suggests that the Nef mediated Lck binding occurs via interactions with the SH3 and SH2 domains. However it is clear from our results that either the affinity of the interaction is not sufficient to perturb the inactive conformation or that the regions in Lck necessary for the interaction are occluded in the inactive conformation of the enzyme. Interestingly, it has recently been reported that c-Src in its C-terminal phosphorylated down regulated

conformation is monomeric (Weijland *et al*, 1997). In contrast structural studies of the Lck SH3-SH2 isolated fragment co-crystallised with a phosphotyrosine peptide or unliganded suggested an ability of this fragment to dimerize. Considering the highly conserved nature of this family of proteins if these results are extrapolated it is possible that in the active conformation where the SH3 and SH2 domains are unrestricted the proteins are capable of dimerisation. This could potentially facilitate intermolecular activation of Lck enzymatic activity analogous to that reported for Src (Barker, 1994; Cooper and MacAuley, 1988) and Hck (Moarefi *et al*, 1997). This would be consistent with Lck activation by for example the aggregation of T-cell receptors. This also raises the possibility that dimerisation of Lck is necessary for Nef recognition or alternatively Nef may prevent Lck dimerisation. The latter proposal would be more consistent with the reduction in Lck activity on Nef binding reported in other studies (Collette *et al*, 1996; Greenway *et al*, 1996). A further potentially relevant factor is the possibility of Nef oligomerisation. While Nef oligomerisation has been demonstrated for HIV-2_{NIH3} Nef (Hodge *et al*, 1995) it has yet to be established whether this characteristic is conserved in HIV-1 and SIV and indeed whether it has any functional significance. Future studies will be required to address the oligomeric status of both Nef and Lck during the interaction and to further evaluate the mechanism of Lck enzymatic inhibition mediated by Nef.

It would be tempting to speculate that as Nef specifically binds the open active conformation of Lck and that Lck activation occurs as a result of CD4 antigen recognition the Lck-Nef interaction may occur immediately on viral entry. Significantly, the avidity of the interaction would be enhanced at this time due to CD4 aggregation. A Nef disruption of Lck signalling could have a drastic impact on cellular responses. Evidence from *in vivo* transgenic *lck* null mice models demonstrated that in the absence of a functional Lck, T-cell development was arrested with a substantial reduction in the double positive (CD4⁺,CD8⁺) thymocyte population (Molina *et al*, 1992). Intriguingly Nef transgenic mice have a similar T-cell profile with a severe depletion in their peripheral CD4⁺ T-cell population (Skowronski *et al*, 1993). Moreover the reduction in Lck enzyme activity in the presence of Nef (Collette *et al*, 1996; Greenway *et al*, 1996) would

effect the Lck phosphorylation of ITAM motifs in the TCR-CD3 receptor complex, thereby preventing ZAP70 recruitment causing an early block in T-cell receptor signalling (Zenner *et al*, 1995).

The requirement of the SH3 and SH2 domains of Lck for Nef binding also suggests that the endogenous cellular interactions of these domains at this stage would be perturbed. Pertinently this would encompass interactions with for example; the phosphatidylinositol 3-kinases (PI3K) (Amrein *et al*, 1993; Vogel and Fujita, 1993; Prasad *et al*, 1993). The identity of the exact PI3K that binds Lck is unknown at present, but all family members phosphorylate hydroxyl groups at position 3 on the inositol ring of the phosphoinositides: phosphatidylinositol (PtdIns), PtdIns (4)P and PtdIns (4,5)P₂. The PI3Ks have been linked to a number of cellular pathways (reviewed (Vanhaesebroeck *et al*, 1997; Sheperd *et al*, 1996)) including for example; the regulation of membrane vesicle trafficking of the prelysosomal system. It is possible that a Nef mediated deregulation of trafficking in this cellular compartment could result in the redirection of CD4 to the lysosomes (Rhee and Marsh, 1994; Aiken *et al*, 1994; Schwartz *et al*, 1995; Sanfridson *et al*, 1997). The PI3K lipid substrates and products are also involved in activating various PKC isozymes which have been implicated in both Nef phosphorylation and the N-terminal Nef complex formations (Coates and Harris, 1995; Bodeus *et al*, 1995; Baur *et al*, 1997). In addition the PI3K contain adaptor molecule binding motifs implicating a role for them in the Nef mediated recruitment of CD4 to clathrin coated pits (Vanhaesebroeck *et al*, 1997; Sheperd *et al*, 1996; Mangasarian *et al*, 1997). Interestingly, it has also been reported that HIV gp120 crosslinking of CD4 results in ~5 fold increase in PI3K activity (Prasad *et al*, 1993). Further studies will be required to determine whether Nef acts to elevate these levels or conversely functions to block the PI3K activity during gp120 mediated receptor crosslinking. Data from a number of SH3 and SH2 domain deletion studies has further highlighted the requirement for these domains in T-cell signalling. Their absence has been demonstrated to result in profound reductions in spontaneous IL-2 production when the deletions are combined with the C-terminal Y505F mutation (Luo and Sefton, 1992; Caron *et al*, 1992) and a reversal of the oncogenic transforming

capabilities of the Y505F mutant (Veillette *et al*, 1992). However the most compelling evidence for the intrinsic involvement of the SH3 and SH2 domains in intracellular signalling pathways came from a study which demonstrated increased T-cell activation levels, relative to wildtype, when the Lck SH3-SH2 domains were expressed in the absence of the catalytic domain (Xu and Littman, 1993).

Studies are currently in progress to corroborate that Lck conformational dependence is maintained in mammalian cells. In order to do this, the lack of CD45 expression in 3T3 fibroblast cells is being exploited. This should result in a constitutively phosphorylated Lck and as a consequence the C-terminal pTyr505 should form intramolecular interactions with its SH2 domain, leading to an inactive conformation of the protein. According to the hypothesis proposed herein this should be incompatible with Nef binding. Conversely, Lck expressed in Jurkat T-cells which express CD45 should be maintained in its open Tyr505 dephosphorylated active conformation, and be compatible with Nef binding. In addition cyanogen bromide cleavage studies would confirm the tyrosine residues phosphorylated in the respective cell lines. Given that a second N-terminal site in Nef was apparently necessary for the Lck binding, mutagenesis studies of the serine residues in this region would enable us to determine whether serine phosphorylation contributes to Lck SH2 domain interactions. Following on from this it would be interesting to evaluate the effect of Nef-Lck complex formation on downstream effectors such as PI3K.

In summary of the results presented in this section: It was successfully demonstrated that the Lck-Nef association was dependent on the Lck open and active conformation and that the interaction occurred independently of Nef myristoylation. The conformational dependency of the interaction was conserved for the laboratory isolate-Bru, the primary Nef isolates and the J5 SIV Nef. The (PXX)₃P motif was found to be necessary for efficient complex formation and N-terminal regions in Nef between residues 7-22 and 36-65 were also found to contribute to the association.

6.3. Interactions of Nef with Hck.

In these studies we demonstrated that the reported interactions of an *E.coli* expressed Nef with the Hck SH3 domain *in vitro* was conserved *in vivo* in the YTHS with a myristoylated Nef and in the context of both full length native proteins expressed in the baculovirus expression system. In addition studies with the BH10 Nef (PXX)₃P motif mutant (PAAP) both *in vivo* and *in vitro* raised questions as to the absolute requirement of this motif for Nef binding to Hck. The possibility of an additional binding site was corroborated by peptide substrate kinase assays which demonstrated that the PAAP Nef mutant had lost its ability to activate Hck.

Firstly, the YTHS was employed to address whether myristoylated Nef was capable of interacting with the Hck SH3 domain. For these studies the SH2 domain and SH3-SH2 domain fusions were also evaluated for Nef binding. These results demonstrated that the co-expression of Nef plus the Hck SH3 domain was toxic to the yeast. This was not Hck specific as similar results were obtained for Lck, Src and Fyn SH3 domains. No binding of Nef to the Hck SH2 domain was detected, however Nef was found to specifically interact with the Hck SH3-SH2 domain fusion. The lack of SH2 binding suggested that the observed Nef-Hck SH3-SH2 binding was mediated by the Hck SH3 domain. These results were consistent with the previous *in vitro* substrate affinity studies and confirmed that native, myristoylated Nef retained its Hck SH3 binding ability in the context of an SH3-SH2 fusion *in vivo*. During the studies Src SH3, SH2 and SH3-SH2 domains were also assessed for Nef binding. It was found the results obtained for each Src domain mimicked those seen for the Hck isolated domains i.e. co-expression of Src SH3 with Nef was toxic to the yeast, the Src SH2 domain gave no detectable interaction with Nef and the Src SH3-SH2 domain fusion exhibited a high affinity for Nef in this system. The relative specificity of these interactions was corroborated by the lack of Nef binding to the isolated Fyn domains. Co-expression of Nef with each of the Lck isolated domains resulted in toxicity therefore potential interactions between Nef and Lck could not be evaluated.

From structural studies on the specificity and selectivity of the Nef interaction with the Hck SH3 domain it was proposed that a single amino acid in the Hck SH3 domain could confer high affinity Nef binding to SH3 domains (Lee *et al*, 1995). This amino acid was located on a variable loop termed the RT loop which projects from the main β -barrel structure of the SH3 domain (Lee *et al*, 1996). Point mutation of the corresponding residue in the Fyn SH3 domain, R96I resulted in a comparable level of Nef binding to that detected for Hck SH3. It was hence proposed that hydrophobic interactions mediated by this isoleucine residue were critical to Nef (PXX)₃P binding. In sequence alignments of a panel of SH3 domains it was noted that Lyn SH3 also contained a similar Ile residue consistent with its binding to Nef during the filter binding studies. This Ile residue was absent in all of the remaining Src family members, therefore no further family members were investigated for Nef binding in subsequent studies. The results obtained in our current study for Src suggest that the presence of an isoleucine residue at position 96 in the RT loop is not a prerequisite for Nef binding and that the criteria governing Nef-SH3 interactions are likely to be more complex.

This conclusion has been recently corroborated in studies by Arold *et al* 1997, who resolved the crystal structures for the liganded and unliganded Nef core domain. These structures revealed that the unbound polyproline type II (PP-II) helix in Nef was partially disordered inferring an intrinsic flexibility. They proposed that SH3 domain interactions restrain the flexibility and stabilize the PP-II helix conformation. The Nef ligand used in the experiments by Arold *et al* was wildtype Fyn SH3. Analysis of the complex formation revealed a differential binding of Arg 77 in the PP-II helix of Nef to Asp100 in the RT loop of Fyn SH3 to that previously reported (Lee *et al*, 1996) which resulted in altered hydrogen bond formation. This allowed the wild type R96 residue to be sequestered into the hydrophobic pocket of Nef and the overall reconfiguration of the RT loop to complement Nef binding. PP-II helices can bind SH3 domains in either “plus” or “minus” orientations, but in the Nef-SH3 complexes binding is restricted to the minus configuration (Lee *et al*, 1996). The orientation of the binding is determined by the residues between the prolines including Arg71, Val74 and Arg77 in Nef. However due to its differential binding

capacity it has been proposed that Arg77 is critical for both the orientation of the interaction and the ligand induced flexibility of the RT loop. As both Asp100 of Fyn and Arg77 of Nef are highly conserved residues it is possible that their association could form the basis of a conserved mechanism of interaction between Nef and all members of the Src kinase family. The observed binding of Nef to Src demonstrated in these current studies is therefore consistent with the proposed more flexible PP-II helix. However the lack of Nef binding seen for Fyn in our study suggests that while a basic affinity between the proteins may exist additional factors may be required to facilitate initial binding prior to the induced RT loop conformational change.

To ascertain whether the Nef interaction with the Hck SH3-SH2 domain fusion was conserved for native Hck recombinant baculoviruses were generated. The authenticity of the recombinant baculovirus expressed proteins was demonstrated. Parameters examined included full length protein expression, authentic acylation and enzyme activity as assayed by both auto- and *trans* phosphorylation. The authenticity of the Nef proteins had been previously demonstrated (Harris and Neil, 1994). These results confirmed the expression of the native full length proteins in the baculovirus expression system. The proteins were subsequently analysed by *in vitro* binding assays for Nef binding ability. The results from these studies demonstrated that Nef retained its ability to bind mHck in the context of the full length proteins. Notably, the efficiency of binding was reduced for the nonmyristoylated Nef *in vitro*. Consistent with results from the YTHS, binding of Nef to Src was also observed, but none was detected for Fyn. A reduction in nonmyristoylated Nef binding to Src was also detected.

Following on from these *in vitro* studies, *in vivo* binding assays were performed on recombinant baculovirus coinfecting Sf9 lysates. The data from these studies revealed the interaction observed between Nef and Hck was specific and stable in an *in vivo* environment. This was consistent with a recent report by Briggs *et al* 1997 who demonstrated the co-immunoprecipitation of Nef and Hck from recombinant retrovirally coinfecting Rat-2 cells. In contrast, Src exhibited non-specific binding to the GA-beads, precluding the analysis of Nef binding during these *in vivo* binding

studies. In future studies alternative affinity reagents such as Nef-6His will be required to confirm the interaction. During the *in vivo* binding assays the Nef-mHck interaction was found to be Nef myristoylation independent with equivalent levels of mHck binding detected for each Nef affinity reagent. This was contrary to the *in vitro* binding results, where nonmyristoylated Nef was found to have a reduced affinity for mHck. Furthermore results from *in vivo* binding studies with $\Delta 78$ hHck concurred with myristoylation enhanced binding, but no difference was seen for G2AhHck. The reduced binding observed for nonmyristoylated Nef and $\Delta 78$ hHck implicated both Nef myristoylation and the unique region of Hck contribute to complex formation although removal of only one was not sufficient to perturb the interactions. The inference being that a number of weak interactions may be necessary to stabilise the Nef-Hck interaction in the context of the native proteins. The discrepancy between the *in vitro* and *in vivo* data suggested that the binding was less efficient *in vitro* and required both an intact myristoylation signal and the Hck unique domain. Overall the data from these studies demonstrated both Nef myristoylation and the Hck unique domain contribute in enhancing the association of the two proteins, probably serving to promote the Nef-Hck interaction *in vivo*. However the loss of either individually is not sufficient to perturb the interaction.

The results from the protease cleavage experiments provided evidence to suggest that both the virion associated N-terminally cleaved species of Nef and the full length myristoylated Nef have equal affinity for native mHck. The results also demonstrated the accessibility of the protease cleavage site in the presence of Hck binding, suggesting this region of Nef is not involved in Hck binding. The implication from these results is that at all times in the viral life cycle Nef retains its ability to interact with Hck. This is indicative of a continued requirement for the interaction throughout the viral life cycle and raises the possibility of Hck inclusion in the virion. From the results of the myristoylation experiments it is likely that the full length myristoylated Nef would have a higher affinity for Hck in solution than the protease cleaved Nef species, therefore intuitively one would predict that an interaction between the cleaved Nef and Hck is most likely to occur in the virion. This could occur either as a result of random Hck incorporation in the virion, or

more likely as a result of specific Hck recruitment to the virion by viral proteins such as Nef. Tyrosine phosphorylation of the Gag MA protein has been demonstrated to be critical for the nuclear import of the preintegration complex (PIC) (Gallay *et al*, 1995) and is a prerequisite of HIV-1 infection of terminally differentiated macrophages (Vonschwedler *et al*, 1994). The ability to infect quiescent cells is unique to the lentiviruses playing a critical role in HIV pathogenesis and is in marked contrast to the oncoretroviruses which require nuclear envelope breakdown at mitosis. It would therefore be tempting to speculate that Nef binds Hck and recruits it to the virion where it is able to phosphorylate Gag MA thereby facilitating HIV infection of non-dividing cells. Protease cleavage of Nef would be required to remove the N-terminal membrane targeting domain of Nef allowing its incorporation into the PIC along with bound proteins such as Hck. This would be consistent with the loss of Nef enhanced viral infectivity in continuous cell lines and its enhancement of viral infectivity in quiescent T cells and PBMCs (Kim *et al*, 1989; de Ronde *et al*, 1992; Miller *et al*, 1994; Spina *et al*, 1994).

An unexpected result obtained during these studies was the ability of the PAAP mutant of Nef to bind Hck with wildtype affinity. In this mutant the 2 central prolines of the conserved (PXX)₃P motif were substituted for alanines, as these mutations had been previously demonstrated to abrogate the Nef-Hck SH3 interaction *in vitro* (Saksela *et al*, 1995; Moarefi *et al*, 1997) (reviewed (Saksela, 1997)). The PAAP Nef binding in our studies was conserved for mHck, G2AhHck and Δ78hHck. The ability of the PAAP mutant to bind Hck suggested that the BH10 Nef isolate could interact with Hck at an alternative site, or that the mutation of the 2 central proline residues had not disrupted the structure of the PP-II helix. The original filter binding assays by Saksela *et al* 1995, demonstrated a loss of Nef binding after the mutation of a C-terminal proline motif at residues 147 and 150. The panel of Nef mutants screened in these current studies did not include a deletion in this region of Nef, possibly providing an explanation for the uniform binding of Hck detected for each of the mutants. Significantly Saksela *et al* utilised a nonmyristoylated PAAP mutant Nef together with an N-terminally truncated Hck lacking the unique domain. From the results of our G2A-G and Δ78hHck binding

studies it is possible that the addition of the proline mutant may have been sufficient to completely perturb the interaction. From the data presented here it can be concluded that the (PXX)₃P motif is not necessary for binding to Hck. This observation implies the existence of additional binding sites.

Clues as to the Nef requirement for Hck binding came from the inability of Bru Nef to interact with Hck. Amino acid sequence alignments revealed only 7 differences between BH10 and Bru, see diagram 5.3. Interestingly 2 of the changes were E151D and L153V proximal to the putative C-terminal proline motif. A dramatic effect for such conserved amino acid substitutions is not unprecedented for SH3 domain interactions, Lee *et al* 1995 demonstrated a single R96I change in the Fyn SH3 RT loop was sufficient to alter a weak interaction with Nef to a binding affinity equal to that obtained for Hck SH3 domains. Other contributing factors to the loss of Nef Bru binding may have been the additional A15T and N52T changes in Bru which introduce further putative phosphorylation sites into the N-terminal region. This could conceivably result in N-terminal structural changes and the loss of the N-terminal PP-II helix recognition. Mass spectrometry studies are currently in progress to determine whether Bru is phosphorylated on these threonine residues. Further mutational analysis will also be required to resolve this apparent loss of binding affinity. Since the completion of these studies it has been demonstrated that the interaction between SF2 Nef and Hck during *in vivo* Rat-2 coinfection experiments was, in contrast to our results, dependent on the (PXX)₃P motif in Nef (Briggs *et al*, 1997). However these studies used RIPA buffer which contains an ionic detergent in contrast to the non-ionic TritonX-100 based detergent used in our studies, it is therefore possible that the increased stringent conditions perturbed interactions with the (PXX)₃P motif mutant. Also notably, they used a different Nef allele to the BH10 Nef allele used here emphasising the variability of Nef isolate interactions with Hck. For future studies it would be interesting to compare T-cell tropic and macrophage tropic Nef derivatives for Hck binding and to determine whether Nef-Hck binding correlates with macrophage tropic HIV strains.

From the results of the study by Moarefi *et al* 1997 it was proposed that SH3 domain ligands cause the rapid activation of Hck. They demonstrated that the presence of Nef dramatically increased the rate of phospho-transfer to a peptide substrate by Hck and that a Nef (PXX)₃P mutant was incapable of similarly activating Hck. Pertinently the conditions employed in this study were comparable to those used by Saksela *et al* 1995 who demonstrated a loss of Hck binding for this Nef mutation. However, the results obtained during the *in vivo* binding assays performed in our current studies suggested that Hck retained the ability to bind the PAAP Nef mutant in the context of the native proteins and that another binding site with equal affinity for Hck existed in the BH10 allele. To attempt to resolve this potential conflict, peptide substrate assays were performed to establish whether the PAAP Nef mutant used here retained the ability to enhance Hck activity. Consistent with the results of Moarefi *et al* the level of Hck activation was enhanced in the presence of Nef. However, the results for the PAAP Nef assays revealed it had no effect on Hck activity. This inferred that PAAP Nef binding to Hck did not involve SH3 recruitment with concomitant enzyme activation. Furthermore the ability of BH10 Nef to activate Hck in contrast to the PAAP mutant confirmed the previous proposal of a critical role for the PXXP motif in activating Hck. Taken together these results suggest that two Hck binding sites exist within Nef only one of which is capable of activating Hck enzymatic activity. Alternatively, it is possibly that PAAP still binds the SH3 domain but with insufficient binding affinity to displace it. From the results of the crystallography studies it was apparent that a number of interactions stabilise the interface between Nef and Fyn SH3. One possibility is that the RT loop of Hck bound to PAAP in our study had not undergone the conformational change necessary for the high affinity interaction, if this is the case washes with an ionic detergent such as RIPA buffer should dissociate the PAAP-Hck complex.

Notably despite alternative Hck binding sites, the dominant effect of the wild type BH10 Nef allele was activation of Hck kinase activity. However the significance of this *in vivo* has been questioned in recent macaque studies by Lang *et al* 1997. These studies demonstrated a lack of reversion of an AxxA Nef allele in macaques

infected with SIV_{mac239} containing this mutation. Furthermore, contrary to expectations the disease pathogenesis was accelerated in these monkeys. These results suggested that PxxP binding alone was not sufficient to perturb the Nef *in vivo* phenotype and that this mutation had enhanced other protein interactions causing accelerated pathogenesis. This is consistent with the results presented herein and infers that the (PXX)₃P mediated Hck activation may not be relevant *in vivo* and other possible (PXX)₃P independent effects on Hck SH3/SH2 signalling events should be investigated. It should be noted that SIV Nef isolates contain only a single PxxP motif at the putative SH3 recognition site, compared to the (PXX)₃P motif in HIV-1 alleles. However if this was critical to viral infectivity it would be anticipated an even greater selection pressure to revert to wild type would be imposed.

Additional studies will be required to further analyse residues important in mediating the Hck interactions with Nef. In future studies it would be interesting to establish which Nef isolates rely on their (PXX)₃P motifs for Hck binding and the functional relevance of the alternative Hck binding site. If sufficient isolates are screened it should be possible to delineate key amino acid residues necessary for this dual binding. Alternatively a recently developed derivative of the YTHS the “reverse” YTHS would allow the rapid screening of randomly generated protein mutants. This system works by detecting the dissociation of known protein binding partners and would allow the rapid screening of the interactions in a eukaryotic system *in vivo* (White, 1996).

In summary the data presented in these studies confirmed that the interaction between native Nef and Hck was conserved *in vivo*. The stability of the association during protease cleavage was also demonstrated raising the possibility of Hck recruitment to the virion by Nef. In addition the PAAP *in vivo* binding assays and peptide substrate data implicated two mechanisms of Nef-Hck binding. The first of which is likely to be PxxP SH3 domain mediated and result in Hck activation. However the second occurs independently from the PxxP motif and given the *in vivo* macaque data may represent a more physiologically relevant Hck binding site.

6.4. Final Discussion:

The remit for these studies was to identify novel interactions between Nef and cellular proteins and to further characterise the Nef associations with the Src tyrosine kinase family. The results from the former study revealed a strong novel interaction between Nef and an uncharacterised polypeptide (clone 39), which had high homology to both human and mouse cDNAs. The strength and specificity of the interaction in the *in vivo* eukaryotic background of *S.cerevisiae* implied the interaction may have a physiological relevance. Intriguingly the polypeptide also exhibited a high affinity binding to p55Gag. As both Nef and p55Gag are myristoylated, membrane associated, virion incorporated proteins it is plausible that they might share common binding partners. Indeed the possibility of Nef complexing with p55Gag or one of its cleavage products would be worth investigating for future studies. Due to the GC rich regions in the cDNA of clone 39 it was difficult to unequivocally determine the polypeptide sequence. However, a short stretch of amino acids were found to have homology to 3',5' cyclic-nucleotide phosphodiesterase. Observations of elevated cAMP levels in infected cells suggest that a Nef interaction with phosphodiesterases might be physiologically relevant, making this an interesting potential Nef binding partner worth evaluating in future binding studies.

While the YTHS is a powerful analytical tool by comparison to traditional methods such as co-immunoprecipitation, crosslinking and copurification through gradients or chromatographic columns none of which result in cDNA isolation, it is limited by the fact that the protein-protein interactions occur in the nucleus. This has recently been overcome by an adaptation of the system. The alternative Sos recruitment system (SRS) relies on the ability of hSos and a Ras guanyl nucleotide exchange factor to activate Ras only when localized to the plasma membrane (Aronheim, 1997). In the system Ras activity is required for *cdc25-2* gene expression and yeast growth at 36°C. Similar to the YTHS, baits and potential interactors are fused to either Sos or Ras guanyl nucleotide exchange factors and interactions between the

two confers growth at 36°C. The system has the advantage that it allows screening of protein-protein interactions to occur in the cytosol. In addition the membrane localisation of the interactions should facilitate the analysis of interactions between myristoylated proteins in their native membrane anchored conformations. This system may therefore represent a better background in which to investigate potential interactors with myristoylated Nef for future studies. One possible drawback of the system for use with the Src tyrosine kinases would be the possible toxicity effects of the localisation of the SH3 and SH2 domains at the membrane, see section 4.7.

The results obtained in the latter part of these studies demonstrated Nef binding to Lck, Hck and Src, but none for Fyn. Data from the YTHS suggested that the Nef interaction was mediated by the SH3 domains of Hck and Src. Although Lck cytotoxicity in the YTHS prohibited its inclusion in these studies, results from the *in vivo* binding assays with the native proteins confirmed the requirement for the Nef (PXX)₃P motif suggesting that the Lck interaction was also SH3 dependent. These results were contrary to the proposed requirement for an Ile residue in the RT loop of the SH3 domains for Nef binding (Lee *et al*, 1995). Instead they infer a conserved ability for the association of Nef and the Src tyrosine kinase domains, consistent with the hypothesis of Arold *et al* 1997.

The results from the Hck *in vivo* binding studies, however suggested mutations in the (PXX)₃P motif were not sufficient to perturb Nef complex formation. This result went against an SH3 mediated domain binding to Nef suggesting the existence of additional interactions. Significantly, when the panel of Nef deletion mutants were screened for Hck binding all were found to have equivalent affinities for Hck. Notably these deletions did not remove a C-terminal single PxxP motif, which in the absence of the (PXX)₃P motif could potentially mediate the SH3 domain interaction. Further studies with the Nef Bru isolate should determine the extent of the interaction with this C-terminal PxxP motif. The Hck results were in direct contrast to those obtained in the Lck binding assays. Notably Lck binding efficiency was impaired for the Δ7-22, Δ36-65 and the PAAP Nef mutants.

Moreover no loss of binding was detected for the Nef Bru isolate to Lck. This suggests that the mechanism of Nef binding to each of the Src tyrosine kinases is very different and that while the SH3 domains of each might be influential in mediating the binding other additional interactions are important in the context of the full length native proteins.

As the criteria governing the Nef interactions with the Src tyrosine kinase members are established the effect of Nef binding will need to be addressed. To date, it has already been demonstrated that Lck activity is inhibited (Greenway *et al*, 1996; Collette *et al*, 1996), while Hck is activated (Moarefi *et al*, 1997). Moreover the relevance of the effect on kinase activity *in vivo* has been called into question by the macaque data (Lang *et al*, 1997). A recently developed cDNA microarray or DNA-chip technology method capable of differentially screening the expression of thousands of mRNA transcripts will make broad scale assessment of these *in vivo* effects possible (reviewed (Ramsay, 1998)). This system not only allows the detailed analysis of mRNA expression but also detects changes in mRNA expression in response to external stimuli. The system utilises a cDNA array (microarray) as a template for hybridization to cDNA probes prepared from RNA samples of cells or tissues. Two sets of cDNA probes are utilised labelled with different fluorescent dyes such that hybridization of either probe individually or simultaneously is distinguishable. This therefore provides both a comparative and quantitative analysis of the tissues under investigation. It would hence be possible to evaluate the effect of mutations on perturbing interactions or more importantly the downstream detrimental effects of such interactions. Similarly, the efficacy of potential therapeutic agents in returning the mRNA profile to normal could also be monitored. This would provide a valuable analytical tool in elucidating the pleiotropic phenotype of Nef during HIV infection and aid in establishing the effect of the Nef interactions with the Src tyrosine kinase interactions on cell signal transduction pathways.

The data presented in this thesis illustrates the enigmatic nature of Nef and emphasises the importance of analysing protein-protein interactions in the context of the native proteins. It further demonstrated combinatorial associations between Nef and cellular proteins can have a profound effect on their binding affinities and that the affinity may vary depending on the strain of HIV.

BIBLIOGRAPHY

- Abraham, N. and Veillette, A. (1990). Activation of p56^{lck} through mutation of a regulatory carboxy-terminal tyrosine residue requires intact sites of autophosphorylation and myristylation. *Molecular and Cellular Biology* 10, 5197-5206.
- Abraham, N., Miceli, M.C., Parnes, J.R., and Veillette, A. (1991). Enhancement of T-cell responsiveness by the lymphocyte-specific tyrosine protein-kinase p56^{lck}. *Nature* 350, 62-66.
- Aderem, A. (1992). The MARCKS brothers: A family of protein kinase C substrates. *Cell* 71, 713-716.
- Adler, H.T., Reynolds, P.J., Kelley, C.M., and Sefton, B.M. (1988). Transcriptional activation of *lck* by retrovirus promoter insertion between two lymphoid-specific promoters. *J. Virol.* 62, 4113-4122.
- Ahmad, N. and Venkatesan, S. (1988). Nef protein of HIV-1 is a transcriptional repressor of HIV-1 LTR [published erratum appears in *Science* 1988 Oct 7;242(4875):242]. *Science* 241, 1481-1485.
- Aiken, C. and Trono, D. (1995). Nef stimulates human-immunodeficiency-virus type-1 proviral DNA-synthesis. *J. Virol.* 69, 5048-5056.
- Aiken, C., Konner, J., Landau, N.R., Lenburg, M.E., and Trono, D. (1994). Nef induces CD4 endocytosis: Requirement for a critical dileucine motif in the membrane-proximal CD4 cytoplasmic domain. *Cell* 76, 853-864.
- Aldrovandi, G.M. and Zack, J.A. (1996). Replication and pathogenicity of human-immunodeficiency-virus type-1 accessory gene mutants in SCID-hu mice. *J. Virol.* 70, 1505-1511.
- Alexandropoulos, K., Cheng, G., and Baltimore, D. (1995). Proline-rich sequences that bind to Src homology 3 domains with individual specificities. *Proceedings of the National Academy of Sciences of the United States of America* 92, 3110-3114.
- Alkhatib, G., Ahuja, S.S., Light, D., Mummidi, S., Berger, E.A., and Ahuja, S.K. (1997). Cc chemokine receptor 5-mediated signaling and HIV-1 co-receptor activity share common structural determinants - critical residues in the third extracellular loop support HIV-1 fusion. *J. Biol. Chem.* 272, 19771-19776.
- Alkhatib, G., Combadiere, C., Broder, C.C., Feng, Y., Kennedy, P.E., Murphy, P.M., and Berger, E.A. (1996). CC CKRS - a RANTES, MIP-1-alpha, MIP-1-beta receptor as a fusion cofactor for macrophage-tropic HIV-1. *Science* 272, 1955-1958.
- Allan, J.S., Coligan, J.E., Lee, T., McLane, M.F., Kanki, P.J., Groopman, J.E., and Essex, M. (1985). A new HTLV-III/LAV encoded antigen detected by antibodies from AIDS patients. *Science* 230, 810-813.

- Ames, J.B., Ishima, R., Tanaka, T., Gordon, J.I., Stryer, L., and Ikura, M. (1997). Molecular mechanics of calcium-myristoyl switches. *Nature* 389, 198-202.
- Ames, J.B., Tanaka, T., Stryer, L., and Ikura, M. (1996). Portrait of a myristoyl switch protein. *Current Opinion In Structural Biology* 6, 432-438.
- Amrein, K.E., Panholzer, B., Flint, N.A., Bannwarth, W., and Burn, P. (1993). The Src homology 2 domain of the protein-tyrosine kinase p56^{lck} mediates both intermolecular and intramolecular interactions. *Proc. Natl. Acad. Sci. U. S. A.* 90, 10285-10289.
- Anderson, S., Shugars, D.C., Swanstrom, R., and Garcia, J.V. (1993). Nef from primary isolates of human immunodeficiency virus type 1 suppresses surface CD4 expression in human and mouse T cells. *J. Virol.* 67, 4923-4931.
- Anderson, S.J., Lenburg, M., Landau, N.R., and Garcia, J.V. (1994). The cytoplasmic domain of CD4 is sufficient for its down-regulation from the cell surface by human immunodeficiency virus type 1 Nef. *J. Virol.* 68, 3092-3101.
- Anderson, S.J., Levin, S.D., and Perlmutter, R.M. (1994). Involvement of the protein-tyrosine kinase p56(lck) in T-cell signaling and thymocyte development. *Advances in Immunology* 56, 151-178.
- Arold, S., Franken, P., Strub, M.P., Hoh, F., Benichou, S., Benarous, R., and Dumas, C. (1997). The crystal structure of HIV-1 Nef protein bound to the Fyn kinase SH3 domain suggests a role for this complex in altered T cell receptor signaling. *Structure* 5, 1361-1372.
- Aronheim, A. (1997). Improved efficiency Sos recruitment system: expression of the mammalian GAP reduces isolation of Ras GTPase false positives. *Nucleic Acids Research* 25, 3373-3374.
- Ashorn, P., Berger, E.A., and Moss, B. (1993). Vaccinia virus vectors for study of membrane-fusion mediated by human-immunodeficiency-virus envelope glycoprotein and CD4. *Methods In Enzymology* 221, 12-18.
- Ashorn, P.A., Berger, E.A., and Moss, B. (1990). Human-immunodeficiency-virus envelope glycoprotein CD4-mediated fusion of nonprimate cells with human-cells. *J. Virol.* 64, 2149-2156.
- Ausubel, F.M., Brent, R., Kingston, R.E., Moore, D.D., Seidman, J.G., Smith, J.A., and Struhl, K. (1993). *Current protocols in molecular biology*. Anonymous Wiley Interscience),
- Backer, J.M., Mendola, C.E., Fairhurst, J.L., and Kovesdi, I. (1991). The HIV-1 Nef protein does not have guanine nucleotide binding, GTPase, or autophosphorylating activities. *AIDS Res. Hum. Retroviruses* 7, 1015-1020.

- Bandres, J. and Ratner, L. (1994). Human immunodeficiency virus type1 Nef protein down-regulates transcription factors NF- κ B and AP-1 in human T cells *in vitro* after T-cell receptor stimulation. *J. Virol.* *68*, 3243-3249.
- Bandres, J.C., Shaw, A.S., and Ratner, L. (1995). HIV-1 Nef protein downregulation of CD4 surface expression: relevance of the ick binding domain of CD4. *Virology* *207*, 338-341.
- Bandres, J.O., Luria, S., and Ratner, L. (1994). Regulation of human immunodeficiency virus Nef protein by phosphorylation. *Virology* *201*, 157-161.
- Barker, S.C.e. (1994). Characterization of pp60^{c-Src} tyrosine kinase activities using a continuous assay: autoactivation of the enzyme is an intermolecular autophosphorylation process. *Biochemistry* *34*, 14843-14851.
- Baur, A.S., Sass, G., Laffert, B., Willbold, D., ChengMayer, C., and Peterlin, B.M. (1997). The N-terminus of Nef from HIV-1/SIV associates with a protein complex containing Lck and a serine kinase. *Immunity* *6*, 283-291.
- Baur, A.S., Sawai, E.T., Dazin, P., Fantl, W.J., Cheng-Mayer, C., and Peterlin, B.M. (1994). HIV-1 Nef leads to inhibition or activation of T cells depending on its intracellular localization. *Immunity* *1*, 373-384.
- Bebenek, K., Abbotts, J., Roberts, J.D., Wilson, S.H., and Kunkel, T.A. (1989). Specificity and mechanism of error-prone replication by human immunodeficiency virus-1 reverse-transcriptase. *J. Biol. Chem.* *264*, 16948-16956.
- Beer, B., Baier, M., Megede, J.Z., Norley, S., and Kurth, R. (1997). Vaccine effect using a live attenuated *nef*-deficient simian immunodeficiency virus of african green monkeys in the absence of detectable vaccine virus replication *in vivo*. *Proceedings of the National Academy of Sciences of the United States of America* *94*, 4062-4067.
- Benichou, S., Bomsel, M., Bodeus, M., Durand, H., Doute, M., Letourneur, F., Camonis, J., and Benarous, R. (1994). Physical interaction of the HIV-1 Nef protein with beta-COP, a component of non-clathrin-coated vesicles essential for membrane traffic. *J. Biol. Chem.* *269*, 30073-30076.
- Berger, E.A. (1997). HIV entry and tropism: the chemokine receptor connection. *AIDS* *11*, S3-S16.
- Berkowitz, R.D. and Goff, S.P. (1994). Analysis of binding-elements in the human-immunodeficiency-virus type-1 genomic RNA and nucleocapsid protein. *Virology* *202*, 233-246.
- Berkowitz, R.D., Ohagen, A., Hoglund, S., and Goff, S.P. (1995). Retroviral nucleocapsid domains mediate the specific recognition of genomic viral RNAs by chimeric gag polyproteins during RNA packaging in-vivo. *J. Virol.* *69*, 6445-6456.

- Berthoux, L., Pechoux, C., Ottmann, M., Morel, G., and Darlix, J.L. (1997). Mutations in the N-terminal domain of human immunodeficiency virus type 1 nucleocapsid protein affect virion core structure and proviral DNA synthesis. *J. Virol.* *71*, 6973-6981.
- Bhatnagar, R.S. and Gordon, J.I. (1998). Understanding covalent modifications of proteins by lipids: where cell biology and biophysics mingle. *Trends In Cell Biology* *8*,
- Bieniasz, P.D., Fridell, R.A., Aramori, I., Ferguson, S.S.G., Caron, M.G., and Cullen, B.R. (1997). HIV-1-induced cell fusion is mediated by multiple regions within both the viral envelope and the CCR-5 co-receptor. *EMBO Journal* *16*, 2599-2609.
- Biffen, M., McMichaelphillips, D., Larson, T., Venkitaraman, A., and Alexander, D. (1994). The CD45 tyrosine phosphatase regulates specific pools of antigen receptor-associated p59(fyn) and CD4-associated p56(lck) tyrosine kinases in human T-cells. *EMBO Journal* *13*, 1920-1929.
- Bleul, C.C., Farzan, M., Choe, H., Parolin, C., Clarklewis, I., Sodroski, J., and Springer, T.A. (1996). The lymphocyte chemoattractant SDF-1 is a ligand for lestr/fusin and blocks HIV-1 entry. *Nature* *382*, 829-833.
- Bleul, C.C., Wu, L.J., Hoxie, J.A., Springer, T.A., and Mackay, C.R. (1997). The HIV coreceptors CXCR4 and CCR5 are differentially expressed and regulated on human T lymphocytes. *Proceedings of the National Academy of Sciences of the United States of America* *94*, 1925-1930.
- Bodeus, M., Mariecardine, A., Bougeret, C., Ramosmorales, F., and Benarous, R. (1995). In-vitro binding and phosphorylation of human-immunodeficiency-virus type-1 Nef protein by serine threonine protein-kinase. *Journal of General Virology* *76*, 1337-1344.
- Boerner, R.J.e. (1996). Correlation of the phosphorylation states of pp60 c-Src with tyrosine kinase activity: the intramolecular pY530-SH2 complex retains significant activity if Y419 is phosphorylated. *Biochemistry* *35*, 9519-9525.
- Bradford, M.M. (1976). A rapid and sensitive method for the quantitation of microgram quantities of protein utilizing the principle of protein-dye binding. *Analytical Biochemistry* *72*, 248-254.
- Brady, H.J.M., Pennington, D.J., Miles, C.G., and Dzierzak, E.A. (1993). CD4 cell surface downregulation in HIV-1 Nef transgenic mice is a consequence of intracellular sequestration. *EMBO Journal* *12*, 4923-4932.
- Briggs, S.D., Sharkey, M., Stevenson, M., and Smithgall, T.E. (1997). SH3-mediated Hck tyrosine kinase activation and fibroblast transformation by the Nef protein. *J. Biol. Chem.* *272*, 17899-17902.
- Broder, C.C. and Collman, R.G. (1997). Chemokine receptors and HIV. *Journal Of Leukocyte Biology* *62*, 20-29.

- Bron, R., Klasse, P.J., Wilkinson, D., Clapham, P.R., Pelchenmatthews, A., Power, C., Wells, T.N.C., Kim, J., Peiper, S.C., Hoxie, J.A., and Marsh, M. (1997). Promiscuous use of CC and CXC chemokine receptors in cell-to-cell fusion mediated by a human immunodeficiency virus type 2 envelope protein. *J. Virol.* *71*, 8405-8415.
- Brown, M.T. and Cooper, J.A. (1996). Regulation, substrates and functions of Src. *Biochimica et Biophysica Acta* *1287*, 121-149.
- Bukovsky, A.A., Dorfman, T., Weimann, A., and Gottlinger, H.G. (1997). Nef association with human immunodeficiency virus type 1 virions and cleavage by the viral protease. *J. Virol.* *71*, 1013-1018.
- Bukrinskaya, A.G., Ghorpade, A., Heinzinger, N.K., Smithgall, T.E., Lewis, R.E., and Stevenson, M. (1996). Phosphorylation-dependent human-immunodeficiency-virus type-1 infection and nuclear targeting of viral-DNA. *Proceedings of the National Academy of Sciences of the United States of America* *93*, 367-371.
- Buonocore, L., Turi, T.G., Crise, B., and Rose, J.K. (1994). Stimulation of heterologous protein degradation by the Vpu protein of HIV-1 requires the transmembrane and cytoplasmic domains of CD4. *Virology* *204*, 482-486.
- Camaur, D. and Trono, D. (1996). Characterization of human-immunodeficiency-virus type-1 vif particle incorporation. *J. Virol.* *70*, 6106-6111.
- Camaur, D., Gallay, P., Swingler, S., and Trono, D. (1997). Human immunodeficiency virus matrix tyrosine phosphorylation: characterization of the kinase and its substrate requirements. *J. Virol.* *71*, 6834-6841.
- Campbell, K., S., Buder, A., and Deuschle, U. (1995). Interactions between the amino-terminal domain of p56^{Lck} and cytoplasmic domains of CD4 and CD8alpha in yeast. *Eur. J. Immunol.* *25*, 2408-2412.
- Cantin, R., Fortin, J.F., Lamontagne, G., and Tremblay, M. (1997). The acquisition of host-derived major histocompatibility complex class II glycoproteins by human immunodeficiency virus type 1 accelerates the process of virus entry and infection in human T-lymphoid cells. *Blood* *90*, 1091-1100.
- Caron, L., Abraham, N., Pawson, T., and Veillette, A. (1992). Structural requirements for enhancement of T-cell responsiveness by the lymphocyte-specific tyrosine protein kinase p56^{lck}. *Molecular and Cellular Biology* *12*, 2720-2729.
- Carrera, A.C., Alexandrov, K., and Roberts, T.M. (1993). The conserved lysine of the catalytic domain of protein kinases is actively involved in the phosphotransfer reaction and not required for anchoring ATP. *Proc. Natl. Acad. Sci. U. S. A.* *90*, 442-446.
- Casnellie, J.H. (1991). Assay of protein kinases using peptides with basic residues for phosphocellulose binding. *Meth. Enzymol.* *200*, 115-120.

- Catling, A.D., Wyke, J.A., and Frame, M.C. (1993). Mitogenesis of quiescent chick fibroblasts by vv-Src: dependence on events at the membrane leading to early changes in AP-1. *Oncogene* 8, 1875-1886.
- Chang, D.K., Cheng, S.F., and Chien, W.J. (1997). The amino-terminal fusion domain peptide of human immunodeficiency virus type 1 gp41 inserts into the sodium dodecyl sulfate micelle primarily as helix with a conserved glycine at the micelle-water interface. *J. Virol.* 71, 6593-6602.
- Chen, C.H., Matthews, T.J., Mcdanal, C.B., Bolognesi, D.P., and Greenberg, M.L. (1995). A molecular clasp in the human-immunodeficiency-virus (HIV) type-1 TM protein determines the anti-HIV activity of gp41 derivatives - implication for viral fusion. *J. Virol.* 69, 3771-3777.
- Chen, J., Wharton, S.A., Weissenhorn, W., Calder, L.J., Hughson, F.M., Skehel, J.J., and Wiley, D.C. (1995). A soluble domain of the membrane-anchoring chain of influenza-virus hemagglutinin (ha(2)) folds in escherichia-coli into the low-ph- induced conformation. *Proceedings of the National Academy of Sciences of the United States of America* 92, 12205-12209.
- Chen, M., Maldarelli, F., Karczewski, M.K., Willey, R.L., and Strebel, K. (1993). Human immunodeficiency virus type 1 vpu protein induces degradation of CD4 *in vitro*: the cytoplasmic domain of CD4 contributes to vpu sensitivity. *J. Virol.* 67, 3877-3884.
- Chou, P.Y. and Fasman, G.D. (1978). Empirical predictions of protein conformation. *Annu. Rev. Microbiol.* 47, 251-276.
- Chowers, M.Y., Spina, C.A., Kwoh, T.J., Fitch, N.J.S., Richman, D.D., and Guatelli, J.C. (1994). Optimal infectivity *in vitro* of human immunodeficiency virus type 1 requires an intact *nef* gene. *J. Virol.* 68, 2906-2914.
- Clark, E.A. (1996). HIV - dendritic cells as embers for the infectious fire. *Current Biology* 6, 655-657.
- Cleghon, V. and Morrison, D.J. (1994). Raf-1 interacts with Fyn and Src in a non-phosphotyrosine dependent manner. *J. Biol. Chem.* 269, 17749-17755.
- Coates, K. and Harris, M. (1995). The human immunodeficiency virus type 1 Nef protein functions as a protein kinase C substrate *in vitro*. *Journal of General Virology* 76, 837-844.
- Coates, K., Cooke, S.J., Mann, D.A., and Harris, M.P.G. (1997). Protein kinase C-mediated phosphorylation of HIV-1 Nef in human cell lines. *J. Biol. Chem.* 272, 12289-12294.
- Colgan, J., Yuan, H.E.H., Franke, E.K., and Luban, J. (1996). Binding of the human-immunodeficiency-virus type-1 gag polyprotein to cyclophilin-a is mediated by the central region of capsid and requires gag dimerization. *J. Virol.* 70, 4299-4310.
- Collette, Y., Chang, H.L., Cerdan, C., Chambost, H., Algarte, M., Mawas, C., Imbert, J., Burny, A., and Olive,

- D. (1996a). Specific th1 cytokine down-regulation associated with primary clinically derived human-immunodeficiency-virus type-1 nef gene-induced expression. *Journal of Immunology* 156, 360-370.
- Collette, Y., Dutartre, H., Benziane, A., Ramosmorales, F., Benarous, R., Harris, M., and Olive, D. (1996b). Physical and functional interaction of Nef with Lck - HIV-1 Nef- induced T-cell signaling defects. *J. Biol. Chem.* 271, 6333-6341.
- Collette, Y., Dutartre, H., Benziane, A., and Olive, D. (1997). The role of HIV1 Nef in T-cell activation: Nef impairs induction of th1 cytokines and interacts with the Src family tyrosine kinase Lck. *Research in Virology* 148, 52-58.
- Collette, Y., Dutartre, H., Benziane, A., Ramosmorales, F., Benarous, R., Harris, M., and Olive, D. (1996). Physical and functional interaction of Nef with Lck - HIV-1 Nef- induced T-cell signaling defects. *J. Biol. Chem.* 271, 6333-6341.
- Cooke, S.J., Coates, K., Barton, C.H., Biggs, T.E., Barrett, S.J., Cochrane, A., Oliver, K., McKeating, J.A., Harris, M.P.G., and Mann, D.A. (1997). Regulated expression vectors demonstrate cell-type-specific sensitivity to human immunodeficiency virus type 1 Nef-induced cytostasis. *Journal of General Virology* 78, 381-392.
- Cooper, J.A. and Howell, B. (1993). The when and how of Src regulation. *Cell* 73, 1051-1054.
- Cooper, J.A. and MacAuley, A. (1988). Potential positive and negative autoregulation of p60^{c-Src} by intermolecular autophosphorylation. *Proc. Natl. Acad. Sci. U. S. A.* 85, 4232-4236.
- Courtneidge, S.A. (1985). Activation of the pp60c-Src kinase by middle T antigen or by dephosphorylation. *EMBO J.* 4, 1471-1477.
- Cross, F.R., Garber, E.A., Pellman, D., and Hanafusa, H. (1984). A short sequence in the p60^{Src} N-terminus is required for p60^{Src} myristoylation and membrane association and for cell-transformation. *Molecular and Cellular Biology* 4, 1834-1842.
- Cullen, B.R. (1996). HIV-1 - is Nef a PAK animal. *Current Biology* 6, 1557-1559.
- Curtain, C.C., Lowe, M.G., Arunagiri, C.K., Mobley, P.W., Macreadie, I.G., and Azad, A.A. (1997). Cytotoxic activity of the amino-terminal region of HIV type 1 Nef protein. *AIDS Res. Hum. Retroviruses* 13, 1213-1220.
- Curtain, C.C., Separovic, F., Rivett, D., Kirkpatrick, A., Waring, A.J., Gordon, L.M., and Azad, A.A. (1994). Fusogenic activity of amino-terminal region of HIV type 1 Nef protein. *AIDS Res. Hum. Retroviruses* 10, 1231-1240

D'Oro, U., Sakaguchi, K., Appella, E., and Ashwell, J.D. (1996). Mutational analysis of Lck in CD45-negative T cells: dominant role of tyrosine 394 phosphorylation in kinase activity. *Molecular and Cellular Biology* 16, 4996-5003.

Daniel, M.D., Kirchhoff, F., Czajak, S.C., Sehgal, P.K., and Desrosiers, R.C. (1992). Protective effects of a live attenuated SIV vaccine with a deletion in the nef gene. *Science* 258, 1938-1941.

Darlix, J.L., Lapadattapolsky, M., Derocquigny, H., and Roques, B.P. (1995). First glimpses at structure-function-relationships of the nucleocapsid protein of retroviruses. *Journal of Molecular Biology* 254, 523-537.

de Ronde, A., Klaver, B., Keulen, W., Smit, L., and Goudsmit, J. (1992). Natural HIV-1 Nef accelerates virus replication in primary human lymphocytes. *Virology* 188, 391-395.

Deacon, N.J., Tsykin, A., Solomon, A., Smith, K., Ludfordmenting, M., Hooker, D.J., McPhee, D.A., Greenway, A.L., Ellett, A., Chatfield, C., Lawson, V.A., Crowe, S., Maerz, A., Sonza, S., Learmont, J., Sullivan, J.S., Cunningham, A., Dwyer, D., Downton, D., and Mills, J. (1995). Genomic structure of an attenuated quasi-species of HIV-1 from a blood-transfusion donor and recipients. *Science* 270, 988-991.

Dean, M., Carrington, M., Winkler, C., Huttley, G.A., Smith, M.W., Allikmets, R., Goedert, J.J., Buchbinder, S.P., Vittinghoff, E., Gomperts, E., Donfield, S., Vlahov, D., Kaslow, R., Saah, A., Rinaldo, C., Detels, R., and O'Brien, S.J. (1996). Genetic restriction of HIV-1 infection and progression to AIDS by a deletion allele of the ckr5 structural gene. *Science* 273, 1856-1862.

Deckert, M., Ticchioni, M., and Bernard, A. (1996). Endocytosis of GPI-anchored proteins in human lymphocytes: role of glycolipid-based domains, actin cytoskeleton and protein kinases. *J. Cell Biology* 133, 791-799.

Deng, H.K., Liu, R., Ellmeier, W., Choe, S., Unutmaz, D., Burkhart, M., Dimarzio, P., Marmon, S., Sutton, R.E., Hill, C.M., Davis, C.B., Peiper, S.C., Schall, T.J., Littman, D.R., and Landau, N.R. (1996). Identification of a major coreceptor for primary isolates of HIV-. *Nature* 381, 661-666.

Desrosiers, R.C., Daniel, M.D., and Yen, L. (1989). HIV-related lentiviruses of nonhuman-primates. *AIDS Res. Hum. Retroviruses* 5, 465-473.

Dewhurst, S., Embretson, J.E., Fultz, P.N., and Mullins, J.I. (1992). Molecular clones from a non-acutely pathogenic derivative of SIVsmmPBj14: Characterization and comparison to acutely pathogenic clones. *AIDS Res. Hum. Retroviruses* 8, 1179-1187.

- Dorfman, T., Bukovsky, A., Ohagen, A., Hoglund, S., and Gottlinger, H.G. (1994). Functional domains of the capsid protein of human-immunodeficiency- virus type-1. *J. Virol.* 68, 8180-8187.
- Dragic, T. and Alizon, M. (1993). Different requirements for membrane fusion mediated by the envelopes of human immunodeficiency virus types 1 and 2. *J. Virol.* 67, 2355-2359.
- Dragic, T., Charneau, P., Clavel, F., and Alizon, M. (1992). Complementation of murine cells for human immunodeficiency virus envelope/CD4-mediated fusion in human/murine heterokaryons. *J. Virol.* 66, 4794-4802.
- Du, Z.J., Lang, S.M., Sasseville, V.G., Lackner, A.A., Ilyinskii, P.O., Daniel, M.D., Jung, J.U., and Desrosiers, R.C. (1995). Identification of a *nef* allele that causes lymphocyte-activation and acute disease in macaque monkeys. *Cell* 82, 665-674.
- Dundr, M., Leno, G.H., Lewis, N., Rekosh, D., Hammarskjold, M.L., and Olson, M.O.J. (1996). Rev-dependent localization and export of HIV-1 gag/pol RNA. *Molecular Biology Of The Cell* 7, 604
- Dwyer, D.E., Ying Chun, G., Wang, B., Bolton, W.V., McCormack, J.G., Cunningham, A.L., and Saksena, N.K. (1997). First human immunodeficiency virus type 1 sequences in the V3 region, *nef* and *vpr* genes from papua new guinea. *AIDS Res. Hum. Retroviruses* 13, 625-627.
- Echarri, A., Gonzalez, E., and Carrasco, L. (1997). The N-terminal arg-rich region of human immunodeficiency virus types 1 and 2 and simian immunodeficiency virus Nef is involved in RNA binding. *European Journal of Biochemistry* 246, 38-44.
- Echarri, A., Gonzalez, M.E., and Carrasco, L. (1996). Human-immunodeficiency-virus (HIV) Nef is an RNA-binding protein in cell-free systems. *Journal of Molecular Biology* 262, 640-651.
- Emerman, M. (1996). HIV-1, vpr and the cell-cycle. *Current Biology* 6, 1096-1103.
- Feng, Y., Broder, C.C., Kennedy, P.E., and Berger, E.A. (1996). HIV-1 entry cofactor - functional cDNA cloning of a 7-transmembrane, G-protein-coupled receptor. *Science* 272, 872-877.
- Fields, S. and Song, O. (1989). A novel genetic system to detect protein-protein interactions. *Nature* 340, 245-246.
- Fields, S. and Sternglanz, R. (1994). The two-hybrid system: an assay for protein-protein interactions. *Trends in Genetics* 10, 286-291.
- Fischer, U., Huber, J., Boelens, W.C., Mattaj, I.W., and Luhrmann, R. (1995). The HIV-1 Rev activation domain is a nuclear export signal that accesses an export pathway used by specific cellular RNAs. *Cell* 82, 475-483.

- Fischer, U., Meyer, S., Teufel, M., Heckel, C., Luhrmann, R., and Rautmann, G. (1994). Evidence that HIV-1 Rev directly promotes the nuclear export of unspliced RNA. *EMBO Journal* 13, 4105-4112.
- Flaherty, K.M., Zozulya, S., Stryer, L., and McKay, D.B. (1993). 3-dimensional structure of recoverin, a calcium sensor in vision. *Cell* 75, 709-716.
- Foster, J.L., Anderson, S.J., Frazier, A.L.B., and Garcia, J.V. (1994). Specific suppression of human CD4 surface expression by Nef from the pathogenic simian immunodeficiency virus SIVmac239^{open}. *Virology* 201, 373-379.
- Foti, M., Carpentier, J.L., Aiken, C., Trono, D., Lew, D.P., and Krause, K.H. (1997). Second-messenger regulation of receptor association with clathrin-coated pits: a novel and selective mechanism in the control of CD4 endocytosis. *Molecular Biology Of The Cell* 8, 1377-1389.
- Foti, M., Mangasarian, A., Piguet, V., Lew, D.P., Krause, K.H., Trono, D., and Carpentier, J.L. (1997). Nef-mediated clathrin-coated pit formation. *Journal Of Cell Biology* 139, 37-47.
- Franchini, G., Robert-Guroff, M., Ghayeb, J., Chang, N.T., and Wong-Staal, F. (1986). Cytoplasmic localization of the HTLVV-III 3'*orf* protein in cultured T cells. *Virology* 155, 593-599.
- Franke, E.K. and Luban, J. (1996). Inhibition of HIV-1 replication by cyclosporine-A or related-compounds correlates with the ability to disrupt the gag-cyclophilin-A interaction. *Virology* 222, 279-282.
- Franke, E.K., Yuan, H.E.H., and Luban, J. (1994). Specific incorporation of cyclophilin-A into HIV-1 virions. *Nature* 372, 359-362.
- Freund, J., Kellner, R., Houthaave, T., and Kalbitzer, H.R. (1994a). Stability and proteolytic domains of Nef protein from human immunodeficiency virus (HIV) type 1. *European Journal of Biochemistry* 221, 811-819.
- Freund, J., Kellner, R., Konvalinka, J., Wolber, V., Krausslich, H.G., and Kalbitzer, H.R. (1994b). A possible regulation of negative factor (Nef) activity of human immunodeficiency virus type 1 by the viral protease. *European Journal of Biochemistry* 223, 589-593.
- Fritz, C.C. and Green, M.R. (1996). HIV Rev uses a conserved cellular protein export pathway for the nucleocytoplasmic transport of viral RNAs. *Current Biology* 6, 848-854.
- Fritz, C.C., Zapp, M.L., and Green, M.R. (1995). A human nucleoporin-like protein that specifically interacts with HIV Rev. *Nature* 376, 530-533.
- Fujita, K., Omura, S., and Silver, J. (1997). Rapid degradation of CD4 in cells expressing human immunodeficiency virus type 1 env and vpu is blocked by proteasome inhibitors. *Journal of General Virology* 78, 619-625.

Fultz, P.N. (1991). Replication of an acutely lethal simian immunodeficiency virus activates and induces proliferation of lymphocytes. *J. Virol.* 65, 4902-4909.

Fultz, P.N., McClure, H., Anderson, D., and Switzer, W.M. (1989). Identification and biological characterization of an acutely lethal variant of simian immunodeficiency virus from sooty mangabeys (SIV/SMM). *AIDS Res. Hum. Retroviruses* 5, 397-409.

Furuta, R.A., Shimano, R., Ogasawara, T., Inubushi, R., Amano, K., Akari, H., Hatanaka, M., Kawamura, M., and Adachi, A. (1997). HIV-1 capsid mutants inhibit the replication of wild-type virus at both early and late infection phases. *FEBS Letters* 415, 231-234.

Gait, M.J. and Karn, J. (1993). RNA recognition by the human-immunodeficiency-virus Tat-protein and Rev-protein. *Trends In Biochemical Sciences* 18, 255-259.

Gallay, P., Swingler, S., Aiken, C., and Trono, D. (1995). HIV-1 infection of nondividing cells - C-terminal tyrosine phosphorylation of the viral matrix protein is a key regulator. *Cell* 80, 379-388.

Gallay, P., Swingler, S., Song, J.P., Bushman, F., and Trono, D. (1995b). HIV nuclear import is governed by the phosphotyrosine-mediated binding of matrix to the core domain of integrase. *Cell* 83, 569-576.

Gallimore, A., Cranage, M., Cook, N., Almond, N., Bootman, J., Rud, E., Silvera, P., Dennis, M., Corcoran, T., Stott, J., McMichael, A., and Gotch, F. (1995). Early suppression of SIV replication by CD8+ nef-specific cytotoxic T-cells in vaccinated macaques. *Nature Medicine* 1, 1167-1173.

Garcia, J.V. and Miller, A.D. (1991). Serine phosphorylation-independent downregulation of cell-surface CD4 by *nef*. *Nature* 350, 508-511.

Garcia, J.V., Alfano, J., and Miller, A.D. (1993). The negative effect of human immunodeficiency virus type 1 Nef on cell surface CD4 expression is not species specific and requires the cytoplasmic domain of CD4. *J. Virol.* 67, 1511-1516.

Geleziunas, R., Morin, N., and Wainberg, M.A. (1996). Mechanisms of down-modulation of CD4 receptors on the surface of HIV-1-infected cells. *Comptes Rendus De L Academie Des Sciences Serie Iii-Sciences De La Vie-Life Sciences* 319, 653-662.

Gervais, F.G. and Veillette, A. (1995). The unique amino-terminal domain of p56(Lck) regulates interactions with tyrosine protein phosphatases in T-lymphocytes. *Molecular and Cellular Biology* 15, 2393-2401.

Gibbs, J.S., Lackner, A.A., Lang, S.M., Simon, M.A., Sehgal, P.K., Daniel, M.D., and Desrosiers, R.C. (1995). Progression to AIDS in the absence of a gene for *vpr* or *vpx*. *J. Virol.* 69, 2378-2383.

- Gietz, R.D., Schiestl, R.H., Willems, A.R., and Woods, R.A. (1995). Studies on the transformation of intact yeast cells by the LiAc/SSS-DNA/PEG procedure. *Yeast* 11, 355-360.
- Glaichenhaus, N., Shastri, N., Littman, D.R., and Turner, J.M. (1991). Requirement for association of p56lck with CD4 in antigen-specific signal transduction in T-cells. *Cell* 64, 511-520.
- Goff, S.P. (1990). Retroviral reverse-transcriptase - synthesis, structure, and function. *Journal of Acquired Immune Deficiency Syndromes* 3, 817-831.
- Goldfarb, D.S. (1995). HIV-1 virology - simply marvelous nuclear transport. *Current Biology* 5, 570-573.
- Goldsmith, M.A., Warmerdam, M.T., Atchison, R.E., Miller, M.D., and Greene, W.C. (1995). Dissociation of the CD4 down-regulation and viral infectivity enhancement functions of human-immunodeficiency-virus type-1 nef. *J. Virol.* 69, 4112-4121.
- Gonfloni, S., Williams, J.C., Hattula, K., Weijland, A., Wierenga, R.K., and Supertifurga, G. (1997). The role of the linker between the SH2 domain and catalytic domain in the regulation and function of Src. *EMBO Journal* 16, 7261-7271.
- Gottlinger, H.G., Sodroski, J.G., and Haseltine, W.A. (1989). Role of capsid precursor processing and myristoylation in morphogenesis and infectivity of human immunodeficiency virus type 1. *Proc. Natl. Acad. Sci. U. S. A.* 86, 5781-5785.
- Greenberg, M.E., Bronson, S., Lock, M., Neumann, M., Pavlakis, G.N., and Skowronski, J. (1997). Co-localization of HIV-1 Nef with the AP-2 adaptor protein complex correlates with Nef-induced CD4 down-regulation. *EMBO Journal* 16, 6964-6976.
- Greenway, A., Azad, A., and McPhee, D. (1995a). Human immunodeficiency virus type 1 Nef protein inhibits activation pathways in peripheral blood mononuclear cells and T-cell lines. *J. Virol.* 69, 1842-1850.
- Greenway, A., Azad, A., and McPhee, D. (1995b). HIV-1 Nef associates with host-cell proteins involved with cellular signaling and activation. *Journal Of Cellular Biochemistry* 190
- Greenway, A., Azad, A., Mills, J., and McPhee, D. (1996). Human-immunodeficiency-virus type-1 Nef binds directly to Lck and mitogen-activated protein-kinase, inhibiting kinase-activity. *J. Virol.* 70, 6701-6708.
- Greenway, A.L., McPhee, D.A., Grgacic, E., Hewish, D., Lucantoni, A., Macreadie, I., and Azad, A. (1994). Nef 27, but not the Nef 25 isoform of human immunodeficiency virus-type 1 pNL4.3 down-regulates surface CD4 and IL-2R expression in peripheral blood mononuclear cells and transformed T-cells. *Virology* 198, 245-256.

- Grzesiek, S., Bax, A., Clore, G.M., Gronenborn, A.M., Hu, J.S., Kaufman, J., Palmer, I., Stahl, S.J., and Wingfield, P.T. (1996a). The solution structure of HIV-1 Nef reveals an unexpected fold and permits delineation of the binding surface for the SH3 domain of Hck tyrosine protein-kinase. *Nature Structural Biology* 3, 340-345.
- Grzesiek, S., Stahl, S.J., Wingfield, P.T., and Bax, A. (1996). The CD4 determinant for down-regulation by HIV-1 Nef directly binds to Nef - mapping of the Nef binding surface by NMR. *Biochemistry* 35, 10256-10261.
- Guy, B., Kieny, M.P., Riviere, Y., Le Peuch, C., Dott, K., Girard, M., Montagnier, L., and Lecocq, J. (1987). HIV F3'orf encodes a phosphorylated GTP-binding protein resembling an oncogene product. *Nature* 330, 266-269.
- Hadida, F., Parrot, A., Kieny, M.P., SadatSowti, B., Mayaud, C., Debre, P., and Autran, B. (1992). Carboxyl-terminal and central regions of human immunodeficiency virus-1 Nef recognized by cytotoxic T lymphocytes from lymphoid organs: an *in vitro* limiting dilution analysis. *Journal of Clinical Investigation* 89, 53-60.
- Hammes, S.R., Dixon, E.P., Malim, M.H., Cullen, B.R., and Greene, W.C. (1989). Nef protein of human immunodeficiency virus type 1: evidence against its role as a transcriptional inhibitor. *Proc. Natl. Acad. Sci. U. S. A.* 86, 9549-9553.
- Hanahan, D. (1983). Studies on transformation of *Escherichia coli* with plasmids. *J. Mol. Biol.* 166, 557-580.
- Harris, M. (1995). The role of myristoylation in the interactions between human immunodeficiency virus type 1 Nef and cellular proteins. *Biochemical Society Transactions* 23, 557-561.
- Harris, M. (1996). From negative factor to a critical role in virus pathogenesis -the changing fortunes of Nef. *Journal of General Virology* 77, 2379-2392.
- Harris, M. and Coates, K. (1993). Identification of cellular proteins that bind to the human immunodeficiency virus type 1 *nef* gene product *in vitro*: a role for myristylation. *Journal of General Virology* 74, 1581-1589.
- Harris, M., Hislop, S., Patsilinos, P., and Neil, J.C. (1992). *In vivo* derived HIV-1 *nef* gene products are heterogeneous and lack detectable nucleotide binding activity. *AIDS Res. Hum. Retroviruses* 8, 537-543.
- Harris, M.P.G. and Neil, J.C. (1994). Myristoylation-dependent binding of HIV-1 Nef to CD4. *Journal of Molecular Biology* 241, 136-142.
- Hengen, P.N. (1997). Methods and reagents - false positives from the yeast two-hybrid system. *Trends In Biochemical Sciences* 22, 33-34.
- Henikoff, S. and Henikoff, J.G. (1994). Protein family classification based on searching a database of blocks.(<http://www.blocks.fhcrc.org/>). *Genomics* 19, 97-107.

- Hewlett, G. (1991). Strategies for optimising serum-free media. *Cytotechnology* 5, 3-14.
- Hill, C.M., Deng, H.K., Unutmaz, D., Kewalramani, V.N., Bastiani, L., Gorny, M.K., Zolla-Pazner, S., and Littman, D.R. (1997). Envelope glycoproteins from human immunodeficiency virus types 1 and 2 and simian immunodeficiency virus can use human ccr5 as a coreceptor for viral entry and make direct CD4-dependent interactions with this chemokine receptor. *J. Virol.* 71, 6296-6304.
- Ho, D.D., Neumann, A.U., Perelson, A.S., Chen, W., Leonard, J.M., and Markowitz, M. (1995). Rapid turnover of plasma virions and CD4 lymphocytes in HIV-1 infection. *Nature* 373, 123-126.
- Hockley, D.J., Nermut, M.V., Grief, C., Jowett, J.B.M., and Jones, I.M. (1994). Comparative morphology of gag protein structures produced by mutants of the gag gene of human-immunodeficiency-virus type-1. *Journal of General Virology* 75, 2985-2997.
- Hodge, D.R., Chen, Y.M.A., and Samuel, K.P. (1995). Oligomerization of the HIV type-2 Nef protein - mutational analysis of the heptad leucine repeat motif and cysteine residues. *AIDS Res. Hum. Retroviruses* 11, 65-79.
- Hoessli, D.C. and Robinson, P.J. (1998). GPI-anchors and cell membranes: a special relationship. *Trends In Cell Biology* 8, 87-89.
- Hofmann, B., Nishanian, P., Nguyen, T., Insixiangmay, P., and Fahey, J.L. (1993). Human immunodeficiency virus proteins induce the inhibitory cAMP/protein kinase A pathway in normal lymphocytes. *Proc. Natl. Acad. Sci. U. S. A.* 90, 6676-6680.
- Hua, J. and Cullen, B.R. (1997). Human immunodeficiency virus types 1 and 2 and simian immunodeficiency virus Nef use distinct but overlapping target sites for downregulation of cell surface CD4. *J. Virol.* 71, 6742-6748.
- Hua, J., Blair, W., Truant, R., and Cullen, B.R. (1997). Identification of regions in HIV-1 Nef required for efficient downregulation of cell surface CD4. *Virology* 231, 231-238.
- Huang, M.J., Orenstein, J.M., Martin, M.A., and Freed, E.O. (1995). P6(gag) is required for particle-production from full-length human- immunodeficiency-virus type-1 molecular clones expressing protease. *J. Virol.* 69, 6810-6818.
- Huang, Y., Zhang, L., and Ho, D.D. (1995). Characterization of *nef* sequences in long-term survivors of human immunodeficiency virus type 1 infection. *J. Virol.* 69, 93-100.
- Iafrate, A.J., Bronson, S., and Skowronski, J. (1997). Separable functions of Nef disrupt two aspects of T cell receptor machinery: CD4 expression and CD3 signaling. *EMBO Journal* 16, 673-684.

Johnson, D.R., Bhatnagar, R.S., Knoll, L.J., and Gordon, J.I. (1994). Genetic and biochemical-studies of protein N-myristoylation. *Annual Review Of Biochemistry* 63, 869-914.

Johnson, L.N., Noble, M.E.M., and Owen, D.J. (1996). Active and inactive protein-kinases - structural basis for regulation. *Cell* 85, 149-158.

Jones, E.Y., Stuart, D.I., Garman, E.F., Griest, R., Phillips, D.C., Taylor, G.L., Matsumoto, O., Darby, G., Larder, B., Lowe, D., Powell, K., Purifoy, D., Ross, C.K., Somers, D., Tisdale, M., and Stammers, D.K. (1993). The growth and characterization of crystals of human-immunodeficiency-virus (HIV) reverse-transcriptase. *Journal Of Crystal Growth* 126, 261-269.

Kaminchik, J., Margalit, R., Yaish, S., Drummer, H., Amit, B., Sarver, N., Gorecki, M., and Panet, A. (1994). Cellular-distribution of HIV type-1 Nef protein - identification of domains in Nef required for association with membrane and detergent- insoluble cellular matrix. *AIDS Res. Hum. Retroviruses* 10, 1003-1010.

Kamps, M.P., Buss, J.E., and Sefton, B.M. (1985). Mutation of NH₂-terminal glycine of p60^{Src} prevents both myristoylation and morphological transformation. *Proc. Natl. Acad. Sci. U. S. A.* 82, 4625-4628.

Karczewski, M.K. and Strebel, K. (1996). Cytoskeleton association and virion incorporation of the human-immunodeficiency-virus type-1 Vif protein. *J. Virol.* 70, 494-507.

Kawano, Y., Tanaka, Y., Misawa, N., Tanaka, R., Kira, J., Kimura, T., Fukushi, M., Sano, K., Goto, T., Nakai, M., Kobayashi, T., Yamamoto, N., and Koyanagi, Y. (1997). Mutational analysis of human immunodeficiency virus type 1 (HIV-1) accessory genes: requirement of a site in the *nef* gene for HIV-1 replication in activated CD4(+) T cells *in vitro* and *in vivo*. *J. Virol.* 71, 8456-8466.

Keen, N.J., Churcher, M.J., and Karn, J. (1997). Transfer of tat and release of tar RNA during the activation of the human immunodeficiency virus type-1 transcription elongation complex. *EMBO Journal* 16, 5260-5272.

Kestler, H.W., Ringler, D.J., Mori, K., Panicali, D.L., Sehgal, P.K., Daniel, M.D., and Desrosiers, R.C. (1991). Importance of the *nef* gene for maintenance of high virus loads and for development of AIDS. *Cell* 65, 651-662.

Kieny, M.P. (1990). Structure and regulation of the human AIDS virus. *Journal of Acquired Immune Deficiency Syndromes* 3, 395-402.

Kim, S., Ikeuchi, K., Byrn, R., Groopman, J., and Baltimore, D. (1989). Lack of a negative influence on viral growth by the *nef* gene of human immunodeficiency virus type 1. *Proc. Natl. Acad. Sci. U. S. A.* 86, 9544-9548.

Kimura, T., Nishikawa, M., and Ohyama, A. (1994). Intracellular membrane traffic of human immunodeficiency virus type 1 envelope glycoproteins: Vpu liberates Golgi-targeted gp160 from CD4-dependent retention in the endoplasmic reticulum. *Journal of Biochemistry* 115, 1010-1020.

- King, L.A. and Possee, R.D. (1992). The baculoviruses. In *The Baculovirus expression system-A laboratory guide*. Anonymous London, New York, Tokyo, Melbourne, Madras: Chapman and Hall), pp. 1-15.
- Kitts, P.A. and Possee, R.D. (1993). A method for producing recombinant baculovirus expression vectors at high frequency. *BioTechniques 14*, 810-817.
- Lang, S.M., Iafrate, A.J., StahlHennig, C., Kuhn, E.M., Nisslein, T., Kaup, F.J., Haupt, M., Hunsmann, G., Skowronski, J., and Kirchhoff, F. (1997). Association of simian immunodeficiency virus Nef with cellular serine/threonine kinases is dispensable for the development of AIDs in rhesus macaques. *Nature Medicine 3*, 860-865.
- Larder, B. (1995). Viral resistance and the selection of antiretroviral combinations. *J. Acquir. Immune. Defic. Syndr. 10 (suppl.1)*, S28-S33.
- Latour, S., Fournel, M., and Veillette, A. (1997). Regulation of T-cell antigen receptor signalling by syk tyrosine protein kinase. *Molecular and Cellular Biology 17*, 4434-4441.
- Lee, C.H., Leung, B., Lemmon, M.A., Zheng, J., Cowburn, D., Kuriyan, J., and Saksela, K. (1995). A single amino-acid in the SH3 domain of Hck determines its high- affinity and specificity in binding to HIV-1 Nef protein. *EMBO Journal 14*, 5006-5015.
- Lee, C.H., Saksela, K., Mirza, U.A., Chait, B.T., and Kuriyan, J. (1996). Crystal-structure of the conserved core of HIV-1 Nef complexed with a Src family SH3 domain. *Cell 85*, 931-942.
- Lee, P.P. and Linial, M.L. (1995). Inhibition of wild-type HIV-1 virus production by a matrix deficient gag mutant. *Virology 208*, 808-811.
- Lee, S., Peden, K., Dimitrov, D.S., Broder, C.C., Manischewitz, J., Denisova, G., Gershoni, J.M., and Golding, H. (1997). Enhancement of human immunodeficiency virus type 1 envelope-mediated fusion by a CD4-gp120 complex-specific monoclonal antibody. *J. Virol. 71*, 6037-6043.
- Lee, Y.M., Tang, X.B., Cimasky, L.M., Hildreth, J.E.K., and Yu, X.F. (1997). Mutations in the matrix protein of human immunodeficiency virus type 1 inhibit surface expression and virion incorporation of viral envelope glycoproteins in CD4(+) t lymphocytes. *J. Virol. 71*, 1443-1452.
- Lenburg, M.E. and Landau, N.R. (1993). Vpu-induced degradation of CD4: Requirement for specific amino acid residues in the cytoplasmic domain of CD4. *J. Virol. 67*, 7238-7245.
- Lewis, A.D. and Johnson, P.R. (1995). Developing animal-models for AIDS research - progress and problems. *Trends In Biotechnology 13*, 142-150.

- Li, S., Couet, J., and Lisanti, M.P. (1996). Src tyrosine kinases, Ga subunits and H-Ras share a common membrane-anchored scaffolding protein, caveolin. *J. Biol. Chem.* *46*, 29182-29190.
- Liu, L.X., Margottin, F., Le Gall, S., Schwartz, O., Selig, L., Benarous, R., and Benichou, S. (1997). Binding of HIV-1 Nef to a novel thioesterase enzyme correlates with Nef-mediated CD4 down-regulation. *J. Biol. Chem.* *272*, 13779-13785.
- Livingstone, C. and Jones, I. (1989). *Nucleic Acids Research* *17*, 2366
- Lock, P., Ralph, S., Stanley, E., Boulet, I., Ramsay, R., and Dunn, A.R. (1991). 2 isoforms of murine Hck, generated by utilization of alternative translational initiation codons, exhibit different patterns of subcellular-localization. *Molecular and Cellular Biology* *11*, 4363-4370.
- Lower, R., Lower, J., and Kurth, R. (1996). The viruses in all of us - characteristics and biological significance of human endogenous retrovirus sequences. *Proceedings of the National Academy of Sciences of the United States of America* *93*, 5177-5184.
- Lu, X.B., Wu, X.N., Plemenitas, A., Yu, H.F., Sawai, E.T., Abo, A., and Peterlin, B.M. (1996). Cdc42 and Rac1 are implicated in the activation of the Nef-associated kinase and replication of HIV-1. *Current Biology* *6*, 1677-1684.
- Luciw, P.A., Cheng-Mayer, C., and Levy, J.A. (1987). Mutational analysis of the human immunodeficiency virus: The orf-B region down-regulates virus replication. *Proc. Natl. Acad. Sci. U. S. A.* *84*, 1434-1438.
- Luo, K.X. and Sefton, B.M. (1992). Activated Lck tyrosine protein-kinase stimulates antigen-independent interleukin-2 production in T-cells. *Molecular and Cellular Biology* *12*, 4724-4732.
- Luo, T., Downing, J.R., and Garcia, J.V. (1997). Induction of phosphorylation of human immunodeficiency virus type 1 Nef and enhancement of CD4 downregulation by phorbol myristate acetate. *J. Virol.* *71*, 2535-2539.
- Luo, T.C. and Garcia, J.V. (1996). The association of Nef with a cellular serine/threonine kinase and its enhancement of infectivity are viral isolate dependent. *J. Virol.* *70*, 6493-6496.
- Luo, T.C., Livingston, R.A., and Garcia, J.V. (1997). Infectivity enhancement by human immunodeficiency virus type 1 Nef is independent of its association with a cellular serine/threonine kinase. *J. Virol.* *71*, 9524-9530.
- Luria, S., Chambers, I., and Berg, P. (1991). Expression of the type 1 human immunodeficiency virus Nef protein in T cells prevents antigen receptor-mediated induction of interleukin 2 mRNA. *Proc. Natl. Acad. Sci. U. S. A.* *88*, 5326-5330.

- Luria, S., Chambers, I., and Berg, P. (1991). Expression of the type 1 human immunodeficiency virus Nef protein in T cells prevents antigen receptor-mediated induction of interleukin 2 mRNA. *Proc. Natl. Acad. Sci. U. S. A.* 88, 5326-5330.
- Macreadie, I.G., Castelli, L.A., Lucantoni, A., and Azad, A.A. (1995). Stress-dependent and sequence-dependent release into the culture-medium of HIV-1 Nef produced in *saccharomyces-cerevisiae*. *Gene* 162, 239-243.
- Macreadie, I.G., Ward, A.C., Failla, P., Grgacic, E., McPhee, D., and Azad, A.A. (1993). Expression of HIV-1 *nef* in yeast: The 27kDa Nef protein is myristylated and fractionates with the nucleus. *Yeast* 9, 565-573.
- Mahalingam, S., Khan, S.A., Jabbar, M.A., Monken, C.E., Collman, R.G., and Srinivasan, A. (1995). Identification of residues in the N-terminal acidic domain of HIV-1 vpr essential for virion incorporation. *Virology* 207, 297-302.
- Malek, S.N. and Desiderio, S. (1994). A cyclin dependent kinase homologue, p130^{PITSLRE}, is a phosphotyrosine independent SH2 ligand. *J. Biol. Chem.* 269, 33009-33020.
- Mangasarian, A., Foti, M., Aiken, C., Chin, D., Carpentier, J.L., and Trono, D. (1997). The HIV-1 Nef protein acts as a connector with sorting pathways in the Golgi and at the plasma membrane. *Immunity* 6, 67-77.
- Maniatis, T., Fritsch, E.F., and Sambrook, J. (1982). *Molecular cloning: A laboratory manual*. Anonymous (New York: Cold Spring Harbor Laboratory),
- Mariani, R. and Skowronski, J. (1993). CD4 down-regulation by *nef* alleles isolated from human immunodeficiency virus type 1-infected individuals. *Proc. Natl. Acad. Sci. U. S. A.* 90, 5549-5553.
- Marth, J.D., Cooper, J.A., King, C.S., Ziegler, S.F., Tinker, D.A., Overell, R.W., Krebs, E.G., and Perlmutter, R.M. (1988). Neoplastic transformation induced by an activated lymphocyte-specific protein tyrosine kinase (pp56^{Lck}). *Molecular and Cellular Biology* 8, 540-550.
- Marth, J.D., Distche, C., Pravtcheva, D., Ruddle, F., Krebs, E.G., and Perlmutter, R.M. (1986). Localization of a lymphocyte-specific protein tyrosine kinase gene (*lck*) at a site of frequent chromosomal abnormalities in human lymphomas. *Proc. Natl. Acad. Sci. U. S. A.* 83, 7400-7404.
- Marth, J.D., Peet, R., Krebs, E.G., and Perlmutter, R.M. (1985). A lymphocyte-specific protein-tyrosine kinase is rearranged and overexpressed in the murine T cell lymphoma LSTRA. *Cell* 43, 393-404.

- Maurer, H.R. (1992). Towards serum-free, chemically defined media for mammalian cell culture. In *Animal cell culture: A practical approach*. R.I. Freshney, ed. (Oxford: IRL Press), pp. 15-46.
- Mayer, B.J. (1997). Clamping down on Src activity. *Current Biology* 7, R295-R298.
- McLaughlin, S. and Aderem, A. (1995). The myristoyl-electrostatic switch - a modulator of reversible protein-membrane interactions. *Trends In Biochemical Sciences* 20, 272-276.
- Mebatsion, T., Finke, S., Weiland, F., and Conzelmann, K.K. (1997). A CXCR4/CD4 pseudotype rhabdovirus that selectively infects HIV-1 envelope protein-expressing cells. *Cell* 90, 841-847.
- Miller, M.D., Warmerdam, M.T., Ferrell, S.S., Benitez, R., and Greene, W.C. (1997). Intravirion generation of the C-terminal core domain of HIV-1 Nef by the HIV-1 protease is insufficient to enhance viral infectivity. *Virology* 234, 215-225.
- Miller, M.D., Warmerdam, M.T., Gaston, I., Greene, W.C., and Feinberg, M.B. (1994). The human immunodeficiency virus-1 *nef* gene product: a positive factor for viral infection and replication in primary lymphocytes and macrophages. *J. Exp. Med.* 179, 101-114.
- Miller, M.D., Warmerdam, M.T., Page, K.A., Feinberg, M.B., and Greene, W.C. (1995). Expression of the human immunodeficiency virus type 1 (HIV-1) *nef* gene during HIV-1 production increases progeny particle infectivity independently of gp160 or viral entry. *J. Virol.* 69, 579-584.
- Moarefi, I., LaFevreBernt, M., Sicheri, F., Huse, M., Lee, C.H., Kuriyan, J., and Miller, W.T. (1997). Activation of the Src-family tyrosine kinase Hck by SH3 domain displacement. *Nature* 385, 650-653.
- Molina, T.J., Kishihara, K., Siderovski, D.P., Vanewijk, W., Narendran, A., Timms, E., Wakeham, A., Paige, C.J., Hartmann, K.U., Veillette, A., Davidson, D., and Mak, T.W. (1992). Profound block in thymocyte development in mice lacking p56(lck). *Nature* 357, 161-164.
- Morikawa, Y., Hinata, S., Tomoda, H., Goto, T., Nakai, M., Aizawa, C., Tanaka, H., and Omura, S. (1996). Complete inhibition of human-immunodeficiency-virus gag myristoylation is necessary for inhibition of particle budding. *J. Biol. Chem.* 271, 2868-2873.
- Muller, A.J., Pendergast, A.M., Havlik, M.H., Puil, L., Pawson, T., and Witte, O.N. (1992). A limited set of SH2 domains binds through a high-affinity phosphotyrosine-independent interaction. *Molecular and Cellular Biology* 12, 5087-5093.
- Mumby, S.M. (1997). Reversible palmitoylation of signaling proteins. *Current Opinion in Cell Biology* 9, 148-154.

- Nakai, M. and Goto, T. (1996). Ultrastructure and morphogenesis of human-immunodeficiency-virus. *Journal Of Electron Microscopy* 45, 247-257.
- Nakashima, I., Pu, M.Y., Nishizaki, A., Rosila, I., Ma, L., Katano, Y., Ohkusu, K., Rahman, S.M.J., Isobe, K., Hamaguchi, M., and Saga, K. (1994). Redox mechanism as alternative to ligand-binding for receptor activation delivering disregulated cellular signals. *Journal of Immunology* 152, 1064-1071.
- Nebreda, A.R., Segade, F., and Santos, E. (1992). The nef gene products: biochemical properties and effects on host cell functions. *Research in Virology* 143, 55-59.
- Nermut, M.V., Hockley, D.J., Jowett, J.B.M., Jones, I.M., Garreau, M., and Thomas, D. (1994). Fullerene-like organization of HIV gag-protein shell in virus-like particles produced by recombinant baculovirus. *Virology* 198, 288-296.
- Niederman, T.M.J., Hastings, W.R., and Ratner, L. (1993). Myristoylation enhanced binding of the HIV-1 Nef protein to T cell skeletal matrix. *Virology* 197, 420-425.
- Nokta, M. and Pollard, R. (1991). Human immunodeficiency virus infection: Association with altered intracellular levels of cAMP and cGMP in MTT-4 cells. *Virology* 181, 211-217.
- Nolan, G.P. (1997). Harnessing viral devices as pharmaceuticals: fighting HIV-1's fire with fire. *Cell* 90, 821-824.
- Nunn, M. and Marsh, J. (1995). Identification of proteins associated with the HIV-1 *nef* gene-product - characterization of a 65,000 dalton kinase. *AIDS Res. Hum. Retroviruses* 11, S 122
- Nunn, M.F. and Marsh, J.W. (1996). Human-immunodeficiency-virus type-1 Nef associates with a member of the p21-activated kinase family. *J. Virol.* 70, 6157-6161.
- Oberlin, E., Amara, A., Bachelier, F., Bessia, C., Virelizier, J.L., Arenzana-Seisdedos, F., Schwartz, O., Heard, J.M., Clarklewis, I., Legler, D.F., Loetscher, M., Baggiolini, M., and Moser, B. (1996). The CXC chemokine SDF-1 is the ligand for lestr/fusin and prevents infection by T-cell-line-adapted HIV-1. *Nature* 382, 833-835.
- Old, S.W. and Primrose, S.B. (1989). *Principles of gene manipulation: an introduction to genetic engineering.* (London, Edinburgh, Boston, Melbourne, Paris, Berlin, Vienna: Blackwell Scientific Publications).
- Oldstone, M.B. (1997). How viruses escape from cytotoxic T lymphocytes: molecular parameters and players. *Virology* 234, 179-185.
- Pandori, M.W., Fitch, N.J.S., Craig, H.M., Richman, D.D., Spina, C.A., and Guatelli, J.C. (1996). Producer-cell modification of human-immunodeficiency-virus type-1 - Nef is a virion protein. *J. Virol.* 70, 4283-4290.
- Parolini, I., Sargiacomo, M., Lisanti, M.P., and Peschle, C. (1996). Signal-transduction and

glycophosphatidylinositol-linked proteins (Lyn, Lck, CD4, CD45, G-proteins, and CD55) selectively localize in triton-insoluble plasma-membrane domains of human leukemic-cell lines and normal granulocytes. *Blood* 87, 3783-3794.

Parton, G.R. (1996). Caveolae and caveolins. *Current Opinion in Cell Biology* 8, 542-548.

Pawson, T. (1995). Protein modules and signalling networks. *Nature* 373, 573-580.

Peitzsch, R.M. and McLaughlin, S. (1993). Binding of acylated peptides and fatty-acids to phospholipid-vesicles - pertinence to myristoylated proteins. *Biochemistry* 32, 10436-10443.

Pelchen-Matthews, A., Parsons, I.J., and Marsh, M. (1993). Phorbol ester-induced downregulation of CD4 is a multistep process involving dissociation from p56^{lck}, increased association with clathrin-coated pits, and altered endosomal

Pendergast, A.M., Muller, A.J., Havlik, M.H., Maru, Y., and Witte, O.N. (1991). BCR sequences essential for transformation by the BCR-ABL oncogene bind to the ABL SH2 regulatory domain in a non-tyrosine-dependent manner. *Cell* 66, 161-171.

Perelson, A.S., Neumann, A.U., Markowitz, M., Leonard, J.M., and Ho, D.D. (1996). HIV-1 dynamics in-vivo - virion clearance rate, infected cell life-span, and viral generation time. *Science* 271, 1582-1586.

Perlmutter, R.M., Marth, J.D., Ziegler, S.F., Garvin, A.M., Pawar, S., Cooke, M.P., and Abraham, K.M. (1988). Specialized protein tyrosine kinase proto-oncogenes in hematopoietic cells. *Biochimica et Biophysica Acta* 948, 245-262.

Prasad, K.V.S., Kapeller, R., Janssen, O., Repke, H., Duke-Cohan, J.S., Cantley, L.C., and Rudd, C.E. (1993). Phosphoinositol (PI) 3-kinase and PI4-kinase binding to the CD4-p56^{lck} complex: the p56^{lck} SH3 domain binds to PI 3-kinase but not PI 4-kinase. *Molecular and Cellular Biology* 13, 7708-7717.

Premkumar, D.R.D., Ma, X.Z., Maitra, R.K., Chakrabarti, B.K., Salkowitz, J., YenLieberman, B., Hirsch, M.S., and Kestler, H.W. (1996). The *nef* gene from a long-term HIV type-1 nonprogressor. *AIDS Res. Hum. Retroviruses* 12, 337-345.

Preston, B.D., Poiesz, B.J., and Loeb, L.A. (1988). Fidelity of HIV-1 reverse-transcriptase. *Science* 242, 1168-1171.

Pu, M.Y., Akhand, A.A., Kato, M., Hamaguchi, M., Koike, T., Iwata, H., Sabe, H., Suzuki, H., and Nakashima, I. (1996). Evidence of a novel redox-linked activation mechanism for the Src kinase which is independent of tyrosine 527-mediated regulation. *Oncogene* 13, 2615-2622.

Quintrell, N., Lebo, R., Varmus, H., Bishop, J.M., Pettenati, M.J., Lebeau, M.M., Diaz, M.O., and Rowley, J.D.

- (1987). Identification of a human-gene (*hck*) that encodes a protein-tyrosine kinase and is expressed in hematopoietic-cells. *Molecular and Cellular Biology* 7, 2267-2275.
- Raja, N.U., Vincent, M.J., and Jabbar, M.A. (1994). Vpu-mediated proteolysis of gp160/CD4 chimeric envelope glycoproteins in the endoplasmic reticulum: Requirement of both the anchor and cytoplasmic domains of CD4. *Virology* 204, 357-366.
- Ramsay, G. (1998). DNA chips: State-of-the art. *Nature Biotechnology* 16, 40-44.
- Re, F., Braaten, D., Franke, E.K., and Luban, J. (1995). Human-immunodeficiency-virus type-1 vpr arrests the cell-cycle in G(2) by inhibiting the activation of p34(cdc2)-cyclin-b. *J. Virol.* 69, 6859-6864.
- Reicin, A.S., Ohagen, A., Yin, L., Hoglund, S., and Goff, S.P. (1996). The role of gag in human-immunodeficiency-virus type-1 virion morphogenesis and early steps of the viral life-cycle. *J. Virol.* 70, 8645-8652.
- Rhee, S.S. and Marsh, J.W. (1994). Human immunodeficiency virus type 1 Nef-induced down-modulation of CD4 is due to rapid internalization and degradation of surface CD4. *J. Virol.* 68, 5156-5163.
- Rhee, S.S. and Marsh, J.W. (1994a). HIV-1 Nef activity in murine T cells: CD4 modulation and positive enhancement. *Journal of Immunology* 152, 5128-5134.
- Rhee, S.S. and Marsh, J.W. (1994b). Human immunodeficiency virus type 1 Nef-induced down-modulation of CD4 is due to rapid internalization and degradation of surface CD4. *J. Virol.* 68, 5156-5163.
- Robbins, S.M., Quintrell, N.A., and Bishop, J.M. (1995). Myristoylation and differential palmitoylation of the Hck protein- tyrosine kinases govern their attachment to membranes and association with caveolae. *Molecular and Cellular Biology* 15, 3507-3515.
- Robert-Guroff, M., Popovic, M., Gartner, S., Markham, P., Gallo, R.C., and Reitz, M.S. (1990). Structure and expression of *tat*-, *rev*-, and *nef*-specific transcripts of human immunodeficiency virus type I in infected lymphocytes and macrophages. *J. Virol.* 64, 3391-3398.
- Robinson, P.J. (1991). Phosphatidylinositol membrane anchors and T cell activation. *Immunology Today* 12, 35-41.
- Rossi, F., Evstafieva, A., PedraliNoy, G., Gallina, A., and Milanesi, G. (1997). Hsn3 proteasomal subunit as a target for human immunodeficiency virus type 1 Nef protein. *Virology* 237, 33-45.
- Rossi, F., Gallina, A., and Milanesi, G. (1996). Nef-CD4 physical interaction sensed with the yeast 2-hybrid system. *Virology* 217, 397-403.
- Rousseau, C., Abrams, E., Lee, M., Urbano, R., and King, M.C. (1997). Long terminal repeat and *nef* gene

variants of human immunodeficiency virus type 1 in perinatally infected long-term survivors and rapid progressors. *AIDS Res. Hum. Retroviruses* 13, 1611-1623.

Rud, E.W., Cranage, M., Yon, J., Quirk, J., Ogilvie, L., Cook, N., Webster, S., Dennis, M., and Clarke, B.E. (1994). Molecular and biological characterization of simian immunodeficiency virus macaque strain 32H proviral clones containing *nef* size variants. *Journal of General Virology* 75, 529-543.

Rud, E.W., Yon, J.R., Larder, B.A., Clarke, B.E., Cook, N., and Cranage, M.P. (1992). Infectious molecular clones of SIVmac32H: Nef deletion controls ability to reisolate virus from rhesus macaques. In *Vaccines92: Modern Approaches To New Vaccines Including Prevention of AIDS*. F. Brown, R.M. Chanock, H.G. Ginsberg, and R.A. Lerner, eds. (Cold Spring Harbor Laboratory Press), pp. 229-235.

Ruprecht, R.M., Baba, T.W., Li, A., Ayehunie, S., Hu, Y.W., Liska, V., Rasmussen, R., and Sharma, P.L. (1996). Live attenuated HIV as a vaccine for AIDS - pros and cons. *Seminars In Virology* 7, 147-155.

Saiki, R.K., Scharf, S., Faloona, F., Mullis, K.B., Horn, G.T., Erlich, H.A., and Arnheim, N. (1985). Enzymatic amplification of β -globin genomic sequences and restriction site analysis for diagnosis of sickle cell anaemia. *Science* 230, 1350-1354.

Saksela, K. (1997). HIV-1 Nef and host cell protein kinases. *Frontiers in Bioscience* (<http://www.bioscience.org/>) 2, d606-d618.

Saksela, K., Cheng, G., and Baltimore, D. (1995). Proline-rich (PxxP) motifs in HIV-1 Nef bind to SH3 domains of a subset of Src kinases and are required for the enhanced growth of *nef*⁺ viruses but not for down-regulation of CD4. *EMBO Journal* 14, 484-491.

Saksena, N.K., Ying Chun, G., Wang, B., Xiang, S.H., Ziegler, J., Palasanthiran, P., Bolton, W., and Cunningham, A.L. (1997). RNA and DNA sequence analysis of the *nef* gene of HIV type 1 strains from the first HIV type 1-infected long-term nonprogressing mother-child pair. *AIDS Res. Hum. Retroviruses* 13, 729-732.

Sanfridson, A., Cullen, B.R., and Doyle, C. (1994). The simian immunodeficiency virus Nef protein promotes degradation of CD4 in human T cells. *J. Biol. Chem.* 269, 3917-3920.

Sanfridson, A., Hester, S., and Doyle, C. (1997). Nef proteins encoded by human and simian immunodeficiency viruses induce the accumulation of endosomes and lysosomes in human T cells. *Proceedings of the National Academy of Sciences of the United States of America* 94, 873-878.

Sanger, F., Nicklen, S., and Coulson, A.R. (1977). DNA sequencing with chain terminating inhibitors. *Proc. Natl. Acad. Sci. U. S. A.* 74, 5463-5467.

Sawai, E.T., Baur, A., Struble, H., Peterlin, B.M., Levy, J.A., and Cheng-Mayer, C. (1994). Human immunodeficiency virus type 1 Nef associates with a cellular serine kinase in T lymphocytes. *Proc. Natl. Acad.*

Sci. U. S. A. *91*, 1539-1543.

Sawai, E.T., Baur, A.S., Peterlin, B.M., Levy, J.A., and ChengMayer, C. (1995). A conserved domain and membrane targeting of nef from HIV and SIV are required for association with a cellular serine kinase-activity. *J. Biol. Chem.* *270*, 15307-15314.

Sawai, E.T., Khan, I.H., Montbriand, P.M., Peterlin, B.M., ChengMayer, C., and Luciw, P.A. (1996). Activation of PAK by HIV and SIV nef - importance for AIDS in rhesus macaques. *Current Biology* *6*, 1519-1527.

Schmid, S.L. (1997). Clathrin-coated vesicle formation and protein sorting: an integrated process. *Annual Review Of Biochemistry* *66*, 511-548.

Schnell, M.J., Johnson, J.E., Buonocore, L., and Rose, J.K. (1997). Construction of a novel virus that targets HIV-1-infected cells and controls HIV-1 infection. *Cell* *90*, 849-857.

Schnitzer, J.E., McIntosh, D.P., Dvorak, A.M., Liu, J., and Oh, P. (1995). Separation of caveolae from associated microdomains of GPI-anchored proteins. *Science* *269*, 1435-1439.

Schwartz, O., DautryVarsat, A., Goud, B., Marechal, V., Subtil, A., Heard J, M., and Danos, O. (1995a). Human immunodeficiency virus type 1 Nef induces accumulation of CD4 in early endosomes. *J. Virol.* *69*, 528-533.

Schwartz, O., Marechal, V., Danos, O., and Heard, J.M. (1995b). Human-immunodeficiency-virus type-1 nef increases the efficiency of reverse transcription in the infected cell. *J. Virol.* *69*, 4053-4059.

Shaw, A.S., Amrein, K.E., Hammond, C., Stern, D.F., Sefton, B.M., and Rose, J.K. (1989). The Lck tyrosine protein kinase interacts with the cytoplasmic tail of the CD4 glycoprotein through its unique amino-terminal domain. *Cell* *59*, 627-636.

Shaw, A.S., Chalupny, J., Whitney, J.A., Hammond, C., Amrein, K.E., Kavathas, P., Sefton, B.M., and Rose, J.K. (1990). Short related sequences in the cytoplasmic domains of CD4 and CD8 mediate binding to the amino-terminal domain of the p56^{lck} tyrosine protein kinase. *Molecular and Cellular Biology* *10*, 1853-1862.

Shenoy-Scaria, A.M., Timson Gaien, L.K., Kwong, J., Shaw, A.S., and Lublin, D.M. (1993). Palmitoylation of an amino-terminal cysteine motif of protein tyrosine kinases p56^{lck} and p59^{fn} mediates interaction with glycosyl-phosphatidylinositol-anchored proteins. *Molecular and Cellular Biology* *13*, 6385-6392.

Shenoyscaria, A.M., Dietzen, D.J., Kwong, J., Link, D.C., and Lublin, D.M. (1994). Cysteine(3) of Src family protein-tyrosine kinases determines palmitoylation and localization in caveolae. *Journal Of Cell Biology* *126*, 353-363.

Sheperd, P.R., Reaves, B.J., and Davidson, H.W. (1996). Phosphoinositide 3-kinases and membrane traffic.

Trends In Cell Biology 6, 92-97.

Shugars, D.C., Smith, M.S., Glueck, D.H., Nantermet, P.V., Seillier-Moiseiwitsch, F., and Swanstrom, R. (1993). Analysis of human immunodeficiency virus type 1 *nef* gene sequences present *in vivo*. J. Virol. 67, 4639-4650.

Sicheri, F., Moarefi, I., and Kuriyan, J. (1997). Crystal structure of the Src family tyrosine kinase Hck. Nature 385, 602-609.

Silver, P. (1991). How proteins enter the nucleus. Cell 64, 489-497.

Simons, K. and Ikonen, E. (1997). Functional rafts in cell membranes. Nature 387, 569-572.

Skowronski, J., Parks, D., and Mariani, R. (1993a). Altered T cell activation and development in transgenic mice expressing the HIV-1 *nef* gene. EMBO Journal 12, 703-713.

Skowronski, J., Parks, D., and Mariani, R. (1993b). Altered T cell activation and development in transgenic mice expressing the HIV-1 *nef* gene. EMBO J. 12, 703-713.

Sleckman, B.P., Shin, J., Igras, V.E., Collins, T.L., Strominger, J.L., and Burakoff, S.J. (1992). Disruption of the CD4-p56^{lck} complex is required for rapid internalization of CD4. Proc. Natl. Acad. Sci. U. S. A. 89, 7566-7570.

Smith, B.L., Krushelnycky, B.W., Mochlyrosen, D., and Berg, P. (1996). The HIV Nef protein associates with protein-kinase-c-theta. J. Biol. Chem. 271, 16753-16757.

Smith, D.B. and Johnson, K.S. (1988). Single-step purification of polypeptides expressed in *Escherichia coli* as fusions with glutathione-S-transferase. Gene 67, 31-40.

Sol, N., Ferchal, F., Braun, J., Pleskoff, O., Treboute, C., Ansart, I., and Alizon, M. (1997). Usage of the coreceptors CCR-5, CCR-3, and CXCR-4 by primary and cell line-adapted human immunodeficiency virus type 2. J. Virol. 71, 8237-8244.

Songyang, Z. (1993). SH2 domains recognise specific phosphopeptide sequences. Cell 72, 767-778.

Songyang, Z. and Cantley, L.C. (1995). Recognition and specificity in protein tyrosine kinase-mediated signalling. TIBS 20, 470-475.

Spearman, P., Wang, J.J., Vanderheyden, N., and Ratner, L. (1994). Identification of human-immunodeficiency-virus type-1 gag protein domains essential to membrane-binding and particle assembly. J. Virol. 68, 3232-3242.

Spina, C.A., Kwoh, T.J., Chowes, M.Y., Guatelli, J.C., and Richman, D.D. (1994). The importance of *nef* in the induction of human immunodeficiency virus type 1 replication from primary quiescent CD4 lymphocytes. J.

Exp. Med. 179, 115-124.

StahlHennig, C., Dittmer, U., Nisslein, T., Petry, H., Jurkiewicz, E., Fuchs, D., Wachter, H., MatzRensing, K., Kuhn, E.M., Kaup, F.J., Rud, E.W., and Hunsmann, G. (1996). Rapid development of vaccine protection in macaques by live-attenuated simian immunodeficiency virus. *Journal of General Virology* 77, 2969-2981.

Stammers, D.K., Somers, D.O., Ross, C.K., Kirby, I., Ray, P.H., Wilson, J.E., Norman, M., Ren, J.S., Esnouf, R.M., Garman, E.F., Jones, E.Y., and Stuart, D.I. (1994). Crystals of HIV-1 reverse-transcriptase diffracting to 2-center-dot-2 angstrom resolution. *Journal of Molecular Biology* 242, 586-588.

Stenberg, P.E., Pestina, T.I., Barrie, R.J., and Jackson, C.W. (1997). The Src family kinases, fgr, fyn, lck, and lyn, colocalize with coated membranes in platelets. *Blood* 89, 2384-2393.

Stevenson, M. (1996). Portals of entry: uncovering HIV nuclear transport pathways. *Trends in Cell Biol.* 6, 9-15.

Stover, D.R., Liebetanz, J., and Lydon, N.B. (1994). Cdc2-mediated modulation of pp60c-Src activity. *J. Biol. Chem.* 269, 26885-26889.

Straus, D.B. and Weiss, A. (1992). Genetic evidence for the involvement of the Lck tyrosine kinase in signal transduction through the T cell antigen receptor. *Cell* 70, 585-593.

Swingler, S., Gallay, P., Camaur, D., Song, J.P., Abo, A., and Trono, D. (1997). The Nef protein of human immunodeficiency virus type 1 enhances serine phosphorylation of the viral matrix (vol 71, pg 4376, 1997). *J. Virol.* 71, 8085

Tamir, A. and Isakov, N. (1991). Increased intracellular cyclic AMP levels block PKC-mediated T cell activation by inhibition of c-jun transcription. *Immunol. Lett.* 27, 95-99.

Tamir, A. and Isakov, N. (1994). Cyclic AMP inhibits phosphatidylinositol-coupled and -uncoupled mitogenic signals in T lymphocytes. Evidence that cAMP alters PKC-induced transcription regulation of members of the jun and fos family of genes. *J. Immunol.* 152, 3391-3399.

Tamir, A., Granot, Y., and Isakov, N. (1996). Inhibition of T lymphocyte activation by cAMP is associated with down-regulation of two parallel mitogen-activated protein kinase pathways, the extracellular signal-related kinase and c-Jun N-terminal kinase. *J. Immunol.* 157, 1514-1522.

Terwilliger, E., Sodroski, J.G., Rosen, C.A., and Haseltine, W.A. (1986). Effects of mutations within the 3'orf open reading frame region of human T-cell lymphotropic virus type III (HTLV-III/LAV) on replication and cytopathogenicity. *J. Virol.* 60, 754-760.

Thali, M., Bukovsky, A., Kondo, E., Rosenwirth, B., Walsh, C.T., Sodroski, J., and Gottlinger, H.G. (1994). Functional association of cyclophilin-a with HIV-1 virions. *Nature* 372, 363-365.

- Timson Gauen, L.K., Tony Kong, A., N., Samelson, L.E., and Shaw, A.S. (1992). p59Fyn tyrosine kinase associates with multiple T-Cell receptor subunits through its unique amino-terminal domain. *Molecular and Cellular Biology* 12, 5438-5446.
- Trono, D. (1995). HIV accessory proteins - leading roles for the supporting cast. *Cell* 82, 189-192.
- Turner, J.M., Brodsky, M.H., Irving, B.A., Levin, S.D., Perlmutter, R.M., and Littman, D.R. (1990). Interaction of the unique N-terminal region of tyrosine kinase p56^{lck} with cytoplasmic domains of CD4 and CD8 is mediated by cysteine motifs. *Cell* 60, 755-765.
- Unutmaz, D. and Littman, D.R. (1997). Expression pattern of HIV-1 coreceptors on T cells: implications for viral transmission and lymphocyte homing. *Proceedings of the National Academy of Sciences of the United States of America* 94, 1615-1618.
- Vanhaesebroeck, B., Leevers, S.J., Panayotou, G., and Waterfield, M.D. (1997). Phosphoinositide 3-kinases: a conserved family of signal transducers. *TIBS* 22, 267-272.
- Varmus, H. (1988). Retroviruses. *Science* 240, 1427-1435.
- Veillette, A., Bookman, M.A., Horak, E.M., and Bolen, J.B. (1988). The CD4 and CD8 T-cell surface-antigens are associated with the internal membrane tyrosine-protein kinase p56^{lck}. *Cell* 55, 301-308.
- Veillette, A., Bookman, M.A., Horak, E.M., Samelson, L.E., and Bolen, J.B. (1989). Signal transduction through the CD4 receptor involves the activation of the internal membrane tyrosine-protein kinase p56lck. *Nature* 338, 257-259.
- Veillette, A., Caron, L., Fournel, M., and Pawson, T. (1992). Regulation of the enzymatic function of the lymphocyte-specific tyrosine protein kinase p56^{lck} by the non-catalytic SH2 and SH3 domains. *Oncogene* 7, 971-980.
- Vogel, L. and Fujita, D.J. (1993). The SH3 domain of p56^{lck} is involved in binding to phosphoinositol 3'-kinase from T lymphocytes. *Molecular and Cellular Biology* 13, 7408-7417.
- Vonschwedler, U., Kornbluth, R.S., and Trono, D. (1994). The nuclear-localization signal of the matrix protein of human-immunodeficiency-virus type-1 allows the establishment of infection in macrophages and quiescent T-lymphocytes. *Proceedings of the National Academy of Sciences of the United States of America* 91, 6992-6996.
- Voronova, A.F. and Sefton, B.M. (1986). Expression of a new tyrosine protein kinase is stimulated by retrovirus promoter insertion. *Nature* 319, 682-686.
- Watanabe, W., Shiratori, T., Shoji, H., Miyatake, S., Okazaki, Y., Ikuta, K., Sato, T., and Saito, T. (1997). A

- novel acyl-coa thioesterase enhances its enzymatic activity by direct binding with HIV Nef. *Biochemical and Biophysical Research Communications* 238, 234-239.
- Weijland, A., Williams, J.C., Neubauer, G., Courtneidge, S.A., Wierenga, R.K., and Supertifurga, G. (1997). Src regulated by C-terminal phosphorylation is monomeric. *Proc. Natl. Acad. Sci. U. S. A.* 94, 3590-3595.
- Weissenhorn, W., Wharton, S.A., Calder, L.J., Earl, P.L., Moss, B., Aliprandis, E., Skehel, J.J., and Wiley, D.C. (1996). The ectodomain of HIV-1 env subunit gp41 forms a soluble, alpha-helical, rod-like oligomer in the absence of gp120 and the N-terminal fusion peptide. *EMBO Journal* 15, 1507-1514.
- Weissenhorn, W., Dessen A., Harrison S.C., Skehel J.J., Wiley D.C. (1997). Atomic structure of the ectodomain from HIV-1 gp41. *Nature* 387 (6631), 426-430.
- Welker, R., Kotler, H., Kalbitzer, H.R., and Krausslich, H.G. (1996). Human-immunodeficiency-virus type-1 Nef protein is incorporated into virus-particles and specifically cleaved by the viral proteinase. *Virology* 219, 228-236.
- Whatmore, A.M., Cook, N., Hall, G.A., Sharpe, S., Rud, E.W., and Cranage, M.P. (1995). Repair and evolution of *nef* in-vivo modulates simian immunodeficiency virus virulence. *J. Virol.* 69, 5117-5123.
- White, M.A. (1996). The yeast two-hybrid system: forward and reverse. *Proc. Natl. Acad. Sci. U. S. A.* 93, 10001-10003.
- Wilkinson, D. (1996). HIV-1 - cofactors provide the entry keys. *Current Biology* 6, 1051-1053.
- Willey, R.L., Buckler-White, A., and Strebel, K. (1994). Sequences present in the cytoplasmic domain of CD4 are necessary and sufficient to confer sensitivity to the human immunodeficiency virus type 1 vpu protein. *J. Virol.* 68, 1207-1212.
- Willey, R.L., Maldarelli, F., Martin, M.A., and Strebel, K. (1992). Human immunodeficiency virus type 1 vpu protein induces rapid degradation of CD4. *J. Virol.* 66, 7193-7200.
- Williams, J.C., Weijland, A., Gonfloni, S., Thompson, A., Courtneidge, S.A., Supertifurga, G., and Wierenga, R.K. (1997). The 2.35Å crystal structure of the inactivated form of chicken Src: a dynamic molecule with multiple regulatory interactions. *J. Mol. Biol.* 274, 757-775.
- Wiskerchen, M. and ChengMayer, C. (1996). HIV-1 Nef association with cellular serine kinase correlates with enhanced virion infectivity and efficient proviral DNA-synthesis. *Virology* 224, 292-301.
- Wu, X., Liu, H., Xiao, H., Conway, J.A., and Kappes, J.C. (1996). Inhibition of human and simian immunodeficiency virus protease function by targeting Vpx-protease-mutant fusion protein into viral particles. *J. Virol.* 70, 3378-3384.

- Wyatt, R., Desjardin, E., Olshevsky, U., Nixon, C., Binley, J., Olshevsky, V., and Sodroski, J. (1997). Analysis of the interaction of the human immunodeficiency virus type 1 gp120 envelope glycoprotein with the gp41 transmembrane glycoprotein. *J. Virol.* *71*, 9722-9731.
- Xu, H. and Littman, D.R. (1993). A kinase-independent function of Lck in potentiating antigen-specific T cell activation. *Cell* *74*, 633-643.
- Xu, W., Harrison, S.C., and Eck, M.J. (1997). Three-dimensional structure of the tyrosine kinase c-Src. *Nature* *385*, 595-601.
- Yamaguchi, H. and Hendrickson, W.A. (1996). Structural basis for activation of human lymphocyte kinase Lck upon tyrosine phosphorylation. *Nature* *384*, 484-489.
- Yu, G. and Felsted, R.L. (1992). Effect of myristoylation on p27 nef subcellular distribution and suppression of HIV-LTR transcription. *Virology* *187*, 46-55.
- Yu, H.T., Chen, J.K., Feng, S.B., Dalgarno, D.C., Brauer, A.W., and Schreiber, S.L. (1994). Structural basis for the binding of proline-rich peptides to SH3 domains. *Cell* *76*, 933-945.
- Zeigler, S.F., March, J.D., Lewis, D.B., and Perlmutter, R.M. (1987). Novel protein-tyrosine kinase gene (*hck*) preferentially expressed in cells of hematopoietic origin. *Molecular and Cellular Biology* *7*, 2276-2285.
- Zenner, G., Zurhausen, J.D., Burn, P., and Mustelin, T. (1995). Towards unraveling the complexity of T-cell signal-transduction. *BioEssays* *17*, 967-975.
- Zhang, W.H., Hockley, D.J., Nermut, M.V., Morikawa, Y., and Jones, I.M. (1996). Gag-gag interactions in the C-terminal domain of human-immunodeficiency-virus type-1 p24 capsid antigen are essential for gag particle assembly. *Journal of General Virology* *77*, 743-751.
- Zhang, Y.Q. and Barklis, E. (1997). Effects of nucleocapsid mutations on human immunodeficiency virus assembly and RNA encapsidation. *J. Virol.* *71*, 6765-6776.
- Zheng, J., Knighton, D.R., Xuong, N.H., Taylor, S.S., Sowadski, J.M., and Eyck, L.F.T. (1993). Crystal structures of the myristoylated catalytic subunit of cAMP-dependent protein kinase reveal open and closed conformations. *Protein Science* *2*, 1559-1573.
- Zhou, W., Parent, L.J., Wills, J.W., and Resh, M.D. (1994). Identification of a membrane-binding domain within the amino-terminal region of human immunodeficiency virus type 1 Gag protein which interacts with acidic phospholipids. *J. Virol.* *68*, 2556-2569.